Development of a model for controlling indoor air quality

Fangfang Guo

UNIVERSITÉ DE STRASBOURG

ÉCOLE DOCTORALE DES SCIENCES DE LA TERRE ET DE L'ENVIRONNEMENT

[LABORATOIRE IMAGE VILLE ENVIRONNEMENT]

THÈSE présentée par :

[FANGFANG GUO]

soutenue le : **26 Octobre 2017**

pour obtenir le grade de : **Docteur de l'université de Strasbourg**

Discipline/ Spécialité : Physique et Chimie de l'Atmosphère

Development of a model for controlling indoor air quality

THÈSE dirigée par :

[Dr. Ponche Jean-luc]	Directeur de thèse, Université de Strasbourg, France
[Dr. Hauglustaine Didier]	Co-directeur de thèse, Université de Strasbourg, France

RAPPORTEURS :

[Dr. Luo Zhiwen]	Assistant professeur, Université de Reading, Royaume-Uni
[Pr. Langlet Thierry]	Professeur, Université de Picardie Jules Verne, France

---

AUTRES MEMBRES DU JURY :

[Dr. Schoemaecker Coralie]	Chargée de recherche, CNRS, France
[Pr. Millet Maurice]	Professeur, Université de Strasbourg, France

UNIVERSITÉ DE STRASBOURG

ÉCOLE DOCTORALE DES SCIENCES DE LA TERRE ET DE L'ENVIRONNEMENT

[LABORATOIRE IMAGE VILLE ENVIRONNEMENT]

THÈSE présentée par :

[FANGFANG GUO]

soutenue le : **26 Octobre 2017**

pour obtenir le grade de : **Docteur de l'université de Strasbourg**

Discipline/ Spécialité : Physique et Chimie de l'Atmosphère

Development of a model for controlling indoor air quality

THÈSE dirigée par :

[Dr. Ponche Jean-luc]	Directeur de thèse, Université de Strasbourg, France
[Dr. Hauglustaine Didier]	Co-directeur de thèse, Université de Strasbourg, France

RAPPORTEURS :

[Dr. Luo Zhiwen]	Assistant professeur, Université de Reading, Royaume-Uni
[Pr. Langlet Thierry]	Professeur, Université de Picardie Jules Verne, France

---

AUTRES MEMBRES DU JURY :

[Dr. Schoemaecker Coralie]	Chargée de recherche, CNRS, France
[Pr. Millet Maurice]	Professeur, Université de Strasbourg, France

Fangfang GUO

Développement d'un modèle pour le contrôle de la qualité de l'air intérieur

Résumé en Français

Ce travail a consisté à analyser et de simuler à l'aide du modèle INCA-Indoor la qualité de l'air intérieur mesurée dans le projet MERMAID, et de développer une nouvelle méthodologie pour étudier les contributions des différents processus aux concentrations de polluants. Cette nouvelle méthodologie se base sur un nouveau programme de sensibilité INCA-Indoor-D, construit à partir du modèle INCA-Indoor. Ce modèle permet d'identifier rapidement les paramètres les plus sensibles qui peuvent influencer la qualité de l'air intérieur.

Le modèle INCA-Indoor a été validé expérimentalement en utilisant les données mesurées lors de la campagne MERMAID (2014-2015). L'application du programme de sensibilité INCA-Indoor-D est pour analyser des sensibilité des concentrations de OH par rapport aux divers paramètres. Une classification de l'importance de ces paramètres (appelée « rang ») en fonction de la sensibilité a ainsi été effectuée. Ce travail de thèse offre une nouvelle analyse de la pollution de l'air ainsi que de nouvelles perspectives d'études possibles dans un bâtiment basse consommation. Il a permis de confirmer que le modèle INCA-Indoor permettait de simuler convenablement la pollution de l'air intérieur. Le modèle de sensibilité a été construit afin d'élaborer un nouvel outil d'aide à la décision capable de calculer à la fois les concentrations et leurs sensibilités aux divers paramètres. Ces sensibilités peuvent ensuite être utilisées pour élaborer, voire optimiser des stratégies de réduction de la pollution de l'air intérieur et d'identifier les paramètres les plus importants.

Mots clés : Qualité de l'air intérieur, modèle INCA-Indoor, sensibilité

Résumé en anglais

This study consisted in the development of a new methodology to study the contributions of different processes taken place indoors and the effect of input data on the indoor air pollution, and especially to develop a fast methodology to identify the most sensitive parameters that could influence indoor air quality. One objective is the development of a tool to support IAQ reduction strategies. The methodology is based on a sensitivity program INCA-Indoor-D for the INCA-Indoor model. This sensitivity program INCA-Indoor-D was built to identify the most important parameters affecting pollutant concentrations.

Since measurement data were newly analyzed and available from MERMAID, it is intended to continue to evaluate the INCA-Indoor model, which was used to analyze the indoor air quality of a low energy building. The first application of the sensitivity program INCA-Indoor-D is performed to develop a comprehensive sensitivity analysis of indoor [OH] with respect to diverse parameters. Sensitivity has been settled with a classification of the parameters. The results in this study provide useful information about roles of different processes controlling indoor air quality and the effects of different parameters on indoor pollutant concentrations. INCA-Indoor model can be used as a powerful tool to investigate indoor air issues. In addition, the tangent linear model of INCA-Indoor model developed can be used to find out the important parameters impacting pollutant concentrations.

Keywords: Indoor air quality, INCA-Indoor model, sensitivity

Acknowledgement

Firstly, I would like to express my sincere gratitude to my advisor Jean-luc Ponche (LIVE, University of Strasbourg) and Dr. Didier Hauglustaine (LIVE&LSCE, CNRS) for the continuous support of my Ph.D study and related research, for their patience, motivation, and immense knowledge. Their guidance helped me in all the time of research and writing of this thesis.

I would like to thank my supervisor Nadège Blond (CNRS). The door to her office was always open whenever I ran into a trouble spot or had a question about my research or writing. She consistently provided help when it was necessary and steered me in the right the direction whenever she thought I needed it.

I appreciate Dr. Isabelle Charpentier (ICUBE, CNRS) who provides me many suggestions and helps during my phd work, especially for the development sensitivity model.

My sincere thanks also goes to Dr. Coralie Schoemaecker (PC2A, CNRS) and Dr. Maxence Mendez (OCTOPUS LAB) who provided me help and suggestion for my work and especially in chemistry.

A very special gratitude goes out to all down at China Scholarship Council for helping and providing the funding for the work.

I thank all the people working at the Laborary of Image, Ville et Environnment at University of Strasbourg. It’s really an excellent experience to work with you.

Last but not the least, I would like to thank my family : my parents and to my brother for supporting me spiritually throughout writing this thesis and my life in general.

Content

List of figures

List of tables

CHAPTER 1

INTRODUCTION

1.1 Indoor air quality

Since the last century, there has been a broad understanding of the threat posed by air pollution to the public's health [1, 2, 3]. The history and evolution of research on Indoor Air Quality is closely intertwined with outdoor air pollution [4]. Indoor air quality(IAQ) generally refers to the air quality within and around buildings and structures and especially relates to the health and comfort of building occupants [5].

Outdoor pollutants may enter the building through infiltration or ventilation. Pollutants of indoor origin may arise from many sources. In the 1980's, the U.S. EPA's Total Exposure Assessment Methodology (TEAM) Study provided a model for comprehensive assessment of the contributions of indoor and outdoor exposures to total personal exposure [6]. Results show that indoor pollution sources were more important contributors to total personal exposure to toxic volatile organic compounds than outdoor pollution sources, including industrial ones.

Indeed, people spend more than 90 percent of their time indoors : at home, at work, in transportation, and in many other public and private places, where concentrations of some contaminants may be higher indoors than outdoors [7]. Indoor environments may contain a variety of air pollutants. Some pollutants are emitted from materials used in the building such as asbestos, formaldehyde and lead [8, 9, 10]. Some pollutants such as pollen, particles, volatile organic

compounds are generated from mold and pollen [11], tobacco smoke [12], household products [13]. Indoor pollution is often exacerbated by poorly designed, badly built, and/or inadequately maintained or operated mechanical ventilation systems [14]. The characteristics of IAQ for one indoor environment vary with time and space, and can be quite different in other residential and commercial buildings.

Indoor air quality affects people's well-being and productivity. Furthermore, risks for diverse diseases are increased by indoor air pollution, which may cause diverse symptoms and illnesses, like the symptom syndrome now most often referred as SBS (sick building syndrome) [15]. Considerable evidences have been revealed about the health consequences of indoor radon, environmental tobacco smoke, formaldehyde, asbestos, latex, and many natural and synthetic allergens [16, 17, 18]. Asbestos, one of the well-known indoor pollutants, can scar lung tissue and cause cancer [19]. Lead poisoning affects virtually every organ system, primarily affects the central nervous system, particularly the developing brain [20]. According to World Health Organization (WHO), 4.3 million people a year die prematurely from illness attributable to the household air pollution caused by the inefficient use of solid fuels (2012 data) for cooking [21].

Many studies present the costs of impact of indoor air pollution and benefits of interventions to reduce it [22, 23, 24]. For example, in France, indoor pollution associated with the pollutants such as benzene, radon, particles (PM2.5 fraction), environmental tobacco smoke (ETS) was estimated at a cost approximately of 20 billion euros in 2004 [25]. The research of Mendell [26] suggests that improving building environments may result in health benefits for more than 15 million of the 89 million US indoor workers, with estimated economic benefits from 5 to 75 billion dollars annually.

Therefore, improving indoor air quality becomes an increasing important topic. Some guides, regulations and specialized databases have established primary standards to set limits related to protection of public health for the primary air pollutant. High priority providing information for indoor air quality applications include ASHRAE Standard 62 [27], National Ambient

Air Quality Standards, etc. OQAI [28] proposed a classification of the pollutants as a function of their health impacts.

1.2 Assessing Indoor Air Quality

With growing recognition of the problems of indoor air pollution and potential benefits of improving indoor environments, two approaches were developed for investigating IAQ problems : measuring and modeling.

1.2.1 Measuring Indoor Air Quality

The measurements of the indoor air quality often highly relies on monitoring instrumentation, that are set up in laboratories or in real building environment (in situ measurements). The in situ long-term measurements provide the opportunity to determine the short-term peak concentrations, average concentrations calculated over any period, and to correlate the concentration variations as a function of time with source generation, infiltration-ventilation, and other characteristics. However, they are very expensive and require frequent calibration and routine maintenance. Thus the short-term measurements are more often performed and offer limited data to fully assess indoor air quality with its diurnal, seasonal or other long-term concentration variations.

Several measurement campaigns were developed in the past. One can cite for example :

In Finland in 1999, an indoor air measurement campaign in Helsinki, Finland 1999 was performed to study the effect of outdoor air pollution on indoor air [29]. Wintertime indoor and outdoor particle size distributions were measured simultaneously with two similar differential mobility particle sizer systems (DMPS) at two places : on the rooftop of a building (30 m above the ground level) in front of a ventilation system corresponding to outdoor concentration, and an office room (first floor). Indoor particle concentrations were observed to vary from 500 to 10^4

cm^{-3} with a high dependence on the outdoor concentrations. This indicates that in this scenario, indoor particles are mainly of outdoor origin.

In US in 1996, nitrous acid, nitrogen dioxide (NO_2), and ozone (O_3) concentrations in occupied houses in Southern California were measured using passive samplers [30]. Measurement results show that the average indoor HONO concentration was 4.6 ppb, compared to 0.9 ppb for outdoor HONO. Average indoor and outdoor NO_2 concentrations were 28 and 20.1 ppb, respectively. Indoor O_3 concentrations were low (average 14.9 ppb) in comparison to the outdoor levels (average 56.5 ppb). The measurements demonstrated the occurrence of substantial residential indoor HONO concentrations and associations among the three indoor air pollutants.

In France in 2002, measurements of outdoor and indoor pollution have been carried out in eight schools in La Rochelle (France) and its suburbs [31]. Ozone, nitrogen oxides (NO and NO_2), and airborne particle (particle counts within 15 size intervals ranging from 0.3 to 15 mum) concentrations were continuously monitored indoors and outdoors for two periods. The indoor humidity, temperature, CO_2 concentration (an indicator of occupancy), window openings and building permeability were also measured. Results show that ozone and nitrogen oxides behave differently but no correlation with building permeability was observed for nitrogen oxides. On the contrary, ozone seem to be strongly influenced by the building air-tightness : the more airtight the building envelope, the lower the ratio [32]. Occupancy, through re-suspension of previously deposited particles and possible particle generation, strongly influences the indoor concentration level of airborne particles.

In US between 1999 and 2001, indoor and outdoor carbonyl concentrations were measured in 234 personal air (RIOPA) homes in three urban areas of the United States [33]. The indoor source strengths for different carbonyl concentrations are reported in this study. For example, formaldehyde, and acetaldehyde had the strongest indoor source strengths with the estimated median values of 3.9 and 2.6 mg h^{-1}, respectively. Hexaldehyde also had large indoor source strengths with a median of 0.56 mg h^{-1}. Acrolein and crotonaldehyde had the weakest indoor

source strengths with no indoor sources detected in the majority of the RIOPA homes that were selected to have only nonsmoker residents.

In France between 2004 and 2005, aldehydes concentrations were measured in 162 homes in the Strasbourg area (East of France) in the context of a case/control study pairing asthmatic and non-asthmatic people [34]. Results show that formaldehyde, acetaldehyde and hexanal were the main encountered aldehydes with mean concentrations of 32.2±14.6, 14.3±9.7 and 8.6±8.1 $\mu g\ m^{-3}$, respectively. However it was difficult to determine the main parameters influencing formaldehyde concentrations in domestic environment. Higher hexanal concentrations were related to new coatings such as painting, wallpapers and laminate flooring. Hexanal concentration decreased with both coating and furniture ages so that this compound may be considered as a tracer of these emissions.

In France between 2009 and 2010, a nationwide monitoring system of indoor air quality in public premises, especially with vulnerable populations such as children, has been performed [35]. The first phase of a pilot study took place from September 2009 to June 2010, and involved 160 schools and daycare centers across 13 regions. The other French regions are taking part in a second wave, begun in September 2010. This campaign focused on several parameters : two chemical pollutants (benzene and formaldehyde) and the air stuffiness. The results show, with respect to the management values put forward by the French committee for public health (HCSP), that air quality is overall acceptable in most of the schools and daycare centers which have taken part in this study. Nonetheless, a few cases require additional diagnoses or corrective measures. Furthermore, 16% of classrooms were found to be insufficiently ventilated (25% in elementary schools). The Mayors and School Principals were notified, and were provided means to identify the main sources of pollution as well as to implement remediation measures.

In France in 2013, SURFin (Les surfaces internes à l'habitat, une source probable d'acide nitreux) [36]. The SURFin campaign has been carried out in an unoccupied classroom in Marseille (France) in order to quantify hydroxyl (OH) and hydroperoxyl (HO_2) radicals, HONO,

photolysis frequencies, O_3 and NOx, relative humidity, temperature, and eight different VOCs (1-pentene, isobutene, d-limonene, isoprene, acetaldehyde, acrolein, toluene and xylenes). For the first time in an indoor environment, field experiments could be carried out to measure the production rates of HONO and OH. Results show that the OH concentrations can reach levels equivalent to those of the outside atmosphere in the sunny areas of the room. The photolysis of HONO, which produced by the heterogeneous reactivity of NO2, was the main source of OH.

In France between 2012 and 2015, MERMAID (Mesures Expérimentales Représentatives et Modélisation Air Intérieur Détaillée) [37]. The ADEME PRIMEQUAL associated project aimed at studying indoor air quality in low energy building. An intensive campaign provides the measurement of physical parameters of the studied room (i.e. volume, surface area), temperature and relative humidity, air exchange rate (AER), the levels of NOx (NO and NO_2), O_3, and fifty different VOCs. The surface interactions with the VOCs were measured also in situ to estimate the emission factors and sorption coefficients of materials.

Specific measurement campaigns in laboratories are usually performed to detail one specific process. Since they are numerous, they will not be detailed here but few of them will be referenced in chapter 2 when discussing the processes occurring indoor.

In principle, the direct measurements of the building interior give the most realistic information concerning the IAQ. Because of the nonuniform distributions of the flows and pollutants, measurements must be made at many locations. Taking direct measurements of the pollutant concentrations at many locations may be not available sometimes or is very expensive and time-consuming when available. In addition, pollutant concentrations are the result of various processes including ventilation, internal emissions, sink effects and chemical reactions. So the pollutant measurements alone do not allow the distinction between the contributions of the above mentioned processes, especially the role of the indoor air chemistry or sources. That is why the IAQ models can be useful.

1.2.2 Modeling Indoor Air Quality

The high costs and complexity of assessing the IAQ experimentally have resulted in the development of the IAQ models. Since a full chapter (chapter two) is dedicated to IAQ modeling, few advantages of IAQ models will be discussed here.

IAQ models provide a way to link sources, sinks and building factors to estimate indoor pollutant concentrations. Furthermore, the IAQ models can be used to investigate many IAQ problems without the expense of large field experiments. The IAQ models have many advantages, for instance :

— They can help to understand the indoor pollutant sources and sinks and to predict the indoor pollutant concentrations ;

— They provide a framework for interpreting experimental results and for designing experiments by providing information on targeted pollutant concentrations ;

— A model is useful to produce results relating indoor pollutant concentrations with various parameters like geometric, materials, ventilation, light, color of walls, use of systems improving indoor quality, etc ;

— Modeling can be used to determine the accuracy and the precision to which various quantities must be reached if the desired accuracy of prediction is to be achieved. It can also be used in sorting out trends with the experimental data ;

— They provide information on the factors that are important and can help to determine what must be measured in priority ;

The most common uses of IAQ models are :

— Estimating the pollutant concentrations ;

— Estimating the impact of individual sources or sinks and IAQ control options on personal exposure ;

Many examples indicate that IAQ models act as powerful tools to study indoor environment. With IAQ models, many IAQ problems can be carefully studied and analyzed with little cost.

A range of models have been developed and adopted for investigating IAQ problems. However, not all of these IAQ models have been validated with experimental results. Since there are not models available which consider all physical and chemical processes indoors and can be used to interpret the experimental results, the model INCA-Indoor, on which the thesis is based, was developed in the framework of the MERMAID (Mesures Expérimentales Représentatives et Modélisation Air Intérieur Détaillée) [37, 38] project to help to understand the measurements. More information on IAQ and especially INCA-Indoor model is available in Chapter two and three.

1.3 Objectives of the thesis

Since indoor air pollution has impacts on human health and people are highly exposed to this air pollution along a day, it is necessary to provide as fast as possible knowledge on the physical and chemical processes that are involved, methodologies that could help to understand the sources and sinks of indoor air pollution, and develop tools to help take decisions to reduce it. This thesis has been carried out in the framework of the PRIMEQUAL MERMAID (2012-2016) [37, 38, 39, 40] project. This project offers several types of results :

— Numerous measurements issued from two campaigns in classrooms and outdoor environments during scholar holidays on April-May 2014 and on February-March 2015 in a low energy building and additional measurements in laboratories to detail few processes ;

— The INCA-Indoor air quality model, that was developed in parallel of the measurement campaigns. Mendez et al. (2015) [41] proposed a model considering diverse indoor physical and chemical processes including emissions, ventilation, gaseous photochemistry, deposition, sorption and heterogeneous chemistry. The model is able to compute the contributions of each processes to the pollutant concentrations ;

— First comparisons of the INCA-Indoor model with measurements issued of the SURFin campaign and other models show that the model offers quite good performance to simulate indoor air quality, and provide new insight of the processes involved indoor air quality. Mendez et al. (2015) assessed the impact of oxidation processes on indoor air quality with INCA-Indoor model [41]. Mendez et al. (2017a) compared simulated concentrations of HOx radicals (OH+HO2) with in situ measurements and provides us information on the sources and sinks of indoor radical oxidants [42]. Mendez et al. (2017b) provides a new indoor HONO formation mechanisms based on in situ measurements and modeling [43] ;

— Preliminary sensitivity analyses showed that sensitivity like Monte Carlo may help to identify the most sensitive input parameters that may influence the simulations and on which it is necessary to improve the estimations (Master Thesis of Fangfang Guo). However, one of the limitations of Monte Carlo method is that it is difficult to evaluate the sensitivity of the impact of parameter variations on model outputs over time. In addition, it is time-consuming to assess the relative importance of parameters for a model with lots of parameters.

All these first results opened new questions to answer : Is the INCA-Indoor model able to re-produce the MERMAID measurements (newly collected and analyzed) and help to understand the indoor air quality in the low energy building that was studied ? What are the main processes involved ? Could we develop a sensitivity methodology to help understand the indoor air pollution and guide reduction strategies ?

Thus the first objective of this thesis aims to fully analyze the measurements collected during the MERMAID campaign using the INCA-Indoor model. This step is very important to understand indoor processes controlling air quality and dynamic but also to evaluate the performance of the model and discuss the measurement methodologies in order to give recommendations for new indoor quality studies. It is also here intended, in a second objective, to present the

development of a new methodology to estimate the sensitivities of the model to diverse parameters. This methodology is developed for several reasons linked to the complexity of the indoor air quality that is the consequence of the effects of many processes : emissions, gaseous and heterogeneous reactions, sorptions, etc :

— Many of the processes are modeled based on the use of uncertain input data. One objective is to be able to detect the most sensitive parameters in order to identify the most important ones which we need to improve the estimate ;

— Taking decision to improve indoor air quality in an efficient way needs to identify the most determinant processes.

1.4 Structure of the thesis

The thesis is organized with five chapters. An overview of indoor air quality models and the need to develop the INCA-Indoor model is based is presented in chapter 2. In chapter 3, the INCA-Indoor model is used in combination with measurement to analyze the indoor air quality as measured in a classroom in a low energy building during the MERMAID campaign. Contribution analysis based on the model is performed in order to analyze the respective role of emission, exchange with outdoor air, indoor chemistry on several pollutants. In chapter 4, the effect of emission rates, air exchange rate, sorptions and light affecting indoor oxidation processes on indoor air quality is investigated. Firstly, INCA-Indoor simulations have been carried out with different emission rates measured during the MERMAID campaign. Secondly, because of the important role of OH radical for the fate of VOC, a parameter affecting indoor photolysis to produce OH radical and indoor air quality is investigated. This parameter is the light transmittance of window, which controls the availability of indoor photons to photolysic the species like the HONO. The characterization of the transmittance of different windows has been studied during the MERMAID campaign. With measured window transmittance, the effect of window

transmittance spectra of different type of window on indoor photolysis and air quality has been assessed with the INCA-Indoor model.

In chapter 5, we explain how the sensitivity program with the INCA-Indoor model was developed and a study on the effects of diverse parameters or processes on the concentration of OH radical is performed. An automatic differentiation tool called TAPENADE is applied to calculate the local fist order sensitivities defined as partial derivatives of indoor species concentrations with respect to the model parameters because of its computational efficiency. The first application of TAPENADE to the INCA-Indoor model is performed to develop a comprehensive sensitivity analysis of indoor OH concentration with respect to diverse parameters (initial NO, NO_2, O_3 and HONO concentrations, indoor VOC emission rates, air exchange rate, outdoor species concentrations, deposition velocities and reaction rate). Sensitivity has been settled with a classification of the parameters. we then provide a conclusion and propose future work directions.

CHAPTER 2

INDOOR AIR QUALITY ASSESSMENT : FOCUS ON MODELING APPROACHES

Abstract

Indoor environment is very complex and the characteristics of indoor pollution vary with different types of buildings. Understanding the processes controlling indoor air pollution is of crucial importance to help decisions focusing on its reduction.

Processes taking place indoors and influencing indoor pollutant concentrations have been studied either by measuring or modeling. Direct measuring indoor pollutant concentrations could provide reliable local information of indoor air quality, however, they are limited in numbers and not sufficient to describe properly the processes. On the contrary, modeling indoor air quality have been demonstrated as a powerful tool to investigate indoor air quality issues but give approximate estimates of the concentrations and contributions taking into account the uncertainties of their inputs and parametrizations of the processes. Thus despite numerous IAQ models have been developed, they showed also some drawbacks and limits. In order to understand them, a review is given in this chapter.

A specific attention is brought to the INCA-INDOOR model recently developed to help to study indoor air quality in low energy buildings in the framework of the PRIMEQUAL ADEME MERMAID project.

2.1 Introduction

To help people who are allergic or sensitive to air pollution to improve the quality of their environment, a series of communications are provided by different services. For example, figure 2.1 is issued from Andatech, a company in Australia, focused on the delivering of breathalyzers and alcohol testing equipment and providing air quality appliances in the market. One of the objectives of this company is to focus on the diversity of the sources that may impact indoor air pollution and aware inhabitants that they are even more exposed to air pollution indoors than outdoors. Others give also recommendations on how to improve indoor air quality using their knowledge on the emission sources. The French agency ADEME (Agence De l'Environnement et de la Maîtrise de l'Energie) provides some propositions to determine if the air at home is polluted through the evaluation of indoor source of pollutants (i.e. the system of ventilation, the human activities, the uses of cleaning products) [44]. Those diagnostics are usually quite qualitative, and not quantitative. The reason is of course linked to the heterogeneity and diversity of the indoor environments, to the costs of measuring and the lack of realistic emission source data and especially detailed models to support these diagnostics.

Nevertheless, to improve the indoor air quality, it is essential to detail and understand the impact of each process taking place indoors and influencing indoor air quality. These processes include the indoor chemistry, ventilation, emissions, sorption and deposition as shown in the figure 2.2. A variety of studies have been carried out to investigate these processes either by measuring or modeling [34, 36, 45, 46, 47].

The objective of this present chapter is not to detail the extensive literature of measuring indoor pollutant concentrations (only few of them are referenced in section 2.2). In these existing studies, it is often difficult to (1) find out the mechanisms of producing and consuming the pollutants, (2) to quantify the contributions of various physical and chemical processes to the pollutant concentrations, and (3) finally to investigate the influence of these various factors. To give just one example, Alvarez et al. (2013) [48] presents direct measuring of significant

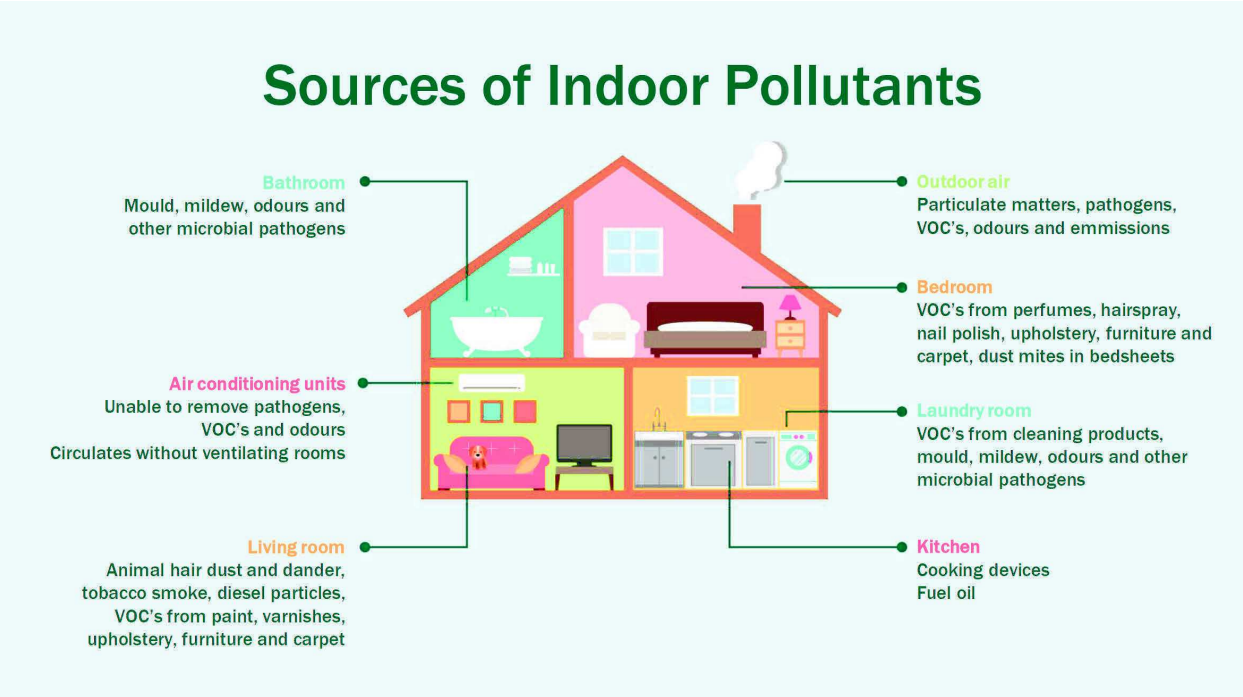

Figure 2.1 – Source of indoor air pollution (reference http ://www.andatech.com.au)

amounts of hydroxyl (OH) radical and nitrous acid (HONO) during an experimental campaign carried out in a school classroom in Marseilles (south east of France). They suggested that HONO is an important source of OH radicals indoors under specific conditions as enough direct solar irradiation inside the room. Only recently, different HONO formation mechanisms were proposed by Mendez et al. (2017) [43] and were compared in the model, which was constrained with experimental data, to explain what was measured by Alvarez et al. (2013). Formal links between both studies are difficult to be detailed but the modeling study showed the effect of HONO formation on indoor chemistry using the indoor air quality model INCA-Indoor and testing different HONO formation mechanisms. The comparison between simulation options with observations point out some keys of understanding, but the study mainly demonstrates the need of more measuring to validate new modeling propositions. Thus measuring and modeling are complementary methodologies that would be very important to develop at the same time but are may be constrained to be developed with a time delay since different expertise are needed.

The objective of the present chapter is to focus on existing indoor air quality models, and their validation. Since recently, there has been a growing interest in understanding indoor air quality, numerous indoor models were developed and few were validated. Strategy of validation using inter-comparison models or comparisons with measuring are discussed.

This chapter is organized in four sections. The following section 2.2 describes the processes controlling indoor air quality. A review of indoor air quality models is given is the section 2.3. The last section 2.4 presents the INCA-Indoor model on which the rest of the PhD work was based.

2.2 The processes controlling indoor air quality

Indoor air quality is controlled by lots of processes and factors that are in interaction. These processes include emissions, indoor chemistry, infiltration, ventilation, sorption and deposition as represented in figure 2.2. Those processes are also affected by indoor moisture and temperature, as well as by outdoor air characteristics (humidity, temperature, wind and outdoor air pollution). Maintenance and operation on building ventilation systems are crucial determinants on indoor air quality.

Each process controlling indoor air quality is presented in the following subsections.

2.2.1 The emissions

Many of the materials used in buildings, either as structural materials or as furnishings, could be the main source of indoor air pollution. Marchand et al. (2005, 2006) [49, 50] reported the formaldehyde and acetaldehyde concentrations measured in indoor environments of various public spaces (railway station, airport, shopping center, libraries, underground parking garage, etc.) of Strasbourg area (east of France). Measuring results show that the formaldehyde concentrations in houses are as high as 100 μg cm^{-3} and glass-cloth glue in refurbished rooms appears to

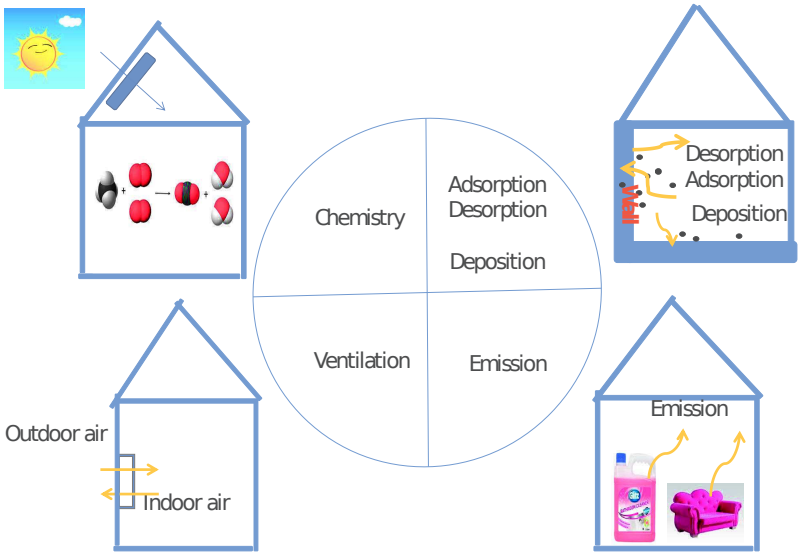

Figure 2.2 – Processes controlling indoor air quality (modified from Schoemaecker et al.,2015) [37]

be a major source of formaldehyde. Statistical tests made on an asthmatic group have highlighted that allergic and asthmatic patients are particularly sensitive to levels of formaldehyde exposure higher than 50 μg cm^{-3}. The volatile organic compounds (VOCs) released from furnishing products and/or household products have been associated with rhinitis, ocular and dermal symptoms, headaches and fatigue [51]. Polymeric materials are used widely in buildings for construction, decorating and furnishing of homes, offices, schools and other non-industrial work places. The slow release of some volatile components from polymeric materials can affect the performance and durability of products and can adversely affect the indoor air quality (IAQ) and the 'well being' of building occupants [52]. Chemical substances (eg. glycol ethers, phosphates, detergents) present in many cleaning products could be responsible for adverse health effects of the skin and the respiratory tract [53, 54].

Emissions are the result of several mass transport and interface processes illustrated in figure 2.3. The emissions can be considered as two main processes including the diffusion of pollution

within the material and the transfer of pollutants from the material/air interface to the room bulk air[55]. Diffusion of pollution within a material can be the result of a concentration, pressure, temperature or density gradient. The transfer of pollutants from the material/air interface to the room bulk air is determined by velocity distributions as well as the flow type (e.g. laminar or turbulent) [55]. A review of emission modeling of volatile and semi-volatile organic compounds from building materials is proposed by Liu et al. 2013 [56].

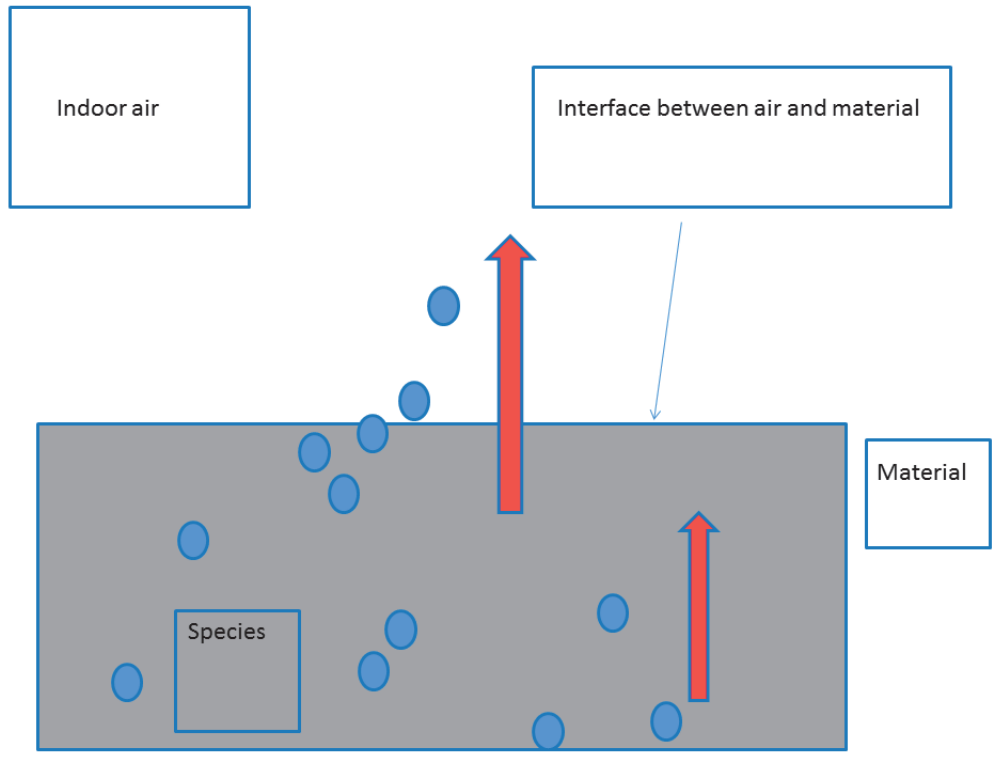

Figure 2.3 – The mechanism of surface emission processes

The emission from materials is usually continuous and may last for many years in a building [57]. The emission rates of materials is affected by temperature, relative humidity and surface air velocity [58]. The emission rates of individual components decrease constantly through time, approaching the equilibrium emission levels [59]. Emissions of Volatile Organic Compounds (VOCs) and carbonyls from carpets of different type (wool, synthetic) measured at four different environmental chambers can reach the maximum concentrations with 2300 microg m^{-3} [60].

VOC emissions range from 5.9 to 38.6 $\mu g\ m^{-3}$ and aldehyde concentrations range from 5.5 to 57.6 $\mu g\ m^{-3}$ measured from a wood based panel [61]. Kelly et al. (1999) [62] compared formaldehyde emissions from new and washed permanent press shirts and found that normal laundering reduced emissions by about 60%.

In addition, emission through human activities is also an important factor influencing indoor air quality. For example, cooking emission is widely recognized as an important source of indoor and outdoor particles and volatile organic compounds with potential deleterious effects on human health [63, 64]. The scented consumer goods emitted more than 100 volatile organic compounds (VOCs), including some that are classified as toxic or hazardous by federal laws [65, 66].

2.2.2 The ventilation and outdoor pollution

The most commons technique for ensuring adequate indoor air quality in buildings is, if the outdoor air quality is good, to dilute the concentration of indoor pollutants with fresh air, either by natural ventilation through open doors and windows, air infiltration through envelope leakage, or mechanical ventilation [67]. Natural ventilation describes air movement through open windows and doors. This can affect the household comfort, and brought new problems like noise or smells. Additionally, natural ventilation can not allow to easily control indoor air pollution and provide an specific thermal comfort level indoors in a hot or cold temperature condition. Therefore, the use of mechanical ventilation is another option. Mechanical ventilation systems are capable to provide controlled ventilation for a given closed space. However, compared to natural ventilation systems, mechanical ventilation systems consume more energy, require more maintenance and may generate higher costs.

Inadequate ventilation possibly leads to health symptoms. A review on relations between ventilation rates and occupant health in 20 studies suggest that ventilation rates below 10 ls^{-1} per person in all building types were associated with statistically significant worsening in one or

more health or perceived air quality outcomes [68]. In addition, ventilation strategies can affect indoor air quality, which is in relation to people's health. Zuraimi et al. (2007) [69] investigated the effect of ventilation strategies of child care centers on indoor air quality and respiratory health of children in Singapore. This study revealed that the risk of current rhinitis among children is significantly higher if they attend mechanically ventilated child care centers (CCCs) compared to natural ventilation CCCs. Air-conditioned CCCs were also associated with higher adjusted prevalence ratio of severe phlegm and dough symptoms and lower respiratory capacity illness.

Ventilation is both a mechanism for removing indoor air pollutants or entering outdoor air pollution, and a potential energy load on the heating or cooling system of a building. In addition to ventilation type, ventilation rate is crucial for IAQ. Fisk (2000) [70] found that, with a doubling of minimum ventilation rates, building energy use would be increased modestly in most buildings. Indeed, there is a tendency to reduce ventilation rates for reducing energy consumption while CO_2 levels can rise to very high levels (about 4000 ppm) in classroom occupancy periods and adversely affect learning of students [71].

2.2.3 The chemical reactions

Indoor pollutants from primary emissions or outdoor lead to secondary pollutant formation due to chemical reactions inside the buildings. Those chemical reactions occur, in the gas-phase, on particles, and on indoor surfaces. The products are formed from such reactions and influence the composition of indoor air.

The gaseous phase Chemistry

Chemical processes in the gaseous phase are linked to reactions between pollutants, photolysis of the pollutants, the presence of oxidants during daytime, reactions at the surfaces, etc. Those oxidants are able to transform rapidly the pollutants present in several oxygenated spe-

cies, which are often more reactive than the initial compounds and so can react with other air contaminants to yield harmful secondary products [72]. The most efficient oxidants indoors are by order of reactivity, the hydroxyl radical (OH), the nitrate radical (NO_3), and the ozone (O_3) [73, 74, 75].

The hydroxyl radical is the key species of the photooxidation cycles in the atmosphere that is able to oxidize rapidly all primary volatile organic compounds (VOCs) including the most stables ones as alcanes, to form secondary oxygenated gas species and aerosols, which can be toxic for most of them [76]. The primary outdoor source of OH is photochemistry. Since sun radiation conditions indoors are much smaller than outdoors during the daytime, the OH production from photolysis reactions is limited [45]. The major indoor sources of OH are the reactions of alkenes with O_3 [77, 78, 46, 79] and the photolysis of HONO [48], that is assumed to be mainly formed by the reaction of NO_2 on the surfaces. The OH oxidation is an important pathway for VOC conversion in the indoor environment [42] (as for the outdoor one), which produce secondary species like formaldehyde and acetaldehyde. The pathway of formation and destruction of OH indoors is shown in figure 2.4.

Ozone/alkene reactions can produce quantities of hydroxyl radicals indoors [77, 78] and also generate semi-volatile products that can contribute to the growth of particles [80, 81]. The products of indoor chemistry, initiated by ozone, can be more irritating, odorous, and/or damaging to materials than their precursors [72, 32].

Nitrate (NO_3) may be of particular importance in some indoor environments. NO_3 is formed by reaction of ozone with nitrogen dioxide (NO_2), which two species may be simultaneously present at high concentrations in some indoor situations [77]. Outdoor, NO_3 is photolyzed fastly during the daytime, so it exists only significant concentrations during the night. Indoors, the normal level of solar irradiation in the daytime would not be enough to cause rapid nitrate photolysis. Hence, during the daytime NO_3 concentrations indoors might sometimes exceed commonly occurring outdoor nitrate levels [82]. Terpene concentrations indoors are commonly

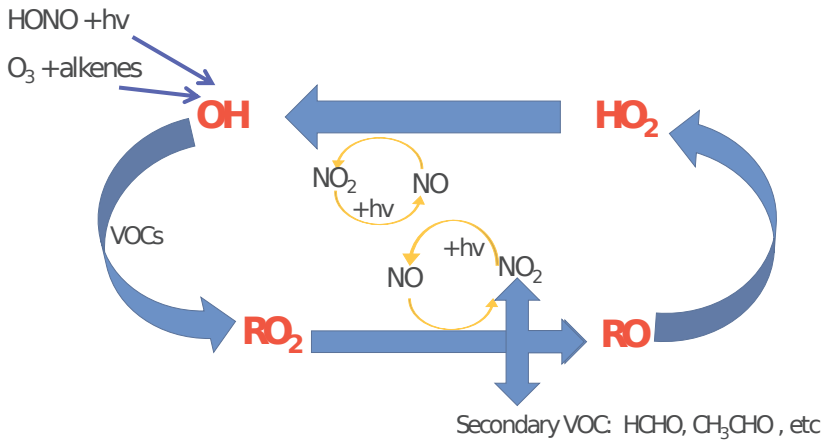

Figure 2.4 – The pathway of formation and destruction for OH indoors (modified from Schoemaecker et al.,2015) [37]

elevated because of the use of solvents and scenting agents in which there are compounds such as d-limonene and alpha-pinene [72]. Reactions of NO_3 with terpenes can produce secondary organic aerosol [83], which are a major component of fine particle pollution, PM.2.5, and these PM2.5 are known to cause lung and heart problems and other health effects.

The heterogeneous Chemistry

Heterogeneous reactions are chemical reactions in which the reactants are components of two or more phases (solid and gas, solid and liquid, liquid and gas, two immiscible liquids) or in which one or more reactants undergo chemical change at an interface (e.g., on the surface of a solid catalyst). Since surface to volume ratio is important indoors, surface reactions play a role in the indoor chemistry [77]. Hugo et al. (2006) [84] investigated the reaction of ozone with nicotine adsorbed on Teflon and cotton surfaces in an environmental chamber and provide the evidence for heterogeneous chemistry. The results of this study indicate that the surface oxidation was competitive with the desorption and the oxidative losses could significantly reduce long-term re-emissions of nicotine from indoor surfaces. Spicer et al. (1993) [85] have demonstrated the existence of indoor nitrous acid (HONO) from the reaction of NO_2 with surfaces inside a test house. Mendez et al. (2017) proposed a model for this heterogeneous reaction in the INCA-indoor model [43]. In addition, the formation of gas-phase nitrous acid (HONO) through the heterogeneous reaction of nitrogen dioxide (NO_2) with sorbed water vapor is impacted by surface type and relative humidity [86]. Finlayson-Pitts et al. (2003) suggested [87] an integrated mechanism for the heterogeneous reaction of NO_2 with water on the surface of laboratory systems. NO_2/surface reactions can also be a source of NO [88]. The heterogeneous hydrolysis of N_2O_5 on moist indoor surfaces is much faster than its homogeneous counterpart [89]. α-terpineol with O_3 reactions on glass and vinyl surfaces generate the largest fraction of oxygenated products even in equal mixtures with other terpene alcohols [90].

2.2.4 The sorption process

The sorption process of a species on a solid material can be considered as several sub-processes consisting of adsorption, absorption, and desorption [91]. The first two ones are described by the steps as followed :

1. Diffusion from bulk air through the boundary layer near the surface
2. Surface adsorption
3. Diffusion into the material
4. Absorption in the interior of the material

Desorption is the opposite process of adsorption, seeing as a re-emissions of adsorbed species (that has to be distinguished from emissions).

Through sorption processes, indoor materials can act as buffers for VOCs, reducing peak concentrations but prolonging the presence of compounds in the air. Many studies were carried out to investigate the sorption of a variety of pollutants to allow a better selection of indoor materials. Aruna et al. (2008) [92] reported the sorption of the malodorant 2-methyl-2-propanethiol, commonly known as tertiary butyl mercaptan (TBM), to two carpets, two wallpapers, a soil, and granular activated carbon (GAC). Results indicated that all solids adsorbed environmentally significant quantities of TBM, with the likelihood of producing concentrations above the odor threshold during subsequent remediation using mechanical ventilation. Won et al. (2001a) [93] reported adsorption and desorption rate coefficients for eight VOCs (isopropanol, MTBE, cyclohexane, toluene, ethylbenzene, tetrachloroethene, 1,2-dichlorobenzene, and 1,2,4-trichlorobenzene) interacting with gypsum wallboard, carpet and cushion, acoustic ceiling tile, wood flooring, vinyl flooring, and fiberglass. Results indicate that carpet was identified as the most significant sorptive sink for non-polar VOCs. Virgin gypsum board was observed to be a significant sink for highly polar VOCs. Jorgensen et al. (1999) [94] presented the influence of combinations of compounds and materials compared to sorption of single compounds on

single materials. The results indicate that the presence of two chemical compounds at the same time gives correspondingly higher sorption compared to experiments with one compound at a time. Furthermore, the combination of two materials at the same time leads to higher sorption than one single material.

The process of sorption of air contaminants and the subsequent desorption may have important consequences for the indoor air quality [95, 96]. Meininghaus [97] presented quantitative experimental results on diffusion and sorption of VOCs in indoor materials and discussed the impact of these processes on indoor air quality. The results indicate that diffusion through the material can contribute to reducing the room air concentration, especially at low ventilation rates. Won et al. (2000) [98] suggested that carpet systems can serve as absorptive sinks with the potential for reductions in peak VOC concentrations and subsequent re-emission of eight VOCs over prolonged periods of time.

The re-emissions (desorption) of adsorbed organic vapors can contribute to elevated concentrations of organics in indoor environments [99, 100]. Occasional release of consumer chemicals leads to momentarily high concentrations in the room air, which in turn results in a strong sorption on material surfaces. Piade et al. (1999) [101] investigated the sorption of nicotine and ethenylpyridine onto different surfaces (glass, cotton, and nylon fabrics) and suggested that as much as 1 mg of nicotine can be adsorbed and re-emitted from 1 m^2 of cotton cloth over a few hours.

2.2.5 The deposition

The surface to volume ratio is generally larger indoors than outdoors and deposition of gases to surfaces is more important in determining gas concentrations indoors than outdoors [32]. The pollutants may be partly removed by deposition in cracks and wall cavities during infiltration [102]. During the particle concentration decay period, when the indoor concentrations are very

high, the losses due to deposition are larger compared to gains due to particle infiltration [103]. Indoor deposition could reduce the effect of toxic gas clouds in ordinary buildings [104].

The mechanism limiting the deposition velocities have been investigated in many studies. Nazaroff et al. (1989) [105] examined the deposition velocities of particles and gases onto indoor surfaces for the case of rapide surface uptake with a removal rate limited entirely by mass transport. Canoruiz et al. [106] investigated the rate of deposition of reactive gaseous pollutants onto indoor surfaces is examined, taking into account mass transport processes and the kinetics of gas-surface interactions.

The deposition velocities vary from material surfaces to others and depend on the air humidity and the temperature. Grøntoft et al. (2004) [107, 104] measured surface deposition velocities of O_3, NO_2 and SO_2 for 24 material classes and at five values of relative air humidity. The results indicate a ranking of deposition velocities with higher values for painted than oiled and than lacquered wood and with particle and fiber boards and plywood than whole wood board.

It is common to simulate a loss of pollutants as a deposition when the loss processes are not very well known and could be due to reactions on the surfaces that cannot be simulated.

2.3 The indoor air quality models

Modeling is the art of developing a set of mathematical equations that allow a user to reproduce a cause-effect relation. Statistical models are based on learning experiments to link inputs to outputs without following all physical and chemical processes. Determinist models aim at representing as possible as the physical and chemical phenomena and then solving the equations to simulate the behavior of real-life systems. This process of using the models to analyze the behavior of the real-life system is called simulation. Simulations are expected to be compared to measured values to show that the processes are well understood, and allows then demonstration of various scenarios in a short time to detail the analysis of the processes or take decisions.

The development of indoor air quality models was going from very simple to complex, and from aiming to one single process to combined processes. The comprehensive indoor air models have been developed considering physical (e.g. emission, ventilation) and chemical processes indoor to predict indoor pollutant concentrations. For example, emission models have been developed to predict the pollutant concentrations emitted from diverse materials. Emission rates are supposed to be constants and the pollutant diffusion in sources is not considered in the emission models. For the later developed emission models, the transfer of pollutants from the interior of sources to the source/air interface is considered and emission rates are described as a sum of several decay rates.

Indoor air quality (IAQ) models are used to predict the pollutant concentrations both spatially and as a function of time within the building environment. They are divided into 3 categories [108] : statistical, mass balance and computational fluid dynamics (CFD) models, as summarized in the table 1.

The statistical models are based on empirical functions that are defined using measuring. Several of them were used to estimate the distribution of indoor pollutant exposures and potential dos distributions for whole populations or sensitive sub-populations using Monte Carlo techniques to combine the databases.

The mass balance models are based on the principle of mass conservation. They can predict well indoor pollutant concentrations under a wide range of conditions and allow rapid analysis of IAQ control options. They were designed to estimate the impacts of sources, sinks and IAQ control options on indoor pollutant concentrations.

The last category, the computational fluid dynamics (CFD) models, are generally used to predict air velocity and pollutant concentrations at several individual points in a room or several rooms in buildings. The transport of pollution from one point to another is computed. This calculation is usually done to the detriment of the chemistry computation. It also usually allows better prediction of personal exposures.

Table 2.1 – Indoor air Model Categories

Type of model	*General purpose*	*Example*
Statistical	Estimating population exposure	CPIEM, Koontz(1998) [109]
Masss balance	Estimating impact of sources and sinks	MIAQ, Nazaroff (1989) [110]
Computational fluid dynamics (CFD)	Estimating pollutant distributins and transport indoors	Brohus (1996) [111]

For the purpose of better understanding the impacts of sources and sinks of indoor pollutants including the chemistry, mass balance models are preferentially used and we choose to detail them in the following section.

2.3.1 The mass balance models monozones or multizones

The mass balance models can be monozones, simulating then only one room, or multizones. simulating exchanges between rooms. The mass balance for a room is given :

$$V\frac{d[C_i]}{dt} = C_{i,in}Q_{i,in} - C_{i,out}Q_{i,out} + R_i - Sink_i \tag{2.1}$$

where V is the volume of the room ;

$[C_i]$ is the bulk room air concentration of species i ;

$C_{i,in}$ is the concentration entering the room ;

$Q_{i,in}$ is the airflow into the room from all locations ;

$C_{i,out}$ is the concentration leaving the room ;

$Q_{i,out}$ is the airflow leaving the room to all locations ;

R_i is the source term ;

$Sink_i$ is the sink and pollutant removal term ;

the subscript i refers to room i and N is the number of rooms.

Different mass balance models were developed to investigate indoor air issues and are listed in Table 2. Many of these models are continually updated to improve their usefulness.

The Mathematical model of Indoor Air Quality (MIAQ) [45] is developed for predicting the concentrations of the main chemically reactive compounds in indoor air. The model accounts for the effects of ventilation, filtration, heterogeneous removal, direct emission, and photolytic and thermal chemical reactions. However, this model does not accommodate processes such as the adsorption and desorption. Additionally, chemical mechanism used by this model is simple considering a little bit more than 50 simultaneous chemical reactions.

A Microsoft Windows-based indoor air quality (IAQ) simulation software package, named Simulation Tool Kit for Indoor Air Quality and Inhalation Exposure (STKi), is designed mainly for advanced users to simulate a wide range of indoor air pollution scenarios [112]. This model can estimate the adequate ventilation rate when some air quality criteria are given. The STKi consists of a general-purpose simulation program and a series of stand-alone, special-purpose programs. The STKi programs assume that a building is divided into air zones and that, within each zone, the air is well mixed. The heating, ventilation, and air-conditioning system is considered as a special air zone with specific features (e.g., air filters are allowed in the paths of return, makeup, and supply air flows) that a regular air zone does not have. However, the STKi only considers gas-phase chemical reactions, the interactions of pollutants with certain surfaces are not considered.

The Indoor Chemistry and Exposure Model (ICEM) [79] for example, allows the simulations of transport processes between outdoor and indoor environments, indoor emissions, indoor chemical reactions and deposition. However, this model only considers homogeneous chemistry and irreversible heterogeneous deposition, other heterogeneous reactions and surface processes like adsorption and desorption are not taken in account in this model.

A probabilistic model (INDAIR) has been developed to predict air pollutant concentrations in home microenvironments in the UK [113]. In the INDAIR model, there are three microenvi-

ronments (MEs) for the residential environment : kitchen, lounge and bedroom. The INDAIR model considers the ventilation, emission, deposition and sorption taken place indoors. According to the distributions of the input parameters and for a large number of iterations (1000, to stabilise the results), the INDAIR model randomly generates values from these distributions for use in the differential equation. There are no explicit chemical mechanism included in this model.

The indoor air detailed chemical model (INDCM) [46, 47] was developed to investigate indoor air chemistry based on a very detailed chemical mechanism (the Master Chemical Mechanism) [114]. But this chemical box model does not consider detailed characterizations of the buildings like emission rates for specific materials and the sorption process.

Another one is the modeling package called INDAIR-CHEM [115], which uses an existing indoor air exposure model [113] and a detailed indoor air chemistry model [46]. It provides an approach to assessing exposure indoors to relevant pollutants indoors. INDAIR-CHEM links emissions of the major pollutants indoors (NOx, ozone, primary VOCs and ultra-fine particles) to the concentrations of key secondary indoor pollutants with suspected adverse health effects. Because of the application of INDCM model as parent model, this model does not solve the problems mentioned for INDCM model, like detailed characterizations of the buildings like the emission rates for specific materials used and sorption processes.

The last one detailed here is the time-averaged model which was developed to explore magnitudes and source strengths of O_3, OH, and NO_3 in residential spaces, as well as the magnitudes and determinants of typical VOC conversion rates by those oxidants [116, 73]. Model inputs were represented as distributions within a Monte Carlo analysis, allowing the statistical influence of inputs on results to be quantified. This model is admittedly a simplified representation of the true kinetics and is not explicit. Only 20 reactions are considered in the model and sorption of VOCs to indoor surfaces is not included.

A simulation tool called MUSICA [117] that enables the dynamic prediction of the trans-

port of gaseous pollutants in the Triomphant class submarines was developed. Four elementary phenomena were identified : airflows between rooms, internal emissions, homogeneous chemistry and heterogeneous chemistry. Care of this model was taken to simulate accurately the homogeneous and heterogeneous indoor chemistry.

Mendez et al. (2015) [41] recently developed INCA-Indoor model that has the advantage to include all the processes existing in confined environments such as : ventilation, emission, deposition, gas phase chemical processes. INCA-Indoor model can be used to simulate the concentrations of indoor chemical species. Furthermore, this model could provide the information of the contributions of each processes to the pollutant concentrations. It is used in this phd report to analyze their relative contributions.

Table 2.2 – Summary of the main mass balanced indoor air models and references

Processes	MIAQ Nazaroff et al. (1986, 1989)[45, 110]	STKi Guo (2000) [112]	ICEM Sarwar et al. (2002, 2003) [79, 118]	INDAIR Dimitroulopoulou et al. (2006) [113]
Chemistry	31 species, 56 reactions	[112]	SAPRC-99	Probabilistic calculation
Number of zones	1-4	1-10	1	3
Exchange with outdoor	15 species	[112]	[79]	NO_2, CO, $PM_2.5$, PM_10
Emission	Experimental values	VOC from water	[79]	[113]
Deposition	Experimental values	Particulate matter deposition	Sarwar, 2002 [79]	[113]
Heterogeneous chemistry	$NO_2 \longrightarrow$ HONO	no	$NO_2 \longrightarrow$ HONO	no
Aerosol	no	no	no	Deposition $PM_2.5$–PM_10

Processes	INDCM Carslaw et al. (2007, 2012) [46, 47]	INDAIR-CHEM Terry et al. (2014) [115]	Time-averaged model Waring et al. (2014,2015) [116, 73]	MUSICA Courtey et al. (2007) [117]	INCA-Indoor Maxence et al (2015, 2017a,b) [41, 43, 42]
Chemistry	MCM	47 reactions + chemistry limonene from MCM(v3.2)	66 species 20 reactions	SAPRC-99, RADM2, RACM, CB04	SAPRC-07,640 COV, about 1500 reactions
Number of zones	1	1	1	1-1000	1
Exchange with outdoor	[79] + species calculated by MCM	[79]	[73]	no	Experimental values
Emission	[79], Emission d-limonene	Emission d-limonene	Emissions of NO, NO_2 and HONO	[117]	Experimental values
Deposition	Sarwar, 2002 [79]	[79]	Deposition of NO_2 and O_3	Nazaroff, 1986 [45, 119]	Experimental values or [79]
Heterogeneous chemistry	[119]	no	no	[120]	[120]
Aerosol	Aerosol of d-limonene	Aerosol of d-limonene	Secondary organic aerosol	no	HO + Coagulation

Verification and validation of the mass balance models

While it was demonstrated that models are useful tools which could provide useful information to assess indoor pollution, simulation models are approximate imitations of real-world systems and they never imitate exactly the real-world system. Due to that, a model should be checked and validated to the degree needed for the models intended purpose or application [121]. The model verification is often defined to ensure that the computer program of the computerized model and its implementation are consistent and correct. Model validation is usually defined to mean substantiation that a computerized model within its domain of applicability possesses a satisfactory range of accuracy consistent with the intended application of the model [122]. Two techniques mostly often used for checking and validating the model are (1) comparison to other models and (2) comparison to experimental data.

Comparison to other models : various results (e.g., outputs) of the simulation model being validated are compared to results of other (valid) models. For example, (1) simple cases of a simulation model are compared to the results of analytic models, and (2) the simulation model is compared to other simulation models that have been validated.

Comparison to experimental data : in given environments, realistic scenarios can be used to make predictions about IAQ, as well as instantaneous changes in scenarios to examine the effects on the results. In addition, room (building) characteristics can be introduced to the system and information about IAQ can be obtained with the possible scenarios. The simulation results for realistic scenarios could be used to compare with the corresponding experimental data.

Quantitative factors and criteria are indispensable for assessing the general agreement between the model predictions and the experimental data. The American Society for Testing and Materials (ASTM) (1991) recommended to use quantitative factors to assess the general agreement between the model predictions and the measuring [123]. The values for the various quantitative criteria recommended by the ASTM are given in the table 2.3. Some quantitative factors are also presented here.

Table 2.3 – Quantitative Criteria for Indoor Air Quality Models

Criteria	Recommended value
Correlation coefficient	>0.9
Normalized mean square error (NMSE)	<0.25
Regression intercept	<25% of average value of the measurements
Regression slope	0.75 to 1.25
Fractional bias (FB)	Absolute value <0.25

A correlation coefficient is a number that quantifies a type of correlation and dependence, meaning statistical relationships between two or more values in fundamental statistics. The correlation coefficient between a series of n measurements of observed concentration C_o and predicted concentration C_p for i = 1, 2, ..., n, is given by

$$\frac{\sum_1^n[(C_o-\overline{C_o})\cdot(C_p-\overline{C_p})]}{\sqrt{[\sum_1^n(C_o-\overline{C_o})^2]\cdot[\sum_1^n(C_p-\overline{C_p})^2]}} \tag{2.2}$$

where $\overline{C_o}$ and $\overline{C_p}$ are the average values of the observed and predicted concentrations, respectively ; The correlation coefficient ranges from -1 to 1, with 1 indicating a strong direct relationship, 0 indicating no relationship, and -1 indicating a strong inverse relationship. It allows to estimate if the model is able to represent correctly the temporal or spatial variability.

The normalized mean square error (NMSE) is an estimator of the overall deviations between predicted and measured values. It is defined as :

$$NMSE = \frac{\overline{(C_p-C_o)^2}}{(\overline{C_o}\cdot\overline{C_p})} \tag{2.3}$$

When the NMSE has a value of 0, it means that there is a perfect agreement for all pairs of C_p and C_o and when the value tends toward higher value as C_p and C_o differ. For example, NMSE is near 0.5 for differences of about 100 percent, and NMSE is near 8 for difference of one order of magnitude.

The least squares best fit regression line between C_p and C_o provides useful information

on how well the model fits the data. The ideal line has a slope of 1, an intercept of 0, and a regression r^2 of 1 ; The slope b of the line is given by

$$b = \frac{\sum_1^n (C_o - \overline{C_o}) \cdot (C_p - \overline{C_p})}{\sum_1^n [(C_o - \overline{C_o})^2]} \tag{2.4}$$

and the intercept a is given by

$$a = \overline{C_p} - b \cdot \overline{C_o} \tag{2.5}$$

The ASTM recommends that the suitability of an IAQ model be determined by an evaluation of all the quantitative factors. A model may meet one or more criteria and still be inadequate, or a model may fail one or more criteria and still be adequate for the task at hand. Zhao et al. (1998) [124] evaluate the COMIS model for multizone air infiltration and pollutant transport. They compared simulation results with measuring results using linear regression analysis. The correlation coefficient between the measured and calculated air change rates was 0.72, and that for pollutant concentration was 0.94. Thunis et al. (2012) [125] recently present the DELTA tool with statistical analysis (i.e.,mean bias, root mean square error, correlation coefficient, standard deviation) to perform diagnostics of outdoor air quality and meteorological model performances [126]. This conceptual tool was not tested in indoor context yet and should be investigated in order to analyze the comparisons as compared to the observation uncertainties. Traditional approaches are used in the present study. The accuracy of the predicted concentrations depends primarily on the adequacy of the source and sink model used in the IAQ model and the type of data available for model input.

2.3.2 Limitations of the mass balance models

The mass balance models are designed to predict average in-room pollutant concentrations and give in this way a first guess of the indoor air quality. But there are obviously limited to simu-

late the impact of the heterogeneity of light distribution, spatial emission variations. Chapter 4 discussed such kind of limitations.

2.4 The INCA-Indoor model

The INCA-Indoor model was developed during the intensive experimental MERMAID campaign [127] (performed during the PRIMEQUAL ADEME MERMAID project, French national project coordinated by University of Lille). The campaign was designed to investigate indoor air quality in low energy buildings. The INCA-Indoor model aims at simulating the concentrations of pollutants considering indoor air specific processes such as emission, infiltration, ventilation, surface interactions (sorption, deposition), gaseous chemistry, heterogeneous chemistry, aerosol formation, etc (see figure 2.5). It is a box time-resolved numerical model developed in order to understand the physical and chemical processes leading to indoor air pollution and identifying the main contributions to pollutant concentrations. The model was built from the box model version of the INteraction with Chemistry and Aerosols (INCA) model described by Hauglustaine et al. (2004) [128] and Folberth et al. (2006) [129]. The present configuration of the model assumes that in a room, the air is completely mixed.

The INCA–Indoor model is based on the Navier Stockes equation in which several terms representing the different processes occurring indoor have been added. The generation and removal of a contaminant in an indoor environment can be mathematically described in the following equation :

$$\begin{aligned} V\frac{d[C_i]}{dt} &= [L[C_i]-P]+[Emission(C_i)]+[Exchange(C_i)] \\ &\quad +[Deposition(C_i)]+[Sorption(C_i)]+[Hetero(C_i)] \end{aligned} \tag{2.6}$$

where V is the volume of a room ;

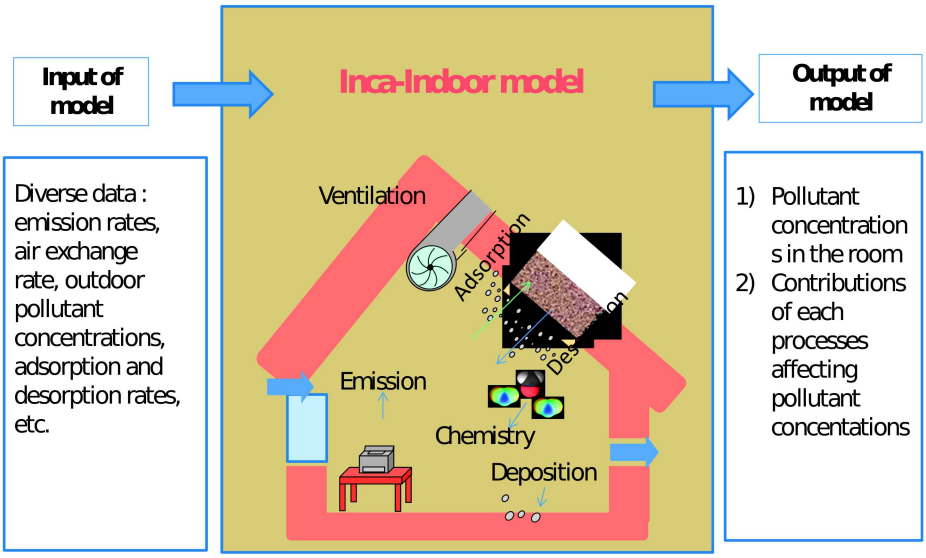

Figure 2.5 – Schematic representation of the INCA-Indoor model

$[C_i]$ is the bulk room air concentration of the specie i ;

$L[C_i]$ is the consumption of the specie i by the chemistry reactions ;

P is the production of the specie i by the chemistry reactions ;

Emission(C_i) is the emission of the species i ;

Exchange(C_i) is the exchange of the species i with outddor air ;

Sorption(C_i) is the sorption of the species i taken place en surfaces.

Hetero(C_i) is the heterogeneous chemistry.

A single room is treated as a single zone or compartment in which no spatial variation of the contaminant concentration occurs (well-mixed assumption). The modeling of each process is detailed below.

2.4.1 Configuration of INCA-Indoor model

The gas phase chemistry

Since the aim of the model is to provide the concentrations of gaseous oxidants but also of some VOCs, reduced mechanisms, in which VOCs are lumped into model species by structure reactivity association, cannot be used. For this reason the chemical mechanism of INCA (Haugustaine et al., 2004 [128]) was updated by the detailed version of SAPRC-07 mechanism [130] that describes the oxidation processes of 640 VOCs through 1400 reactions. In order to limit the size of the mechanism, some simplifications have been done. Secondary species that can be formed are detailed up to 3-carbon chain length. Stable products with carbon chains greater than 3 carbons are lumped together. To reduce the number of chemical reactions, the degradation of the RO_2 species by NO to form RO species is not detailed. Generally, the oxidation of a VOC leads to the formation of RO_2 and HO_2 (that is formed by reaction of RO radicals with O_2).

The emissions

The emission of species i is calculated for each material considering its surface S_M (cm^2), an emission factor of the species i, $E_{i,S}$ (in molecules cm^{-2} s^{-1}) which is considered to be constant during the simulation period, and the total volume of the room V (cm^3).

$$\frac{d[C_i]}{dt} = \frac{E_{i,S} S_M}{V} \tag{2.7}$$

where $[C_i]$ is the indoor concentration of species i in phase gazeuse.

The outdoor air exchange

The outdoor air exchange is treated as a function of the outdoor concentration, $[C]_{i,out}$ (molecule cm^3), the ventilation flow, Q(cm^3 s^{-1}), the filtration factor f (set to 1 representing that in natu-

rally ventilated buildings, the building fabric presents no barrier to particulate or gas pollutants [46] simulations), and the volume of the room, V (cm^3) :

$$\frac{d[C_i]}{dt} = \frac{Q}{V} f([C_{i,out}] - [C_i]) \tag{2.8}$$

The deposition process

The deposition mechanism suggested by Mendez et al. (2015) is adopted here [41]. The loss rate due to deposition of species i on the surfaces is given by the product of its deposition velocity, $V_{D,i,M}$ (cm s^{-1}) and the surface to volume ratio S/V (cm^{-1}, S is the total surface area of the room) :

$$\frac{d[C_i]}{dt} = -V_{D,i,M} \frac{S}{V} [C_i] \tag{2.9}$$

The deposition velocity is considered as a process integrating the transport from the indoor air to the boundary layer and the loss rate of the species on the surface and is consistent with the Nazaroff and Cass (1986) [45] approach, attributing transport-limited values of deposition velocities to the radical species (0.07 cm s^{-1}). In the absence of available experimental data, the Sarwar et al. (2002) [79] values of deposition velocities were assigned.

The sorption process

The sorption process can be important for VOCs and has to be taken into account in the indoor air quality simulation [41]. VOCs are actually adsorbed in a reversible way on building surfaces. The so called sorption dynamics can either be modeled by a macroscopic or an elemental model (Blondeau et al., 2008 [131]). The most widely used macroscopic reversible sink model is the so-called one-sink model based on the Langmuir isotherm and proposed by Tichenor et al.

(1991) [132]. It considers that at any time, the mass flux at the material surface is the difference between the adsorption and the desorption rates of the material. The sink model is

$$R_{sink} = k_a[C_i]S_M - k_d[C_{i,M}]S_M \tag{2.10}$$

where R_{sink} is the net rate at which mass enters or leaves the sink;

k_a is the adsorption constant;

$[C_i]$ is the bulk room air concentration;

S_M is the area of the sink;

k_d is the desorption constant;

$[C_{i,M}]$ is the the pollutant mass per unit area collected in the sink ($k_a[C_i]S_M$ is the adsorption rate and $k_d[C_{i,M}]S_M$ is the desorption rate)

Tichenor et al. (1991) reported the Langmuir sink model predicted the sorption of VOCs by indoor materials reasonably well. However, the Langmuir model underestimated the re-emissions phase.

Elemental models account for the concentration gradient in materials. They consist of a series of coupled diffusion equations describing the VOCs transport in the boundary layer, and in each material layer constituting the walls or furnishings [131]. For example, Axley (1991, 1995) [133, 134] suggests a sink model that accounts for mass transport to the sink/air interface, mass transport from the interface into the sink, and other processes. The approaches suggested by Axley are promising, because re-emissions from sinks are an example of source-phase-limited sources. These physically-based models have the advantage that they are more accurate than the one-sink model, and they can serve as source or sink models [135]. On the other hand, they call for several input parameters that may be difficult to determine (adsorption isotherms, effective diffusion coefficients, initial concentration in the materials, etc.), and require computational efforts to solve the diffusion equations.

As a compromise between macroscopic and elemental models, Mendez et al. (2015) [41]

suggests an intermediate model to represent exchanges between the room surfaces and the indoor air (VOCs only). The diffusion of the gas phase pollutant in the material is not considered. In the model, the concentration of species i in the boundary layer ($[C_i^*]$) and adsorbed at the surface of M ($[C_{i,M}]$) ($[C_i^*]$ and $[C_{i,M}]$ expressed in molecules cm^{-2}) have to be considered. The sorption model proposed by Mendez et al. (2015) can be summarized by the following equations :

$$V\frac{d[C_i]}{dt} = h_{M,i}S_M([C_i] - [C_i^*]) \tag{2.11}$$

$$V^*\frac{d[C_i^*]}{dt} = h_{M,i}S_M([C_i] - [C_i^*]) - k_aS_M[C_i^*] + k_dS_M[C_{i,M}] \tag{2.12}$$

$$\frac{d[C_{i,M}]}{dt} = k_a[C_i^*] - k_d[C_{i,M}] \tag{2.13}$$

The mass transfer velocity ($h_{M,i}$) is calculated as a function of the Sherwood numbers (Sh_i), D_i is the diffusivity of a pollutant i in the air ($m^2\ s^{-1}$), and a mixing length :

$$h_{M,i} = \frac{Sh_iD_i}{l_M} \tag{2.14}$$

The Sherwood number Sh is given by :

$$Sh_i = 0.664Re^{1/2}Sc_i^{1/3} \qquad \text{if } Re < 5*10^5 \tag{2.15}$$

$$Sh_i = 0.037Re^{4/5}Sc_i^{1/3} \qquad \text{if } Re > 5*10^5 \tag{2.16}$$

with Re represents the Reynolds numbers and Sc_X the Schmidt number :

$$Re = \frac{U l_M}{\nu} \tag{2.17}$$

$$Sc_i = \frac{\nu}{D_i} \tag{2.18}$$

where U is the air velocity (m s^{-1}), lm is the characteristic length of the material, ν is kinematic viscosity of the air ($\nu = 1.57 \times 10^{-5} m^2 s^{-1}$). Since V* is very small compared to the total volume of the room, equations (7)–(9) can be simplified as follows :

$$V\frac{d[C_i]}{dt} = S(\frac{-k_a h_{M,i}}{h_{M,i}+k_a}[C_i] + \frac{h_{M,i}k_d}{h_{M,i}+k_a}[C_{i,M}]) \tag{2.19}$$

$$\frac{d[C_{i,M}]}{dt} = \frac{k_a h_{M,i}}{h_{M,i}+k_a}[C_i] + \frac{h_{M,i}k_d}{h_{M,i}+k_a}[C_{i,M}] \tag{2.20}$$

Finally, when comparing equation (5) with 14 and 6 with 15, one can note that this model is equivalent to Tichenor et al.'s one-sink model but with k_a^* and k_d^* defined as :

$$k_a^* = \frac{k_a h_{M,i}}{h_{M,i}+k_a} \tag{2.21}$$

$$k_d^* = \frac{k_d h_{M,i}}{h_{M,i}+k_a} \tag{2.22}$$

The heterogeneous chemistry

For the INCA-Indoor model, the effect of heterogeneous reactions on the concentration of a species i is considered through classical uptake theory where the uptake coefficient represents the reaction probability of a chemical species to stick on a surface and depends on the reactive

uptake coefficient,γ, and ω the thermal speed of the species (cm s^{-1}). S is the total surface areas of the room, and V is the total volume of the room.

$$\frac{d[C_i]}{dt} = \frac{\gamma\omega S}{4V}[C_i] \tag{2.23}$$

2.4.2 The INCA-Indoor model validation

Verification and experimental validation of the model to check the accuracy and establish the model's limitations are extremely important. In order to verify and validate the INCA-Indoor model, Mendez et al. (2015, 2017) compared the predicted results of INCA-Indoor model with the experimental results [43] and with other models [41]. The comparison results are presented in the following sections.

Comparison to other Models

In Mendez et al. (2015) [41] work, the INCA-Indoor model has been firstly evaluated with the test cases based on Carslaw (2007) [46]. Carslaw (2007) [46] defined several scenarios to assess the sensitivity of the modeling system to various parameters such as the ozone deposition rate, the air exchange rate (AER), the limonene emission rate and the S/V ratio. These scenarios conditions were reproduced with INCA-Indoor in order to verify the pollutant concentrations evolved in Carslaw (2007). However, there are some differences with Carslaws's work including the chemical schemes used, the photolysis rates that are adapted to indoor environments and the outdoor concentrations. The INCA-Indoor model implements a semi-explicit chemical mechanism SAPRC-07, and the explicit mechanism MCM v3.1 is used in Carslaw's model. The photolysis rates were calculated with the tropospheric ultraviolet and visible radiation (TUV) model [136] with the attenuation factors measured by Nazaroff et al. (1986) [45] also used by Carslaw (2007). The photon flux calculated by the MCM model may be different from our data coming from TUV model. In Carslaw's work, outdoor and indoor chemistry are compu-

ted simultaneously with the same reference model. Mendez et al. (2015) [41] adopted outdoor concentrations of HNO_3, H_2O_2, NH_3 (all of them at 2.0 ppb) and 49 primary VOC taken from Sarwar et al. (2002) [79] and indoor source for 46 species.

Predicted variations of concentrations of OH, HO_2, O_3, NO, NO_2, PANs, d-limonene, HCHO obtained with the scenarios performed with INCA-Indoor model showed good agreement with the ones obtained by Carslaw (2007)[46]. The dynamic of main pollutants can be simulated with mean absolute variation differences ranging from 1.6% for ozone dynamic to 19.7% for PAN variations. Direct comparisons of concentrations were not possible because no information was available on outdoor concentrations and interaction between outdoor and indoor could not be simulated by INCA-Indoor as well as by INDCM.

Comparison with experimental results

Alvarez et al. (2013) [48] reported that the photolysis of HONO in indoor environnments was the major oxidation process to produce OH through the measuring during the campaign SURFin [48]. In order to interpret the experimental results and to investigate the mechanism of HONO, INCA-Indoor has been set-up following the configuration of the classroom studied. The concentrations of ozone, NOx, and the eight VOCs, the temperature, the relative humidity and air exchange rate (AER) have been constrained to their measured values in the model.

The HONO concentrations calculated by INCA-Indoor model have been compared with the experimental temporal profiles of HONO obtained during the SURFin [48] campaign. The results shows that even if the HONO formation mechanism proposed by Mendez et al. (2017) [43] is not yet fully supported by laboratory experiments, it seems to provide a good parameterization for fitting the experimental data. The comparisons with this measuring campaign have been helpful to adjust the INCA-Indoor model settings and to validate the model, even partially at least.

2.5 Conclusion

The indoor environment is complex and the air quality of this environment is controlled by diverse physical and chemical processes. To improve indoor air quality, it is important to identify the main processes affecting the pollutant concentrations. Indoor air quality models provides a way to study indoor air quality, which links sources and sinks of pollutants. IAQ models could be used to predict the evolution of pollutant concentrations over time and allow to quantify the contributions of the different processes taking place indoors to balance the pollutant concentrations.

Among numerous IAQ model, the mass balance models are preferred for such study as our, aiming to estimate the pollutant concentrations and effect of different factors on pollutant concentrations. The INCA-Indoor model is based on the principle of the mass balance and has moreover the advantage to include the different processes existing in confined environments such as the ventilation, the emissions, the deposition, all the major gas phase chemical processes, to simulate as well as possible the concentrations of indoor chemical species. The results of the study of Mendez et al ., (2015, 2017a, 2017b) [41, 42, 43] have shown that the INCA-Indoor model is capable to simulate the pollutant concentrations and identify the major processes affecting indoor concentrations of selected species. Furthermore, this model can be used to investigate the generation and consumption mechanism of chemical species.

The verification and the experimental validation of this model to check the accuracy and also establish the model's limitations are extremely important. New comparisons and validation are presented in next chapter 3 : the INCA-Indoor model will be used to simulate the selected pollutant concentrations in a representative classroom in France. This model has been validated with experimental data collected during MERMAID campaign [37, 38] and the modeled results have been compared with measured results. The objective of our work was to study indoor air quality in a realistic environment with the INCA-Indoor model.

CHAPTER 3

MEASUREMENT AND SIMULATION OF INDOOR AIR QUALITY IN A REALISTIC CLASSROOM

Abstract

An indoor air quality model called INCA-Indoor has been developed taking into account all the processes taking place in indoor environment. This model allows to predict the time evolution of the concentrations of the gas-phase species and particulate matter. It can also evaluate the contribution of different processes to the pollutant concentrations. INCA-Indoor model is applied to simulate the concentrations of volatile organic compounds, NO, NO_2 and O_3 measured in a classroom of a low energy school building in France. Measurement were performed during the MERMAID (Mesures Expérimentales Représentatives et Modélisation Air Intérieur Détaillée) campaign in April-May 2014. The comparison with the measurements shows that INCA-Indoor model is able to reproduce the profiles for most of the species measured indoors. It is showed that indoor emissions, outdoor air pollution, ventilation, and chemistry are important processes controlling indoor air quality, but their relative effect depends on the air pollutant.

3.1 Introduction

Air quality in public buildings and especially in schools is a growing concern. The children spend much of their time [137] in schools and poor indoor air quality may cause health diseases like asthma [138]. Measurement campaigns have been carried out to characterize the sources and concentration levels of pollutants in schools [139, 140, 2, 141, 142]. These campaigns have shown that indoor levels of many volatile organic compounds (VOCs), PM_10 were higher than outside levels [139]. Among the volatile organic compounds (VOCs) detected and identified in indoor environments, benzene and formaldehyde are confirmed as a human carcinogen [143].The other VOCs, such as hexane, heptane and octane (all alcanes in fact) can affect the central nervous system. Therefore, the studies related to indoor air pollution due to VOCs are important as they are directly associated with the public health.

As presented in chapter 2, pollutant concentrations are controlled by several chemical and physical processes in indoor environments. Identifying the major processes affecting pollutant concentrations is critical to reduce their concentrations and to improve indoor air quality. Only few studies have been performed to understand the contributions of chemical and physical processes in indoor environment involving high temporal measurements of outdoor and indoor concentrations of a large range of pollutants (20 VOCs, O_3, NO, NO_2, HONO, OH, HO_2, PM) and experimental conditions (light intensity, temperature, humidity) coupled to an indoor air quality model. Previous studies were usually focused on the analyses of measurements in specific environments ([144, 145, 146]) or the influence of specific processes (i.e. emission, sorption) involving the pollutant concentrations. Drakou et al. (1998) reported in a study the measurement and simulation results of indoor O_3 and NOx (NO and NO_2) in two buildings without mentioning VOCs. Carslaw (2007) [46] developed a model to study the indoor air quality in a typical urban residence in the UK without real measurements comparisons. In addition, to our knowledge, there is no study which focuses both on chemical and physical processes taken place in low energy buildings, where the conditions of emissions by new materials and ventilation are

specific. The aim of the MERMAID [37, 38] project is to assess the air quality in these low energy buildings. An intensive campaign provides the measurement of a large range of indoor pollutant concentrations. The surface emission factors and sorption coefficients of materials of several VOCs were measured. During the MERMAID project, the INCA-Indoor model has been evaluated with other model results [41] and the SURFin data [42] (MERMAID were at the same time collected and the data not yet analyzed and available).

With data collected during SURFin campaign [48], Mendez et al. (2016) has compared the concentrations of OH and HO_2 between experimental and modeled profiles using the INCA-Indoor model and the comparison results shows same order of concentrations for OH and variations for both radicals (OH and HO_2) [42]. However, precise comparisons were not possible as information on building configuration and materials were missing. In addition, OH and HO_2 are two species very sensitive to lighting conditions, and probably very heterogeneously distributed in a room, while measurements are done at one place and INCA-Indoor simulate only an average. Since HONO is an important source of OH [41, 42], INCA-Indoor model has also been used with different HONO formation mechanisms. A new mechanism was proposed with assumptions on surface processes that now need to be confirmed by more measurements. This mechanism allowed at least better simulations of the HONO concentrations, as measured during SURFin campaign.

The aim of the present study is now to assess the ability of INCA-Indoor model to simulate the pollutant concentrations, newly measured and analyzed in the classroom studied during the MERMAID project. Based on the simulation results, INCA-Indoor model is used to quantify the contributions of different processes to the concentrations of VOCs, NOx and O_3 and to identify the role of the various processes in determining these concentrations.

The section 3.2 presents the data collected during the MERMAID campaign which have been used as input in the INCA-Indoor model. Then the section 3.3 shows the results of 12 priority VOCs, NOx, and O_3 that were all measured during MERMAID campaign and modeled

by the INCA-Indoor model. The modeled results have been compared with the experimental concentrations. In addition, contribution analysis was realized to identify the role of different processes and to evaluate the impacts of these processes on the concentrations of these selected species and better understand the observations. The results obtained have been discussed and concluded in the last section 3.4.

3.2 Methodology

3.2.1 The MERMAID campaign

The MERMAID (Mesures Expérimentales Représentatives et Modélisation Air Intérieur Détaillée Representative Experimental Measurement Indoor Air Detailed Model) project was coordinated by the PC2A-Lille University, France (C.Schoemaecker et al., 2015 [37]). The main objective was to identify and classify the physical and chemical processes responsible for the presence of pollutants inside typical low energy public buildings.

The MERMAID project was based on experimental and modeling approaches. The experimental field campaigns were carried out to study the dynamics of the concentrations of pollutants and of the oxidants species as a function of environmental conditions (i.e. ventilation, outdoor concentrations, temperature), and to identify precisely the evolution of pollutants from outdoor source (like NOx, ozone), from indoor source (like formaldehyde, toluene), and from mixed source (like xylenes). In order to choose a representative building school to carry out measurements, a field measurement was conducted in ten low energy school buildings in France to characterize indoor and outdoor pollutant concentrations. Among the ten low energy school buildings, only one building (called THPE 3) was selected as representative according to the concentration levels of the species measured, ventilation levels, orientation of the classrooms and possibilities to perform intensive campaigns with minimum disturbances. This THPE3 building is located in the north of France (50.2746°N, 3.9415°E) and presents access facilities to

conduct intensive field campaigns. A classroom of this building was selected as test location where all furnishings were removed to allow measuring the emission and sorption on main building materials. All measurements were conducted in this classroom during scholar holidays on April-May 2014 and on February-March 2015. These two periods were chosen to represent two different seasons (spring/winter) in order to evaluate also the potential effect of heating systems.

The modeling part of the MERMAID project aims to develop a detailed indoor air quality model called INCA-Indoor, which considers the physical and chemical processes influencing indoor air quality and which is able to reproduce the concentration profiles of species. The application and validation of the INCA-Indoor model was realized with the help of measurement data during the first MERMAID campaign. The measurement data used as inputs by the INCA-Indoor model and the ones that were used for validation are presented in the following sections.

Measurement campaign description

Field measurements for the first MERMAID campaign, which have been used and are reported in this chapter, were carried out from 23 April 2014 to 2 May 2014. The measured parameters include physical parameters of the studied room (i.e. volume, surface area), temperature and relative humidity, air exchange rate (AER), the levels of NOx, O_3, and VOCs. The selected classroom for intensive MERMAID measurements is described in the figure 3.1 hereafter. The 5 windows of the classroom are exposed to the south (210°) in order to favor the solar heating. Two air intakes from a double-flow air treatment unit with heat recovery are present in the classroom on the side of the windows, and an extraction is installed on the side of the corridor. The characteristics of the classroom are also detailed in the table 3.1. Measurements were carried out in 5 different places in and out of the classroom (see figure 3.2) : Inside : at the ventilation inlet in the room M2,

Inside : in the middle of the room M2,

Outside : on the terrace (O1),

Outside : in the playground, air intake from air treatment center (O2),

Inside : at the exit of the air treatment unit.

The instruments for the measurements by sampling lines were installed in I1 and I2 for measurements in M2 and O1, and in I3 for O2 measurements. The instruments which have required in-situ measurements were installed in M2. More information can be found in Schoemaecker et al. (2015) [37].

Table 3.1 – Characteristics of the classroom

Volume (m^3)	Total surface (m^2)	length (m)	width (m)	height(m)
138.5	181.5	7.6	6.6	2.7

Measurement of air exchange rate

The ventilation rate was measured by two methods :

- with an anemometer (Swemaflow) measuring the flow entering or leaving the ventilation inlet and extraction vents.

- by following the decrease in CO_2 concentration after its injection as a tracer. Note that the CO_2 can be considered as a good tracer because of its non–reactivity during the duration of the measurements.

Both techniques yielded similar results. When the ventilation was active, the air flow measured by the decay of CO_2 was 300 m^3 h^{-1}, giving an air change rate of 2.17 h^{-1} for the classroom with a volume of 138.5 m^3. When the ventilation was inactive, the air flow was 30-60 m^3 h^{-1}, corresponding to an air change rate of 0.22-0.43 h^{-1}. The ventilation system in the tested classroom worked only during teaching periods and was stopped during the weekends. For the needs of the campaign and the specificity of specific instruments, these operating schedules have been

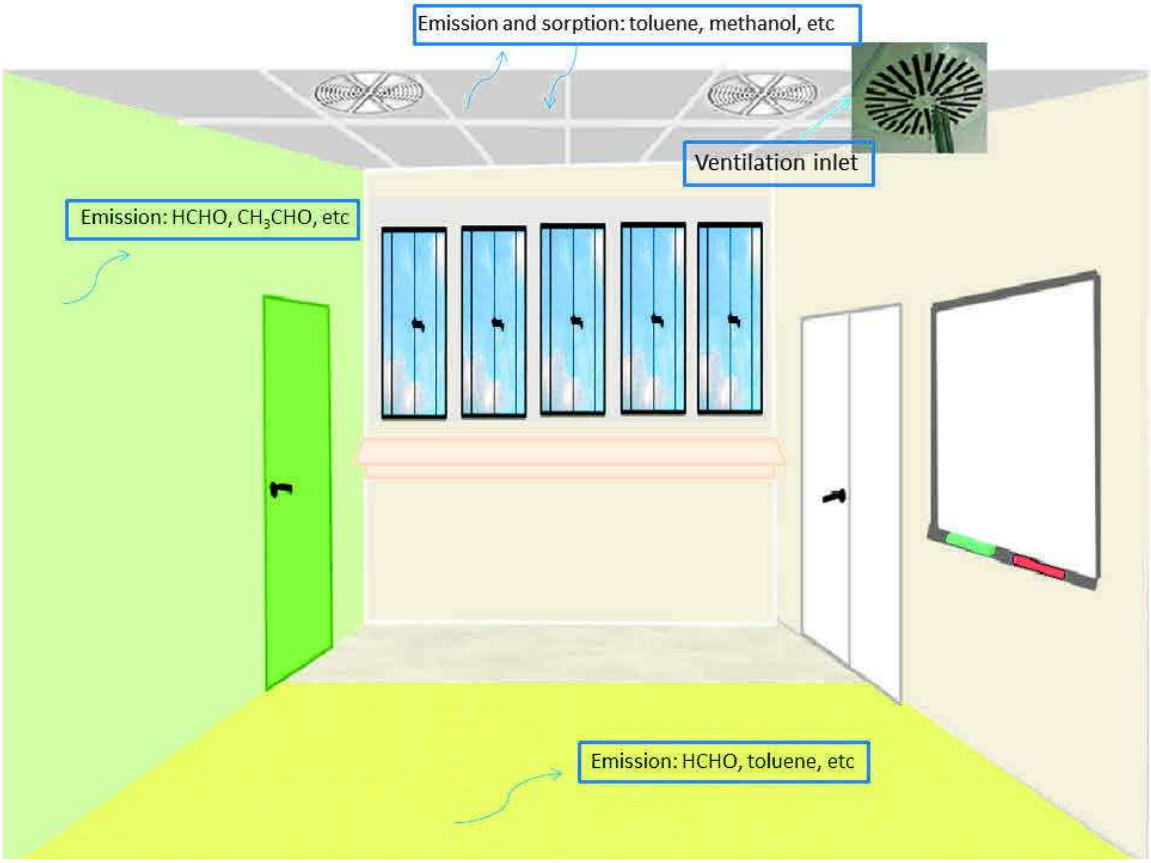

Figure 3.1 – The classroom as test location (from Rizk et al., 2015 [147])

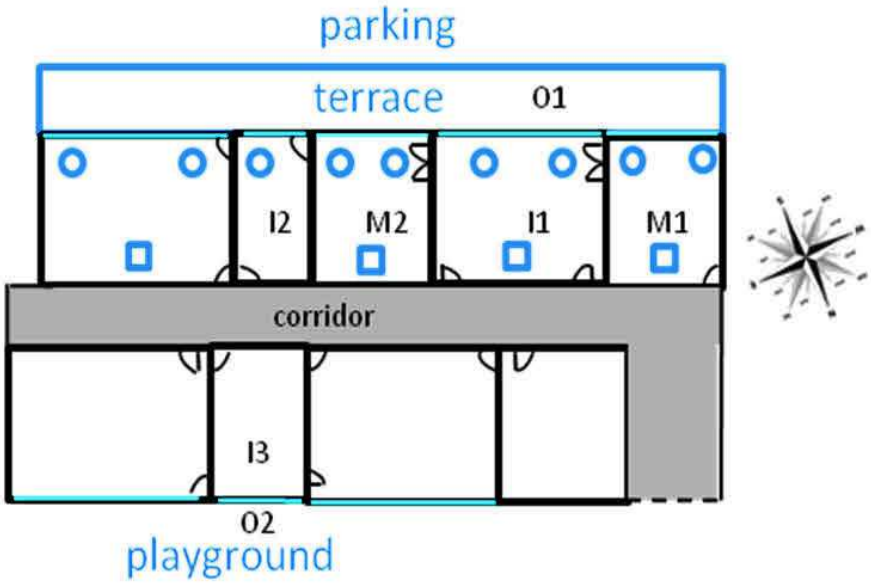

Figure 3.2 – Measured points inside and outside of the classroom (from Schoemaecker et al.,2015 [37])

modified at some times. The table 3.2 shows the operating schedules of ventilation in the tested classroom during the first campaign.

Table 3.2 – Operating hours of ventilation during the first Campaign

Date		Ventilation 1 begin end	Ventilation 2 begin-end	Ventilation 3 begin-end	Ventilation 4 begin-end
Monday	21/04/2014	08 :10-09 :45	10 :10-11 :45	13 :35-15 :00	15 :25-17 :15
Tuesday	22/04/2014	08 :10-09 :45	10 :10-11 :45	13 :35-15 :00	15 :25-17 :15
Wednesday	23/04/2014	08 :10-09 :45	10 :10-11 :45	13 :35-15 :00	15 :25-17 :15
Thursday	24/04/2014	08 :10-09 :45	10 :10-11 :45	13 :35-15 :00	15 :25-17 :15
Friday	25/04/2014	08 :10-09 :45	10 :10-11 :45	13 :35-15 :00	15 :25-17 :15
Saturday	26/04/2014	no ventilation			
Sunday	27/04/2014	no ventilation			
Monday	28/04/2014	08 :20-09 :45	10 :10-11 :45	13 :35-15 :00	15 :25-17 :15
Tuesday	29/04/2014 injection(O_3)	08 :20-09 :45	10 :10-11 :45 10 :13-10 :14 ;11 :49-11 :53	13 :35-15 :00	15 :25-17 :15
Wednesday	30/04/2014	08 :20-09 :45	10 :10-11 :45	13 :35-15 :00	no ventilation
Thursday	01/05/2014	07 :20-09 :45	10 :10-11 :45	13 :35-15 :00	no ventilation
Friday	02/05/2014	07 :20-09 :45	10 :10-11 :45	13 :35-15 :00	15 :25-17 :15

Measurement of temperature and the relative humidity

The temperature (T) and the relative humidity (RH) were measured continuously throughout the campaign. The table 3.3 summarizes the measurements obtained : the minimum, mean, maximum of the temperature and relative humidity outside and inside of the classroom.

Table 3.3 – Minimum, mean, maximum of the temperature and relative humidity during the first Campaign

	Outside		Inside	
	T(^{o}C)	RH(%)	T(^{o}C)	RH(%)
Minimum	6.0	33.5	19.0	22.0
Mean	13.5	65.0	23.0	36.1
Maximum	21.5	96.0	26.5	59.0

Measurement of the concentrations of VOCs, NOx and O_3

There were 23 VOCs measured during MERMAID campaign. The major part of the species are oxygenated ones : acetone, 2-butanone, formaldehyde and acetaldehyde. In addition, concentrations of NOx and O_3 are measured during the first MERMAID campaign. Hereafter are detailed the concentration levels of 12 VOCs listed in the table 3.4, nine of them are classified as hazardous air pollutants by the United States Environmental Protection Agency (EPA) [148], and three (d-limonene, acetone and isoprene) can produce hazardous air pollutants due to reactions with O_3 and radicals (i.e. OH, NO_3) [149, 150, 151]. Annexe 8 gives guidance values that are recommended to protect health. The mean, maximum and minimum concentrations of 12 VOCs, NOx and O_3 measured in the center of the classroom during the first campaign are also presented in the table 3.4.

Table 3.4 – Concentrations (in ppb) measured at the center of the room (indoor)

Species	maximum	mean	minimum
NO	2.50	0.91	0.69
NO_2	14.79	4.29	2.22
O_3	79.98	11.03	2.49
methanol	45.91	33.15	15.70
formaldehyde	23.35	17.96	9.34
acetaldehyde	6.96	4.57	2.46
acrolein	10.46	7.79	4.12
acetone	11.90	8.91	4.58
benzene	0.60	0.45	0.28
toluene	25.58	16.02	4.09
o-xylene	2.11	1.12	0.54
chlorobenzene	0.95	0.78	0.57
p-dichlorobenzene	0.78	0.50	0.17
isoprene	2.00	1.42	0.75
d-limonene	3.82	1.88	0.74

In addition to the measurements of these concentrations, the surface characteristics were carried out by emission measurements (Ecole des Mines de Douai and ICPEES) and sorption

using the FLEC (Field and Laboratory Emission Cell) coupled to the PTR-MS, GC analyzers and cartridges post analyzer. The emission rate (in ppb m^{-2} h^{-1}) of all detected VOCs were investigated on the 10 main surfaces of the classroom (table 4.4). There are only 13 species within the 23 measured species emitted by these surfaces at levels above detection limits (ranging from 0.005 to 0.100 ppb m^{-2} h^{-1} depending on species). Measurement results show that toluene, formaldehyde and methanol are the most emitted species in the classroom. The results of emission rates are listed in the table 3.6 .

The sorption coefficients have been measured for the VOCs within a few hours for each surface (<17 hours/surface) and are presented in the table 3.7. Measurement methodologies are fully described in Rizk (2015) [147] and Rizk et al.(2016) [152].

Table 3.5 – Area of the surfaces present in the classroom

Building material	Number	Surface area (m^2)	Percentage of surface (%)
Green vinyl flooring	1	43.69	24.07
Ceiling tiles	1	47.40	26.12
White painted concrete wall	2	25.47	14.04
Green painted gypsum board	1	18.68	10.29
White PVC board	2	11.97	6.6
White painted gypsum board	1	16.73	9.22
White vinyl flooring	1	6.24	3.44
White painted wood shelf	2	4.75	2.62
White painted wood door	1	3.33	1.83
Green painted wood door	2	3.22	1.77
Total surface area		181.5	

3.2.2 Configuration of the INCA-Indoor model

To compare simulation results with the measurements performed during MERMAID, INCA-Indoor was set-up following the configuration of the classroom (i.e. volume = 138.5 m^3, 10 surface areas as described in table 4.4). The temperature and the relative humidity were constrained

Table 3.6 – Measured VOC mean emission rates (mol.m^{-2}.h^{-1}) for tested surfaces in the classroom

Species	Ceiling tiles	Green vinyl flooring	White vinyl flooring	White painted concrete wall	Green painted gypsum board	White painted gypsum board	White PVC board	White painted wood shelf	White painted wood door	Green painted wood door
formaldehyde	2.07E-10	1.79E-11	0.	1.73E-11	1.81E-11	0.	1.76E-11	0.	2.34E-11	1.98E-11
acetaldehyde	4.26E-12	3.31E-12	3.78E-12	5.04E-12	3.94E-12	0.	0.	6.94E-12	1.01E-11	4.41E-12
toluene	0.	2.29E-10	1.74E-10	0.	0.	0.	0.	0.	0.	0.
o-xylene	0.	1.38E-12	8.30E-13	0.	0.	0.	0.	0.	0.	0.
styrene	3.47E-12	0.	1.33E-12	0.	0.	0.	0.	0.	0.	0.
alpha-pinene	2.45E-12	7.24E-13	9.48E-13	0.	0.	0.	0.	0.	0.	0.
beta-pinene	2.55E-12	7.44E-12	9.58E-12	0.	0.	0.	0.	0.	0.	0.
Camphene	3.23E-11	1.74E-12	2.21E-12	0.	0.	0.	0.	0.	0.	0.
d-limonene	5.51E-12	0.	3.66E-13	0.	0.	0.	0.	0.	0.	0.
methanol	0.	4.16E-11	6.07E-11	1.04E-10	0.	0.	0.	0.	1.56E-10	1.82E-10
n-octane	0.	1.70E-11	0.	0.	0.	0.	0.	0.	0.	0.
n-nonane	0.	4.41E-12	4.22E-12	0.	0.	0.	0.	0.	0.	0.
n-undecane	2.37E-12	0.	0.	0.	0.	0.	0.	0.	0.	0.

Table 3.7 – Measured VOC mean sorption rates for tested surfaces in the classroom, * : indicates that the limit of detection is determined theoretically for the couple of parameters (ka, kd) using the FLEC-PTR method. MEK : Ketones and other non-aldehyde oxygenated products that react with OH radicals faster than 5×10^{-13} but slower than 5×10^{-12} cm^3 molecule^{-2} second^{-1}.

Species	Ceiling tiles		Green painted concrete wall	
	ka(m h^{-1})	kd(h^{-1})	ka(m h^{-1})	kd(h^{-1})
acrolein	17.1	259.1	<0.07*	<0.07*
acetone	39.0	609.0	<0.07*	<0.07*
MEK	5.3	55.9	<0.07*	<0.07*
benzene	3.5	40.2	<0.07*	<0.07*
toluene	2.0	9.9	<0.07*	<0.07*
ethyl benzene	1.7	2.9	0.31	13.6
styrene	2.6	3.0	1.1	17.11
alpha-pinene	1.0	4.0	<0.07*	<0.07*
methanol	6.9	43.8	<0.07*	<0.07*

to their measured values in the model. The operating schedules of ventilation follow the program of measurements during the first campaign. The infiltration rates were measured only one day during the campaign by following the decrease in CO_2 concentration and it varies between 30 and 60 m^3h^{-1}. The infiltration rates used as input in the model were 45 m^3h^{-1} (AER :0.43 h^{-1}) corresponding to the maximum infiltration rate with the ventilation switched off and 300 m^3h^{-1} (AER : 2.2h^{-1}) with the ventilation switched on. In order to identify potential differences between the outdoor concentration and the concentration at the ventilation inlet due to losses in the system or at the contrary contamination, measurements at both locations were performed during the campaign. In addition, the concentrations entering the room considered as intake concentration for the model are either the measured outdoor concentrations or the ones measured at the ventilation inlet. Both types data are tested here and discussed in the following sections. The VOC emission and sorption rates of the 10 main surfaces measured during the campaigns [147] are used in the model. All the simulations start from the April 29th 2014 at midnight and ended the 30th of April 2014 at midnight with a time step of 60 seconds.

Photolysis frequencies

The chemical mechanism of INCA is based on the detailed version of SAPRC-07 mechanism [130] that contains about 1628 reactions, with 885 species describing gas-phase chemistry, surface reactions, deposition, emissions, surface emission, exchange, adsorption and desorption. Within these 1628 reactions, 174 are photolysis reactions involving the photolysis of 88 species (or lumped species). Direct indoor measurements of the actinic fluxes in the classroom have been used. The absorption cross sections and quantum efficiency used to calculate the photolysis frequencies are based on 34 reference species from SAPRC-07 [130] (e.g. propanal data used for C4-C8 aldehydes) for which accurate data are available.

Deposition velocities

The deposition velocities of 37 species have been considered and many were taken from Sarwar et al (2002) [79]. The deposition velocities used in the model have the following values :

0.036 cm s^{-1} for O_3 ;

0.06 cm s^{-1} for NO_2 ;

0.07 cm s^{-1} for HONO, HNO_3, HO_2NO_2, H_2O_2, NO_3, N_2O_5, HO_2 and OH ;

0.005 cm s^{-1} for HCHO and CH_3CHO ;

Concerning the other compounds, due to the fact that most of the indoor deposition velocities are 10-100 times smaller than those of outdoors, we have adjusted the deposition velocities values to the following ones :

0.002 cm s^{-1} for PAN and organic nitrate organic,

0.07 cm s^{-1} for organic peroxides

0.005 cm s^{-1} for aldehydes other than HCHO and CH_3CHO

Initial concentrations

The indoor concentrations of NO, NO_2 and O_3 and of 14 VOCs have been initialized from the measured values obtained during the campaign and listed in the table 3.8. All other modelled species were initialized at zero.

3.3 Results and discussion

In order to validate the INCA-Indoor model, the predicted instantaneous concentrations of 12 VOCs, NOx and O_3 based upon the model are compared with the experimental results from MERMAID campaign. The 29th of April 2014 has been chosen because it was representative of the situations observed in this field campaign in terms of ventilation conditions.

From midnight on 29th of April in 2014 to midnight on 30th of April in 2014, the VOC

Table 3.8 – Initial concentrations (MEK : Ketones and other non-aldehyde oxygenated products that react with OH radicals faster than 5×10^{-13} but slower than 5×10^{-12} cm^3 $molecule^{-2}$ $second^{-1}$.))

Species	Initial concentrations (ppb)
NO	0.81
NO_2	3.17
O_3	4.19
methanol	41.82
acetaldehyde	5.33
acrolein	9.62
acetone	10.90
isoprene	1.64
crotonaldehyde	2.29
MEK	1.19
benzene	0.51
toluene	23.69
o-xylene	0.91
d-limonene	3.82
chlorobenzene	0.92
p-dichlorobenzene	0.46
formaldehyde	20.43

measurements were available for the center of the classroom, ventilation inlet and outdoor. The concentrations measured in the center of the classroom were considered to represent the mean concentrations in the classroom, which were used to compare with the modeled concentrations. When the ventilation was switched on, the concentrations entering the room considered as intake concentration for the model were either the measured outdoor concentrations or the ones measured at the ventilation inlet. When the ventilation was switched off, the classroom can be considered as a "closed box" with just an infiltration of outdoor air (leaks around the doors and windows). Considering measured data outdoors as input of the model, the losses in the ventilation system or at the contrary contamination are not considered during the simulation when the ventilation is switched on, but the concentrations entering the room due to the infiltration with the ventilation switched off are well represented. With measured data at the ventilation inlet as input of the model, the concentrations entering the room due to the infiltration with the ventilation switched off are not well considered but taken into account as any other process that could produce a difference between indoor concentrations and concentrations observed at the ventilation inlet (usually closed except when the ventilation is switched on). In this chapter, two types of simulations have been performed with measured data outdoors (both the ventilation switched on and off) and at the ventilation inlet (both the ventilation switched on and off).

The comparison of concentration profiles between measured and modeled leads to point out the model's ability to simulate the behaviors of different species. To identify the major processes responsible for the concentrations of the species of interest and to evaluate the contributions of the different processes on the budget of the priority pollutants, contributions analysis have been realized to compare the production and loss rates for these selected species. In this chapter, contribution analysis between 8h :20 and 17h :15 was based on the simulations with measured outdoor concentrations as model input. To favor the analysis of the behaviors of these 15 targeted species, they are grouped into 3 types : species mainly originated from outdoors (concen-

trations increase with the ventilation on), indoors (concentrations decrease with the ventilation on), both from indoors and outdoors (peaks form of concentrations with the ventilation on).

3.3.1 Analysis of the pollutants mainly originated from outdoors

Analysis of the concentration levels of O_3

Due to the lack of outdoor measurement for O_3, the daily ozone concentrations have been considered as shown in the figure 3.3 for the measurement at the center of the room and at the ventilation inlet, as well as for the modeled profile. Since ozone is a common initiator for indoor gas-phase oxidation processes [72], it has been also experimentally injected to the classroom with the ventilation switched on and off in order to investigate the influence of forced conditions on chemical reactions.

O_3 concentrations are the lowest (equivalent between at the ventilation inlet and in the center of the room) when the ventilation remains inactive and increase when the ventilation is switched on. Due to the injection of O_3 at 10h :13 and during five minutes from 11h :49 to 11h :54, O_3 rises rapidly to almost 80 ppb and 60 ppb, respectively. During the last two periods of ventilation, O_3 remains stable at around 25 ppb with higher levels at the ventilation inlet than in the center of the room, which is the consequence of indoor loss by deposition and to a lesser extent by consumption due to reactions with other species.

Contribution analysis based on the INCA-Indoor model between 8h :20 and 17h :15 presented in the figure 3.4 indicates that O_3 is mainly from the outdoor-to-indoor transport, which contributes 93.40% to the total production rates of O_3. The production of O_3 via indoor chemical reactions accounts for 6.60%. Indoor the great part of O_3 is removed by the deposition (85.9%), while the minor contributions to removal are the reaction of O_3 with NO (10.80%) and the reactions of O_3 with other species (3.3%).

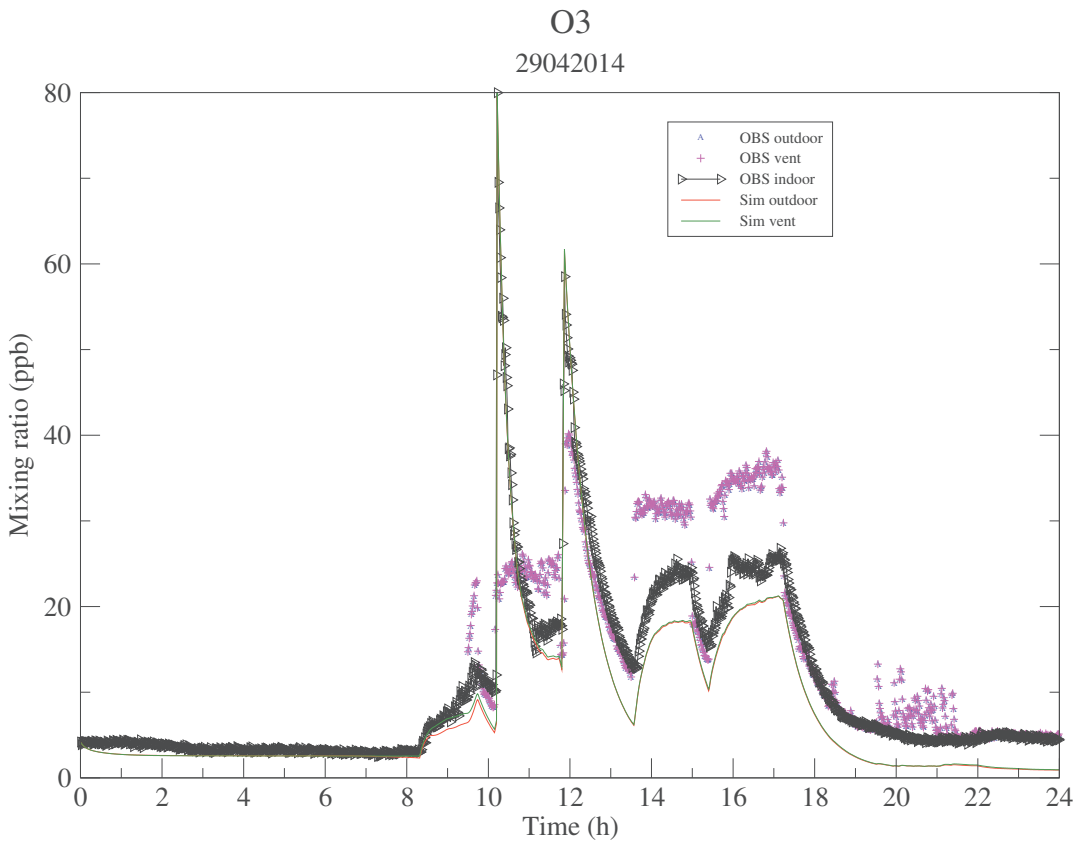

Figure 3.3 – Measured concentrations of O_3 for the ventilation inlet (OBS vent, magenta +) and the center of the classroom (OBS indoor, black line with triangle right). Modeled concentrations with data for the ventilation inlet (Sim vent, green line) with INCA-Indoor model.

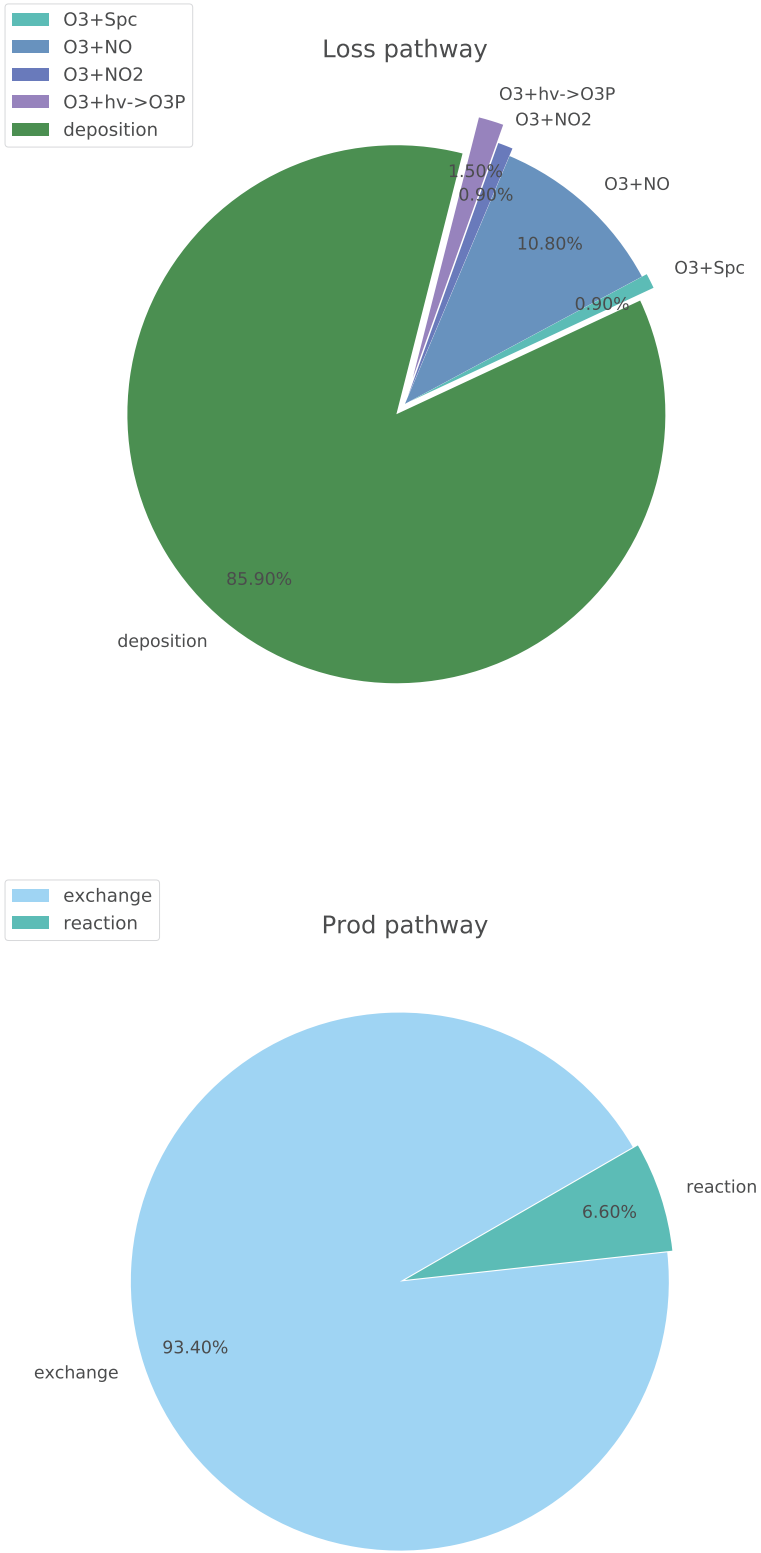

Figure 3.4 – Contributions of production and loss pathways of O_3. "spc" represents the organic species reacting with O_3.

Analysis of the concentration levels of NO and NO_2

The concentration profiles of NO and NO_2 measured at the center of the classroom (OBS indoor), at the ventilation inlet (OBS vent), outdoor (OBS outdoor) and modeled with data of outdoors (Sim outdoor) and the ventilation inlet (Sim vent) are presented for the 29th of April in figure 3.5. The outdoor concentration profiles of NO (figure 3.5) shows that this compound increases markedly from 7h :00 and reaches the peak concentration at about 8h :30 with 10.42ppb, and then decrease rapidly. The average outdoor concentration of NO after 13h :00 is lower than 1ppb. There is a significant fluctuation for outdoor NO_2 concentration before 8h :00 with a maximum of 23.30 ppb at 8h :15. Because the outdoor concentrations of NO and NO_2 are dominated by the rush-hour traffic [46, 153], the time reaching maximum concentrations in the morning corresponds to the morning rush-hour traffic. The evening rush hour is only distinct for the NO_2 data, with several peak concentration between 17h :00 and 23h :00. Without ventilation, NOx concentration measured indoor and at the ventilation inlet are similar. When the ventilation is switched on, the NOx concentrations measured for these two places increase significantly due to the outdoor-to-indoor transport, but indoor peak concentration is smaller than at the ventilation inlet, which is probably is due to indoor reactions.

The predicted indoor NO and NO_2 concentrations followed their outdoor concentrations. When the ventilation is switched on, the modeled concentrations for NO from the simulation with data at the ventilation inlet are lower than those with outdoor data, which are closer to measured indoor concentrations. There is probably an offset on the analyzer for NO indoors during the campaign. For NO_2, simulation with data of the ventilation inlet is closer to the measured indoor concentrations. When the ventilation was switched on, modeled concentrations of NO and NO_2 with measured outdoor data were higher than with the measured ones at the ventilation inlet. That is because that measured outdoor concentrations were higher than at the ventilation inlet. It needs to note that there is the problem of calibration of the NO and NO_2 analyser for the outdoor measurement.

Contribution analysis between 8h :20 and 17h :15 (see figure 3.6) shows that NO comes mainly from the transport outdoor-to-indoor (83.8%) and the photolysis of NO_2 (15.9%). The loss pathways for NO are the chemical reactions, of which the reaction of NO with O_3 is the most important accounting for 77.7%. The major production pathways for NO_2 are the reaction of NO with O_3 (53.30%), the decomposition of HNO_4 (21.1%), reactions of NO with specific radicals like hydroperoxide radicals or methyl peroxy radicals (13.8%) and other reactions producing NO_2 (10.4%) (see figure 3.7). The contribution of the exchange with outdoor air to indoor NO_2 concentration accounts for 27.7%, which is much smaller than that to NO concentration. That can be explained by the fact that some reactions (i.e NO_2 with surfaces) occur at a rate greater than air-exchange rates, so the contribution of ventilation to NO_2 becomes less important compared to these reactions. NO_2 is consumed by the reactions of NO_2 with HO_2 (18.8%), NO_2 with surfaces (29.1%) contributing to the formation of nitrous acid (HONO), the photolysis of NO_2 (9.6%) and the reactions of NO_2 with other oxidants or radicals (i.e. O_3, OH) (14.8%). One can note that these contributions need to be analyzed in a global way, summing the full effect of the chemistry (production and consumption), as proposed later in text (cf. summary of this section) for whole species.

Analysis of the concentration levels of o-xylene

The concentration profiles of o-xylene have been measured in the center of classroom (OBS indoor), in the ventilation inlet (OBS vent) and outdoor (OBS outdoor) on the 29nd of April and are shown in the figure 3.8. Two types of simulations (considering the data with of outdoors (Sim outdoor) and the ventilation inlet (Sim vent) are also presented in the figure 3.8.

For the two simulations (Sim outdoor and Sim vent), the modeled indoor o-xylene concentrations follow its outdoor concentrations. For o-xylene, indoor concentrations increase with the increase of outdoor concentrations before the first ventilation episode starts. Those increases indoors are due to progressive infiltration of the o-xylene from outdoors. The delay between the

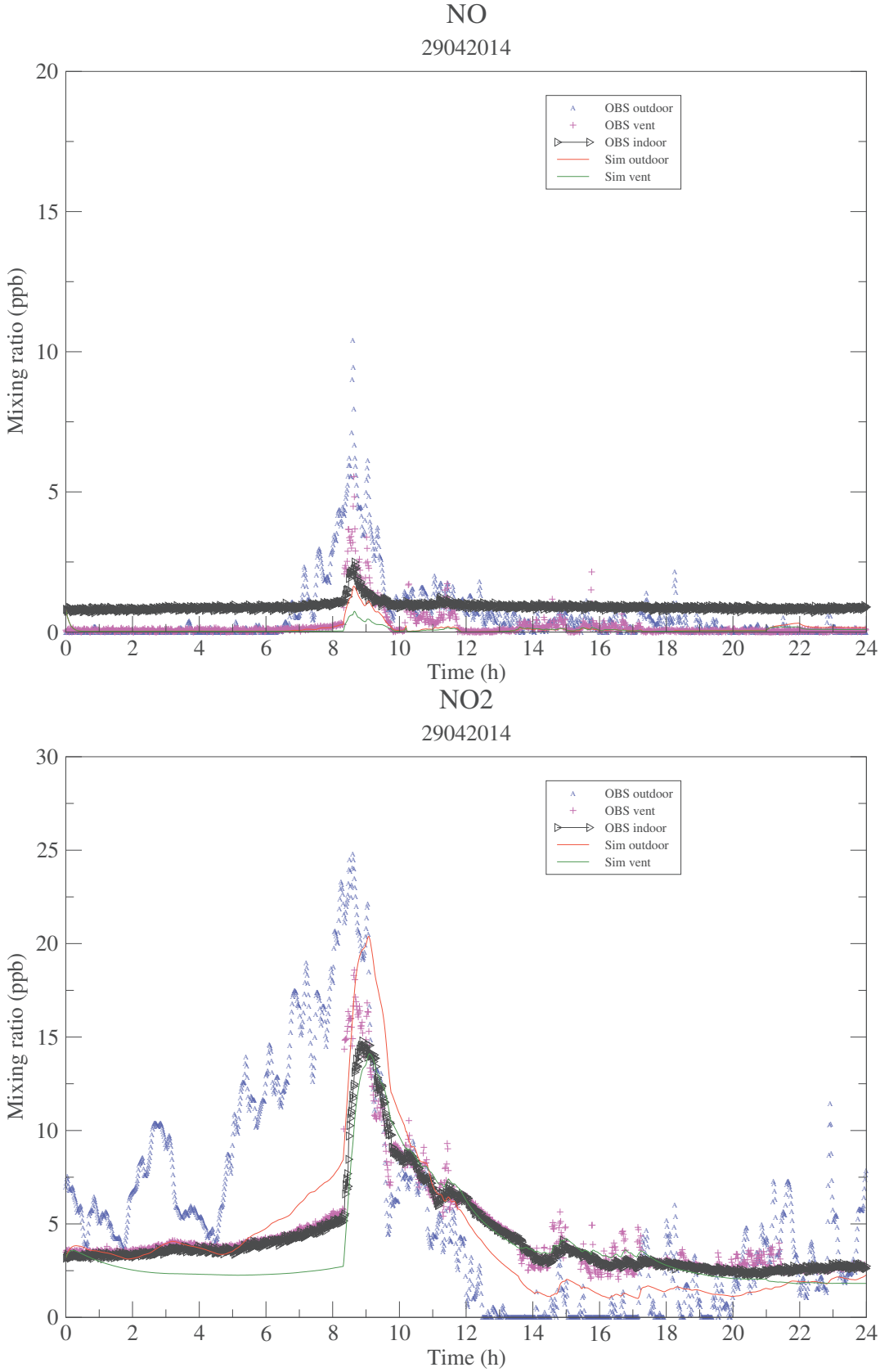

Figure 3.5 – Measured concentrations of NO and NO_2 for outdoor (OBS outdoor, blue char), the ventilation inlet (OBS vent, magenta +) and the center of the classroom (OBS indoor, black line with triangle right). Modeled concentrations with data for outdoor (Sim outdoor, red line), the ventilation inlet (Sim vent, green line) with INCA-Indoor model.

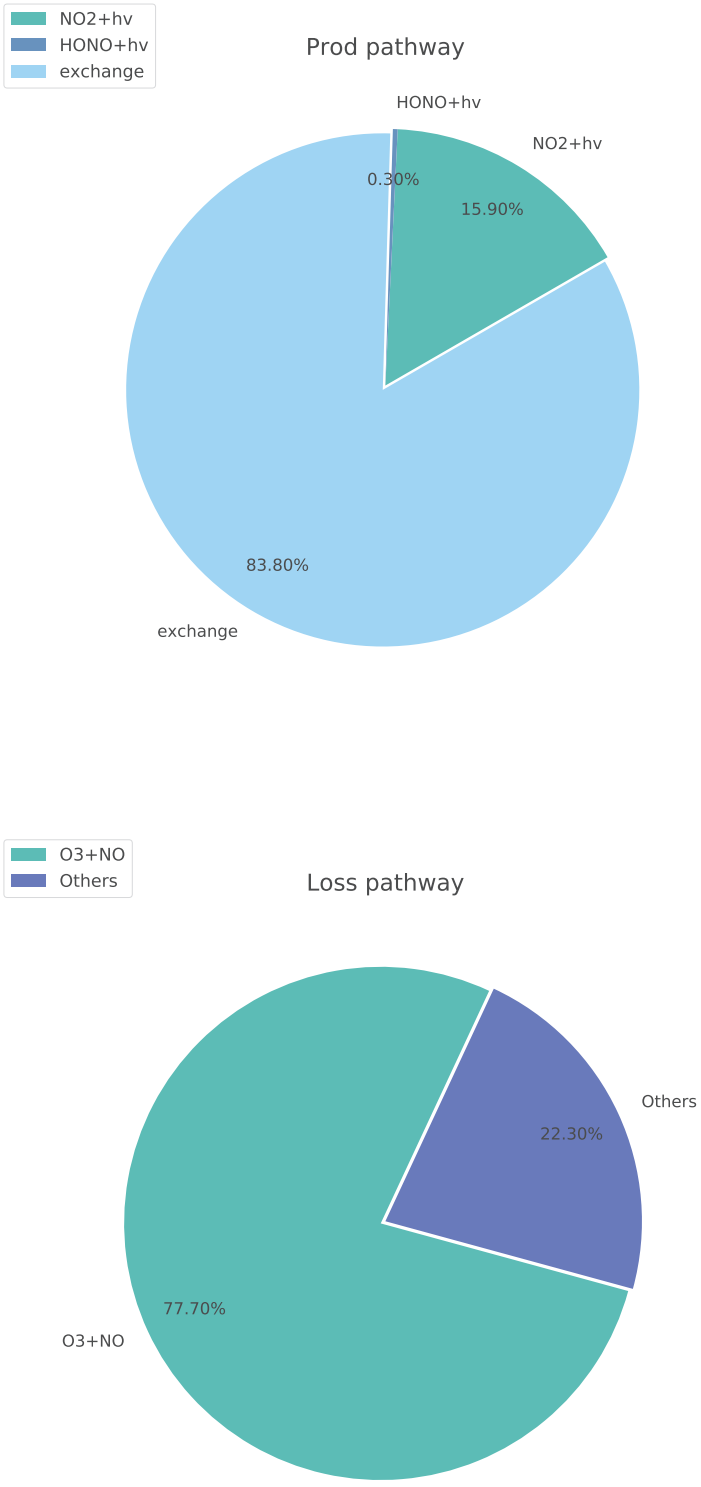

Figure 3.6 – Contributions of production and loss pathways of NO. "Others" includes reactions of NO with some radicals (i.e. peroxyacyl, hydroperoxide)

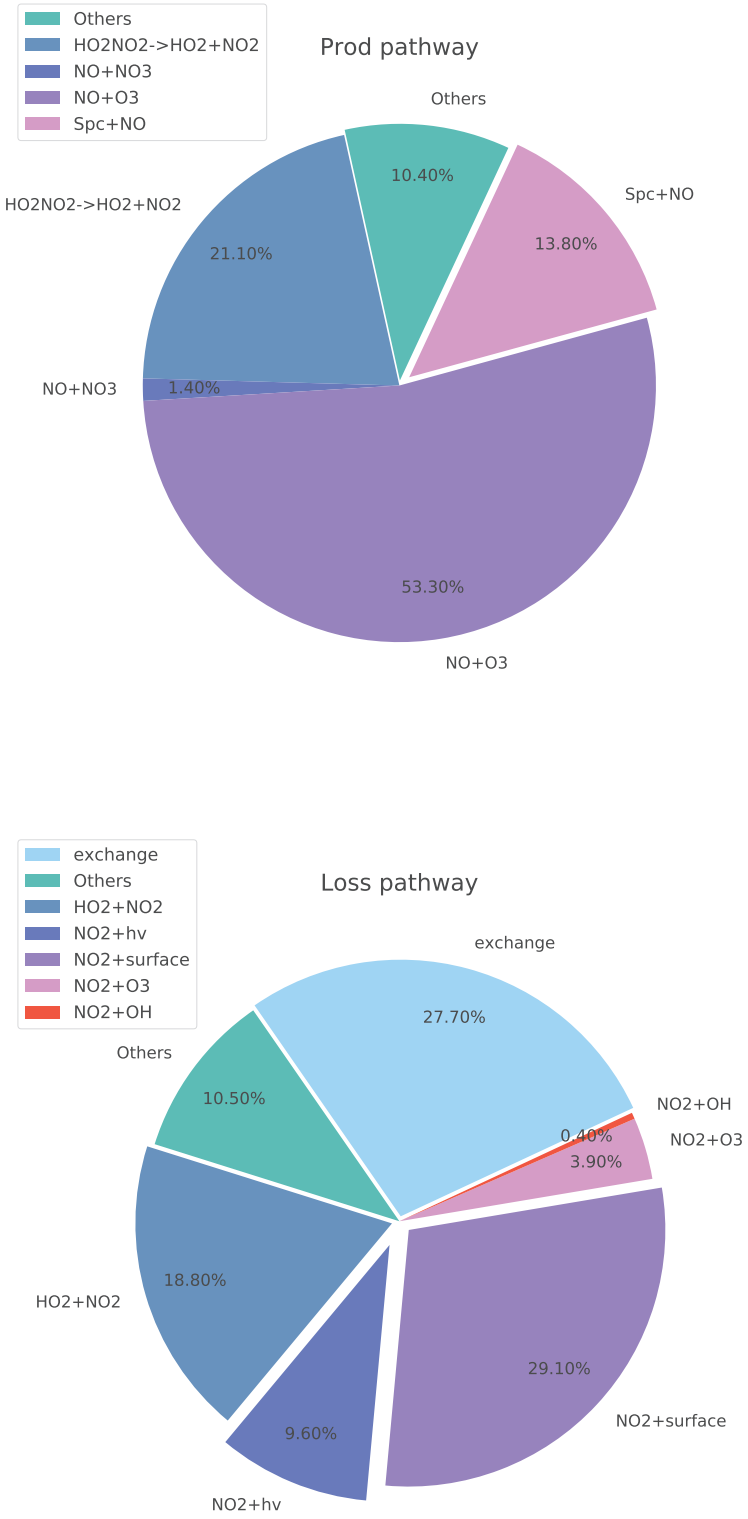

Figure 3.7 – Contributions of production and loss pathways of NO_2. "Others" includes reactions of NO_2 with some radicals (i.e. peroxyacyl, acetyl peroxy radical). "spc" represents some radicals (i.e. hydroperoxide radicals, methyl peroxy radicals) reacting with NO.

simulation using outdoor concentrations compared to observations indicate that the infiltration rate is probably overestimated (i.e. the o-xylene is entering too fast in the room). When the ventilation is switched on, indoor o-xylene concentrations first decrease because the indoor concentration is higher then start to increase also because outdoor concentrations increased. The simulation with measured outdoor concentrations was underestimated probably due to the underestimation of the emission rate of the o-xylene.

The contribution analysis based on the simulation with outdoor data as model input between 8h :20 and 17h :15 presented in the figure 3.9 indicates that the indoor o-xylene concentrations were produced via emissions. This seems not coherent with our choice to identify o-xylene as an pollutant from outdoor due to the period choosed to analysis. Before 8h :20 during the ventilation is switched off, indoor concentrations of o-xylene increase with outdoor concentrations increasing and decrease with outdoor concentrations decreasing, however there is a delay between the peak outdoor and indoor concentrations. It indicates that indoor concentrations is mainly impacted by outdoor concentrations. Between 8h :20 and 17h :15, the emission appears as the main production process because of low outdoor concentrations playing a role as a sink of o-xylene. The o-xylene loss was mainly due to the ventilation (98.4%). Those results are not here fully representative of what happened during the whole day because of fast change in outdoor concentration. The reactions of o-xylene with OH plays a minor role in reducing o-xylene concentrations and accounts for 1.6% of the total consumption rates.

3.3.2 Analysis of the pollutants mainly originated from indoors

Analysis the concentration levels of methanol

The concentration profiles of methanol measured in the center of classroom (OBS indoor), in the ventilation inlet (OBS vent) and outdoor (OBS outdoor) on the 29nd of April are shown in

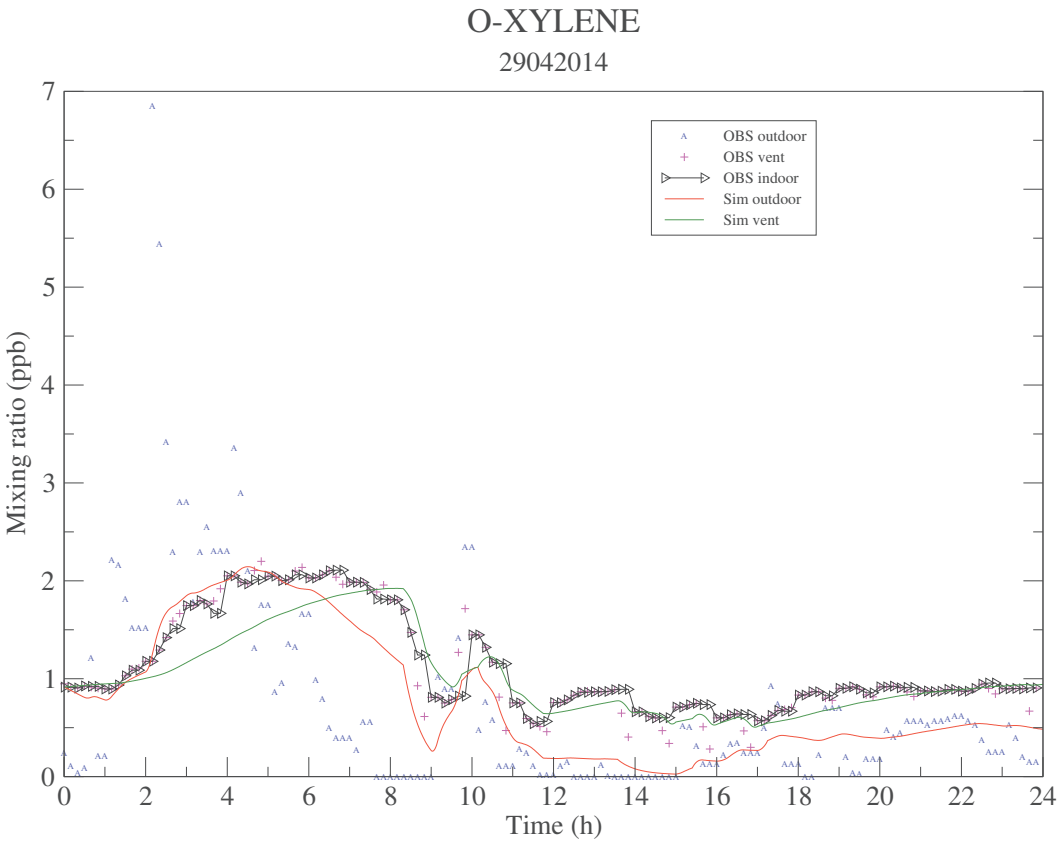

Figure 3.8 – Measured concentrations of o-xylene for outdoor (OBS outdoor, blue char), the ventilation inlet (OBS vent, magenta +) and the center of the classroom (OBS indoor, black line with triangle right). Modeled concentrations with data for outdoor (Sim outdoor, red line), the ventilation inlet (Sim vent, green line) with INCA-Indoor model.

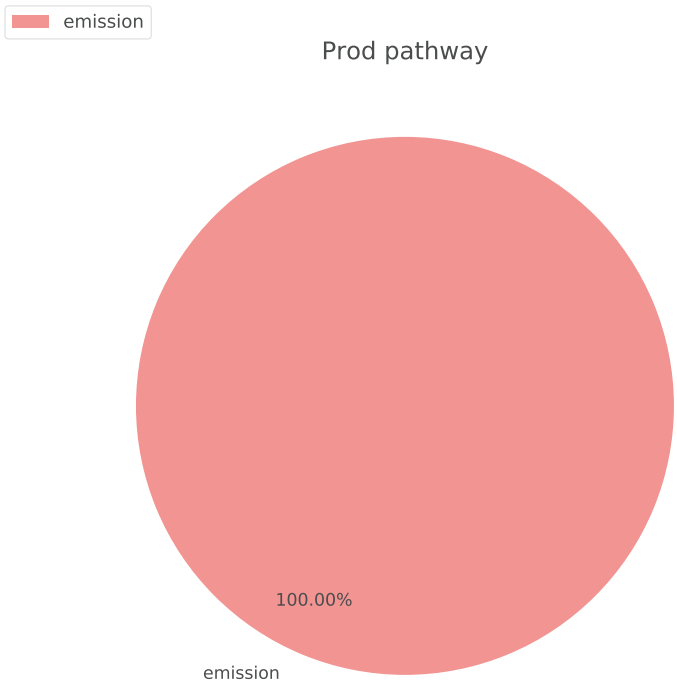

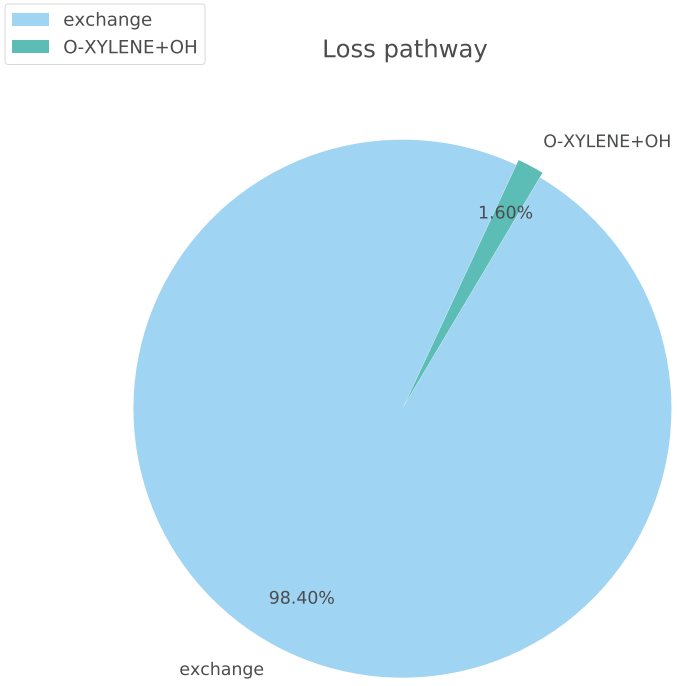

Figure 3.9 – Contributions of production and loss pathways of o-xylene

the figure 3.10. Two types of simulations (considering the data outdoor (Sim outdoor) and at the ventilation inlet (Sim vent)) are also presented in this figure.

Before the ventilation is switched on, the measured indoor methanol concentrations reach a plateau. Two reasons may explain this plateau : (1) there is an equilibrium between the production of methanol (mainly emitted indoors) and the losses (infiltration) (2) the air of the room is so stabilized that the concentrations in the middle of the room are constants, and the gradient just existed near surfaces and infiltration sources. Taking into account results of o-xylene, the second is not accepted since a transport between outdoor and indoor is seen in the observations. During the periods of the ventilation switched on intermittently four times between 8h20 and 17h15, the measured indoor methanol concentrations decrease significantly as soon as the ventilation is active but increase rapidly when the ventilation becomes inactive. When the ventilation is active, methanol concentrations at the ventilation inlet are significantly lower than the indoor ones because outdoor air enters indoor with lower concentrations of methanol than that of indoor. However the concentrations of methanol at the ventilation inlet are higher than those of outdoors, indicating that methanol is probably impacted by the ventilation system. In addition, higher indoor concentrations compared with outdoors and at the ventilation inlet indicate an important contribution from indoor sources of methanol.

With outdoor data as input of the model, the modeled concentrations underestimate the indoor ones probably due to an underestimation of the emission rate.

With data at the ventilation inlet as input of the model, the modeled methanol concentrations are closer to the concentrations measured indoor than the ones obtained with outdoor concentrations. When the ventilation is switched on, the model simulates properly the concentration variability. This allows us to say that the involved processes are well simulated. However, one can note that when the ventilation is switched off at around 18h :00, the fast increase of methanol is not enough well reproduced by the model and underestimated. This is coherent with an underestimations. Methanol is one of the most emitted species in the classroom observed

during the campaign and the predicted concentrations with the model are impacted by the emission rate, which varies with the environment conditions [154, 155]. The emission factors are maybe underestimated. The INCA-Indoor model considers the emission rates as constants and uses the mean emission rate for all the simulation, which may be lower than the realistic data, leading to the underestimation by the model.

Compared two types of simulation, simulation with measured outdoor data is more reasonable. In the figure 3.11 are illustrated the contributions of the different processes to the methanol concentration based on the simulation with outdoor data. The indoor emissions are considered as the most important sources for methanol due to the negligible contributions of the others production pathways. The major loss pathway for methanol are exchange with outdoor (91.7%) and sorption (8.3%).

Analysis of the profiles of other VOC concentration levels

The other species with similar profile shapes to the methanol include the formaldehyde, acetaldehyde, acrolein, acetone, toluene and isoprene (figure 3.12-3.14). When the ventilation is switched off, the concentrations measured at the ventilation inlet for these species are equaled to those measured in the center of the room but becomes lower than the indoor ones when the ventilation is switched on. In addition, the indoor concentrations of these species decrease significantly when the ventilation is switched on and increase rapidly when the ventilation is switched off. The emissions of most species are probably underestimated, except toluene.

The contribution analysis based on the simulation with measured outdoor data between 8h :20 and 17h :15 (see figure 3.15-3.19) indicates that the emissions are the major indoor source for formaldehyde (97.7%), acetaldehyde (95.3%) and the only source for toluene. In the absence of indoor emissions, the oxidation of VOC becomes the only indoor source of acetone. There are no available measurements of indoor source for isoprene and acrolein.

Under the conditions of this study, the concentrations of these 6 species could be reduced

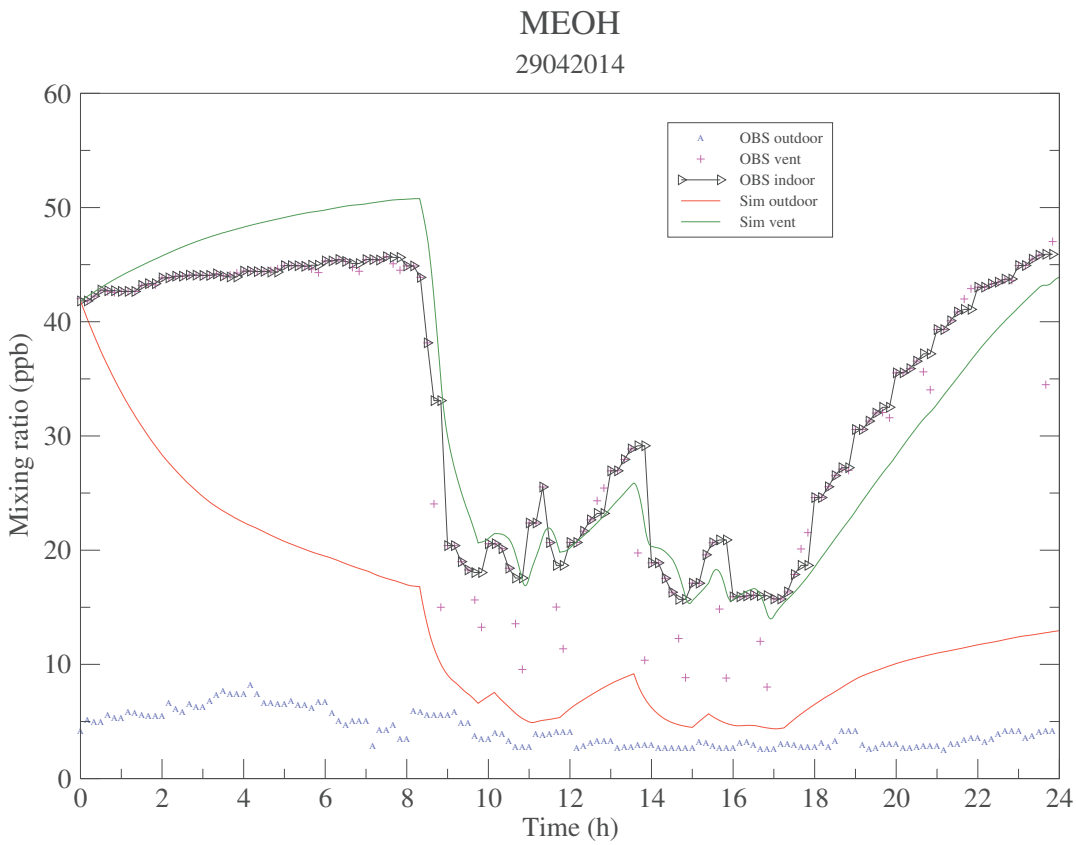

Figure 3.10 – Measured concentrations of methanol (MEOH) for outdoor (OBS outdoor, blue char), the ventilation inlet (OBS vent, magenta +) and the center of the classroom (OBS indoor, black line with triangle right). Modeled concentrations with data for outdoor (Sim outdoor, red line), the ventilation inlet (Sim vent, green line) with INCA-Indoor model.

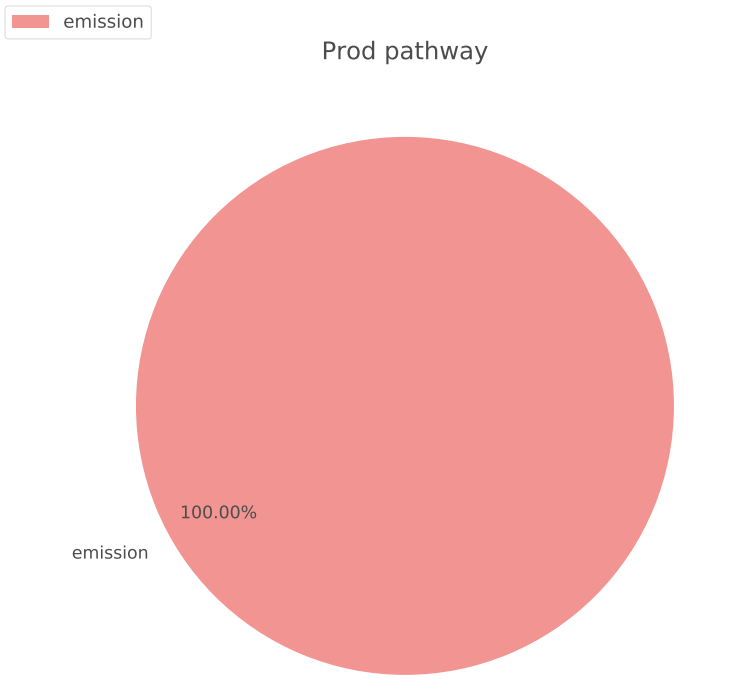

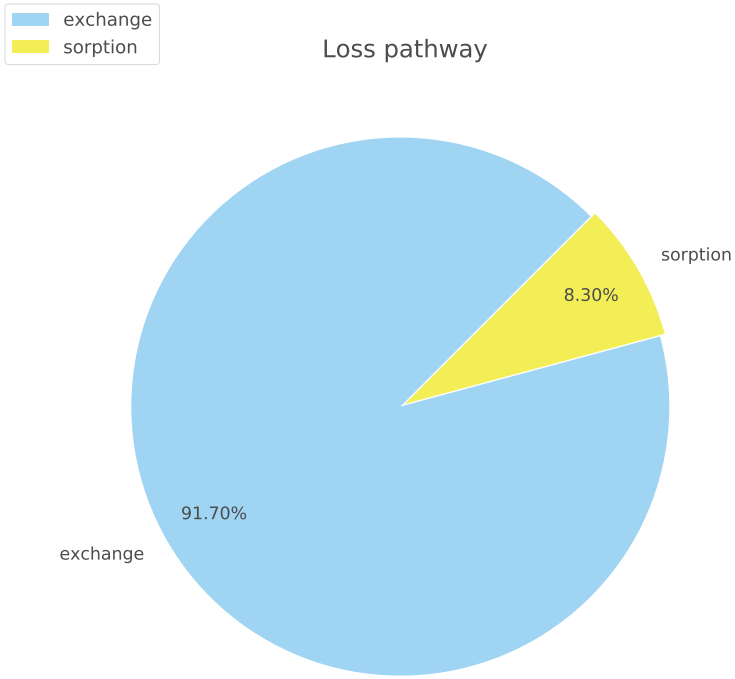

Figure 3.11 – Contributions of production and loss pathways of methanol

significantly by exchanging with outdoor air, which serves as a major loss pathway for all these 6 species. The deposition acts as an important sink for formaldehyde (HCHO) and acetaldehyde (CCHO) and accounts for 35.9% and 12.6% of their total consumption rates. For acetone and acrolein, the sorption is also an important loss pathway, which contributes 27.13% and 61.4%, respectively to their consumption. The oxidation by OH radical is also an important loss pathway for isoprene (31.3%) and acrolein (8.9%).

3.3.3 Analysis of the pollutants originated from indoors and outdoors

Analysis of the concentration levels of benzene

The concentration profiles of benzene have been measured under the same conditions as the previous compounds, and is described are represented in the figure 3.20. There is no emission of benzene measured during the campaign.

In this figure, one can notice the diurnal fluctuations in indoor benzene concentrations but without any significant concentration variations. The maximum, averaged and minimum measured for the indoor concentrations are respectively 0.6 ppb, 0.45 ppb and 0.28 ppb. In addition, the outdoor profile of benzene is not realistic because of the detection limitation of benzene about 1 ppb with the PTR used outdoors with lots of noise for benzene increasing the uncertainty in the model using these data. That is why the simulation with measured outdoor data could not follow the indoor concentration profiles. The simulation with data at the ventilation inlet well represents the indoor concentration profiles but underestimates the indoor ones due to the underestimation of the benzene emission rate. However, with the ventilation inlet data, those underestimations are slightly corrected when the ventilation is switched off. Comparing two types of simulation, the outdoor profile can't be used because of the uncertainty of the measurement. With the data at the ventilation inlet as model input, the difference between the

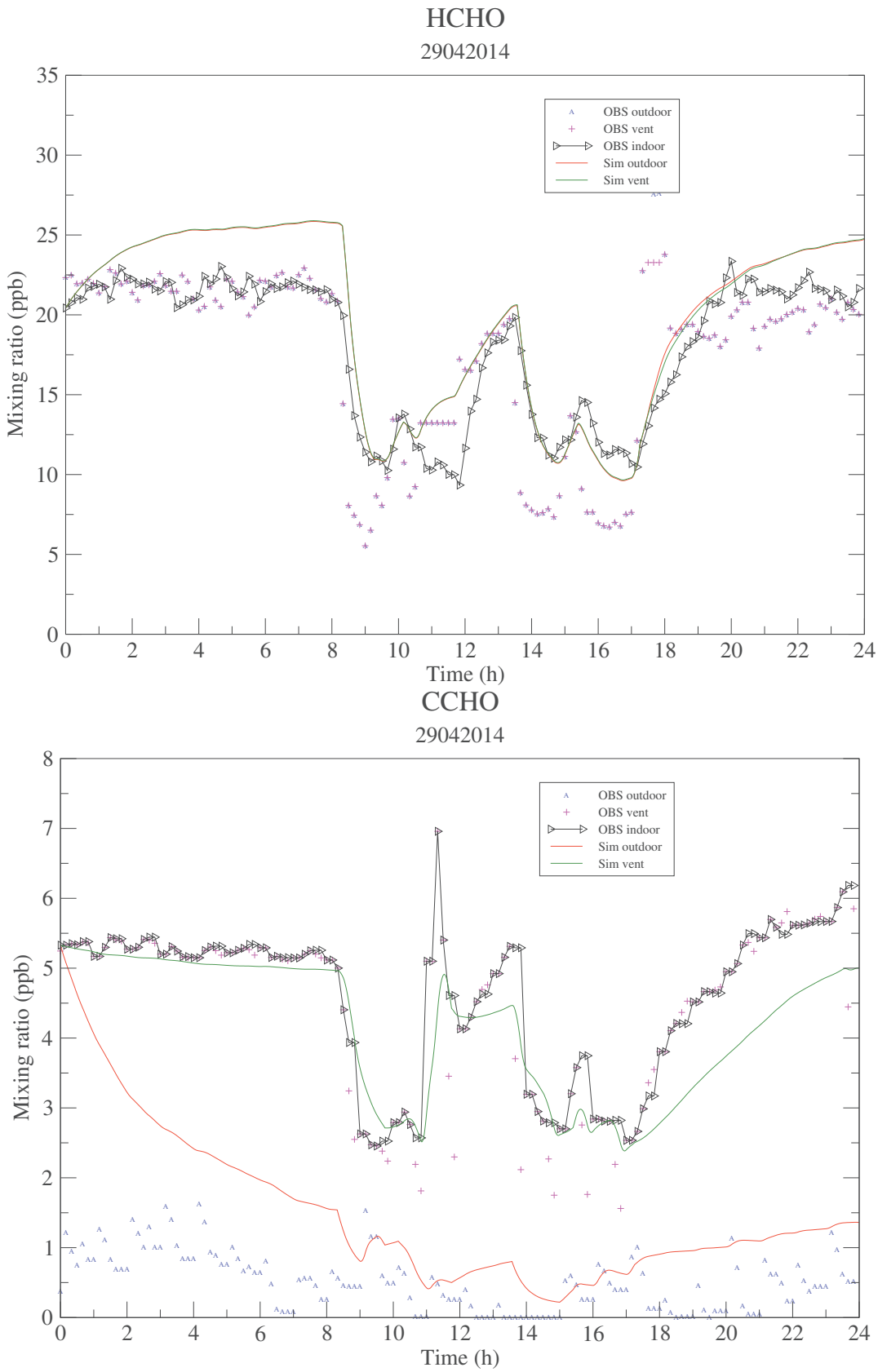

Figure 3.12 – Measured concentrations of formaldehyde (HCHO), acetaldehyde (CCHO) for outdoor (OBS outdoor, blue char), the ventilation inlet (OBS vent, magenta +) and the center of the classroom (OBS indoor, black line with triangle right). Modeled concentrations with data for outdoor (Sim outdoor, red line), the ventilation inlet (Sim vent, green line) with INCA-Indoor model.

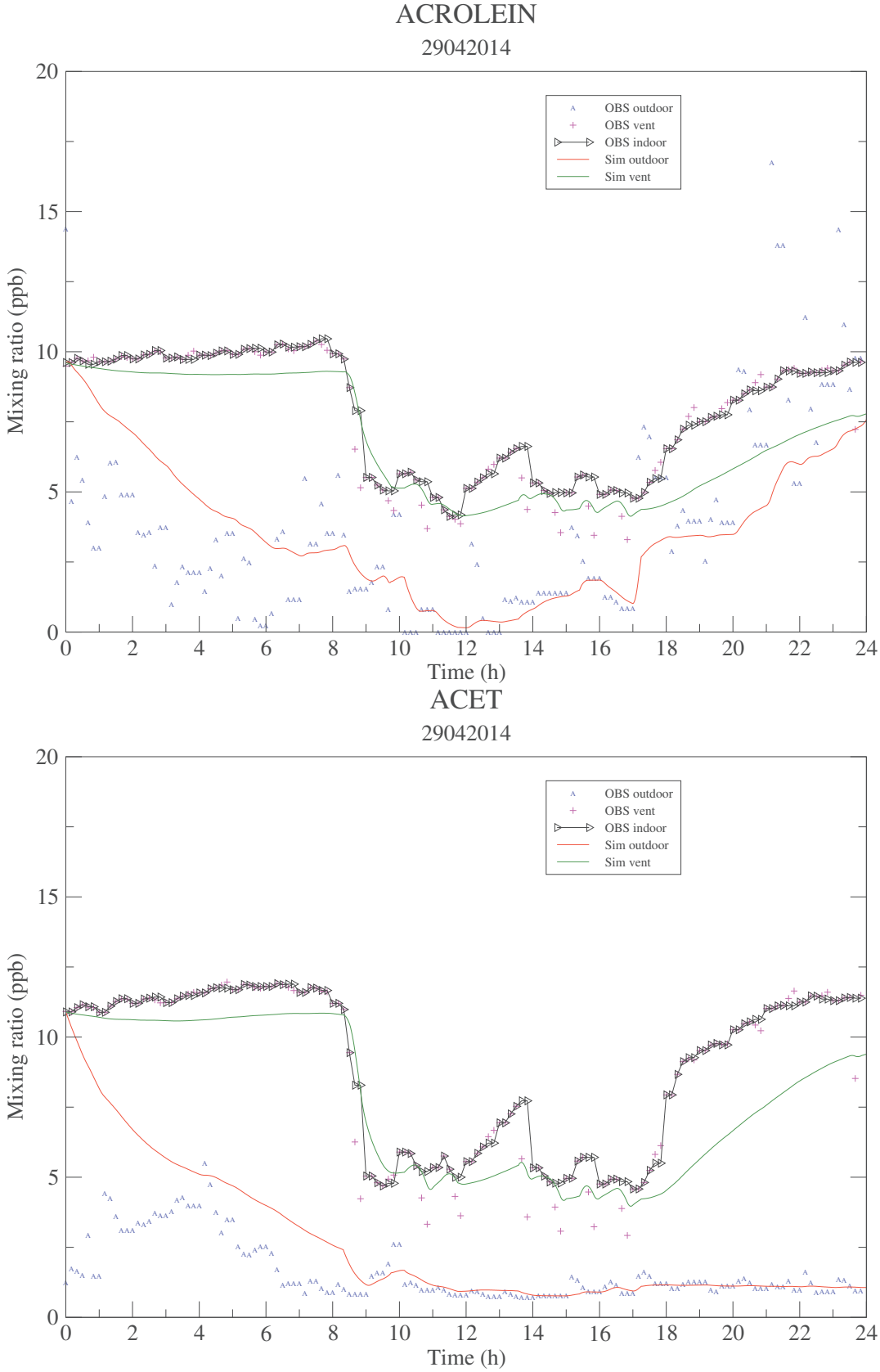

Figure 3.13 – Measured concentrations of acrolein and acetone (ACET) for outdoor (OBS outdoor, blue char), the ventilation inlet (OBS vent, magenta +) and the center of the classroom (OBS indoor, black line with triangle right). Modeled concentrations with data for outdoor (Sim outdoor, red line), the ventilation inlet (Sim vent, green line) with INCA-Indoor model.

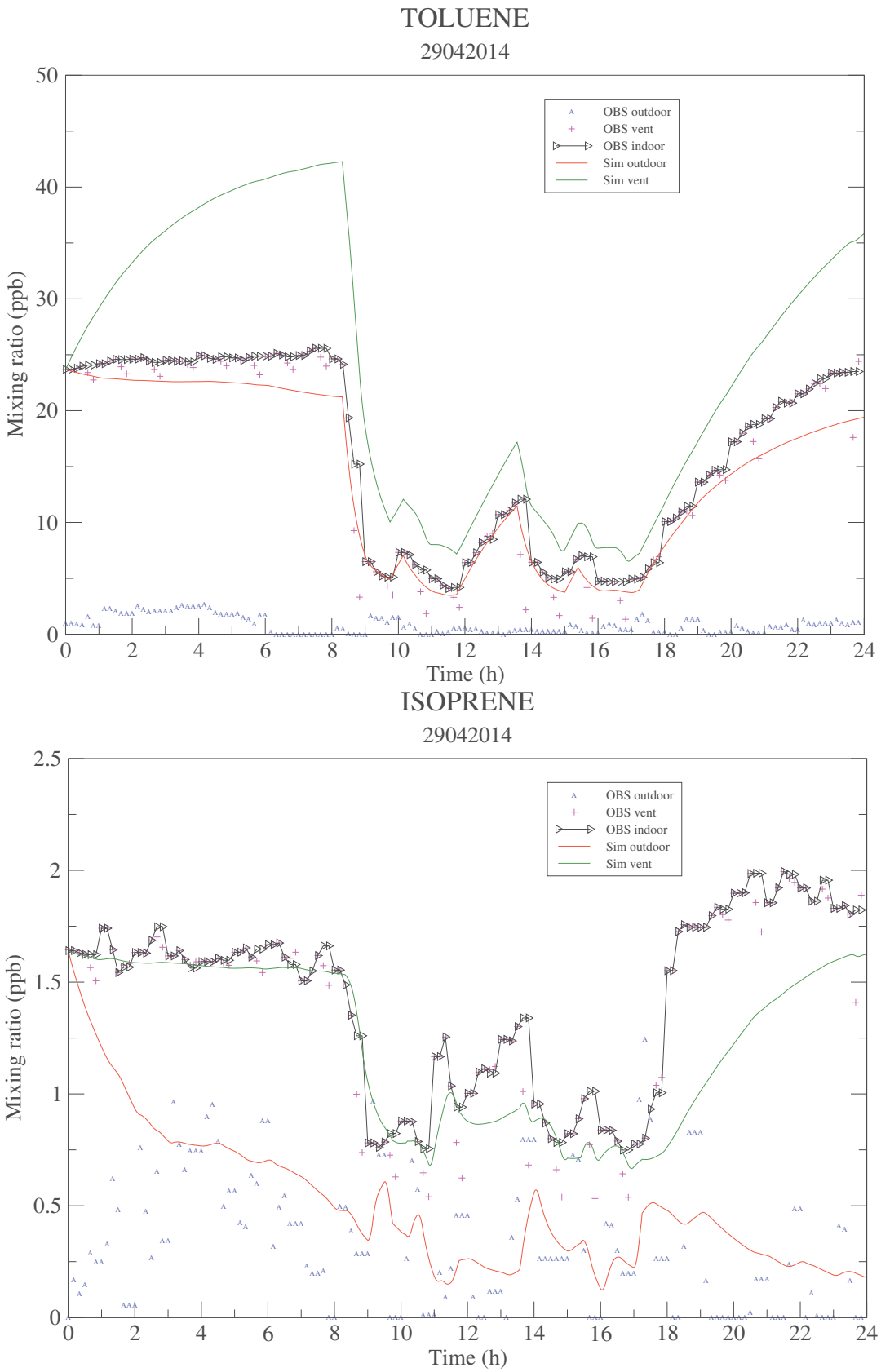

Figure 3.14 – Measured concentrations of toluene (TOLUENE) and isoprene (ISOPRENE) for outdoor (OBS outdoor, blue char), the ventilation inlet (OBS vent, magenta +) and the center of the classroom (OBS indoor, black line with triangle right). Modeled concentrations with data for outdoor (Sim outdoor, red line), the ventilation inlet (Sim vent, green line) with INCA-Indoor model.

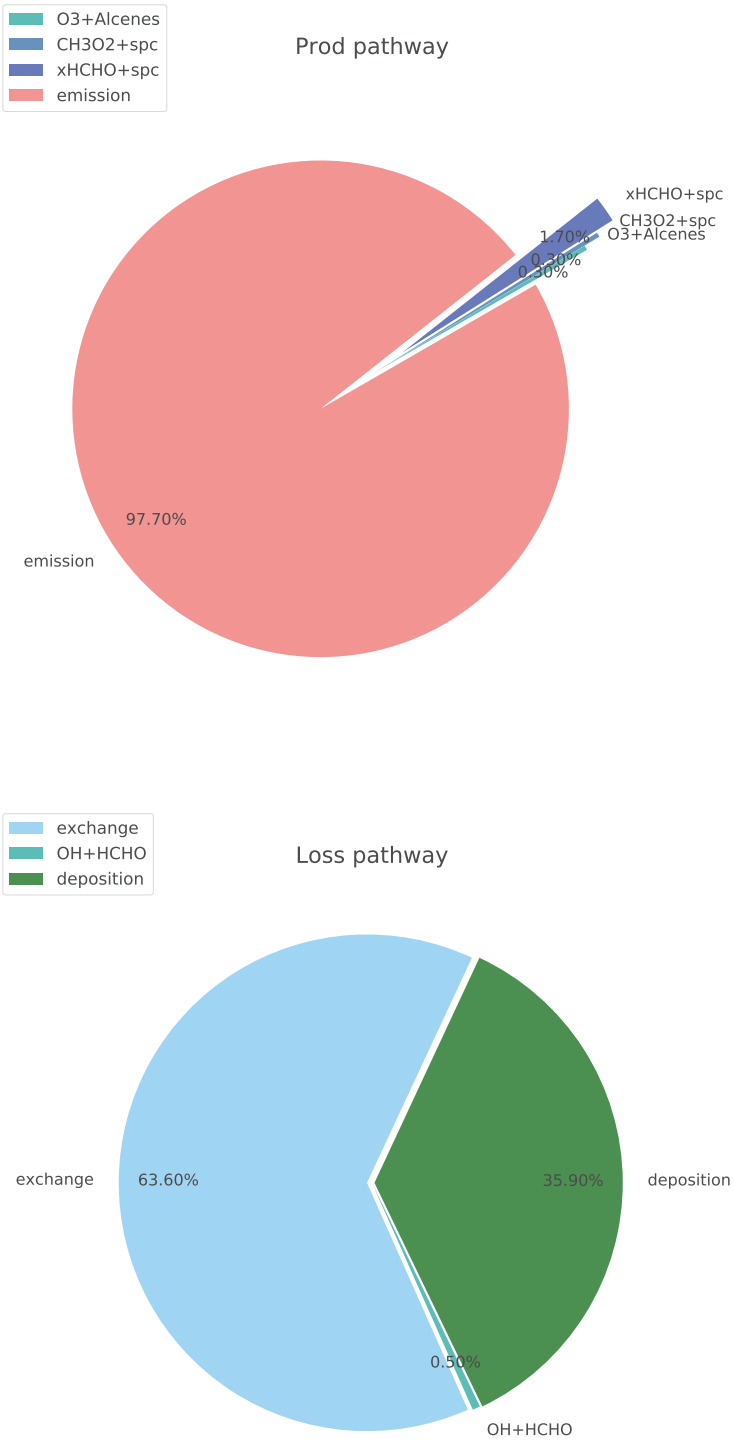

Figure 3.15 – Contributions of production and loss pathways of formaldehyde (HCHO). "Others" represents other reactions producing HCHO. xHCHO represents the chemical species added in SAPRC07 in order to parametrize the formation of HCHO from alkoxy radicals formed in peroxy radical reactions with NO and NO_3 and RO_2.

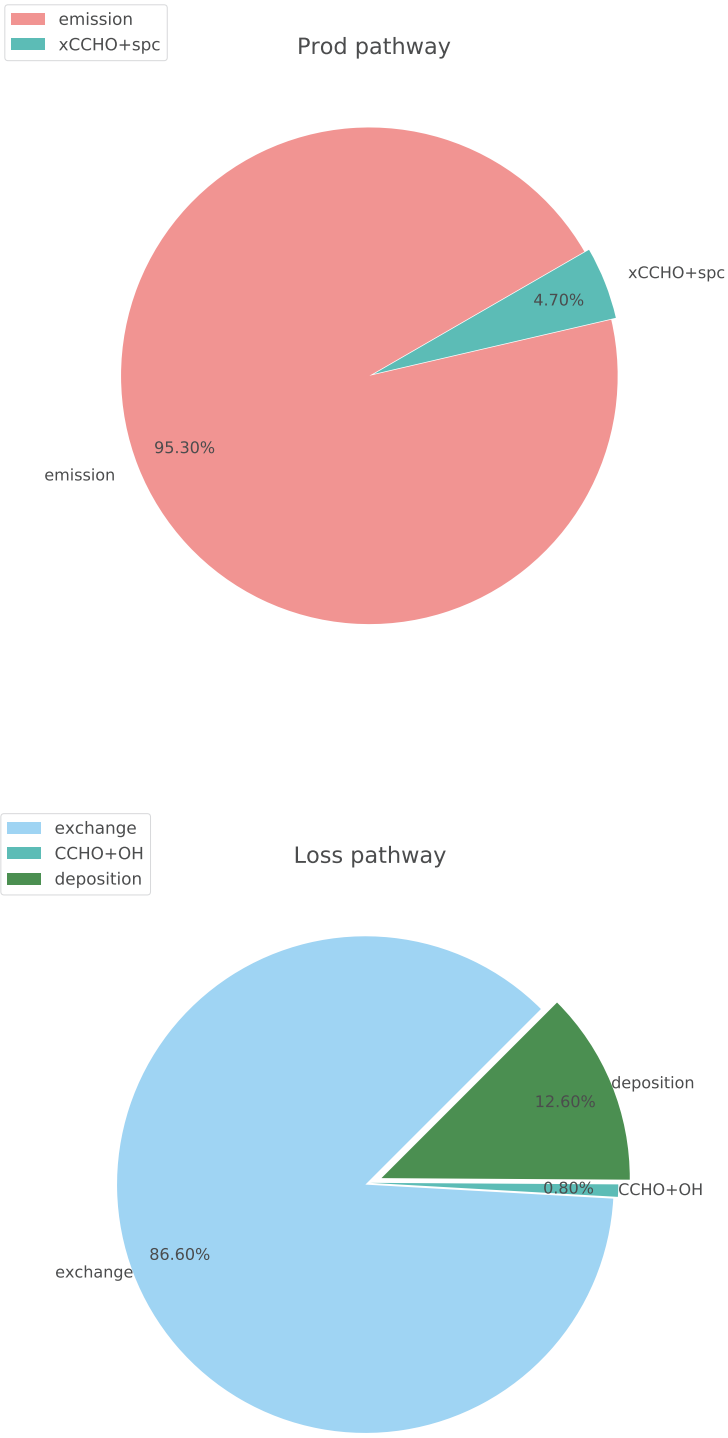

Figure 3.16 – Contributions of production and loss pathways of acetaldehyde (CCHO). xCCHO represents the chemical species added in SAPRC07 in order to parametrize the formation of CCHO from alkoxy radicals formed in peroxy radical reactions with NO and NO_3 and RO_2. "spc" represents species (i.e. NO, methyl peroxy radicals)

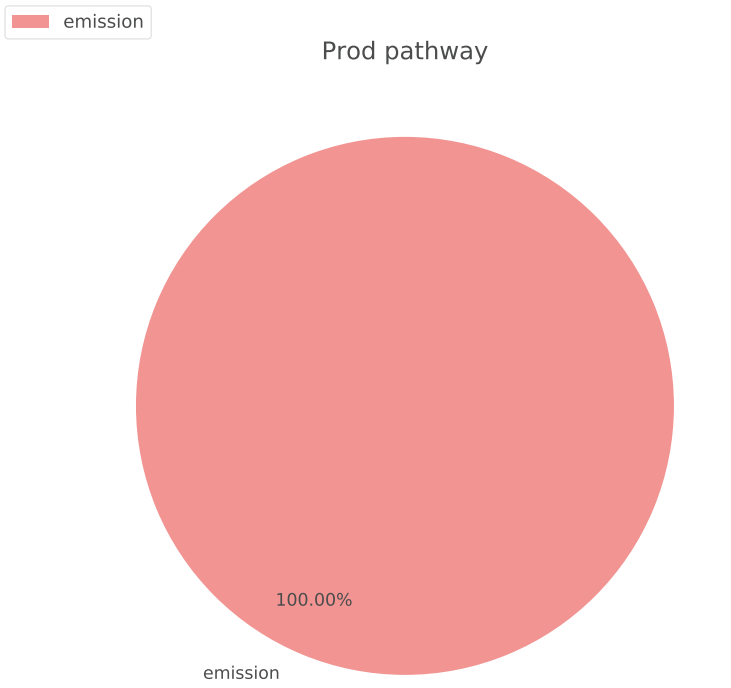

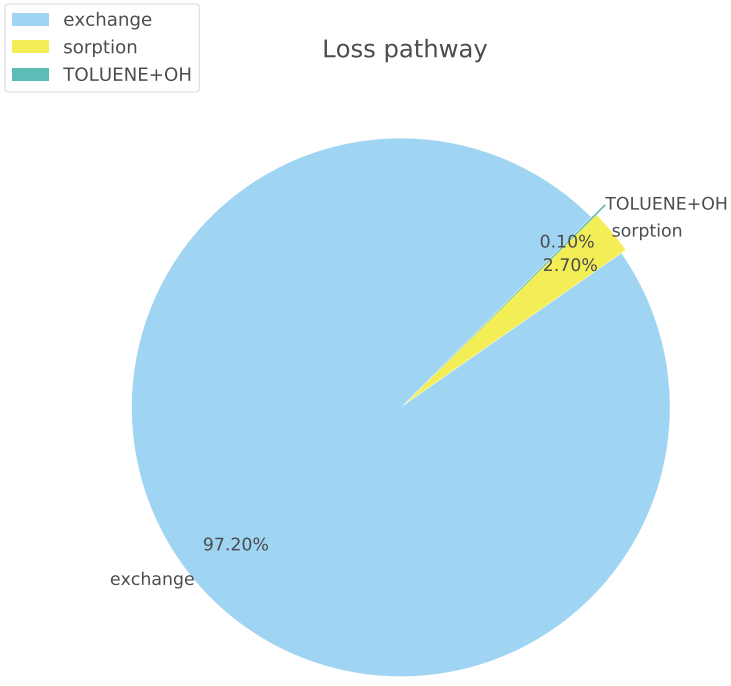

Figure 3.17 – Contributions of production and loss pathways of toluene (TOLUENE)

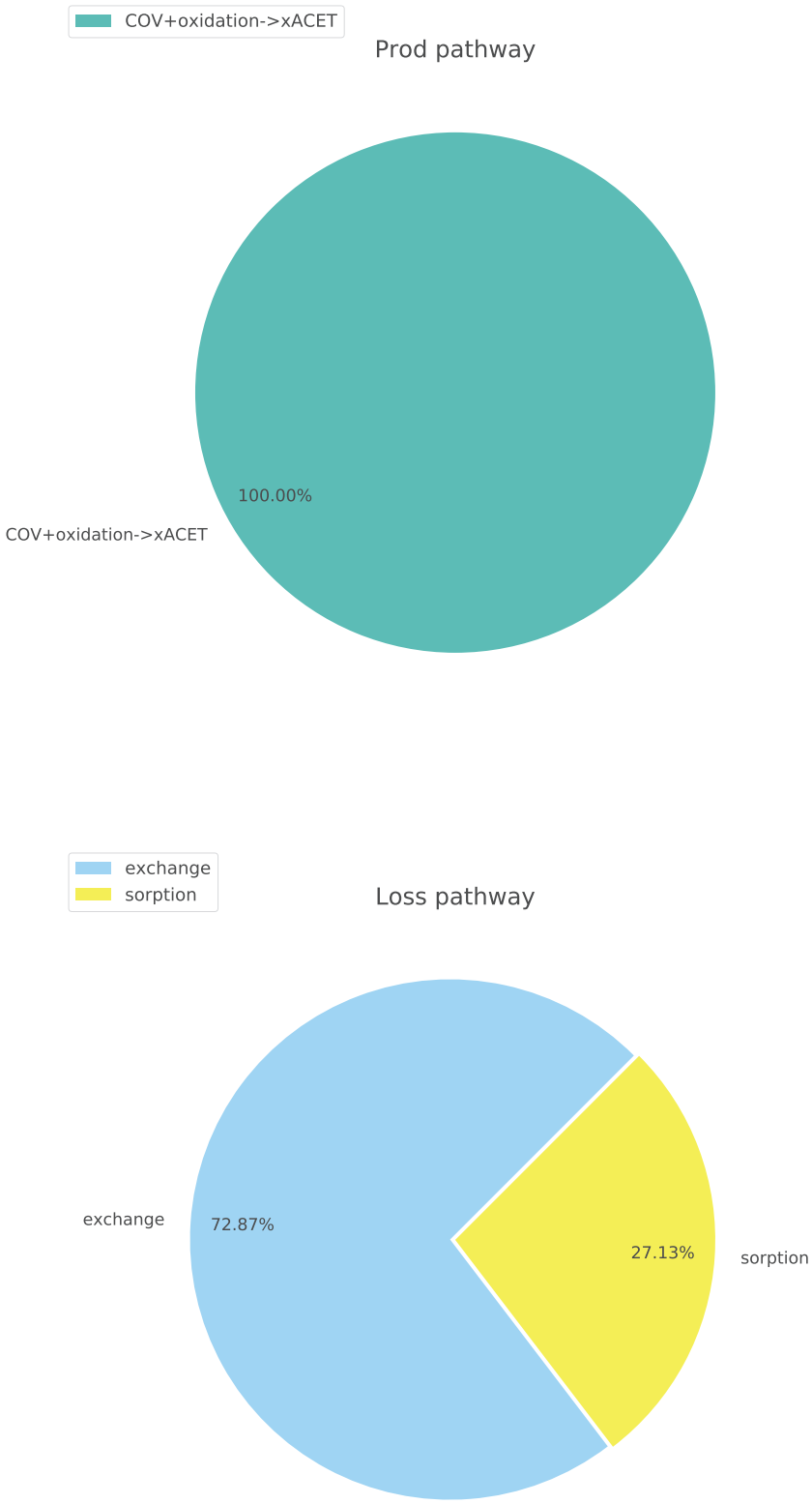

Figure 3.18 – Contributions of production and loss pathways of acetone (ACET)

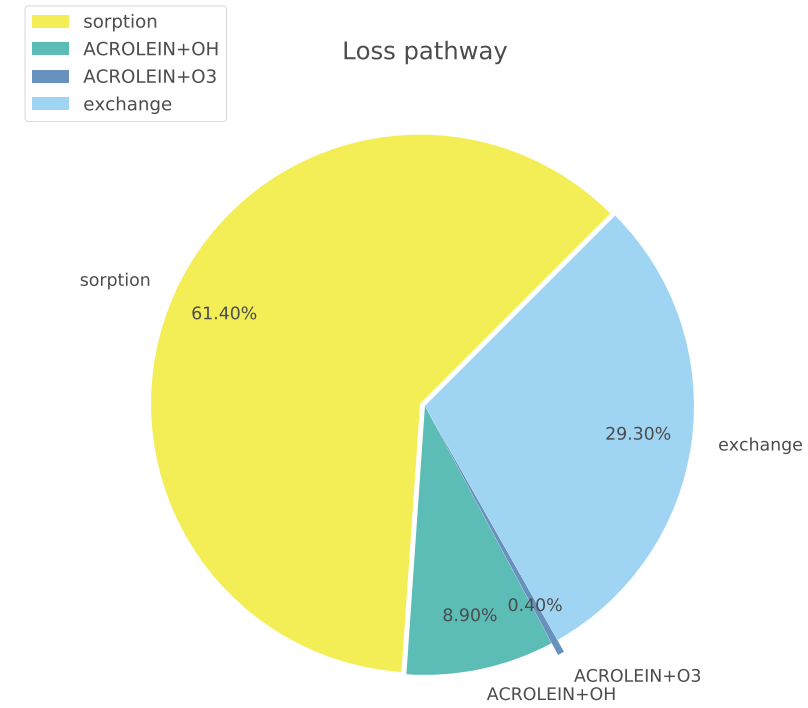

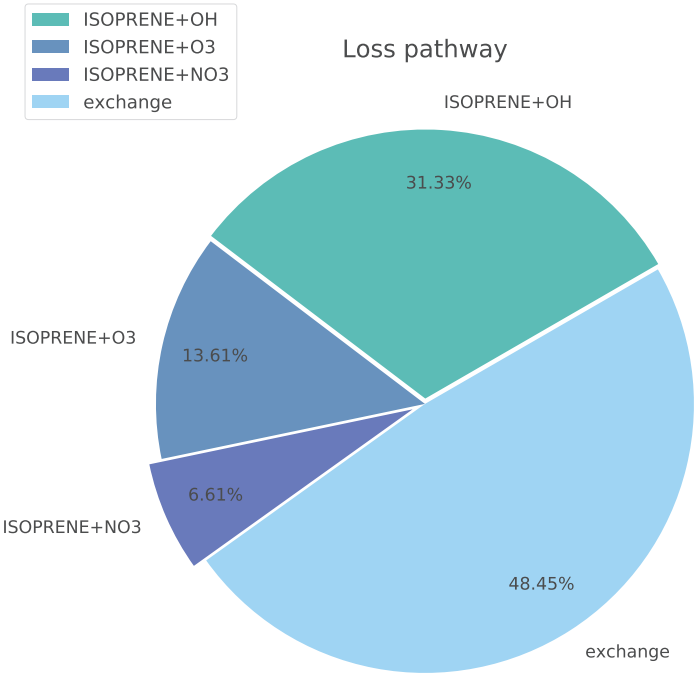

Figure 3.19 – Contributions of loss pathways of acrolein (ACROLEIN) and isoprene (ISOPRENE). There is no indoor source observed for acrolein and isoprene.

measured indoor concentration and the modeled ones is caused probably by the underestimation of the emission rate, which should be partly taken into account in the model.

The contribution analysis based on the simulation with data at the ventilation inlet are presented in figure 3.21. There is no indoor source for benzene. The major loss pathways for benzene are the exchange with outdoor (72.8%) and the sorption (26.9%). There is a minor contribution of reaction of benzene with OH (0.3%) to indoor benzene concentrations.

Analysis of the concentration levels of chlorobenzene and p-dichlorobenzene

The profiles of chlorobenzene and p-dichlorobenzene concentrations are similar to that of benzene (see figure 3.22). No significant variation on the concentration levels measured in the center of the classroom can be noticed for chlorobenzene and p-dichlorobenzene. Same with benzene, there is the uncertainty of measurement for outdoor concentrations and no emission of chlorobenzene and p-dichlorobenzene measured during the campaign. Hence, measured outdoor data should not be used for the simulation. The simulation with data at the ventilation inlet is better for representing indoor ones because the experimental data are of better quality with the indoor instrument. Although the simulation with data at the ventilation inlet well represents indoor ones, the underestimation of the emission rate of chlorobenzene and p-dichlorobenzene was compensated because the effect of infiltration with the ventilation switched off was negligible. Here, it is not suitable to conclude that the simulation with data at the ventilation is better than with outdoors because of the effect the quality of measured data for the species with concentration close to the limitation detection of the instrument used.

The contribution analysis based on the simulation with data at the ventilation inlet between 8h :20 and 17h :15 (see figure 3.23) shows that the ventilation is the most important loss pathway for chlorobenzene and p-dichlorobenzene accounting for 99.7%. In addition, there is no indoor source measured for these two species.

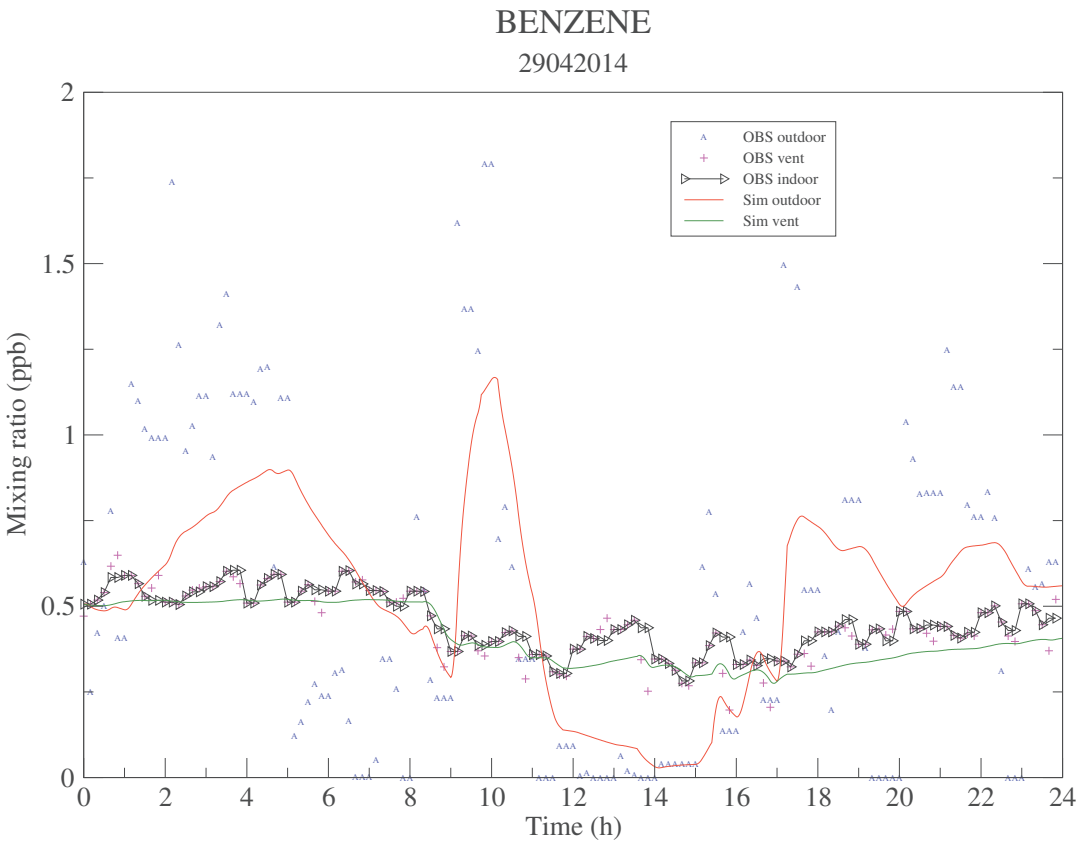

Figure 3.20 – Measured concentrations of benzene for outdoor (OBS outdoor, blue char), the ventilation inlet (OBS vent, magenta +) and the center of the classroom (OBS indoor, black line with triangle right). Modeled concentrations with data for outdoor (Sim outdoor, red line), the ventilation inlet (Sim vent, green line) with INCA-Indoor model.

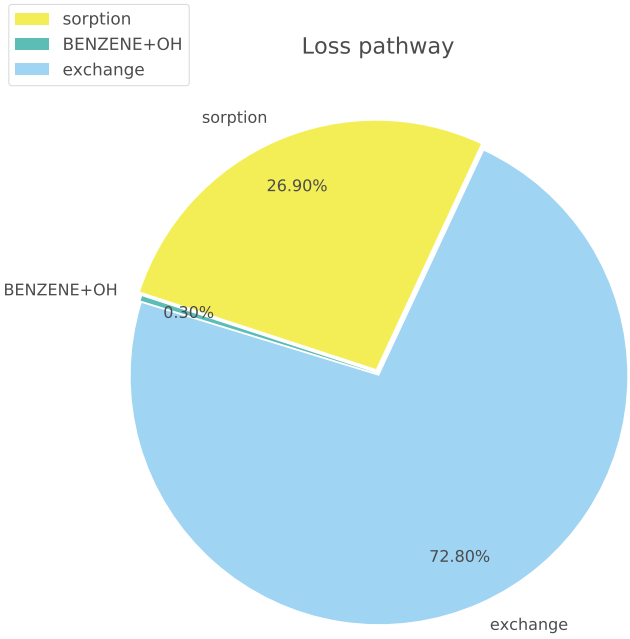

Figure 3.21 – Contributions of loss pathways of benzene. There is no indoor source observed for benzene.

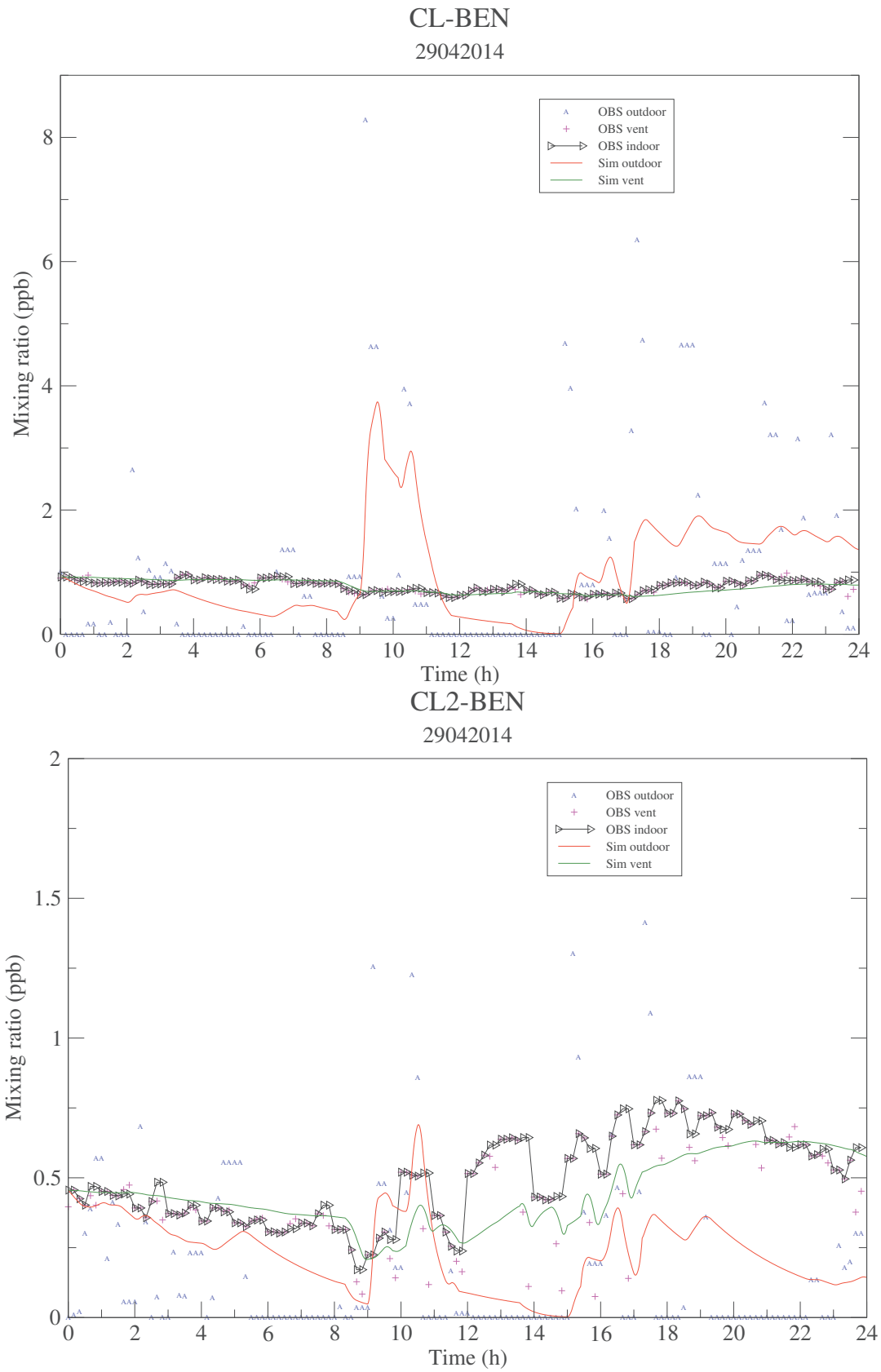

Figure 3.22 – Measured concentrations of chlorobenzene (CL-BEN) and p-dichlorobenzene (CL2-BEN) for outdoor (OBS outdoor, blue char), the ventilation inlet (OBS vent, magenta +) and the center of the classroom (OBS indoor, black line with triangle right). Modeled concentrations with data for outdoor (Sim outdoor, red line), the ventilation inlet (Sim vent, green line) with INCA-Indoor model.

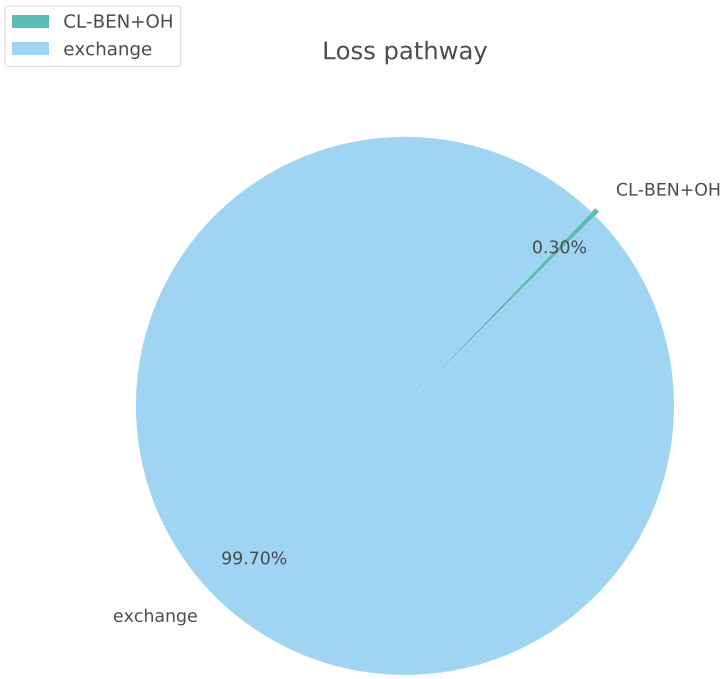

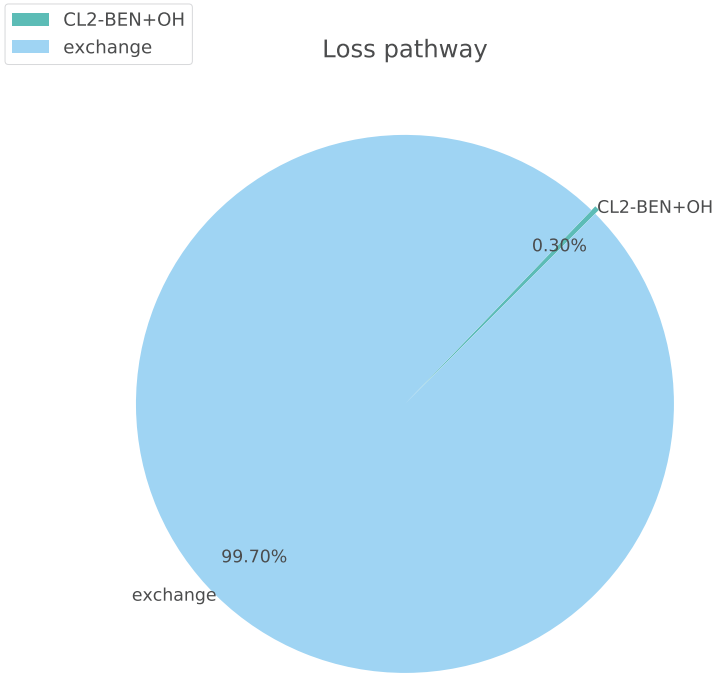

Figure 3.23 – Contributions of loss pathways of chlorobenzene (CL-BEN) and p-dichlorobenzene (CL2-BEN). There is no indoor source observed for chlorobenzene and p-dichlorobenzene

Analysis of the concentration levels of d-limonene

The concentration profiles of d-limonene measured in the center of classroom (OBS indoor), in the ventilation inlet (OBS vent) and outdoor (OBS outdoor) on the 29nd of April are detailed in the figure 3.24. Two types of simulations are also presented in this figure.

The maximum of measured d-limonene concentrations in the center of the classroom reached approximately 3.82 ppb while the minimum was 0.74 ppb obtained during the periods of ventilation. The d-limonene concentrations measured in the center of the classroom tends to decrease before the ventilation is switched on due to the consumption by the reactions of d-limonene with O_3, nitrate radical (NO_3) and hydroxyl radical (OH). Meanwhile, the observed visible fluctuations of d-limonene concentration may point out the contributions of the chemical reactions, the emissions and the infiltration of outdoor air to d-limonene concentration. When the ventilation is switched on, the evolution of d-limonene concentrations is complicated and depends on the balance of production and consumption rates of d-limonene. The combined d-limonene consumption rate of all reactions of d-limonene with O_3 and the radicals NO_3 and OH is 0.46 ppb h^{-1}, while the combined production rate from the emissions and ventilation is 0.27 ppb h^{-1}. Thus the d-limonene concentration decreases from 2.56 ppb at the beginning of the first time of ventilation to 1.18 ppb at the end of the last time of ventilation. When the ventilation is switched off after 17h :15, the d-limonene concentration tends to be stable.

The simulation with measured outdoor data underestimates the indoor ones probably due to the underestimation of emission rate. The simulation results obtained with the data collected from the ventilation inlet are closer to indoor measured concentrations than those obtained with the outdoor data. The INCA-Indoor model using the data collected from the ventilation inlet reproduces well the profile of d-limonene. As discussed in section 3.3.1 for the o-xylene, the simulation with data at the ventilation inlet does not consider the influence of the infiltration with the ventilation switched off and ignore the underestimation of the emission rate.

The contribution analysis based on the INCA-Indoor model between 8h :20 and 17h :15

presented in the figure 3.25 indicates that the indoor d-limonene concentrations were produced primarily via emissions. The reactions of d-limonene with ozone (39.9%) appears as a major sink for d-limonene compared to reactions of d-limonene with the NO_3 (26.2%), the exchange with outdoor air (23.4%) and reaction with OH radicals (10.5%).

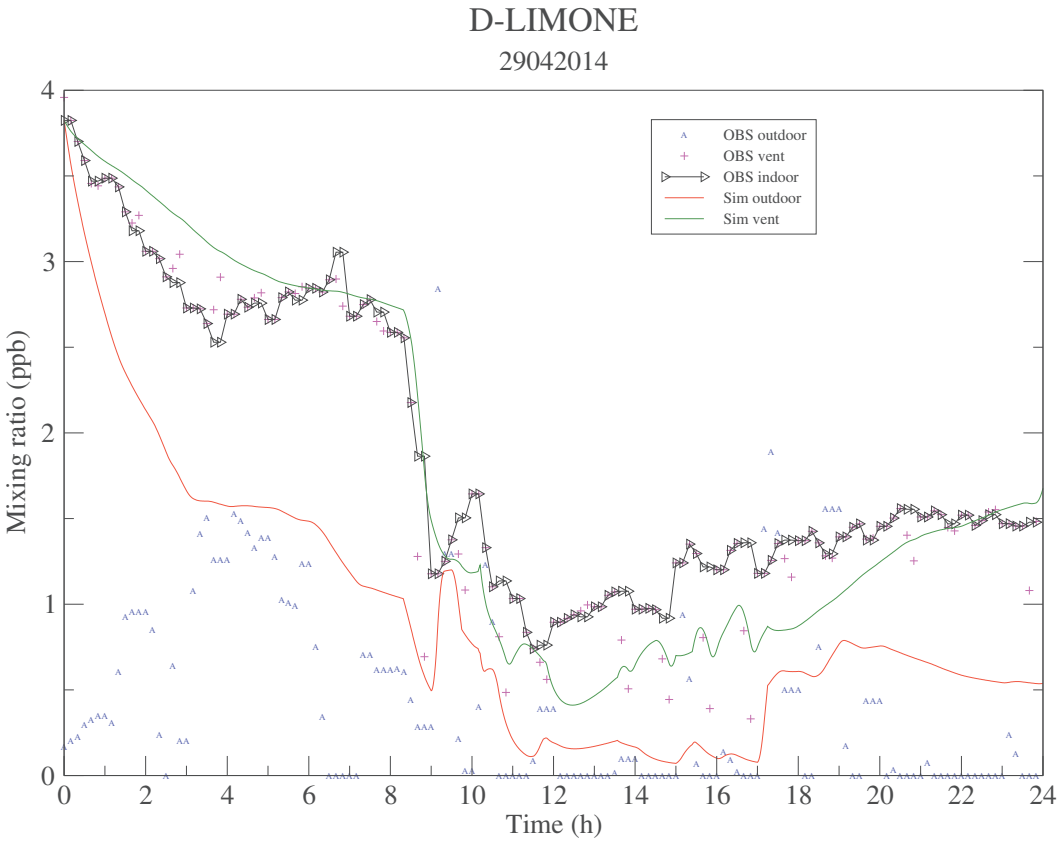

Figure 3.24 – Measured concentrations of d-limonene (D-LIMONE) for outdoor (OBS outdoor, blue char), the ventilation inlet (OBS vent, magenta +) and the center of the classroom (OBS indoor, black line with triangle right). Modeled concentrations with data for outdoor (Sim outdoor, red line), the ventilation inlet (Sim vent, green line) with INCA-Indoor model.

3.3.4 Summary

The indoor averaged concentrations for these 15 species measured during MERMAID campaign are regrouped in the table 3.9 for the three periods (before the first episode of the ventilation

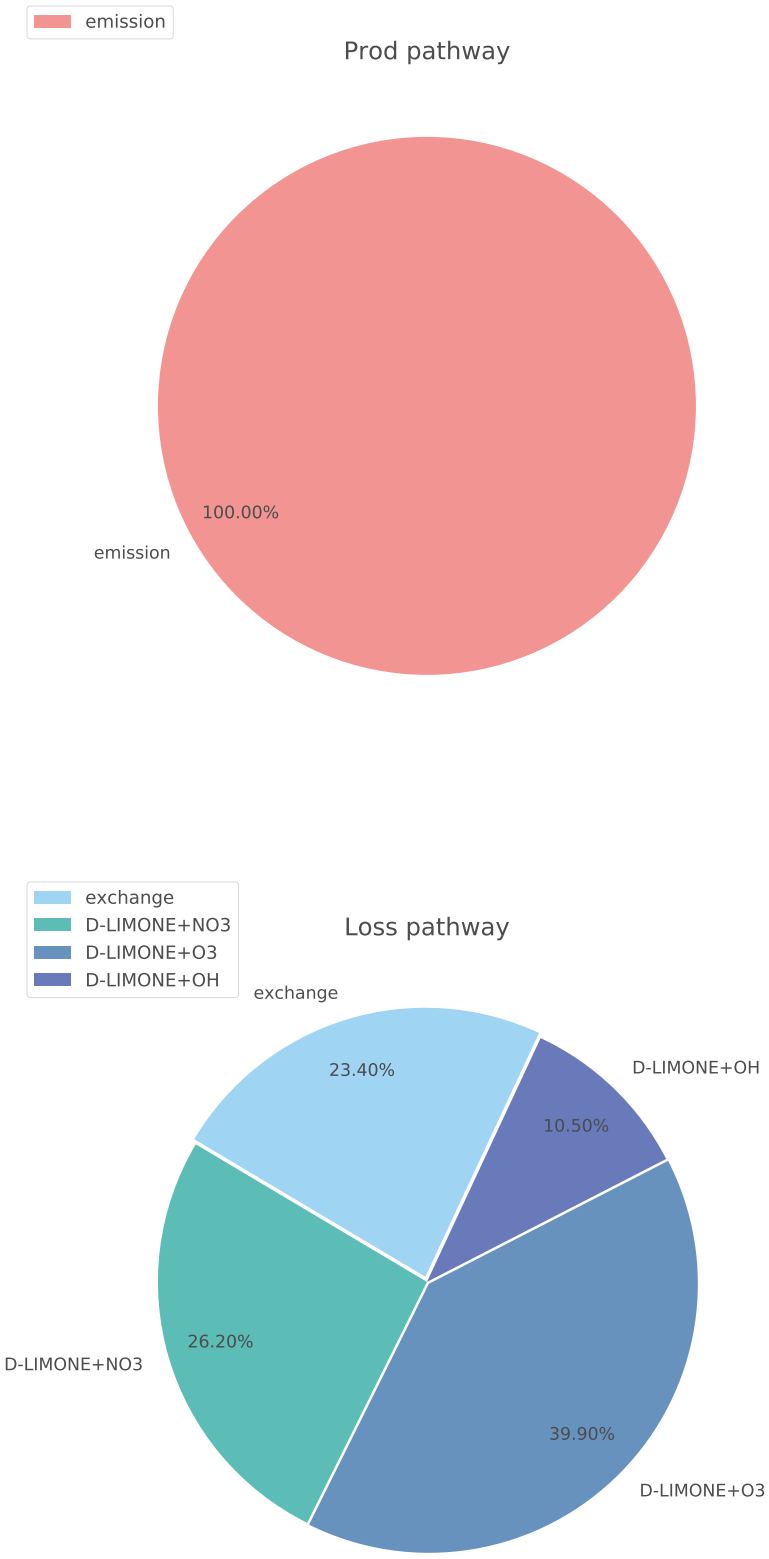

Figure 3.25 – Contributions of production and loss pathways of d-limonene

switched on (00h :00-8h :20), during the ventilation switched on or off (8h :20-17h :15) and after the ventilation switched off (17 :15-24 :00)). Compared with the concentrations measured before the ventilation is active, the indoor NO, NO_2 and O_3 concentrations during the ventilation active increase markedly due to the outdoor-to-indoor transport. Indoor O_3 concentration increases of 521.11%, which is mainly caused by the injection of O_3. Indoor dichlorobenzene concentration increases by 26.32% but the concentrations of the other 11 VOCs decrease by significantly between 22.09% and 70.08%. Especially for toluene, the concentration decreases up to 70.08%. This reflects the importance of the ventilation to decrease indoor concentrations of some VOCs, but not all.

The contribution of different processes to NOx, O_3 and VOCs concentrations from 8h :20 to 17h :15 when the ventilation active have also been quantified. Results show that ventilation is the major loss pathway for VOC except for d-limonene with an air exchange rate (AER) of 2.17 h^{-1}, which is higher than averaged AER of 0.76 h^{-1} for residential setting [156]. With high air exchange rate, the chemical formation and loss pathways for most of VOC are insignificant compared to the physical processes.

After the ventilation is switched off, indoor averaged concentrations of 12 VOCs increase but the NOx and the O_3 decrease compared to those measured during the ventilation active. But compared with those measured before the ventilation active, indoor averaged concentrations of O_3, isoprene and dichlorobenzene increase but other species decrease. Figures 3.19 and 3.21 show that after the ventilation is switched off, some VOC concentrations increase slowly up to the levels similar to those measured before the ventilation is switched on. These VOCs include formaldehyde, acetaldehyde, acrolein, acetone, toluene and isoprene, which have indoor source.

Mean contributions (%) of different processes for targeted species between 8h :20 and 17h :15 are shown in table 3.10. Indoor concentrations of NO and NO_2 are mainly controlled by the exchange with outdoor air and indoor chemistry. The deposition of O_3 is a major loss pathway for O_3. Due to the injection of O_3 as one of its sources, the contributions of the ventilation

to O_3 concentrations become less important than those to NO and NO_2. Furthermore, indoor chemistry contributes little to O_3 concentrations. Most of VOCs concentrations are significantly impacted by the ventilation. For VOCs originated from indoors and outdoors, the contributions of the ventilation accounts for up to 74.4%-99.5% (i.e. o-xylene, p-dichlorobenzene). Major source of VOC mainly originated from indoors is the emission, which accounts for 44.5% to 43.9% for their concentrations (i.e. formaldehyde, toluene). Indoor chemistry is an important loss pathway for isoprene and d-limonene, but not important for other VOC concentrations. For organic compounds in this study, only the concentrations of formaldehyde and acetaldehyde are impacted by the deposition, whose contributions are 19.7% and 7.0%, respectively. The sorption can be important for some VOCs like benzene, acrolein and acetone but has negligible influence for other organic compounds.

Table 3.9 – Comparasion of indoor concentrations measured before, during and after the ventilation

Species	before vent (00h :00-8h :20)	vent (8h :20-17h :15)	Biais relative(%)	after vent (17h :15-24h :00)	Biais relative(%)
NO	0.86	1.02	18.60	0.85	-1.16
NO_2	3.78	6.04	59.79	2.64	-30.16
O_3	3.41	21.18	521.11	7.15	109.68
formaldehyde	21.64	13.12	-39.37	19.89	-8.09
methanol	44.21	21.36	-51.69	35.24	-20.29
acetaldehyde	5.27	3.65	-30.74	4.95	-6.07
acrolein	9.93	5.53	-44.31	8.17	-17.72
acetone	11.47	5.78	-49.61	9.92	-13.51
toluene	24.63	7.37	-70.08	16.92	-31.30
isoprene	1.62	0.98	-39.51	1.76	8.64
d-limonene	2.95	1.20	-59.32	1.45	-50.85
o-xylene	1.64	0.83	-49.39	0.87	-46.95
benzene	0.55	0.38	-30.91	0.44	-20.00
chlorobenzene	0.86	0.67	-22.09	0.82	-4.65
p-dichlorobenzene	0.38	0.48	26.32	0.66	73.68

Table 3.10 – Mean contributions (%) of different processes between 8h :20 and 17h :15. *Emission of O_3 indicates its injection.

Species	exchange	deposition	sorption	emission	chemistry
NO	49.8	0	0	0	50. 2
NO_2	63.1	0	0	0	36.9
O_3	26.1	44.8	0	25.5*	3.6
formaldehyde	34.8	19.7	0	44.5	0.8
methanol	53.0	0	4.8	42.2	0.0
acetaldehyde	47.6	7.0	0	43.7	1.8
acrolein	29.2	0	61.2	0	9.4
acetone	55.9	0	20.8	0	23.1
toluene	54.5	0	1.5	43.9	0.1
isoprene	48.4	0	0	0	51.6
d-limonene	13.4	0	0	42.5	44.0
o-xylene	74.4	0	0	24.3	1.2
benzene	72.8	0	26.9	0	0.3
chlorobenzene	99.7	0	0	0	0.3
p-dichlorobenzene	99.5	0	0	0	0.5

3.3.5 Quantitative assessement of the model

The American Society for Testing and Materials (ASTM) (1991) recommended quantitative factors used to assess the general agreement between the model predictions and measurements [123]. The values for the various quantitative criteria recommended by the ASTM are given in the second chapter.

The correlation coefficient is useful to evaluate the ability of the model to reproduce the temporal variability of the observations. The fractional bias allows the detection of the global underestimations or overestimation, but this index may hide error compensation. The NMSE allows to evaluate the mean error without any compensation (because taking the square of the error).

The ASTM recommends that a model may meet one or more criteria and still be inadequate, or a model may fail one or more criteria and still be adequate for the task. In the table 3.11 are summarized the results of statistical analysis between measured and predicted concentrations.

According to the linear regression analysis, the ideal agreement condition is indicated by a slope of unity and an intercept of zero. The slope and the intercept were generally very close to unity and zero, respectively, which imply that the measured concentrations were in good agreement with the predicted concentrations.

The linear regression between the measurements and predictions for selected species shows relatively good agreement, with a slope between 0.40 and 1.34, an absolute intercept between 0.0 and 5.59, and R^2 between 0.49 and 0.96. Although the results of statistic analysis for NO, HCHO and p-dichlorobenzene fail the criteria recommended by the ASTM, the INCA-Indoor model reproduces well the concentration profiles for these species.

Table 3.11 – Quantitative comparison of predictions of model based on measured outdoor data with experimental indoor data

Species	biais relative	Correlation coefficient	NMSE	Regression slope	Regression intercept	Regression r^2
NO	87.55	0.84	5.25	1.07	-0.84	0.70
NO_2	30.56	0.96	0.16	1.52	-2.33	0.93
O_3	34.25	0.98	0.15	0.95	-2.18	0.95
methanol	61.09	0.76	0.94	0.60	-6.16	0.57
formaldehyde	12.68	0.95	0.02	1.16	-0.97	0.90
acetaldehyde	68.47	0.49	1.56	0.49	-0.74	0.24
acrolein	57.65	0.75	0.73	0.86	-3.12	0.56
acetone	72.68	0.56	1.95	0.49	-1.70	0.31
benzene	48.30	0.48	0.27	1.55	-0.17	0.22
toluene	12.88	0.99	0.02	0.90	-0.26	0.98
o-xylene	40.97	0.93	0.20	1.22	-0.59	0.86
chlorobenzene	80.60	0.0	0.82	-0.04	1.01	0.0
p-dichlorobenzene	51.80	0.04	0.94	0.03	0.22	0.00
isoprene	63.16	0.26	1.43	0.20	0.22	0.07
d-limonene	57.15	0.93	0.56	0.87	-0.71	0.86

3.4 Conclusion

The measurements obtained during the MERMAID campaigns allow to detect the main indoor pollutants and identify the behaviors of these compounds over time. In this chapter, the mea-

sured data for a typical day (29th of April in 2014) in a classroom of a low energy school buildings in France is presented and analyzed. The measurement results show temporal variability in concentrations of NOx, O_3 and 12 VOCs classified as hazardous air pollutants. Thus we distinguished between several types of air pollutant that were, in the classroom studied here, mainly issued from outdoor sources, indoor sources, or both.

Although the measurements during MERMAID campaign provide useful information about temporal variabilities in the concentrations of NOx, O_3 and 12 VOCs and indicate some sources and sinks for these compounds, there are no available data to assess the relative importance of different chemical and physical processes for the concentrations of targeted species. Thus the INCA-Indoor model also helped to quantify the contributions of different processes to pollutant concentrations.

Two types of simulations (considering the data outdoor (Sim outdoor) and at the ventilation inlet (Sim vent)) were performed for the 15 species of interest in this chapter. The simulation with data at the ventilation inlet well represents the indoor concentration profiles but underestimates the indoor ones due to the underestimation of the emission rate when the ventilation is switched on (i.e. 3.10). However, when the ventilation is switched off, simulations with measured at the ventilation inlet do not consider the effect of infiltration. Simulations with outdoor data represent the evolution of the concentration profiles but underestimate the indoor ones due to the underestimation of the emission rates (i.e. 3.8). However, simulations with measured outdoor data could not always follow the indoor concentration profiles (i.e. 3.20, 3.22) because of the detection limitation of instruments used outdoors causing the increase of the uncertainty in the model using outdoor data.

Contribution analysis based on the simulation with measured outdoor data confirms that indoor emissions are the major sources for most of VOCs (i.e. methanol, formaldehyde and acetaldehyde) and that the oxidation of VOCs can be an important source for several compounds like acetone.

Simulations with measured outdoor data as model input indicate that indoor O_3 and NOx concentrations showed a critical dependence on the outdoor values. The concentrations of indoor O_3 and NOx increase when the ventilation is switched on. Although there is o-xylene emitted by indoor materials, the comparisons of the data measured and simulated showed that indoor o-xylene was mainly issued from outdoor through the ventilation when the ventilation is switched on. The delay between peaks in outdoor and indoor concentrations allowed us to conclude that the model probably underestimates the infiltration processes, that were not measured everyday during the MERMAID campaign, but are varying from one day to another as function of the local meteorology. One of our first recommendation would be to measure continuously this infiltration rate in future indoor air quality campaign. The underestimation of modeled o-xylene concentration is probably due to the underestimation of the emission rates.

Most of the other VOCs concentrations are almost constant during night when the ventilation is switched off, and then decrease as soon as the ventilation is switched on but increase when the ventilation is again switched off. These VOCs include formaldehyde, acetaldehyde, methanol, toluene, acrolein, acetone and isoprene. It is showed that INCA-Indoor model does simulate these night concentrations while our simulations probably underestimate the infiltration processes using measured data at the ventilation inlet. The model very well simulates the decrease of these VOC concentrations due to the ventilation but tends to underestimate the increase of VOC concentrations at the end of the day and when the ventilation is switch off again. This increase is due to the surface emission factors. The underestimations of the model tends to show that the surface emission factors are also underestimated.

The evolution of d-limonene concentration is more complex to explain. The d-limonene concentration tends to decrease before the ventilation is switched on due to the consumption by reactions of d-limonene with O_3, nitrate radical (NO_3) and hydroxyl radical (OH). When the ventilation is switched on, the d-limonene concentration depends on the balance of production and consumption rates of d-limonene. According to the no-regular fluctuations in d-limonene

concentration, it suggests that chemical reactions may play a more important role for d-limonene concentration compared to other VOCs concentrations.

For benzene, chlorobenzene and p-dichlorobenzene, there is no indoor source observed during MERMAID campaign and the measurements are showing low concentrations close to the limit of their uncertainties (see 3.20, 3.22). Simulations with measured data at the ventilation inlet show that the concentrations of benzene and chlorobenzene are not significantly impacted by the ventilation. However, modeled concentrations of benzene, chlorobenzene and p-dichlorobenzene with measured outdoor data were strongly affected by the outdoor concentrations. However, the outdoor profile of benzene, chlorobenzene and p-dichlorobenzene are not realistic because of the detection limitation of instruments used outdoors causing the increase of the uncertainty in the model using outdoor data.

The ventilation is a major pathway to reduce most of VOC concentrations. In addition, the deposition is also important for reducing the concentrations of formaldehyde and acetaldehyde. For acetone and acrolein, the sorption accounts for 35.08% and 49.60% respectively of the total consumption rates. The indoor chemistry appears as important loss pathway for acrolein, isoprene and d-limonene through their reactions with OH radical or O_3.

We can conclude that emissions, exchange with outdoor air are very sensitive processes that would need to be better represented in the model, especially infiltration. Deposition and indoor chemistry (OH + VOC) were other important processes impacting specific species like d-limonene, actaldehyde, etc. The effect of these processes will be discussed in next chapter. In addition, the accuracy of the simulations is impacted by the experimental limitations like the infiltration rate, emission rate and the detection limitation of instruments used.

CHAPTER 4

IMPACT OF SELECTED PARAMETERS ON INDOOR AIR QUALITY IN A LOW ENERGY BUILDING

Abstract

The effect of emission and sorption rates, air exchange rate and the light intensity transmitted by different windows on indoor air quality has been investigated in this chapter. With data collected during MERMAID campaign, simulations have been carried out under indoor conditions to assess the effect of these parameters.

Results show that VOC concentrations increase with increasing their emission rates. With increasing AER (from 2.16 to 4.32 h^{-1}) when the ventilation switched on, for the species originated mainly from outdoors, the maximum concentrations of NO, NO_2 and O_3 increase by 60.86%, 17.08% and 3.4% respectively. The concentrations for methanol, toluene and o-xylene decrease with increasing AER. With increasing AER from 1.08, 2.16 to 4.32 h^{-1}, the maximum concentrations of formaldehyde and acetaldehyde increase, but the mean and minimum concentrations decrease. There is minor change for acrolein and acetone, benzene, isoprene, d-limonene, chlorobenzene and p-dichlorobenzene with increasing AER.

The variation of sorption rates (k_a and k_d) has a minor influence on benzene concentration and negligible influence for other VOC and NOx concentrations. The photolysis of HONO increases with increasing the transmittance for UV and visible light and more OH produced by the HONO photolysis. In addition, some VOC (i.e d-limonene, o-xylene, isoprene) decrease due to the reactions with OH.

4.1 Introduction

The principal indoor pollutants found in indoor environments include nitrogen oxides, ozone and airborne particles originated outdoors [157], aldehyde, radon, asbestos, tobacco smoke and volatile organic compounds (VOC) arising from indoor sources [158], etc. The diverse aspects of indoor pollutants have been investigated like sources, concentrations and health effects. Over two hundred volatile organic compounds (VOCs) have been identified in the indoor environment [159]. Volatile organic compounds (VOCs) are ubiquitous pollutants emitted by several indoor sources like building products (paint, flooring, carpet, gypsum board. . . etc) and household products (waxes, detergent, deodorizers. . . etc). They have hazardous effects on human heath like asthma, wheezing, allergic rhinitis, and eczema [160, 161]. Mainly originated outdoors, NO_2 acts mainly as an irritant affecting the mucous of the eyes, nose, throat and respiratory tract [162] and O_3 has reversible effects on respiratory symptoms and pulmonary function [163].

Indoor air quality are controlled by diverse physical and chemical process, such as air exchange with outdoor, gas-surface interactions of trace gases onto/from indoor surfaces such as emission, sorption or heterogeneous reactivity, and gas-phase chemical reactions [48]. The concentration of an indoor pollutant depends not only on its indoor emission rate, but also on the rate at which it is being transported from outdoors to indoors, and the rates at which it is scavenged by indoor surfaces, consumed by indoor chemistry and removed by ventilation or filtration [158]. As discussed in chapter 3, emission and ventilation are the two main processes impacting indoor air quality. In addition, indoor chemistry and sorption play a role as source or sink for some species.

Quantifying the VOC emissions from the building materials and furnishings is challenging and important because the pattern of VOC emissions can vary greatly between materials under diverse conditions [164], which significantly influence indoor air quality. To investigate the effect of emission rates, a series of simulations with INCA-Indoor model have been carried out with the measured emission rates during MERMAID campaign within their uncertain range.

In addition, air exchange is one of several crucial variables in understanding indoor–outdoor relationships and therefore, as such, can have an important influence on indoor pollution levels [165]. Air exchange rate (AER) is the rate at which outdoor air replaces indoor air in a given space. Within the range of air exchange rates reported in literature, the effect of air exchange rates has been investigated in this chapter.

The results in chapter 3 also show that indoor chemistry could be important for indoor air quality. Studies suggest that the gas phase indoor chemistry is initiated by the concomitant presence of oxidants and species re acting with them. Two major oxidants have been identified indoors : ozone from outdoors and equipment like air cleaners or printers [166] and hydroxyl radical (OH) from ozonolysis [72, 167] or photolysis of HONO [48]. Important sources for indoor OH include the reactions of some alkenes with O_3 and the photolysis of HONO [**?** 48]. The processes leading to OH production through photolytic sources like the photolysis of HONO are less known. Especially, the photolysis depends on the availability of photons indoors able to photolysed species such as HONO (λ<400 nm) and the characterization of light indoors are little known. Consequently, the effect of transmitted light by windows on indoor air quality has been studied with INCA-Indoor model using the measured window transmittance spectra during the MERMAID campaign.

In this chapter, we first characterize the emission and sorption rates of tested surfaces, the air exchange rate and the light transmittance of different windows measured during the MERMAID campaign [37] in section 4.2. A series of simulation scenarios with INCA-Indoor model have been chosen to investigate the effect of emission rates, air exchange rate, sorption rates and the light transmitted by different windows. Data collected during MERMAID campaign have been used as input of model. The section 4.3 presents the results. Simulated results with different emission rates based on model have been compared with the measured ones. The impact of window transmittance on indoor concentrations of species of interest has been discussed. In section 4.4, we conclude the effect of these parameters on indoor air quality.

4.2 Methodology

The INCA-Indoor model [41] allows simulating pollutant concentrations in indoor environment. It was designed in the framework of the MERMAID project [38] and based on the INCA model [129, 128] and the SAPRC-07 chemical mechanism [130]. This model accounts for indoor chemistry, the exchange of species between outdoor and indoor, the indoor emission of primary pollutants and surface processes (sorption, uptake, deposition).

Data collected during the MERMAID campaign are presented in detail in chapter 3 and some of them are used as input in the INCA-Indoor model. The data of April 29th 2014 was selected for the simulation according to the available measurements for indoor, ventilation inlet (used for all the simulations in this chapter) and outdoor (used only for the simulations with the different emission rates in this chapter). INCA-Indoor was set-up following the configuration of the classroom (i.e. volume = 138.5 m^3, 10 surface areas). The temperature and the relative humidity were constrained to their measured values for the simulation. The operating schedules of ventilation follow the program measured during the first campaign. The air flows measured are 60 m^3h^{-1} (AER : 0.43 h^{-1}) with the ventilation switched off and 300 m^3h^{-1} (AER : 2.2h^{-1}) with the ventilation switched on. Concentrations measured in ventilation inlet represent outdoor concentrations. To investigate the influence of different parameters listed in table 4.1 on indoor air quality, a series of simulations is carried out with varying these parameters. All the simulations start from April 29th 2014 at midnight to April 30th 2014 at midnight and the time step is 60 seconds.

Table 4.1 – Parameters for the simulations

Parameters for the simulations	Corresponding paragraph number for the parameters
Emission rates (Femi)	Figures 4.3-4.6
Air exchange rate (AER)	Figures 4.7-4.14
Sorption rates (k_a, k_d)	Figues 4.15-4.22
Window transmittance spectra	Figures 4.23-4.26

4.2.1 Modeling with different emission rates

The VOC emission rates were measured for the ten surfaces present in the classroom during MERMAID campaign and 23 VOCs were identified. VOCs with emission rates less than the detection limits (LOD) for all the measured surfaces are not represented in the figure 4.1. The measurement results show that the emission rates can be different between similar surfaces as painted gypsum boards with different colors. In addition, the emission rate determined on different location of the same material showed variability between 9% and 85% respectively depending on the VOC and the surface. This heterogeneity is may be due to aging of surface caused by different exposure to the sunlight.

To investigate the effect of emission rates on indoor pollutant concentrations, sensitivity tests are performed using INCA-Indoor model with different emission rates (average, minimum and maximum) measured for targeted VOC in 10 surfaces present in the classroom. The modeled profiles are then compared with experimental profiles obtained during the MERMAID campaign. All modeled scenarios are listed in table 4.2.

VOC	Measurement method	Ceiling tiles	Green vinyl flooring	White vinyl flooring	White painted concrete wall	Green painted gypsum board	White painted gypsum board	White PVC board	White painted wood shelf	White painted wood door	Green painted wood door
Formaldehyde	HPLC	22 ± 7.5 (n=5)	1.9 ± 0.94 (n=6)	<1.5 (n=2)	1.9 ± 0.81 (n=3)	2.0 ± 1.1 (n=5)	<1.5 (n=1)	1.9 (n=2)	<1.5 (n=1)	2.5 (n=1)	2.1 ± 1.2 (n=6)
Acetaldehyde	HPLC	0.68 ± 0.35 (n=4)	0.53 ± 0.05 (n=4)	0.6 (n=2)	0.8 (n=1)	0.63 ± 0.25 (n=4)	<0.5 (n=1)	<0.5 (n=1)	1.1 (n=1)	1.6 (n=1)	0.70 ± 0.52 (n=4)
Acetone	HPLC	<1.8 (1<n<2)									
Toluene	GC	<0.9 (n=3)	76 ± 44 (n=5)	58 (n=2)	<0.9 (n=2)	<0.9 (n=2)	<0.9 (n=1)	<0.9 (n=1)	<0.9 (n=1)	<0.9 (n=1)	<0.9 (n=4)
1.2.3-TMB	GC	1.3 (n=2)	<0.2 (n=5)	0.5 (n=2)		<0.2 (n=2)	<0.2 (n=1)	<0.2 (n=1)	<0.2 (n=1)		<0.2 (n=2)
Styrene	GC	1.3 (n=2)	<0.2 (n=5)	0.5 (n=2)		<0.2 (n=2)	<0.2 (n=1)	<0.2 (n=1)	<0.2 (n=1)		<0.2 (n=2)
o-Xylène	GC	<0.1 (n=3)	0.53 ± 0.50 (n=4)	0.32 (n=2)		<0.1 (n=2)			<0.1 (n=1)	<0.1 (n=1)	<0.1 (n=1)
m,p-Xylene	GC	<1.2 (1<n<5)									
Octane	GC	<0.4 (n=2)	7.0 ± 14 (n=4)	<0.4 (n=2)	<0.4 (n=1)		<0.4 (n=2)		<0.4 (n=1)		
Nonane	GC	<0.1 (n=3)	2.0 ± 1.6 (n=5)	2.0 (n=2)		<0.1 (n=3)	<0.1 (n=1)		<0.1 (n=1)	<0.1 (n=1)	<0.1 (n=4)
α-pinene	GC	1.2 (n=2)	0.4 ± 0.3 (n=3)	0.5 (n=2)		<0.4 (n=2)	<0.4 (n=1)	<0.4 (n=1)	<0.4 (n=1)	<0.4 (n=1)	<0.4 (n=2)
B-pinene + decane	GC	1.3 (n=2)	3.7 (n=2)	4.7 (n=1)	<0.4 (n=1)	<0.4 (n=1)	<0.4 (n=1)	<0.4 (n=1)	<0.4 (n=1)	<0.4 (n=1)	<0.4 (n=1)
Camphene + 1.2.4-TMB	GC	16 (n=2)	0.9 ± 0.7 (n=5)	1.1 (n=2)							<0.5 (n=2)
Limonene	GC	2.7 (n=2)	<0.1 (n=3)	0.18 (n=2)							
Undecane	GC	1.3 ± 1.1 (n=3)	<1.3 (n=5)	<1.3 (n=5)	<1.3 (n=2)	<1.3 (n=2)	<1.3 (n=3)	<1.3 (n=1)	<1.3 (n=1)	<1.3 (n=1)	<1.3 (n=2)

Figure 4.1 – Measured VOC emission rates (μg.m^{-2}.h^{-1})for tested surfaces using GC and HPLC measurements. The standard deviation is calculated for 1σ on the number of measurements performed (n) for each surface

Table 4.2 – The modeled scenarios with the emission rates

Modeled scenarios	Emission rate
S_{min}	minimum
S_{avg}	average
S_{max}	maximum

4.2.2 Modeling with different air exchange rate (AER)

Limited measurements of air exchange in schools have been found in the literature. Generally, it is difficult to estimate the air exchange rates in schools, since they depend on the different habits of children and teachers regarding the opening of the windows. Measurements in 8 primary schools in England give air exchange rates of 4.0 ± 0.3 h^{-1} and 0.6 ± 0.1 h^{-1} when the ventilation system was providing fresh and re-circulated air respectively [168]. Wålinder et al. (1998) suggested that the general air exchange rate in the 12 schools was 1.9 on average, with absolute values ranging from 0.5-5.2 [169]. Guo et al. (2008) reported the air exchange rate measured in a classroom for different conditions associated with window opening and the operational status of air conditioners (A/C) and fans were tested [170]. Results in that study show that the lowest AER (0.12 h^{-1}) was found when the windows were closed and A/C and fans were off. In contrast, the highest AER (7.92 h^{-1}) was observed when the windows were opened and A/C and fans were all on. Considering the range of observed values reported above and the absence of air conditioners and fans in the classroom, the sensitivity of the model to AER has been tested with AER observed during MERMAID (2.16 h^{-1} with ventilation switched on), 2 times of AER observed and 0.5 times of AER observed. When the ventilation is switched off, AER remains as 0.43 h^{-1} for three scenarios. Other simulation conditions were kept same for each simulation. The modeled scenarios are listed in table 4.3.

Table 4.3 – The modeled scenarios with different air exchange rate

Scenarios	AER(ventilation off, h^{-1})	AER(ventilation on, h^{-1}) 08 :20-09 :45 10 :10-11 :45 13 :35-15 :00 15 :25-17 :15
Sim AER1.08	0.43	1.08
Sim AER2.16	0.43	2.16
Sim AER4.32	0.43	4.32

4.2.3 Modeling with different sorption rates

The adsorption rate (k_a) and the desorption rate (k_d) for 27 VOC on the 10 types of material surface (see table 4.4) in the classroom are measured during MERMAID campaign. Measurement methodologies are fully described in Rizk (2015) [147, 171] and Rizk et al.(2016) [152]. Measurement results show that most of materials do not exhibit any interactions with any VOC present in the tested mixture, such as the white PVC board, the vinyl flooring and the green painted wood door, the ceiling tiles and green painted gypsum board exhibit sorption parameters in the range 0.25-7.52 $m.h^{-1}$ for k_a and 2.28-93.73 h^{-1} for k_d. The k_a and k_d for the ceiling tiles and green painted gypsum board are presented in table 4.5.

To investigate the effect of k_a and k_d on indoor concentration of species, sensitivity tests are performed using INCA-Indoor model with different sorption rates (average, minimum and maximum) measured. The modeled scenarios are listed in table 4.6.

4.2.4 Modeling with the experimental data of indoor solar radiation

Characteristics of the solar radiation of the room

Spectrally and temporally resolved solar radiance measurements and real time measurements of the spatial distribution of the indoor light have been performed during the MERMAID campaign

Table 4.4 – Area of the surfaces present in the classroom

Building material	Number	Surface area (m^2)	Percentage of surface (%)
Green vinyl flooring	1	43.69	24.07
Ceiling tiles	1	47.40	26.12
White painted concrete wall	2	25.47	14.04
Green painted gypsum board	1	18.68	10.29
White PVC board	2	11.97	6.6
White painted gypsum board	1	16.73	9.22
White vinyl flooring	1	6.24	3.44
White painted wood shelf	2	4.75	2.62
White painted wood door	1	3.33	1.83
Green painted wood door	2	3.22	1.77
Total surface area		181.5	

[38]. A classroom located at the first floor of one low energy school building called Mroom-1st and other rooms (Lroom-grd and Lroom-1st) in another low consumption building have been selected to investigate the light characteristics. There are 5 windows in this classroom Mroom-1st exposed to the south (210^o) in order to favor the solar heating. The windows are composed by two Planilux glasses : the first one of 4 mm and the second of 6 mm, coated on one face with a Planitherm coating. In the rooms Lroom-grd and Lroom-1st, three different types of windows have been studied :

— Lroom-grd-LEHP (Low Emissivity High Performance window at the ground floor) : Saint Gobain 44.2 Cool lite SKN154/14 argon /33.2 with film. The windows is composed of two glasses of 4 mm of thickness (Planilux glass) assembled together by a layer of 200 μm of PVB film (Stadip type : polyvinyl butyral) cutting the UV light and finished by thermal coating (Cool lite coating, in silver), a space of 14 mm of Argon and two glasses of 3 mm (Planilux type, with one layer of 200 μm of PVB film) ;

— Lroom-grd-LE (Low Emissivity window at the ground floor), Saint Gobain 44.2 Planistar /16 Argon/44.2, with film ;

Table 4.5 – Measured VOC mean sorption rates for tested surfaces in the classroom. * : indicates that the limit of detection is determined theoretically for the couple of parameters (k_a ($cm.s^{-1}$), k_d (s^{-1})) using the FLEC method.

Species	ceiling tiles						green painted gypsum board					
	min	mean	max	min	mean	max	min	mean	max	min	mean	max
formaldehyde	<0.07*	<0.07*	<0.07*	<0.07*	<0.07*	<0.07*	<0.07*	<0.07*	<0.07*	<0.07*	<0.07*	<0.07*
acetaldehyde	<0.07*	<0.07*	<0.07*	<0.07*	<0.07*	<0.07*	<0.07*	<0.07*	<0.07*	<0.07*	<0.07*	<0.07*
acrolein	0.207	0.476	0.929	0.036	7.200	0.135	<0.07*	<0.07*	<0.07*	<0.07*	<0.07*	<0.07*
acetone	0.413	1.080	1.750	0.067	16.900	0.271	<0.07*	<0.07*	<0.07*	<0.07*	<0.07*	<0.07*
butanone	0.090	0.147	0.197	0.010	1.550	0.020	<0.07*	<0.07*	<0.07*	<0.07*	<0.07*	<0.07*
isoprene	<0.07*	<0.07*	<0.07*	<0.07*	<0.07*	<0.07*	<0.07*	<0.07*	<0.07*	<0.07*	<0.07*	<0.07*
benzene	0.056	0.097	0.124	0.004	1.120	0.022	<0.07*	<0.07*	<0.07*	<0.07*	<0.07*	<0.07*
toluene	0.031	0.055	0.076	0.002	0.275	0.004	<0.07*	<0.07*	<0.07*	<0.07*	<0.07*	<0.07*
ethyl benzene	0.032	0.048	0.060	0.001	0.081	0.001	0.009	0.009	0.009	0.004	0.377	0.004
m-xylene	0.032	<0.07*	0.060	0.001	<0.07*	0.001	0.009	<0.07*	0.009	0.004	<0.07*	<0.07*
p-xylene	0.032	<0.07*	0.060	0.001	<0.07*	0.001	0.009	<0.07*	0.009	0.004	<0.07*	<0.07*
o-xylene	<0.07*	<0.07*	<0.07*	<0.07*	<0.07*	<0.07*	<0.07*	<0.07*	<0.07*	<0.07*	<0.07*	<0.07*
styrene	0.049	0.073	0.104	0.001	0.084	0.001	0.015	0.029	0.042	0.003	0.475	0.006
alpha-pinene	0.019	0.027	0.036	<0.07*	0.112	0.002	<0.07*	<0.07*	<0.07*	<0.07*	<0.07*	<0.07*
beta-pinene	<0.07*	<0.07*	<0.07*	<0.07*	<0.07*	<0.07*	<0.07*	<0.07*	<0.07*	<0.07*	<0.07*	<0.07*
1,2,4-trimethyl benzene	<0.07*	<0.07*	<0.07*	<0.07*	<0.07*	<0.07*	<0.07*	<0.07*	<0.07*	<0.07*	<0.07*	<0.07*
n-decane	<0.07*	<0.07*	<0.07*	<0.07*	<0.07*	<0.07*	<0.07*	<0.07*	<0.07*	<0.07*	<0.07*	<0.07*
Camphene	<0.07*	<0.07*	<0.07*	<0.07*	<0.07*	<0.07*	<0.07*	<0.07*	<0.07*	<0.07*	<0.07*	<0.07*
1,3,5-trimethyl benzene	<0.07*	<0.07*	<0.07*	<0.07*	<0.07*	<0.07*	<0.07*	<0.07*	<0.07*	<0.07*	<0.07*	<0.07*
d-limonene	<0.07*	<0.07*	<0.07*	<0.07*	<0.07*	<0.07*	<0.07*	<0.07*	<0.07*	<0.07*	<0.07*	<0.07*
Terpinolene	<0.07*	<0.07*	<0.07*	<0.07*	<0.07*	<0.07*	<0.07*	<0.07*	<0.07*	<0.07*	<0.07*	<0.07*
methanol	0.119	0.191	0.381	0.004	1.220	0.023	<0.07*	<0.07*	<0.07*	<0.07*	<0.07*	<0.07*
n-octane	<0.07*	<0.07*	<0.07*	<0.07*	<0.07*	<0.07*	<0.07*	<0.07*	<0.07*	<0.07*	<0.07*	<0.07*
n-nonane	<0.07*	<0.07*	<0.07*	<0.07*	<0.07*	<0.07*	<0.07*	<0.07*	<0.07*	<0.07*	<0.07*	<0.07*
n-undecane	<0.07*	<0.07*	<0.07*	<0.07*	<0.07*	<0.07*	<0.07*	<0.07*	<0.07*	<0.07*	<0.07*	<0.07*
n-dodecane	<0.07*	<0.07*	<0.07*	<0.07*	<0.07*	<0.07*	<0.07*	<0.07*	<0.07*	<0.07*	<0.07*	<0.07*
1,2,3-trimethyl benzene	<0.07*	<0.07*	<0.07*	<0.07*	<0.07*	<0.07*	<0.07*	<0.07*	<0.07*	<0.07*	<0.07*	<0.07*

Table 4.6 – The modeled scenarios with sorption rates (k_a and k_d)

Modeled scenarios	Sorptio rates
$kakd_{min}$	minimum
$kakd_{mean}$	average
$kakd_{max}$	maximum

— Lroom-1st-LE (Low Emissivity window at the first floor), Saint Gobain 4 Planistar/16 Argon/4 located at the first floor.

A calibrated spectroradiometer LICOR (LICOR-LI 1800, spectral range : 300-850 nm, resolution : 1 nm) with a PTFE-dome cosine receptor with a 180° field of view was used to measure the spectrally resolved radiance. With the radiance measurement I(λ) at the wavelength λ (in nm), the actinic flux F(λ) can be calculated in condition of direct sunshine following the equation :

$$F(\lambda) = \frac{I(\lambda)}{cos\theta} \tag{4.1}$$

where F(λ) is the actinic flux (in photons.cm^{-2}.nm^{-1}.s^{-1}), θ being the azimuth angle. The calculated F(λ) is used to calculate the photolysis frequencies J (of HONO, for example) using the following equation :

$$J = \int_{\lambda_{min}}^{\lambda_{max}} F(\lambda)\sigma(\lambda)\phi(\lambda)d\lambda \tag{4.2}$$

where σ(λ) is the absorption cross section of the molecule (in cm^2) at the wavelength of light λ (nm) and ϕ(λ) is the quantum yield or the probability of photodissociation of the molecule after absorption of a photon at the wavelength λ.

During the MERMAID project, window transmittance has been measured with the LICOR instrument placed just behind the window in the room Mroom-1st. The transmittance measured for different types of windows have been compared with those reported in the literature [172, 46, 110] and are shown in figure 4.2. The windows at the ground floors (L0-LEHP and L0-LE) systematically include a intrusion retarding film that cuts the transmittance of UV radiation (below 380nm). LEHP windows have an extra coating allowing to reflect more Infrared radiation (IR) and thus reduce the energy consumption from heating. The transmission levels in room 1 are similar to those of Drakou [172] and much higher than those used in Carslaw's

modeled base scenario [46] and measured in a Gallery by Nazaroff and Cass [110]. In Nazaroff and Cass (1986) study, the window transmission was measured in a Gallery where the windows are coated most of the time to cut the UV in order to protect the art works. That could explain why the values reported by Nazaroff and Cass (1986) are lower than those measured during MERMAID campaign.

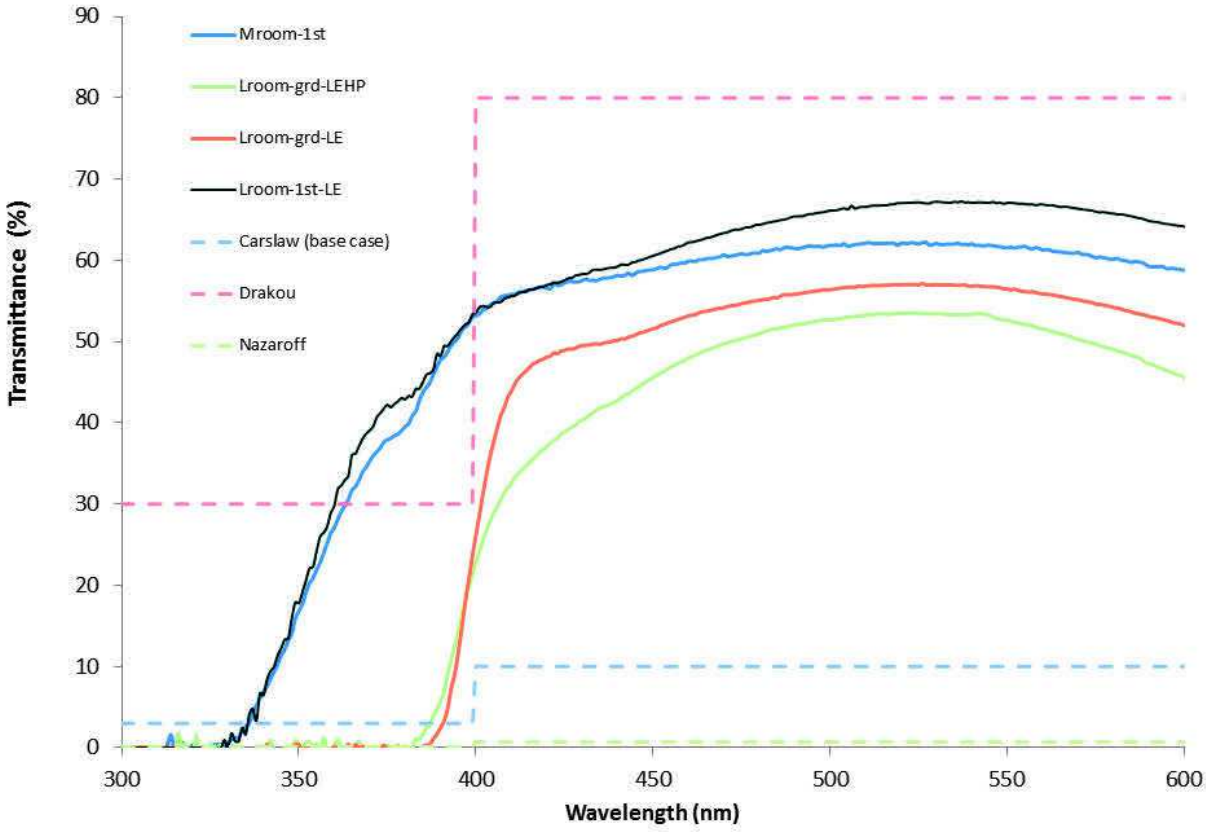

Figure 4.2 – Window transmittance measured in Mroom-1st in 04/18/2014 between 10 :00 and 15 :00 for Lroom-grd and Lroom-1st). The transmittance used in the different case of (Carslaw, 2007),(Drakou, 1998) and (Nazaroff, 1986) are represented as dashed lines. Source of figure : report of MERMAID [37]

Modeling with solar radiation transmitted by different types of windows

In order to analyze the impact of the actinic flux on the indoor chemistry, simple scenarios favorable to the production of HOx by photolysis (high HONO level : 10 ppb, case 1 :no indoor light) have been chosen under indoor conditions on the April 29th 2014 during MERMAID campaign and using the light transmittance of the windows measured. The same photon fluxes from natural outdoor light (TUV spectrum on 2010/06/21 at noon latitude 50°, longitude 0°) have been used for all simulations in order to test the influence of the different window transmittance spectra (figure 4.2) on the indoor chemistry. No artificial light has been added as their emission is weak compared to the sun radiation. Simulation scenarios with different window transmittances spectra presented in the figure 4.2 are performed and listed in table 4.7.

Table 4.7 – Simulation scenarios with different window transmittance spectra

Conditions	UV transmitted (%)	Visible transmitted (%)
nolight	0.	0.
Nazaroff	0.15	0.7
Lroom-grd-LE	1.48	46.29
Lroom-grd-LEHP	1.86	39.23
Carslaw	3	10
Mroom-1st	20.05	56.27
Lroom-1st-LE	21.33	57.33
Drakou	30	80

4.3 Results

4.3.1 Effects of emission rates on indoor VOC concentration

Figure 4.3-4.6 shows a comparison of concentration profiles measured and modeled with different emission rates for 7 VOCs emitted indoors. The modeled concentration profiles are similar for three types of simulations with different emission rates. Modeled concentrations of these

7 species increase with increasing the emission rates. These figures show that modeled concentrations with the maximum emission rates are closer to indoor measured concentrations except for formaldehyde (HCHO) and Toluene. For Toluene, simulation with the minimum emission rate are closer to indoor measured concentrations and the other two simulation overestimate the experimental concentrations. During the first night (04/29/2014 00 :00 to 04/29/2014 08 :00) the modeled toluene profile S_{avg} overestimates the experimental concentrations. This is because that the infiltration is not considered during the simulation with measured data at the ventilation inlet. For formaldehyde during this period, modeled concentrations with S_{avg} and S_{max} overestimate the experimental concentrations and simulation with S_{min} is close to the measured concentrations. In addition, an indoor peak of concentration for HCHO was observed during the second ventilation period (10h :10-11h :45) due to the peak concentrations with 32.7ppb observed at the ventilation inlet, and that were following outdoor concentrations. This confirm that this HCHO is due to outdoor pollution entering in the room. One can notice that the model is not fast enough to eliminate the HCHO as what happens in reality in the room.

4.3.2 Effects of air exchange rate on indoor pollutant concentrations

Concentration profiles modeled with different air exchange rates for NOx, 12 VOCs are presented in figures 4.7-4.14. Since the ventilation begins from 8h20 and the AER are changed for the periods when the ventilation is switched on, the results after 8h20 are considered and analyzed. The maximum, mean and minimum concentrations of species of interest for three simulated scenarios are listed in table 4.8. Figure 4.7 and 4.8 show that concentrations of NOx and O_3 increase with AER increasing. Taking the scenario AER 2.16 h^{-1} as base case, NO concentrations ranged from 0.01 to 0.69 ppb, with an average mean NO concentration of 0.09 ppb. With 2 times of measured AER (4.32h^{-1}) when the ventilation switched on, the maximum and mean concentrations of NO increase by 60.86% and 33.33% receptively. With 0.5 times of measured AER (1.08h^{-1}) when the ventilation switched on, the maximum and the mean of NO concen-

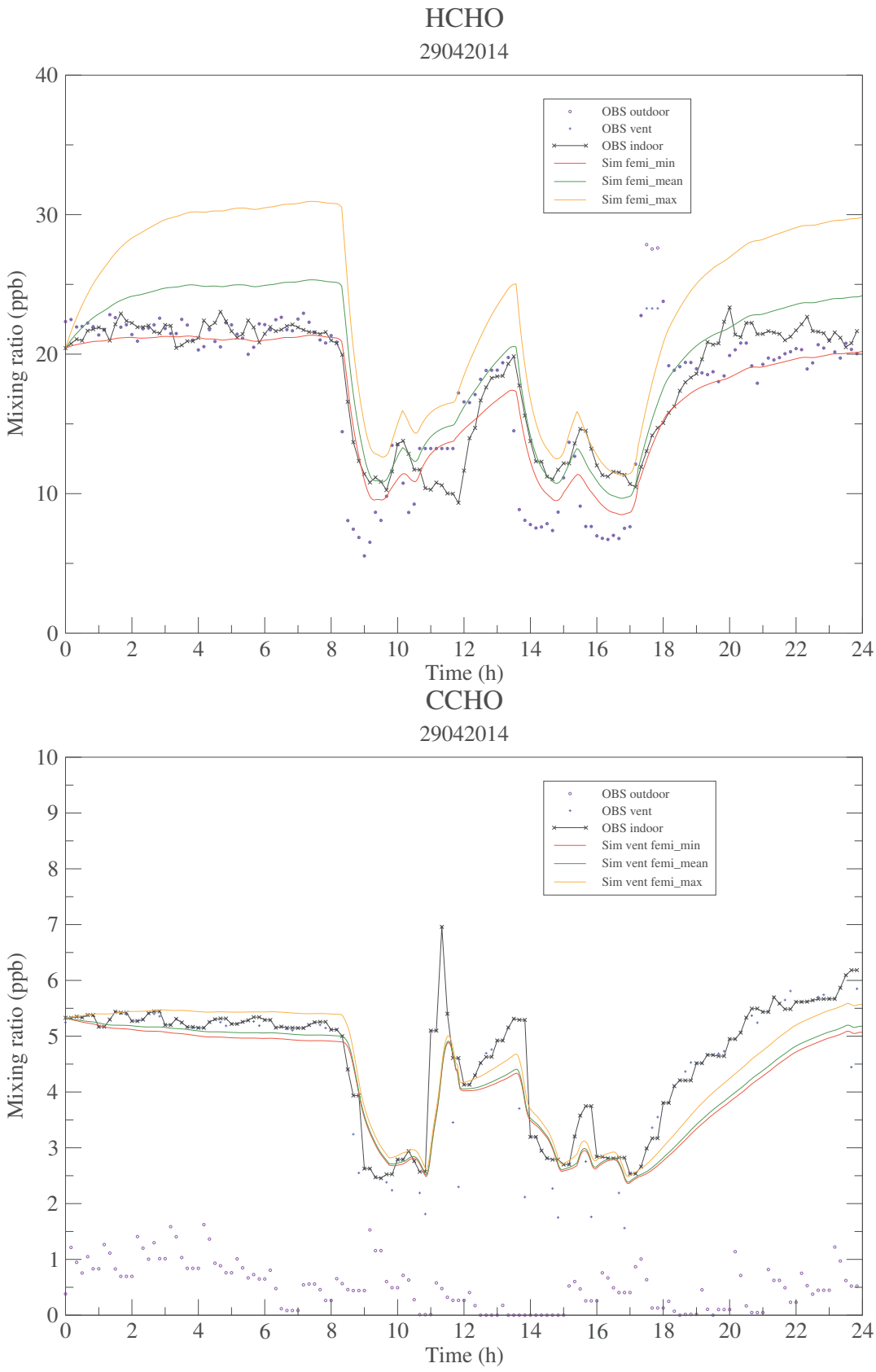

Figure 4.3 – Measured (OBS) concentrations of formaldehyde (HCHO) and acetaldehyde (CCHO) for outdoor (OBS outdoor), the ventilation inlet (OBS vent) and the center of the classroom (OBS indoor). Modeled concentrations with data at the ventilation inlet (Sim vent) and outdoor (Sim outdoor) and different emission rates with INCA-Indoor model.

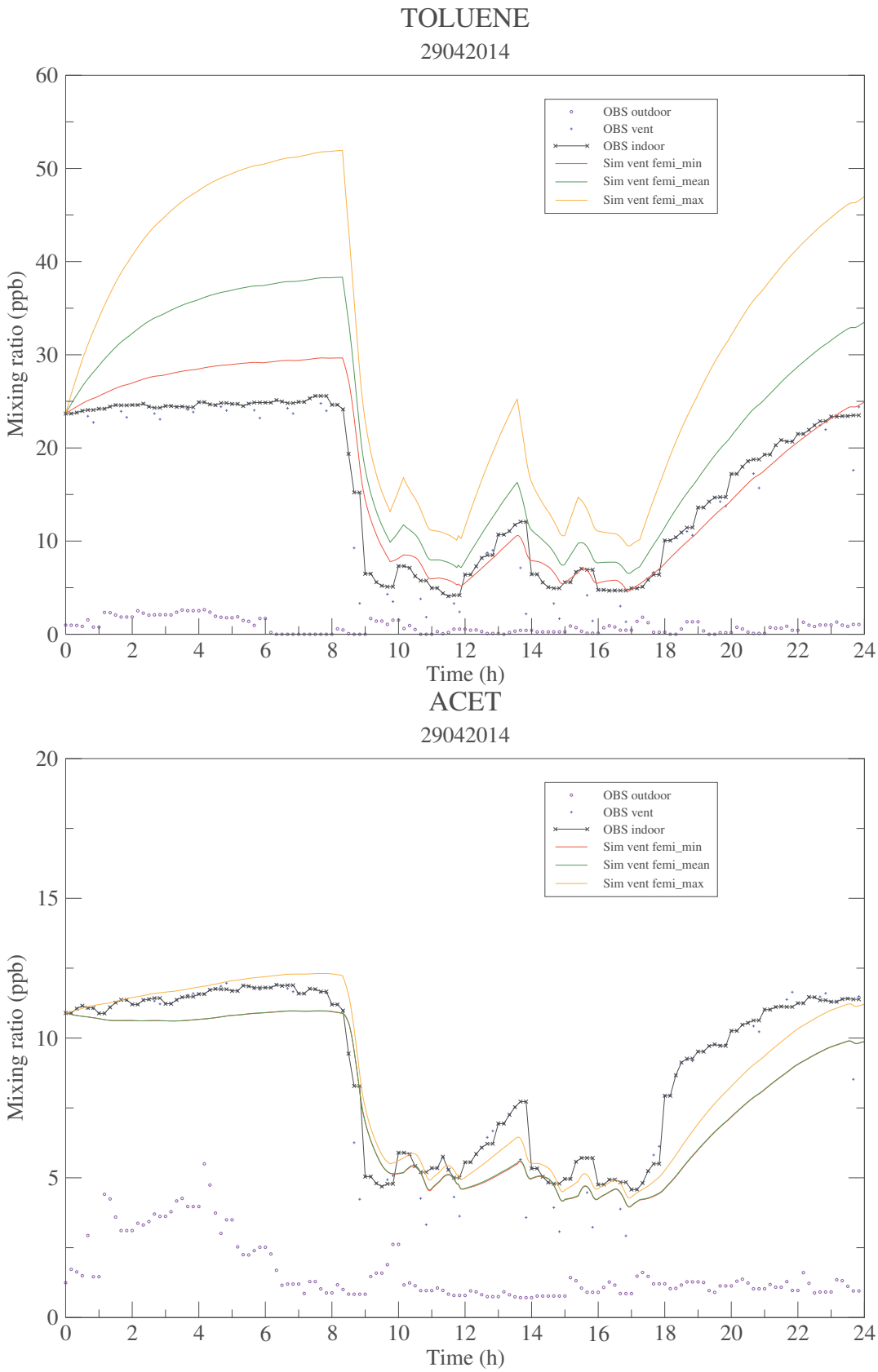

Figure 4.4 – Measured (OBS) concentrations of toluene (TOLUENE) and acetone (ACET) for outdoor (OBS outdoor), the ventilation inlet (OBS vent) and the center of the classroom (OBS indoor). Modeled concentrations with data at the ventilation inlet (Sim vent), outdoor (Sim outdoor) and different emission rates with INCA-Indoor model.

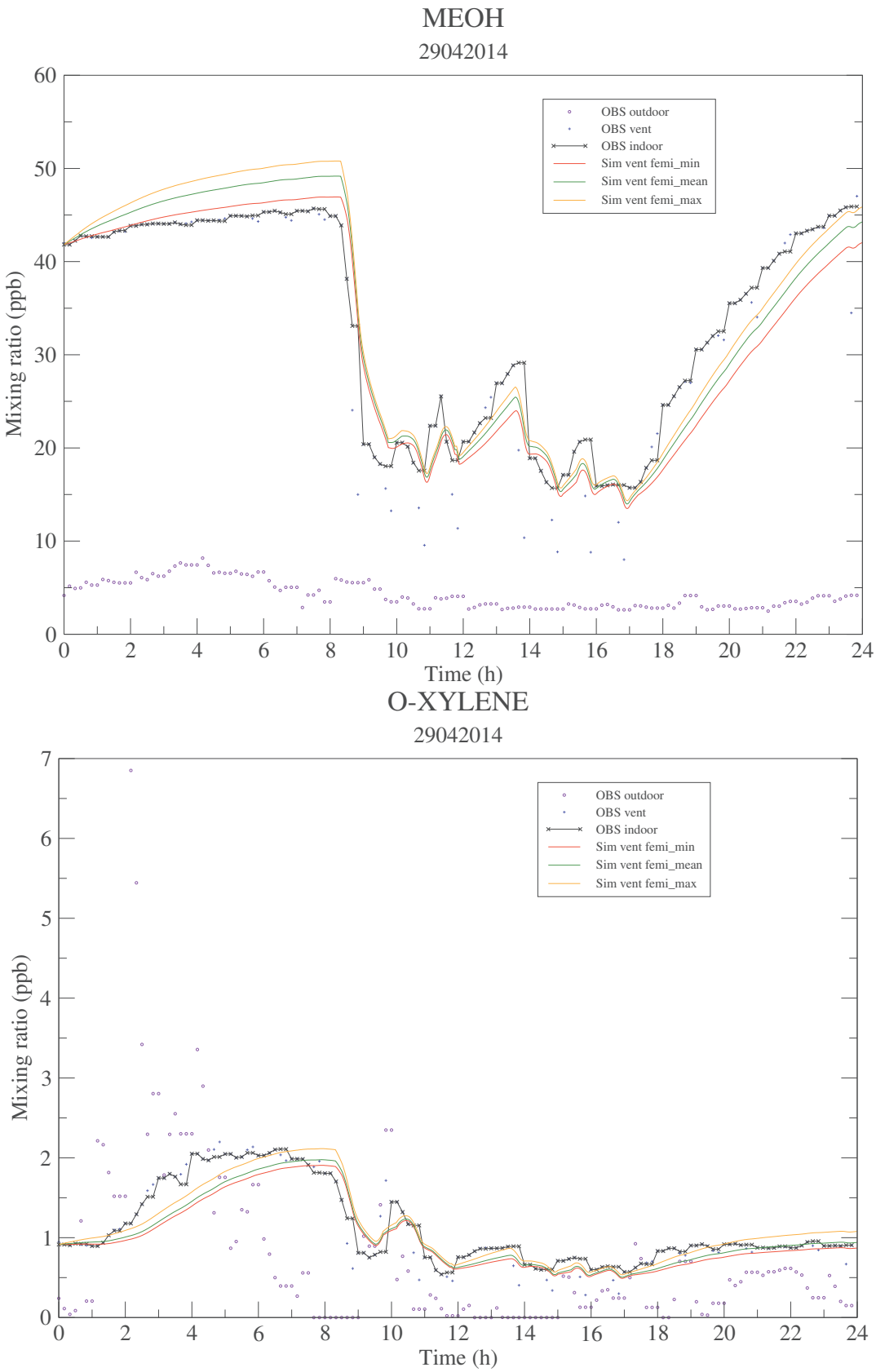

Figure 4.5 – Measured (OBS) concentrations of methanol (MEOH) and o-xylene (O-XYLENE) for outdoor (OBS outdoor), the ventilation inlet (OBS vent) and the center of the classroom (OBS indoor). Modeled concentrations with data at the ventilation inlet (Sim vent), outdoor (Sim outdoor) and different emission rates with INCA-Indoor model.

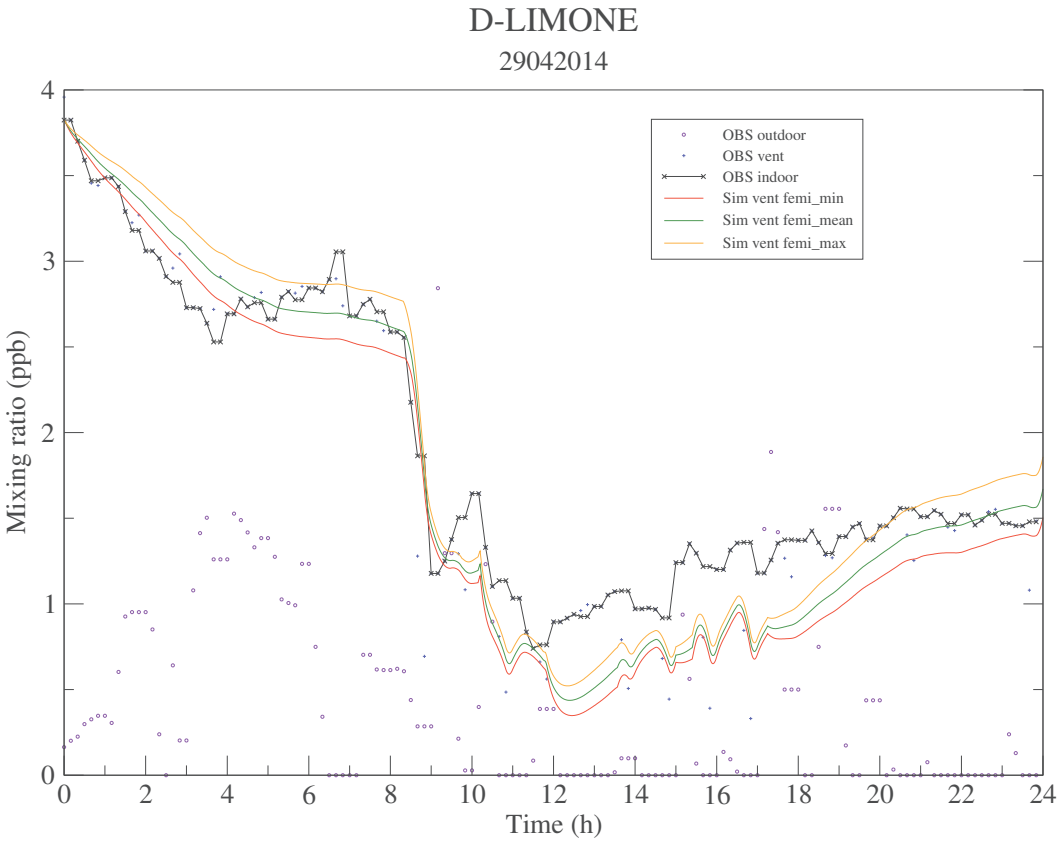

Figure 4.6 – Measured (OBS) concentrations of methanol (MEOH), o-xylene (O-XYLENE) and d-limonene (D-LIMONE) for outdoor (OBS outdoor), the ventilation inlet (OBS vent) and the center of the classroom (OBS indoor). Modeled concentrations with data at the ventilation inlet (Sim vent), outdoor (Sim outdoor) and different emission rates with INCA-Indoor model.

trations decrease by 42.03% and 11.1 % receptively compared to the scenario AER 2.16 h^{-1}. The similar behavior is observed for NO_2 and O_3 concentrations. With respect to the maximum concentrations of NO_2 and O_3 for scenario AER 2.16 h^{-1}, the maximum concentrations of NO_2 and O_3 increase by 17.08% and 3.4% respectively with 2 times of measured AER (4.32h^{-1}) and decrease by 24.46% and 2.66% respectively with 0.5 times of measured AER (1.08h^{-1}).

With increasing AER from 1.08h^{-1} to 4.32h^{-1}, the maximum concentrations of acetaldehyde increase, but the mean and minimum concentrations decrease. Compared to the concentrations for scenario AER2.16 h^{-1}, the maximum concentrations acetaldehyde for scenario AER4.32 h^{-1} increase by 7.4% and mean concentrations decrease by 3.08% and 1.86%. Figure 4.9 show that acetaldehyde reach the peak concentration between 11h :00 and 12h :00, during which the concentrations of NO and O_3 increase with increasing AER. The increase of concentrations of NO and O_3 allows more NO and O_3 to react with some radicals (i.e. methyldioxidanyl, peroxyacyl) and to produce more acetaldehyde. That's why the maximum concentrations of acetaldehyde increase. The concentrations of formaldehyde and acetaldehyde decrease when the ventilation is switched on. The effect of ventilation diluting the concentrations of formaldehyde and acetaldehyde is more important than the reactions producing HCHO (i.e. methyldioxidanyl+NO,peroxyacyl+NO), hence, mean and minimum concentrations of formaldehyde and acetaldehyde decrease.

The maximum, mean and minimum concentrations for methanol, toluene and o-xylene decrease with increasing AER due to the exchange with outdoor air. Compared with concentrations for scenario AER 1.08 h^{-1}, an increase of 3 times of AER (4.32h^{-1}) reduce by 11.4%, 24.46% and 11.49% receptively of the mean concentrations of methanol, toluene and o-xylene.

For acrolein and acetone, there is almost no change for the maximum concentrations but mean and minimum concentrations reduce sightly with increasing AER. Furthermore, there is no significant change for the maximum, mean and minimum concentrations of benzene, isoprene, d-limonene, chlorobenzene and p-dichlorobenzene with increasing AER.

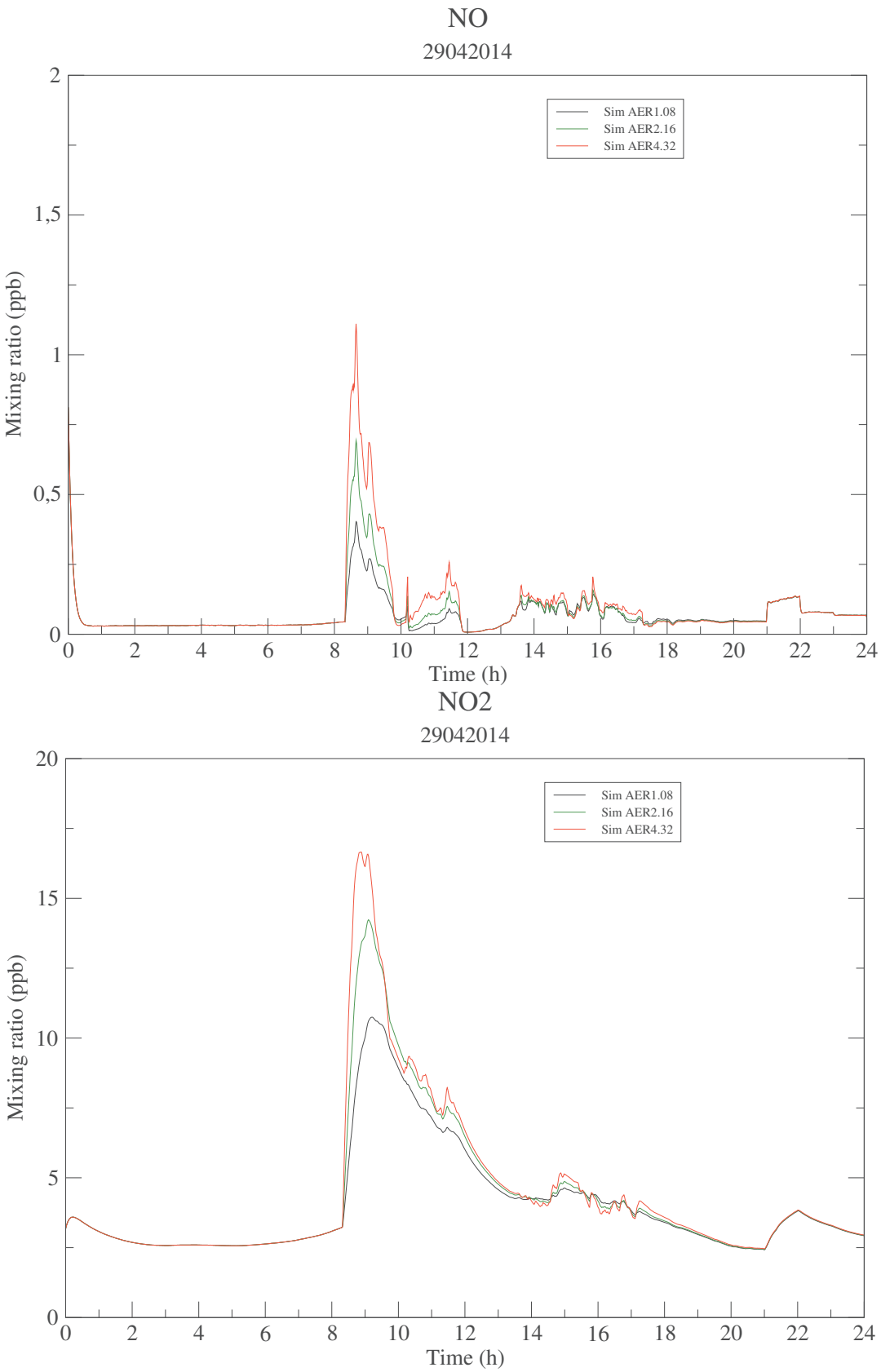

Figure 4.7 – Modeled concentrations of NO and NO_2 with AER1.08 h^{-1}(black line), AER2.16h^{-1} (green line), AER4.32h^{-1} (red line)

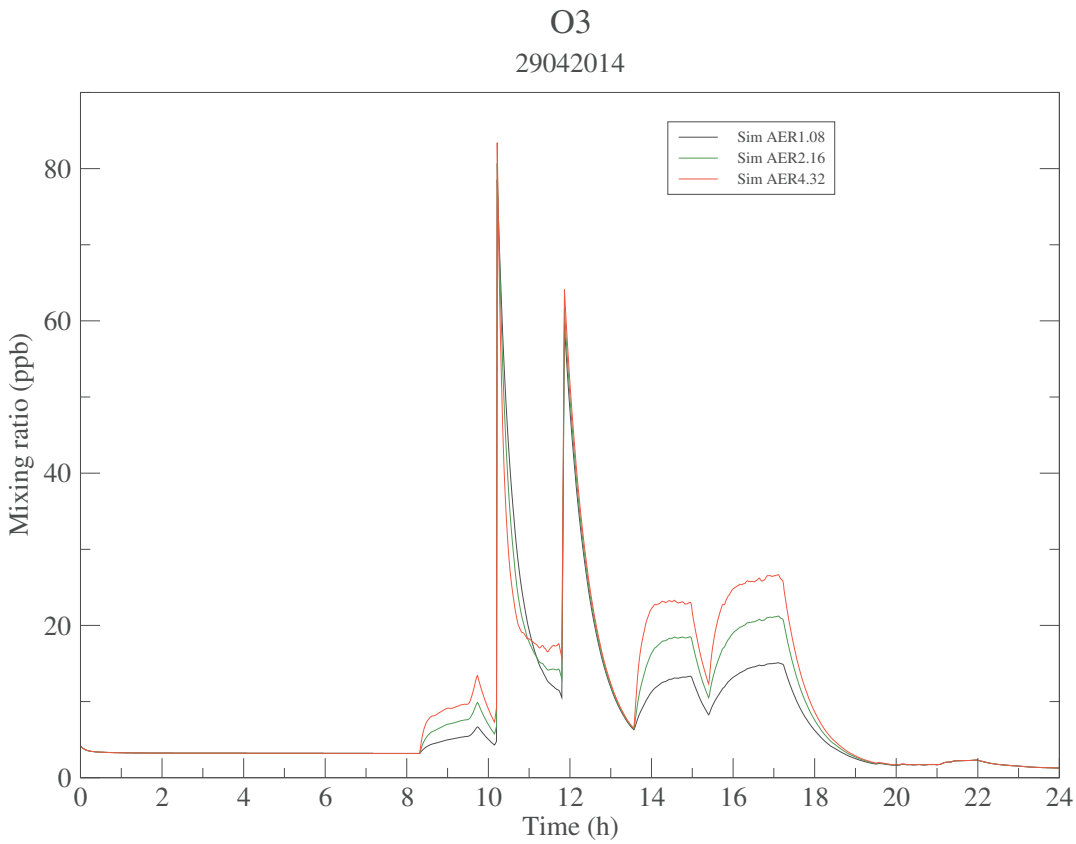

Figure 4.8 – Modeled concentrations of O_3 with AER1.08 h^{-1}(black line), AER2.16h^{-1} (green line), AER4.32h^{-1} (red line)

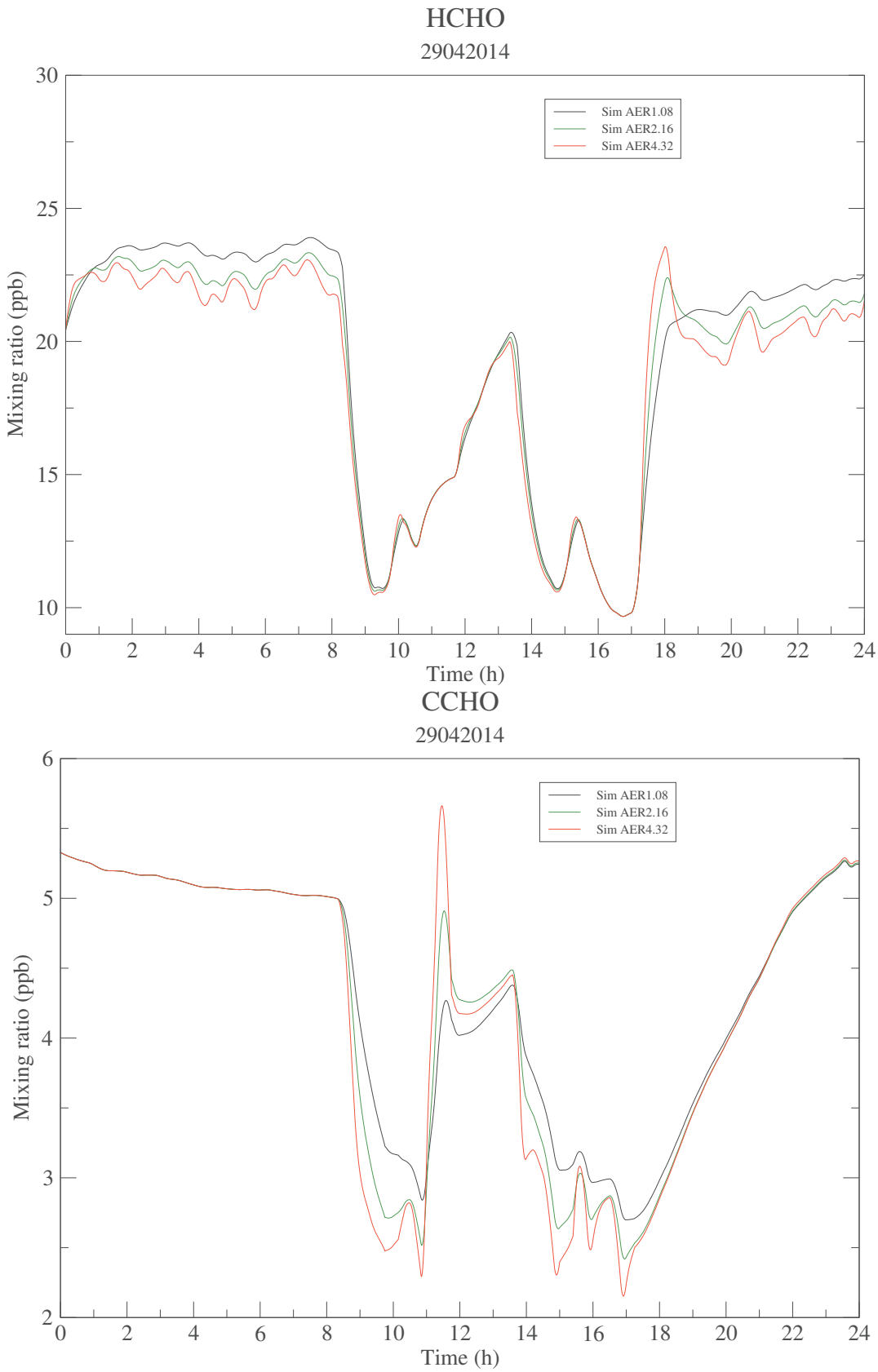

Figure 4.9 – Modeled concentrations of formaldehyde (HCHO) and acetaldehyde (CCHO) with AER1.08 h^{-1}(black line), AER2.16h^{-1} (green line), AER4.32h^{-1} (red line)

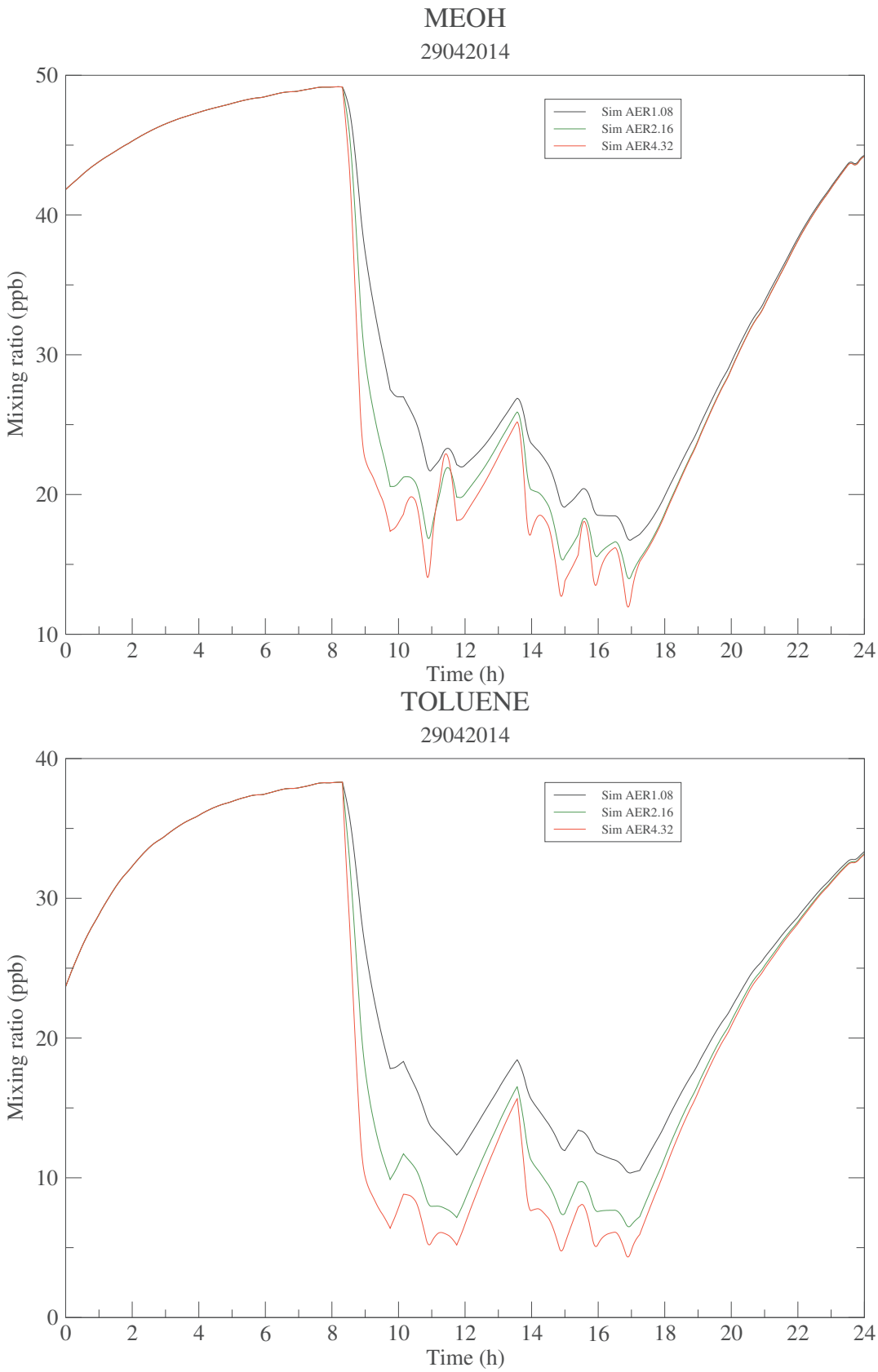

Figure 4.10 – Modeled concentrations of methanol (MEOH) and toluene (TOLUENE) with AER1.08 h^{-1}(black line), AER2.16h^{-1} (green line), AER4.32h^{-1} (red line)

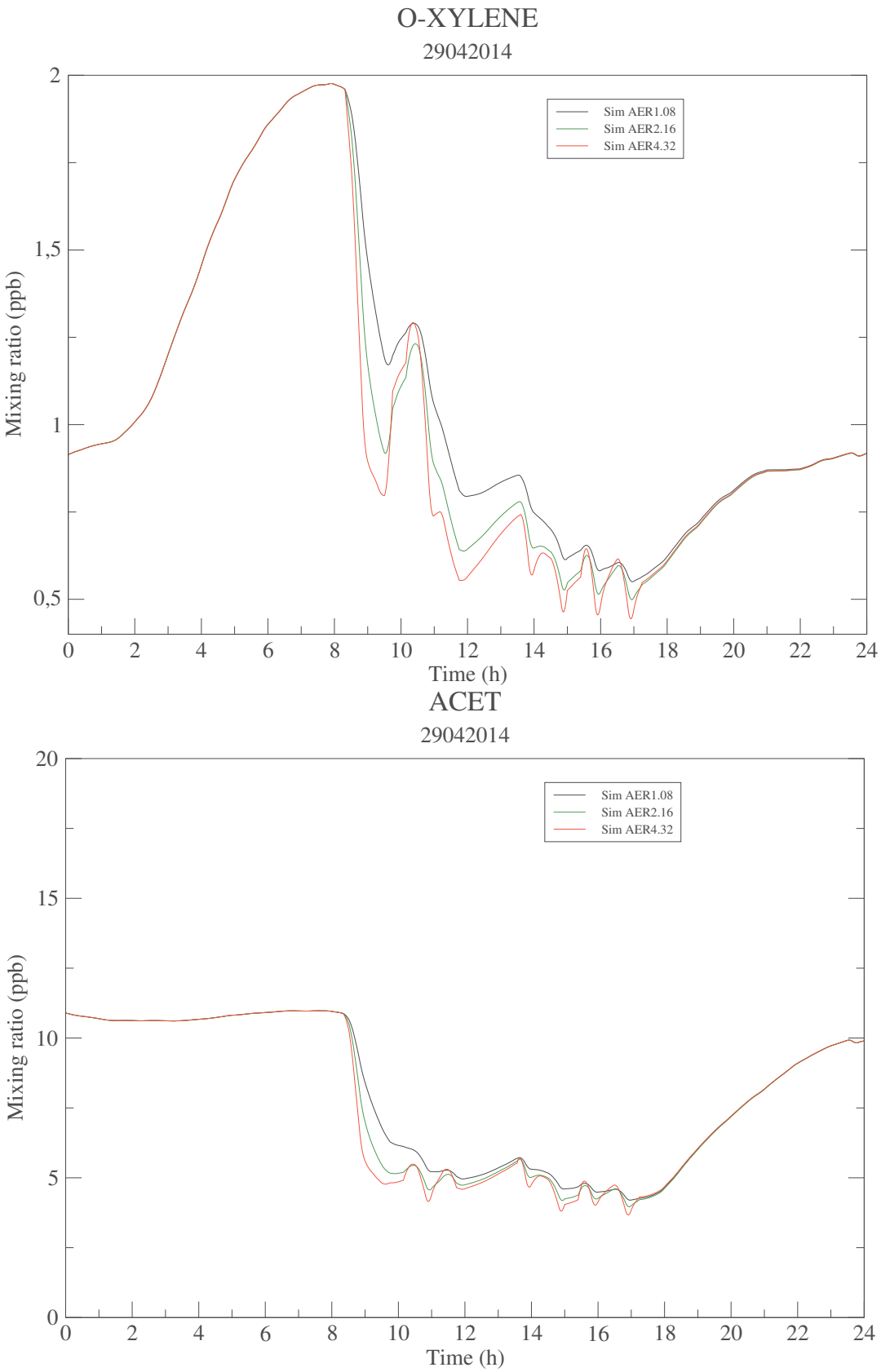

Figure 4.11 – Modeled concentrations of o-xylene (O-XYLENE) and acetone (ACET) with AER1.08 h^{-1}(black line), AER2.16h^{-1} (green line), AER4.32h^{-1} (red line)

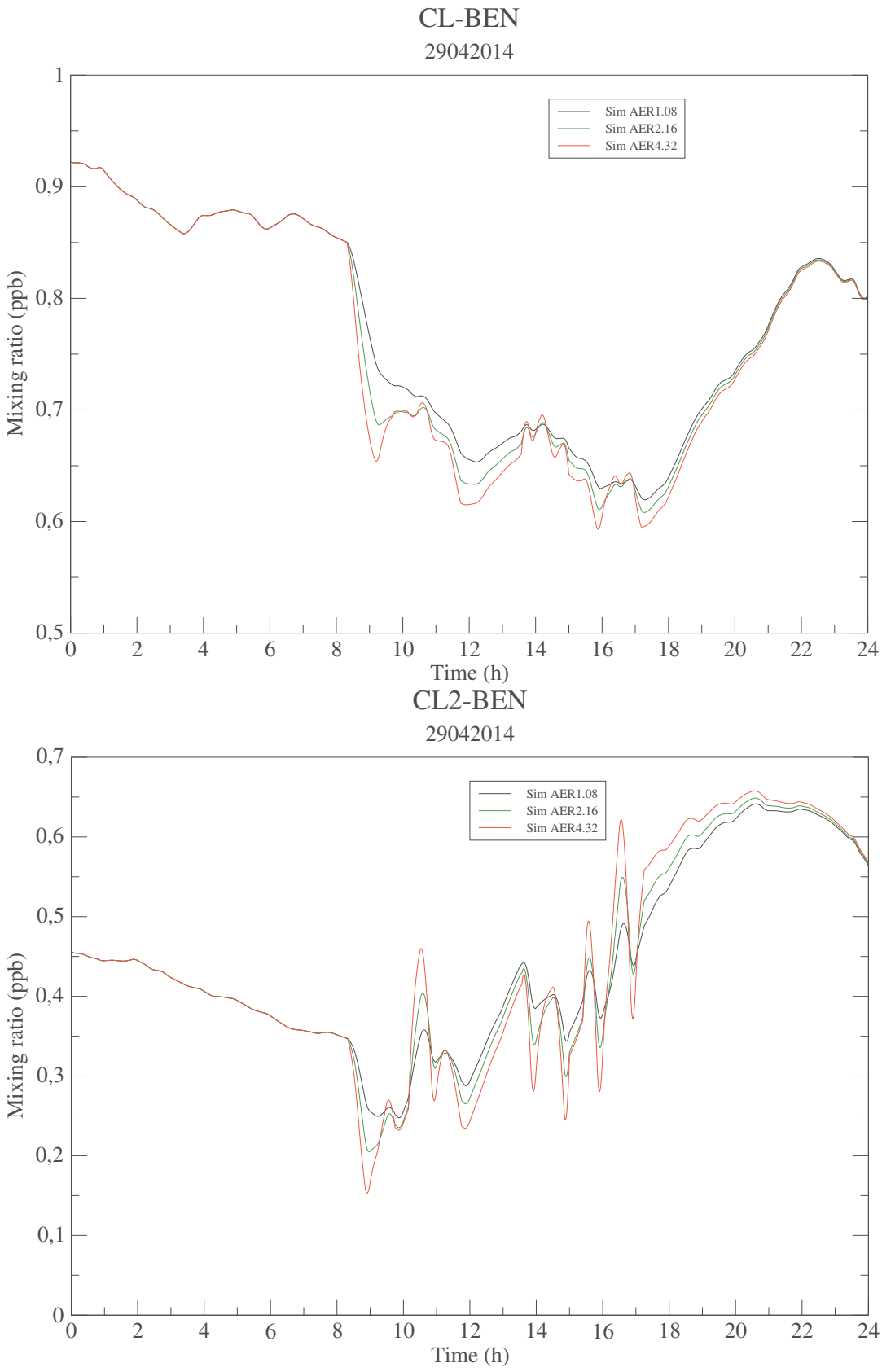

Figure 4.12 – Modeled concentrations of chlorobenzene (CL-BEN) and p-dichlorobenzene (CL2-BEN) with AER1.08 h^{-1}(black line), AER2.16h^{-1} (green line), AER4.32h^{-1} (red line)

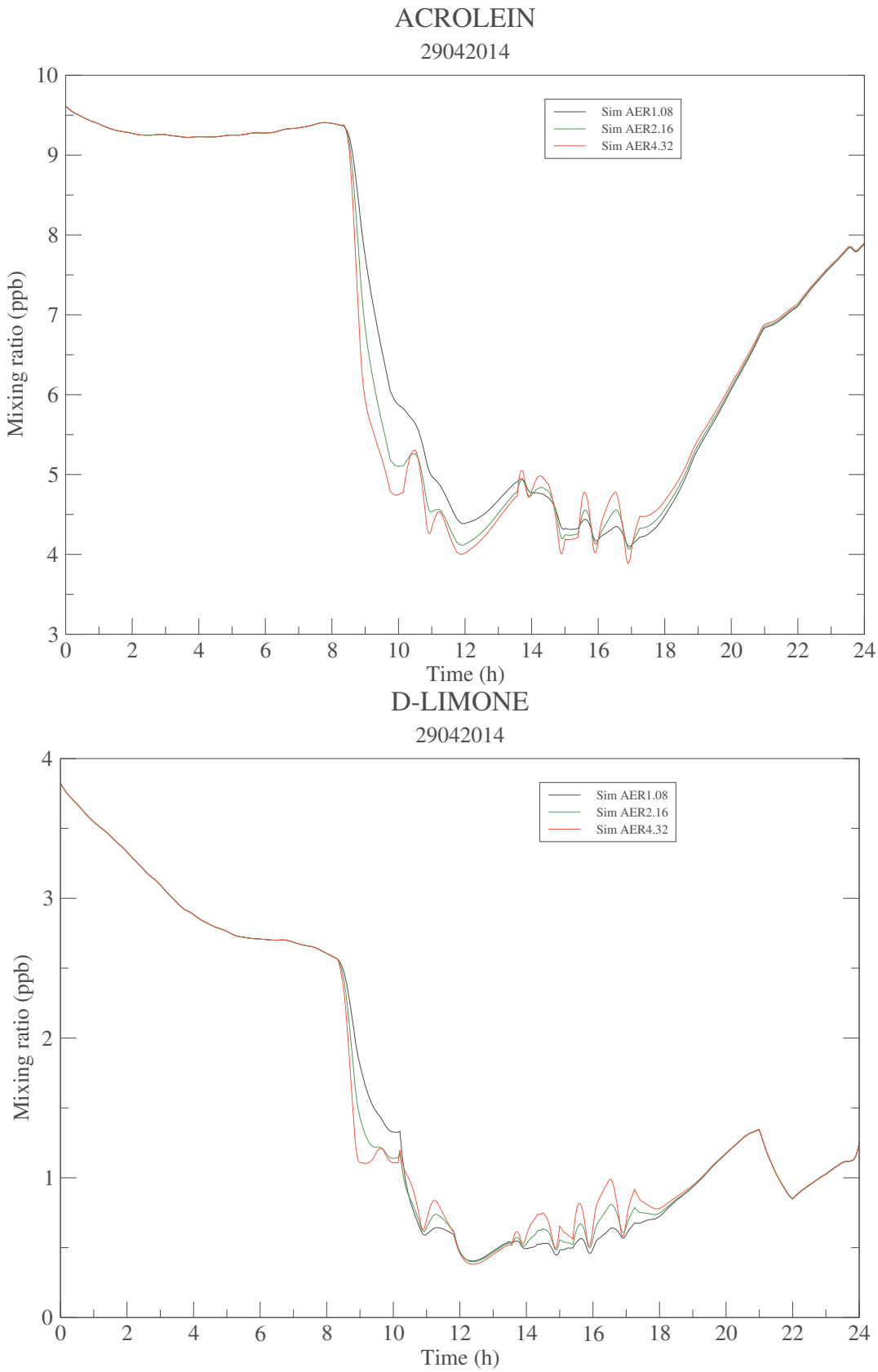

Figure 4.13 – Modeled concentrations of acrolein and d-limonene (D-LIMONE) with AER1.08 h^{-1}(black line), AER2.16h^{-1} (green line), AER4.32h^{-1} (red line)

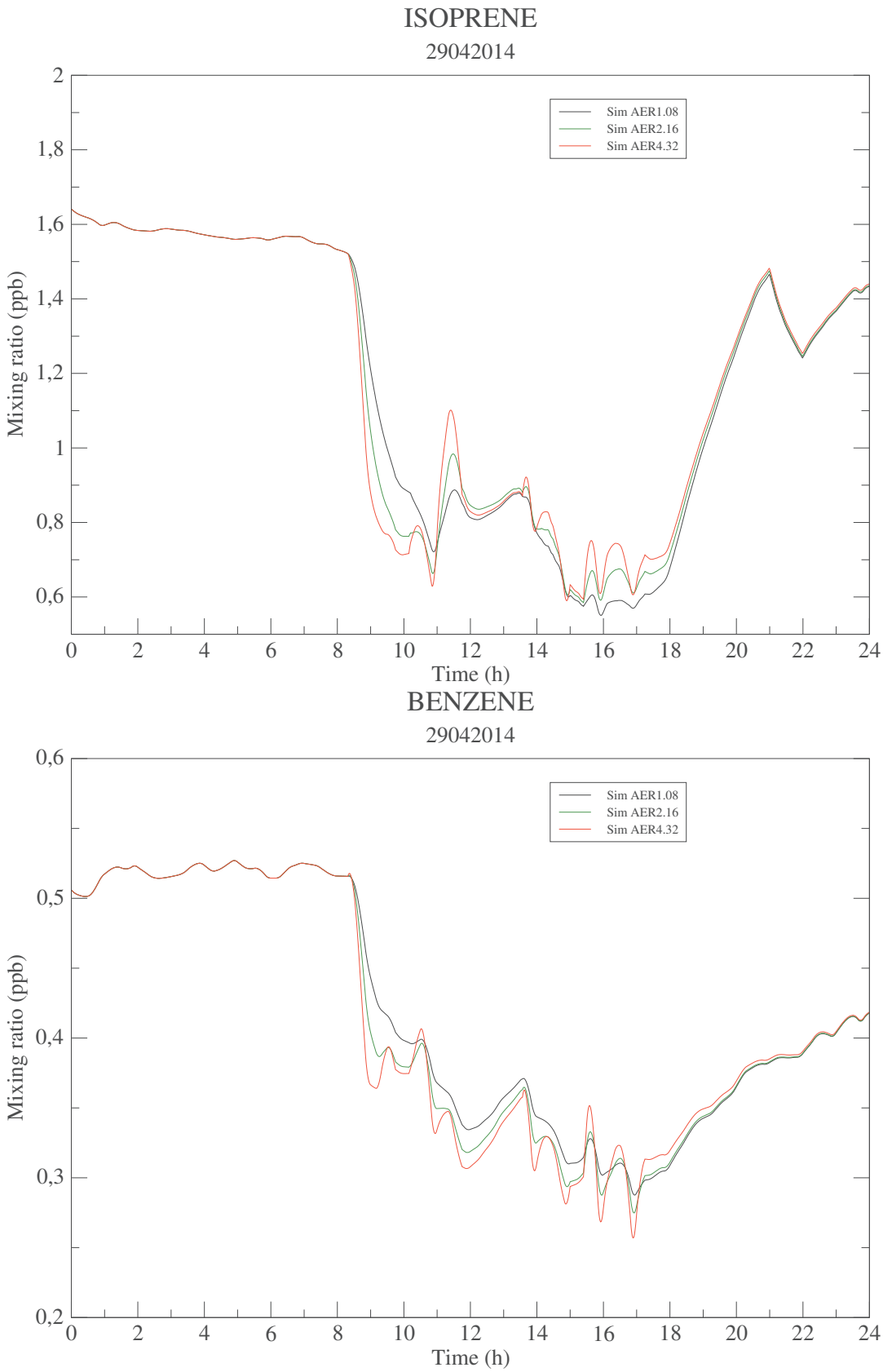

Figure 4.14 – Modeled concentrations of isoprene and benzene (BENZENE) with AER1.08 h^{-1} (black line), AER2.16h^{-1} (green line), AER4.32h^{-1} (red line)

Table 4.8 – Comparaison of modeled concentrations (ppb) with different air exchange rate

Species	AER1.08h^{-1}			AER2.16h^{-1}			AER4.32h^{-1}		
	max	mean	min	max	mean	min	max	mean	min
NO	0.40	0.08	0.01	0.69	0.09	0.01	1.11	0.12	0.01
NO_2	10.75	4.71	2.42	14.23	5.09	2.43	16.66	5.31	2.45
O_3	78.53	10.07	1.28	80.68	11.61	1.28	83.40	13.14	1.28
formaldehyde	27.12	20.18	12.34	30.01	19.17	9.79	32.11	18.58	8.10
acetaldehyde	5.26	3.85	2.70	5.27	3.76	2.42	5.66	3.69	2.15
methanol	49.08	27.80	16.73	48.96	25.72	13.98	48.75	24.63	11.95
toluene	38.15	19.34	10.35	37.88	16.26	6.50	37.36	14.61	4.34
o-xylene	1.96	0.87	0.55	1.95	0.81	0.50	1.94	0.77	0.44
acrolein	9.37	5.66	4.10	9.37	5.54	4.06	9.38	5.49	3.89
acetone	10.88	6.48	4.20	10.88	6.24	3.96	10.88	6.13	3.67
benzene	0.52	0.36	0.29	0.52	0.36	0.27	0.52	0.35	0.26
isoprene	1.52	0.97	0.55	1.52	0.97	0.58	1.52	0.98	0.59
d-limonene	2.56	0.90	0.40	2.56	0.89	0.40	2.56	0.91	0.38
chlorobenzene	0.85	0.71	0.62	0.85	0.70	0.61	0.85	0.70	0.59
p-dichlorobenzene	0.64	0.46	0.25	0.65	0.46	0.20	0.66	0.46	0.15

4.3.3 Effects of sorption rates on indoor pollutant concentrations

Modeled concentrations for NOx and 12 VOC are presented in figues 4.15-4.22. Results show that the variation of sorption rates (k_a and k_d) has a slight influence on benzene concentration, but there is almost no impact for other VOC and NOx concentrations. For benzene, with increasing k_a and k_d, the maximum and mean concentrations of benzene (see table 4.9 increase by 3.92% and 2.5% respectively compared with those simulated with minimum k_a and k_d . However, the concentrations of benzene remain unchanged for simulations with mean k_a, k_d and maximum k_a, k_d .

4.3.4 Effects of window transmittance spectra on indoor air quality

From the observation of an overlap range between the transmitted light and the absorption spectra, it is showed that, with or without films, the wavelengths indoors are available to photolyse

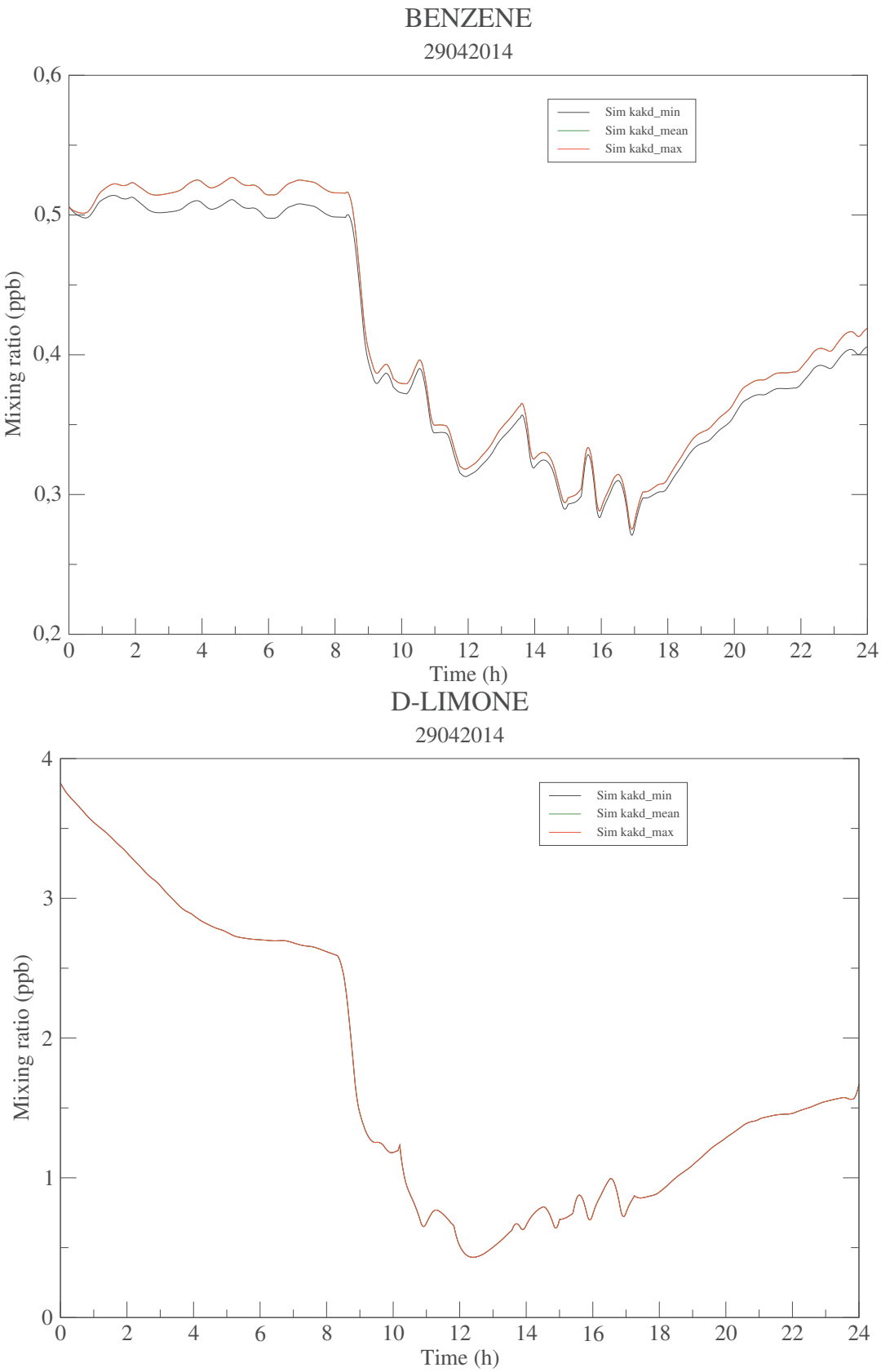

Figure 4.15 – Modeled concentrations of benzene (BENZENE) and d-limonene (D-LIMONE) with $k_a k_d$ minimum(black line), $k_a k_d$ mean (green line), $k_a k_d$ maximum (red line)

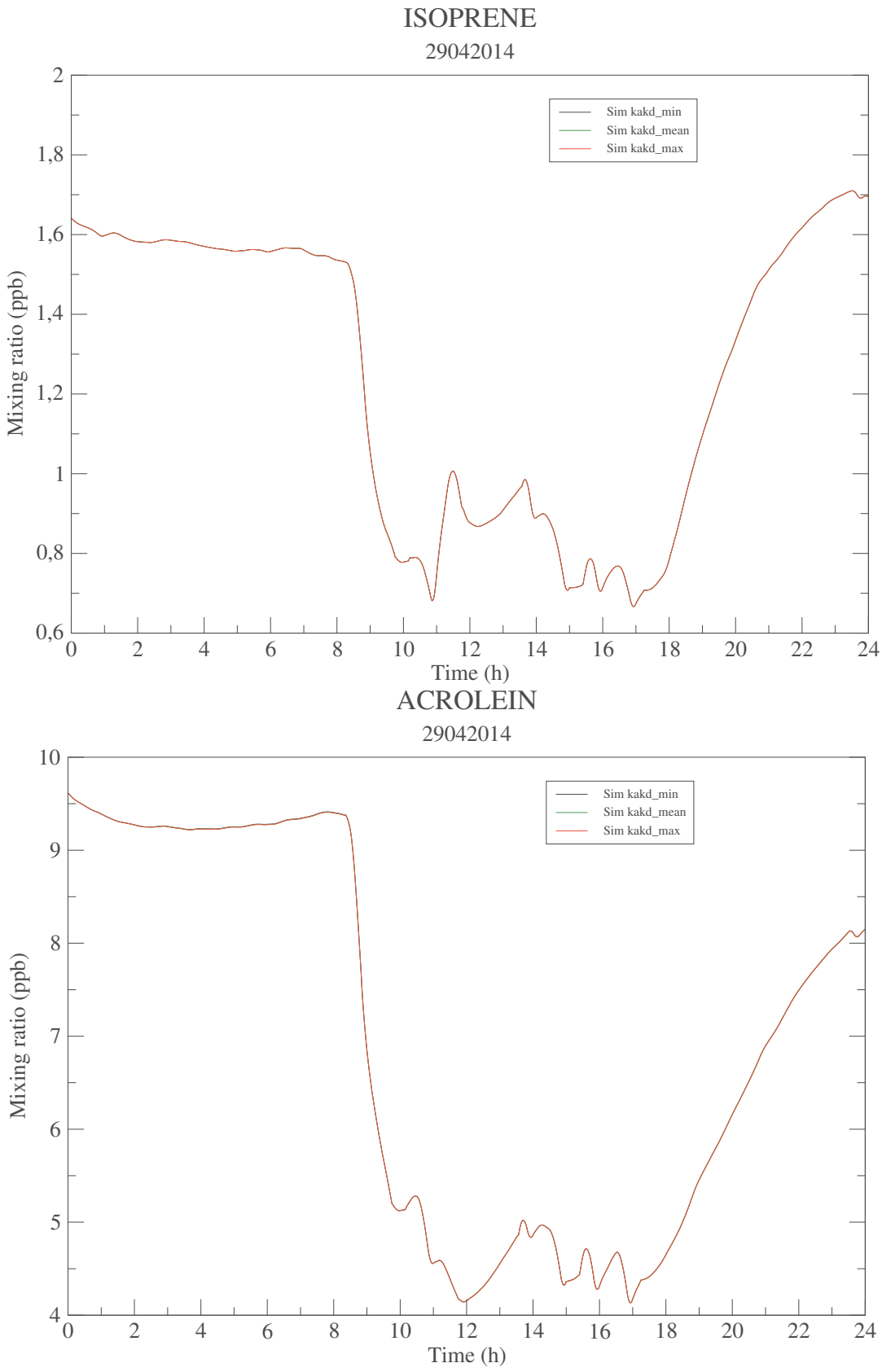

Figure 4.16 – Modeled concentrations of isoprene and acrolein with $k_a k_d$ minimum(black line), $k_a k_d$ mean (green line), $k_a k_d$ maximum (red line)

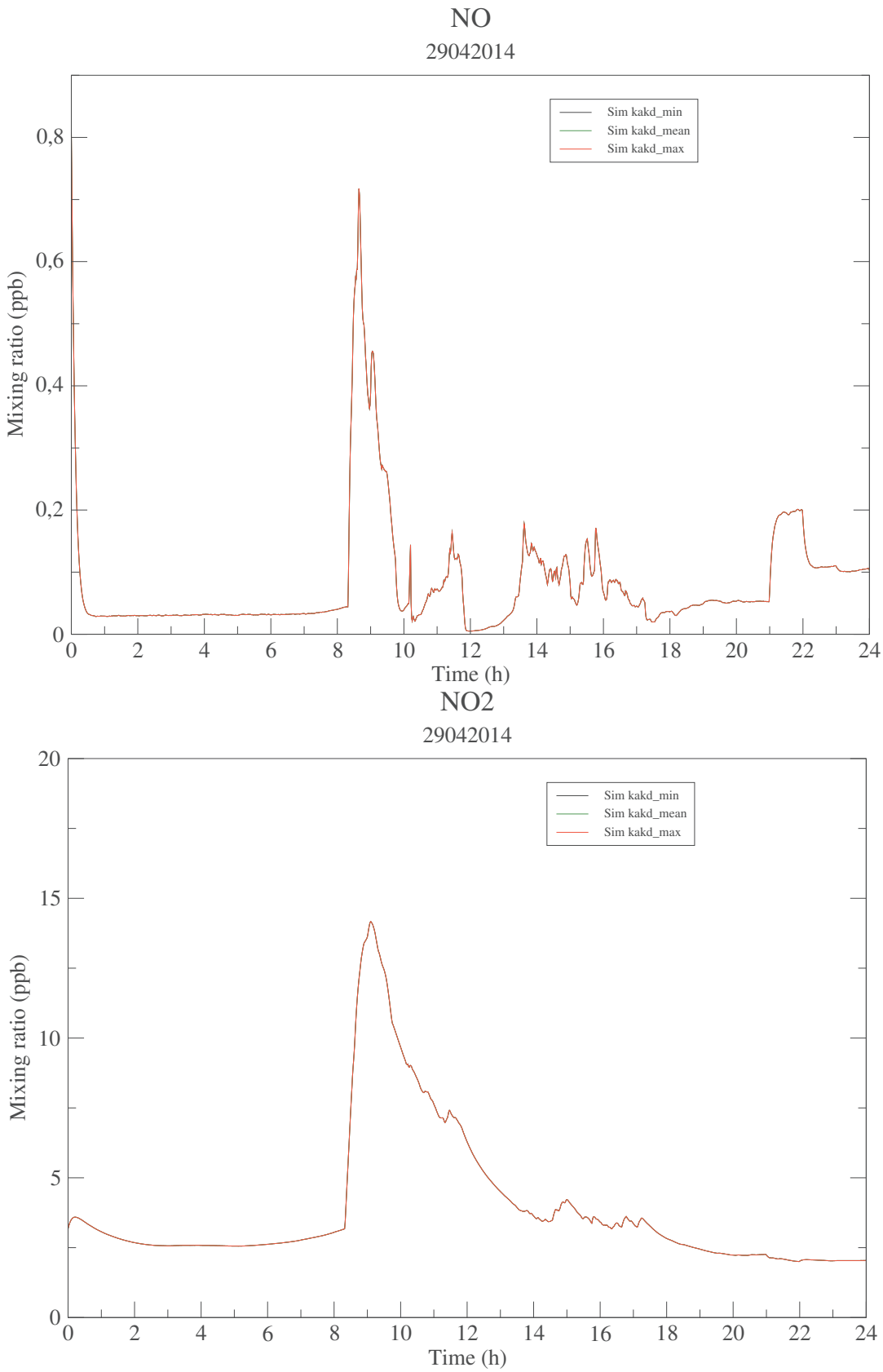

Figure 4.17 – Modeled concentrations of NO and NO_2 with $k_a k_d$ minimum(black line), $k_a k_d$ mean (green line), $k_a k_d$ maximum (red line)

Table 4.9 – Comparaison of modeled benzene concentrations (ppb) with different sorption rates

Species	$k_a k_d$ min			$k_a k_d$ mean			$k_a k_d$ max		
	max	mean	min	max	mean	min	max	mean	min
benzene	0.51	0.40	0.27	0.53	0.41	0.28	0.53	0.41	0.28

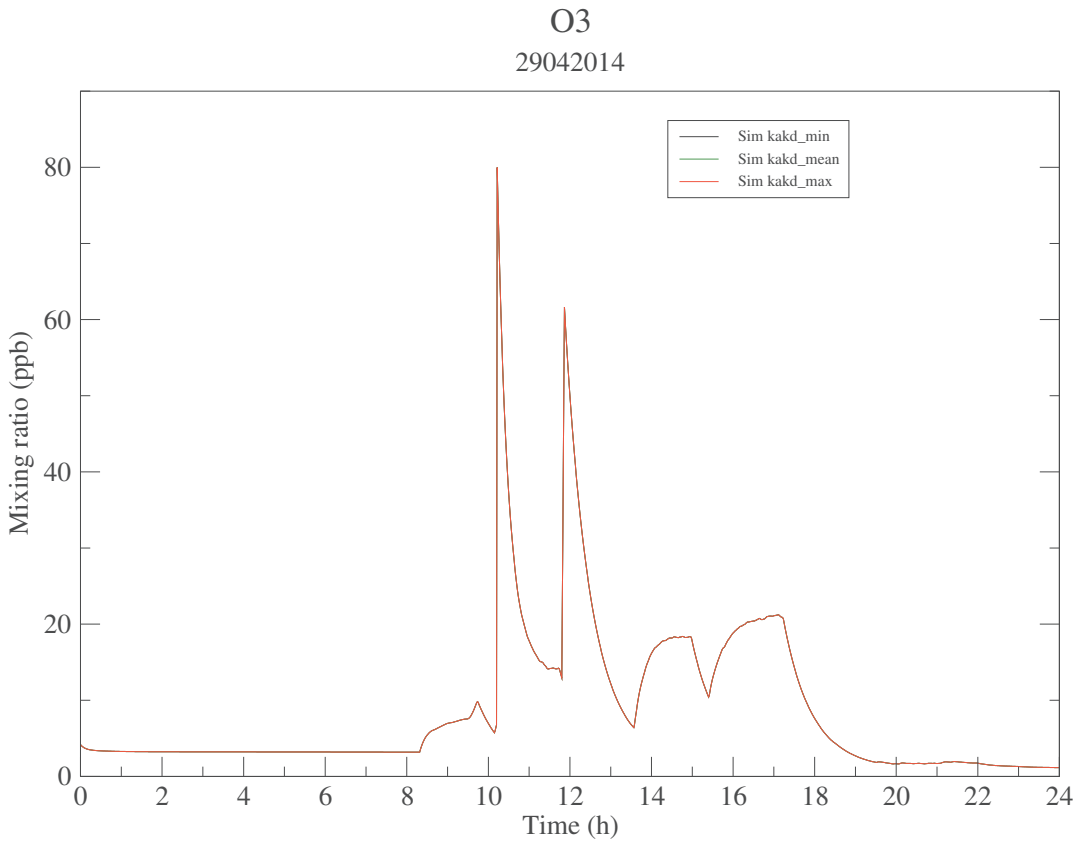

Figure 4.18 – Modeled concentrations of O_3 with $k_a k_d$ minimum(black line), $k_a k_d$ mean (green line), $k_a k_d$ maximum (red line)

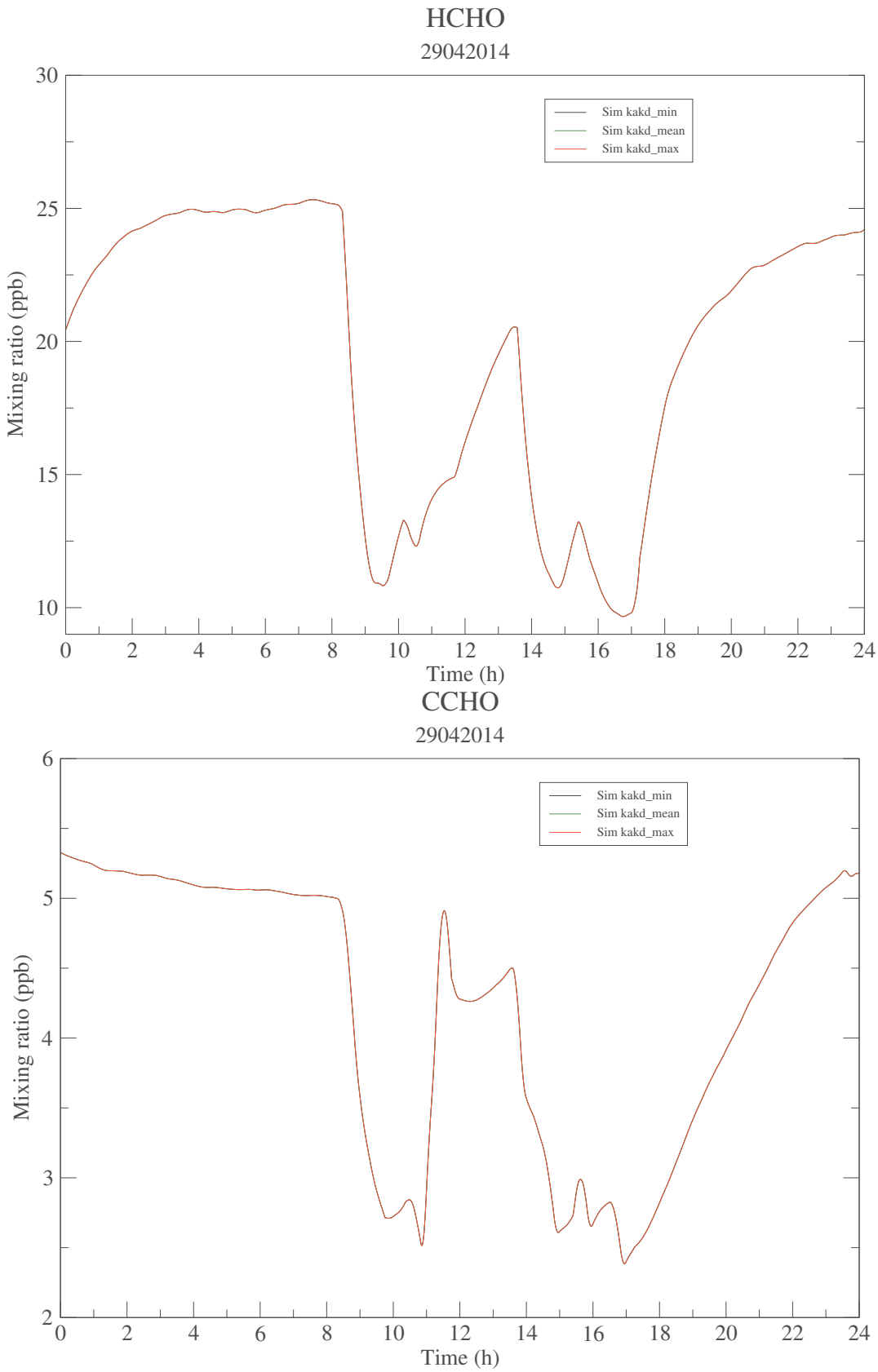

Figure 4.19 – Modeled concentrations of NO, NO_2 O_3, formaldehyde (HCHO) and acetaldehyde (CCHO) with $k_a k_d$ minimum(black line), $k_a k_d$ mean (green line), $k_a k_d$ maximum (red line)

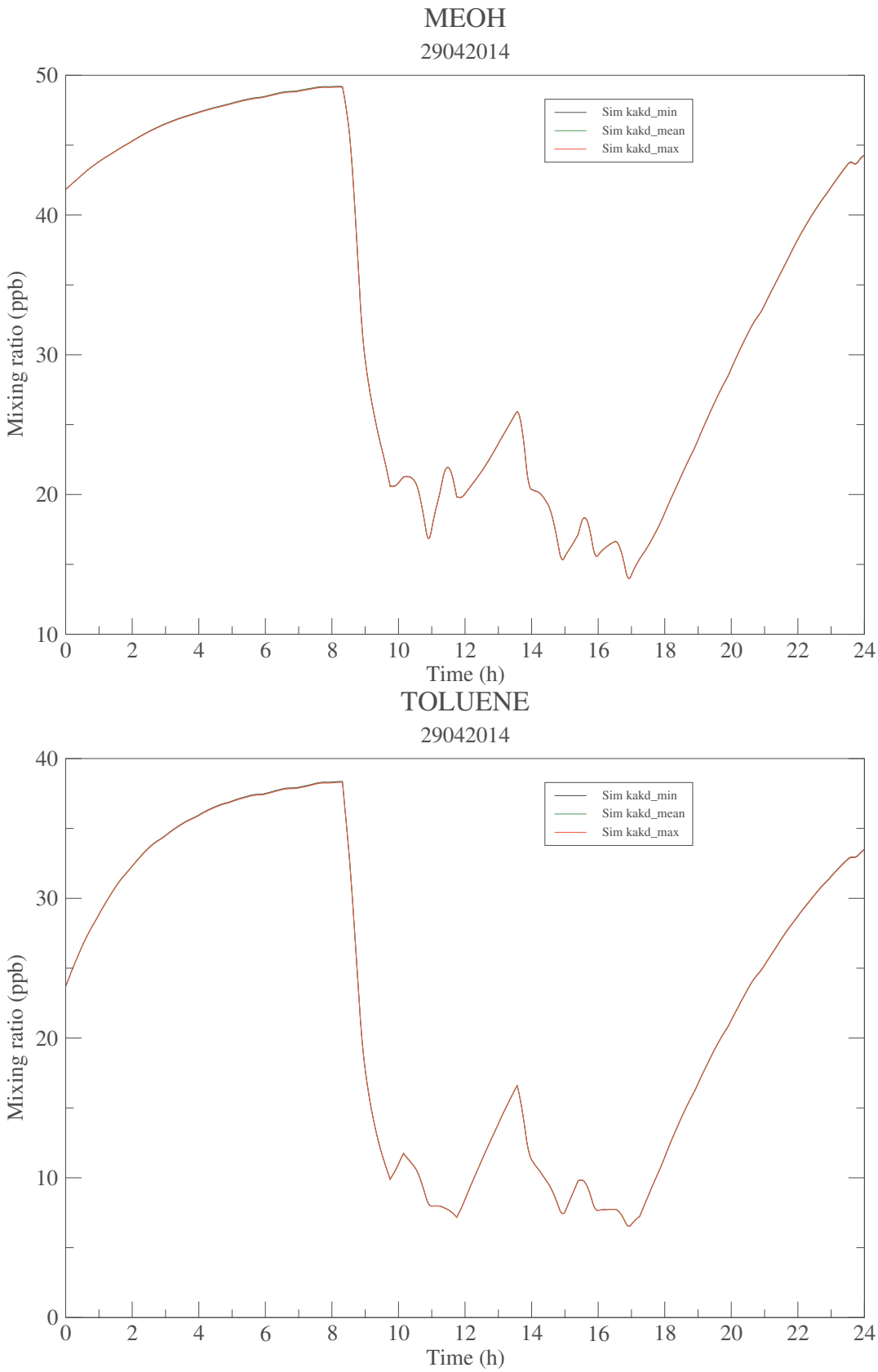

Figure 4.20 – Modeled concentrations of methanol (MEOH) and toluene with $k_a k_d$ minimum(black line), $k_a k_d$ mean (green line), $k_a k_d$ maximum (red line)

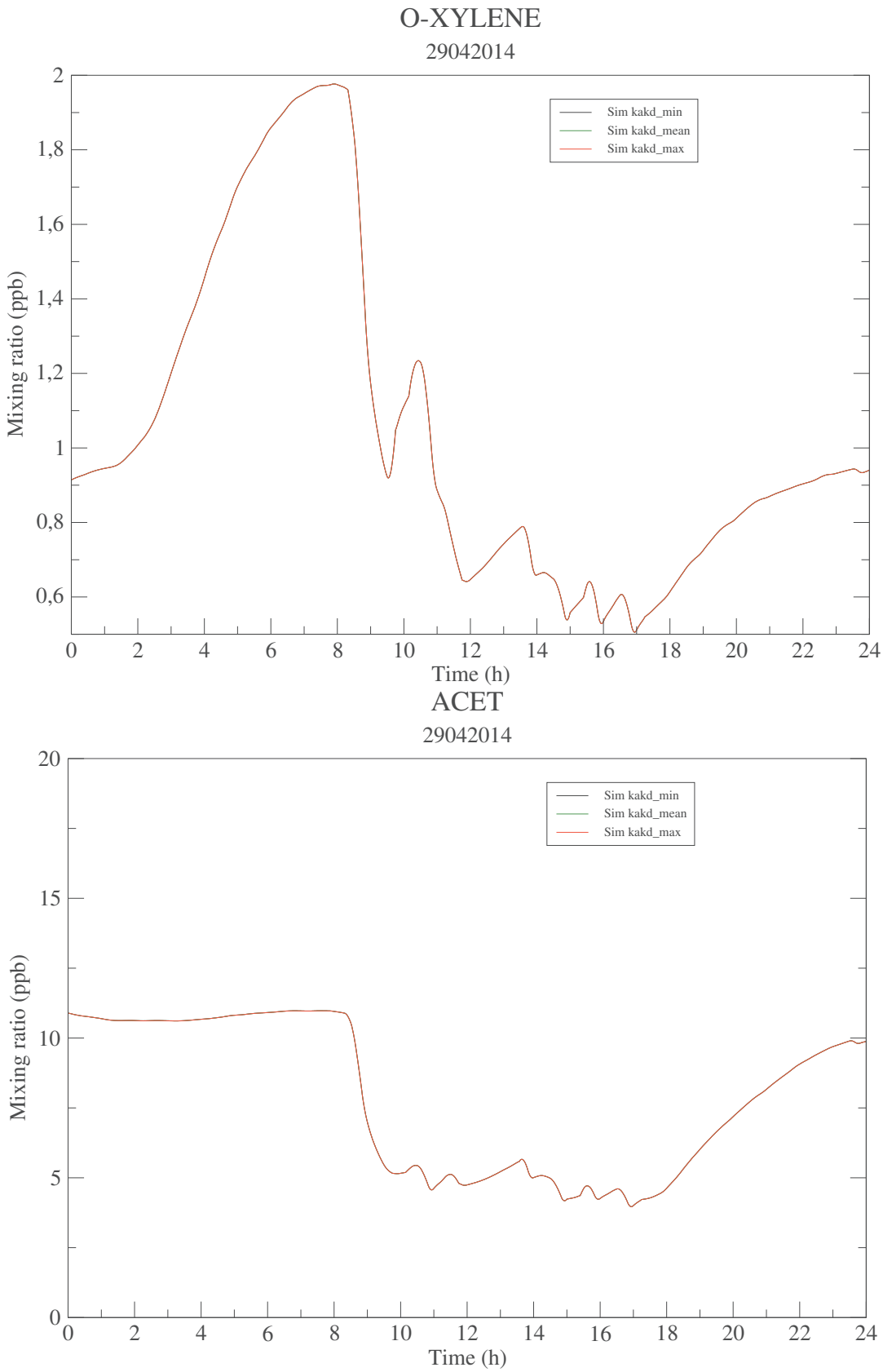

Figure 4.21 – Modeled concentrations of o-xylene (O-XYLENE) and acetone (ACET) with $k_a k_d$ minimum(black line), $k_a k_d$ mean (green line), $k_a k_d$ maximum (red line)

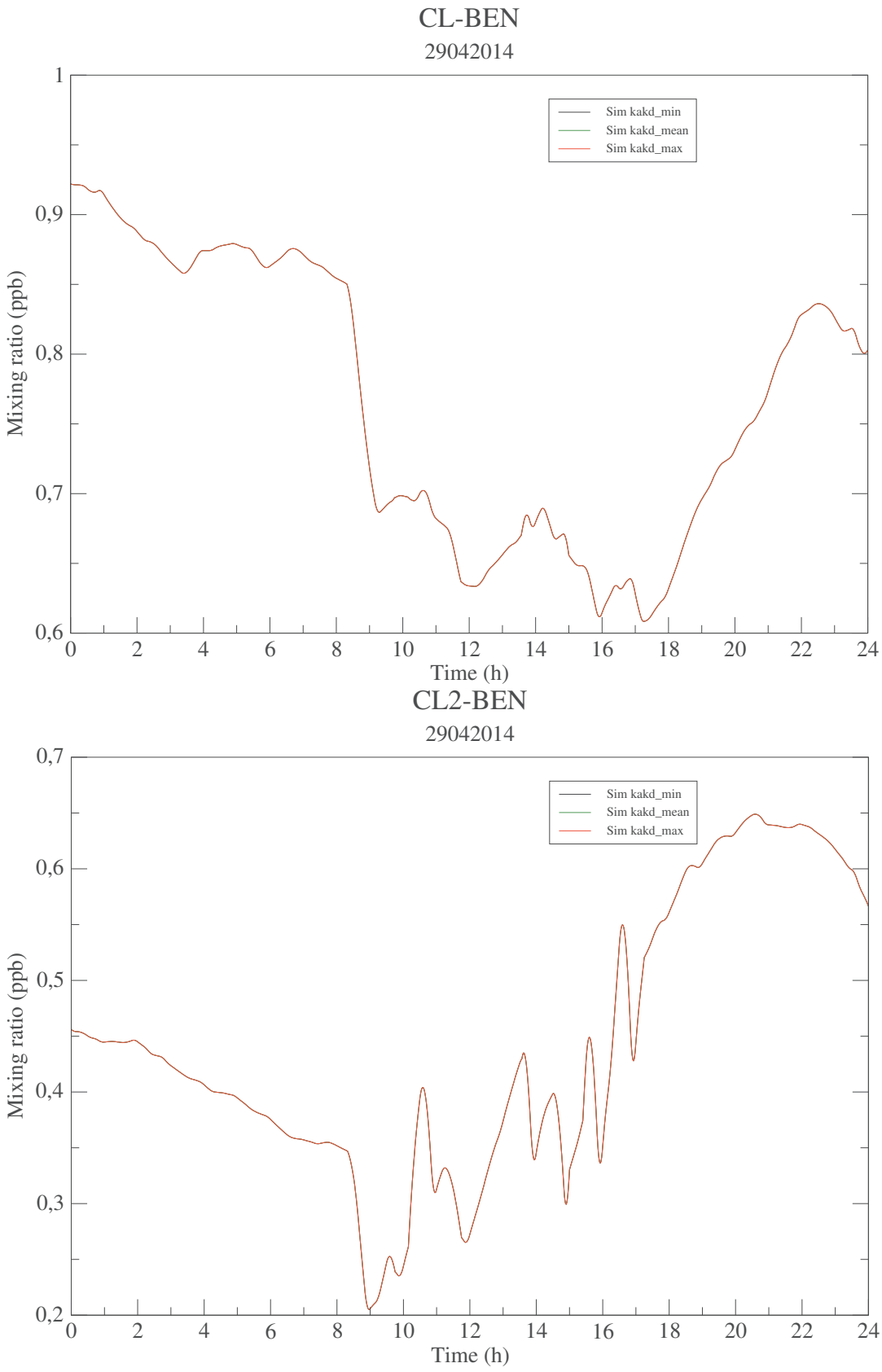

Figure 4.22 – Modeled concentrations of chlorobenzene (CL-BEN) and p-dichlorobenzene (CL2-BEN) with $k_a k_d$ minimum(black line), $k_a k_d$ mean (green line), $k_a k_d$ maximum (red line)

NO_2 and NO_3. The photolysis of ozone as the main source of OH in the atmosphere is negligible indoors. It is noticed that the photolysis of HONO only takes place in rooms having windows without UV films (these films are commonly installed at the ground floor as intrusion retarding). In addition, the photolysis of HONO has been demonstrated as an important source of OH radical [173, 48]. Taking into account the different types of transmittance spectra (see figure 4.2), the photolysis frequencies of HONO has been compared in table 4.10. Results show that photolysis frequencies of HONO increase with increasing the transmittance for UV light.

Table 4.10 – Average photolysis frequencies calculated with different transmittance for one day and without artificial light

Conditions	J_{HONO} (HONO + hv = OH + NO)
nolight	0.00e+00
Nazaroff	9.68e-07
L0-LE	8.52e-07
LEHP	2.94e-06
Carslaw	1.94e-05
M1	1.61e-04
L1-LE	1.76e-04
Drakou	1.94e-04

Figures 4.23-4.26 show the influence of the light intensity on the mean concentration of the HOx radicals, HONO, ozone, NOx and some VOC. There is no visible variation for these species mentioned with the average transmittance for UV light (300-400 nm) between 0 to 3% but their concentration change significantly with the transmittance for UV light between 20.05% and 30%. With increasing the transmittance for UV light (20.05% to 30%), HONO mean concentration decreases by the most larger factor of 15% due to more HONO photolysis. Indoor OH radical and NO concentrations increase with increasing the transmittance for UV light causing more HONO photolysis to produce OH and NO. More indoor OH causes decreasing of d-limonene, o-xylene and isoprene via their reactions with OH. As products of reactions of VOC with OH, formaldehyde (HCHO) and acedaldehyde (CH_3CHO) increases little but HO_2

increases largely. Ozone production increase by about 7 ppb, due to the light increase in the visible increasing the photolysis of NO_2 . This shows the importance of light transmittance to study the indoor chemistry as it will impact the oxidant levels.

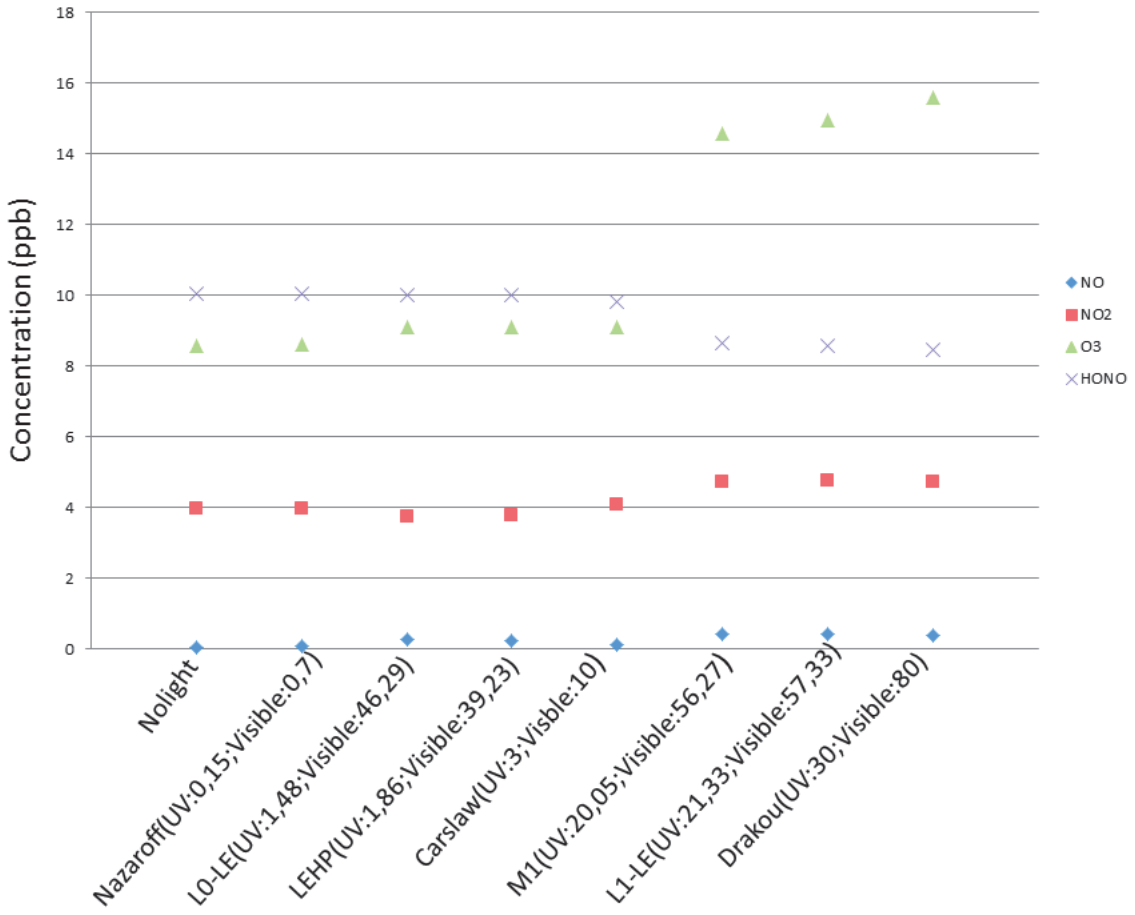

Figure 4.23 – Influence of the window transmittance spectra on the mean concentration of HONO, ozone and NOx

4.4 Discussion and Conclusion

In this chapter, the effect of changes of surface emission rates, and sorption rates in their range of spatial variabilities on indoor air quality is investigated. Scenarios with varying air exchange rate and the light intensity transmitted by different windows are also analyzed.

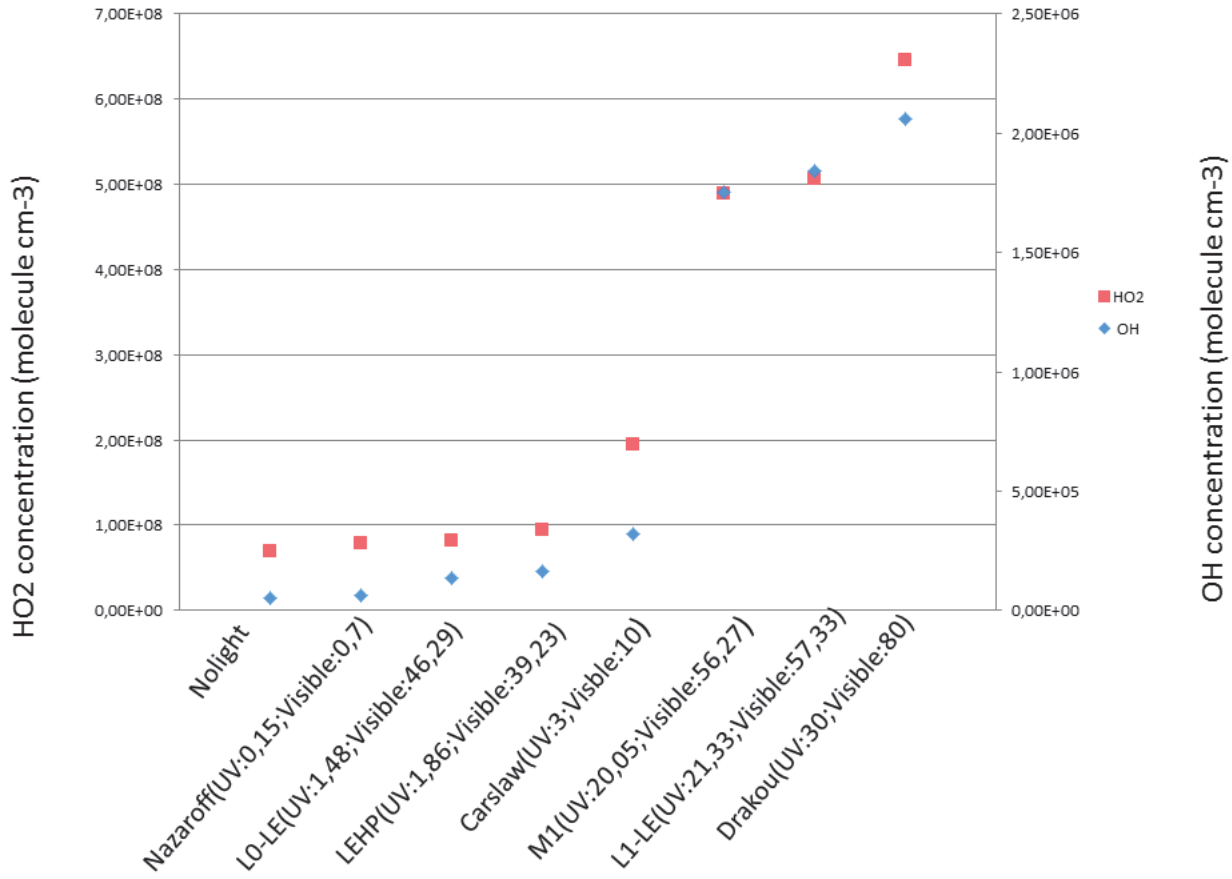

Figure 4.24 – Influence of the window transmittance spectra on the mean concentration of the HOx radicals

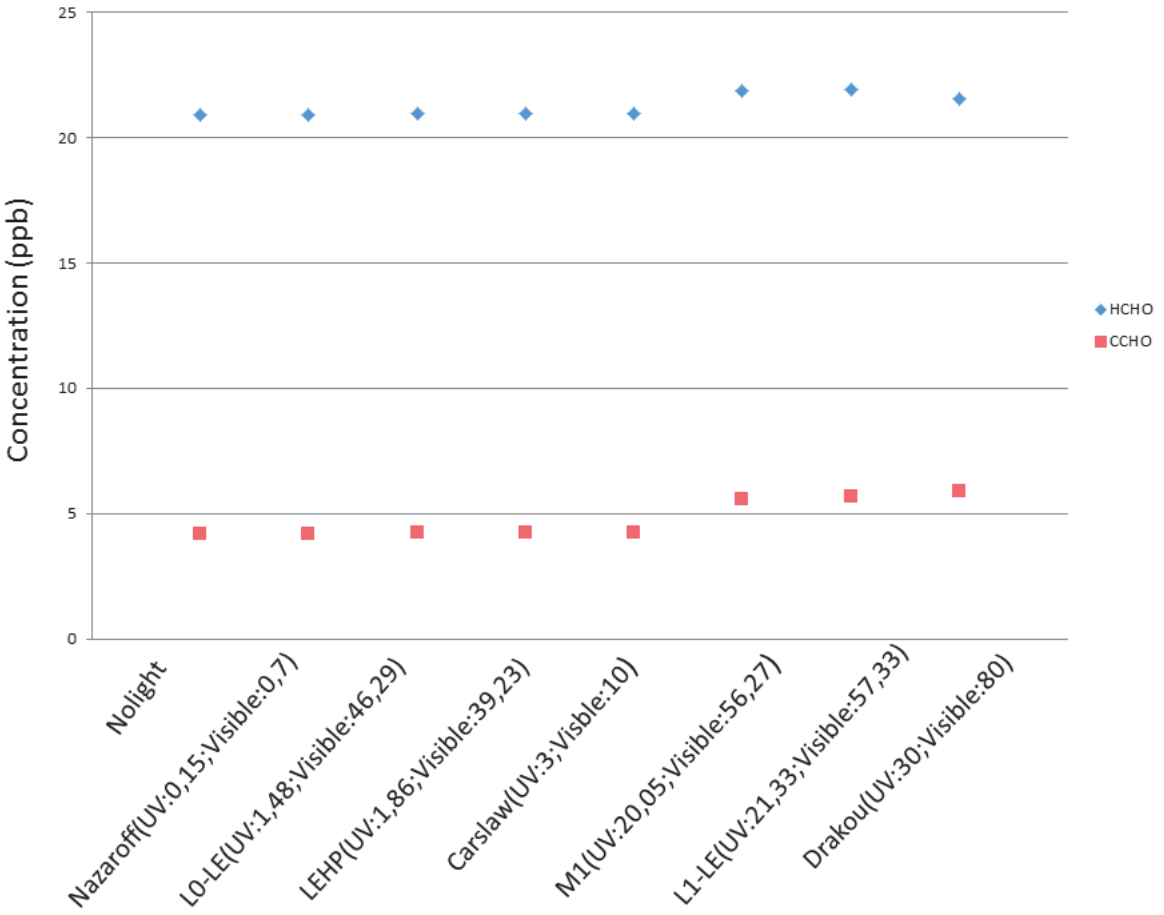

Figure 4.25 – Influence of the window transmittance spectra on the mean concentration of formaldehyde and acedaldehyde

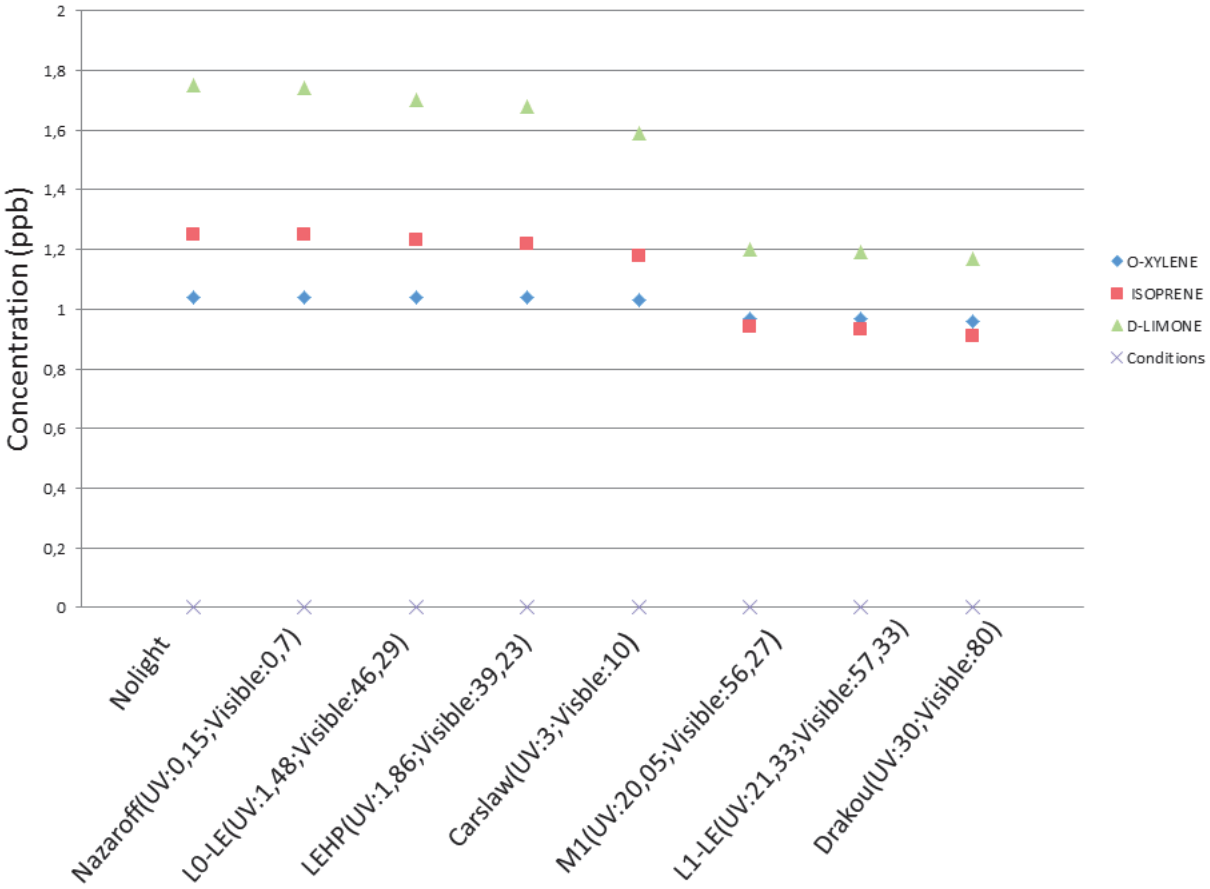

Figure 4.26 – Influence of the window transmittance spectra on the mean concentration of some VOC

The VOC emission rates were measured for the ten main surfaces present in a classroom of an energy efficient school building during the MERMAID campaign. The measurement results show that the emission rates can be different between similar surfaces. In addition, the emission rate determined on different locations of the same material showed variability between 9% and 85% respectively depending on the VOC and the surface. This heterogeneity is maybe due to aging of surface caused by different exposure to the sunlight.

In the INCA-Indoor model, mean emission rate factors and sorption rates are used. To study the influence of the emission rates of VOCs on the indoor air quality, simulations with the different measured emission rates (minimum, mean, maximum) have been performed on a selected day of the field campaign. Simulation results show that VOC emissions have, in the conditions of this study, a major impact on the measured concentration indoor of formaldehyde, toluene and d-limonene (variations could reach 20%, 30% and 30% respectively around the mean). It is noted that the use of maximum surface emission factors for acetaldehyde and acetone is not sufficient to well represent the fast increase of the concentrations of those pollutants in the classroom when the ventilation is off in late afternoon. This could be due to an underestimation of the emission rates and the influence of the deposition and also an underestimation of NOx, O_3, or a lack of VOC species considered in the model (some VOC productions are parametrized and their impact on the formation of HCHO and CH_3CHO through oxidation process may be reduced).

Concentrations of NOx and O_3 increase with AER increasing. With an increase of one time of measured AER ($4.32h^{-1}$) when the ventilation switched on, the maximum and mean concentrations of NO increase by 60.86% and 33.33% receptively and the maximum concentrations of NO_2 and O_3 increase by 17.08% and 3.4% respectively. The increase of O_3 concentrations enhances the oxidation of some VOC (i.e d-limonene, isoprene) by O_3 or reactions of NO (or O_3) with some radicals (i.e. methyldioxidanyl, peroxyacyl) to produce more HCHO. More NO

increases the productions of HCHO and CH_3CHO via reactions of the organic peroxy radical (RO_2) with NO.

With increasing one time of AER (from 1.08 h^{-1} to 4.32 h^{-1}), the maximum concentrations of acetaldehyde increase, but the mean and minimum concentrations decrease. Compared to the concentrations for scenario with AER 2.16 h^{-1}, the maximum concentrations of acetaldehyde increase by 7.4% and mean concentrations decrease by 1.86% with an AER 4.32 h^{-1}. The maximum concentrations of acetaldehyde increase as a consequence of the increase of concentrations of NO and O_3, allowing more NO and O_3 to react with some radicals (i.e. methyldioxidanyl, peroxyacyl) and to produce more acetaldehyde. However, the effect of ventilation diluting the concentrations of formaldehyde and acetaldehyde is more important than the reactions producing formaldehyde and acetaldehyde (i.e. methyldioxidanyl+NO, peroxyacyl+NO). Consequently, the mean concentrations of formaldehyde and acetaldehyde reduce.

The maximum, mean and minimum concentrations for methanol, toluene and o-xylene decrease with increasing AER. Compared with concentrations for scenario with AER 1.08 h^{-1}, an increase of 3 times of AER (4.32h^{-1}) reduce 11.4%, 24.46% and 11.49% receptively for the mean concentrations of methanol, toluene and o-xylene.

For acrolein and acetone, there is almost no change for the maximum concentrations but mean and minimum concentrations reduce slightly with increasing AER. Furthermore, there is no significant change for the maximum, mean and minimum concentrations of benzene, isoprene, d-limonene, chlorobenzene and p-dichlorobenzene with increasing AER.

The variation of sorption rates (k_a and k_d) has a minor influence on benzene concentration, and there is almost no impact for other VOC and NOx concentrations. With increasing of k_a and k_d For benzene, the maximum and mean concentrations of benzene increase by 3.92% and 2.5% respectively compared with those simulated with minimum k_a and k_d.

The characterization of the transmittance of different windows has been studied during MERMAID campaign. With the measured transmittance spectra of different type of windows,

a series of simulations with INCA-Indoor model have carried out to investigate the effect of the transmitted light. Simulation results show the transmitted light depends on the type of window and has direct impact on photolysis phenomena occurring indoors and pollutant concentrations. In addition, the distribution of indoor light intensity also has impact on indoor chemistry and pollutant concentrations like HCHO and O_3. Under indoor conditions of this study, with increasing the transmittance for UV and visible light, concentrations of the HOx radicals, O_3 increase and some VOC (i.e d-limonene, o-xylene, isoprene) decrease due to the reactions of VOC with OH.

Results in this chapter demonstrated the important role of emission rate and air exchange rate in impacting indoor air quality and quantified their impact on indoor air quality. However, the important parameters influencing pollutant concentrations may be different with respect to different species. For example, the role of indoor chemistry may be more important than that of air exchange rate for some species (i.e. d-limonene), especially when the reactions act at a rate competitive or greater than AER. If little information is given about the effect of parameters on pollutant concentration, how to find the important parameters is an important question before making decision to reduce indoor air pollution. Furthermore, it is critical to compare the importance of different parameters and find the important parameters. For a model with a number of parameters, it is time-consuming to assess the effect of parameters with the method of changing the values of parameters one by one. Hence, how to find a method more convenient to assess all the influence of diverse parameters on pollutant concentration levels is important. That is why we have developed a sensitivity model using automatic differentiation to investigate the effect of parameters. More information will be discussed in next chapter.

CHAPTER 5

DEVELOPMENT OF A SENSITIVITY METHODOLOGY USING THE LINEAR TANGENT MODEL : APPLICATION TO INDOOR OH RADICAL CONCENTRATION ANALYSIS

Abstract

The tangent linear model of the indoor air quality model, INCA-Indoor, was built using the TAPENADE model. This so-called new model INCA-Indoor-D allows to compute local first order derivatives of pollutant concentrations with respect to input parameters that are defined as sensitivities. Sensitivities of OH concentration ([OH]) are here quantified and classified at the time of the [OH] peak concentration and the maximum growing velocity in an objective way without redefine scenarios. The sensitivity results confirm that [OH] is firstly and highly sensitive to the air exchange rate and to the photolysis of HONO which produces OH. The photolysis of NO_2 also shows an important positive impact on [OH]. Indoor [OH] is affected by outdoor concentrations of NOx (NO and NO_2) and O_3. In the presence of a variety of VOCs in the model, the main sink reactions of OH are reactions of d-limonene with OH and ethanol with OH. The reaction of d-Limonene with OH or O_3 is much less important.

KEYWORDS INCA-INDOOR, INCA-Indoor-D, Sensitivity analysis, IAQ model, automatic differentiation, Tapenade, hydroxyl radical, photolysis

5.1 Introduction

Since people live 80 to 90 percent of their time indoors and it was largely demonstrated that indoor air pollution often exceeds health recommendation standards [146, 72, 174], it is very important to develop methods to better assess air quality in indoor environments and subsequently the global exposures of the inhabitants. It is also important to design tools helping to define efficient measures to reduce this exposure.

On the one hand, measurement campaigns allow direct and precise evaluations of the indoor air quality states. However, they are very local and usually in insufficient number to fully understand the processes involved. On the other hand, indoor air quality (IAQ) models are tools that allow to first estimate the indoor air quality as supplementary to existing measurements or in case where measurements are not possible but keep still approximates of the real state of the IAQ. These models are also useful to understand the influence of each process on the air pollutant concentrations, and to predict indoor air pollution following several scenarios of reconstruction, renovation, ventilation, emission reduction, etc.

Different indoor air quality models were developed. An Indoor Chemistry and Exposure Model (ICEM) [173] for example, allows for the simulations of transport processes between outdoor and indoor environments, indoor emissions, indoor chemical reactions and deposition. This model considers homogeneous chemistry and irreversible heterogeneous deposition. Other heterogeneous reactions and surface processes like adsorption and desorption are not taken in account. The indoor air detailed chemical model (INDCM) [46, 47, 175] was developed to investigate indoor air chemistry based on a detailed chemical mechanism (the Master Chemical Mechanism, MCM) [114]. This chemical box model does not consider detailed characterizations of the buildings like the emission rates for specific materials used and the sorption processes. Mendez et al. (2015) [41] developed the INCA-Indoor model that has the advantage to include the processes existing in confined environments such as ventilation, emission, deposition, gas phase chemical processes, to simulate the concentrations of indoor chemical species.

The chemistry mechanism is based on SARPC [130]. Although it is less detailed than the MCM of INDCM but as it is, the INCA-Indoor model shows good performance when simulations were compared with measurement data collected during SURFin [42] and MERMAID [37] and results in Carslaw et al. (2007) [41].

The accuracy of the simulated concentrations depends both on the capacity of the model to represent the real environment (depending on our knowledge or computing skills), and the quality of the input data used to perform the simulations. Indoor environments are so complex, involving many types of materials that can release or adsorb chemical compounds and processes, that it is impossible to correctly represent all of them. Thus it is crucial to evaluate the sensitivity of the model to each input and each process taken into account. One challenge is to be able to identify the most important parameters. It is thus crucial to evaluate the sensitivity of the model to each input and each process taken into account in order to improve their modeling by order of priority.

Sensitivity analysis (SA) is usually defined as the evaluation of the impacts on the model outputs due to changes in model input parameters [176]. A key feature of SA is parameter ranking, which aims at generating the ranking of the input factors according to their relative contribution to the output variability [177]. The application of SA to the model can provide insights into the dominant controls of the system and can support decision-making. The SA methods most widely used are grouped into five classes including perturbation and derivatives methods, multiple-starts perturbation methods, correlation and regression analysis methods, Monte-Carlo sensitivity analysis and Variance-based methods [177]. These methods have one or several of the following limitations : inaccuracy in the results, high cost in human effort, difficulty in mathematical formulation and computer program implementation [178].

To support derivatives analyses, automatic differentiation (AD) has the ability to built tangent or adjoint model of computer programs using a large number of input parameters. AD is a program transformation technique aiming at computing the derivatives of the function defined

by a computer program. It is based on the fact that any function, regardless of its complexity, can be viewed as a sequence of elementary operations and elementary functions [179, 180, 181]. By applying the chain rule repeatedly to these elementary operations and functions, one can compute derivatives automatically. This method produces a code that exactly evaluates the derivatives (up to the precision of the machine while saving human efforts).

The first objective of this chapter is to present the development of a linear tangent model (called NCA-Indoor-D) using the AD tool TAPENADE. TAPENADE [182] has been chosen because of its capabilities in terms of code generation, computational efficiency and performance in several applications [183, 184, 185]. The second objective of the chapter is to discuss an application of INCA-Indoor-D in order to objectively analyze further the main determinant of the OH indoor concentrations by applying INCA-Indoor-D.

Sensitivity analysis of indoor [OH] with respect to the different parameters involved, is used to find out the most important parameters and reactions impacting [OH] and helps to understand contributions of different physical and chemical processes.

Indeed, Sarwar et al. (2002) [79] investigated effects of selected parameters on indoor [OH] like outdoor O_3, NO concentrations, indoor alkene emission rates and air exchange rate. Mendez et al. (2015) [41]also studied the effects of selected pollutant concentrations, HONO, NO and the VOC concentrations, on the HOx concentrations [HOx] ([HO_2] + [OH]) budget, following the work of Carslaw (2007) [46] who also assessed the effect of light intensities, deposition, air exchange rate, species concentrations and temperature and relative humidity on indoor [OH]. In these studies referred above, the investigation of the effect of selected parameters on indoor [OH] is realized by varying the parameter value from its nominal value one at a time and then assesses the impacts on the simulation results. The first problem of this method is that a sensitive parameter does not necessarily identify which processes are occurring in the actual environment. Rather, it indicates that a parameter variation within a specific range of values strongly influences indoor [OH], and the absence of a process can impact indoor [OH] just as

much as the presence of one. The second problem is that it could not diagnose to what extent and at which sensitivity level the parameters can impact indoor [OH] in different time periods, due to the parameter sensitivities of indoor [OH] changing significantly through time. The third one is that it could not be used to compare the effects of reactions and model parameters on indoor [OH] and to indicate the most important reactions or parameters for [OH] under specific conditions.

In this study, the tangent linear code of AD technique allows to calculate sensitivity coefficients at a prescribed time with respect to all the parameters without rerunning the model. A temporal sensitivity analysis is conducted to analyze the temporal dynamic of parameter sensitivity. This analysis helps to diagnose the time periods where specific processes like photolysis of HONO or the ventilation dominate indoor [OH] take place. Secondly, we have evaluated the sensitivities of indoor [OH] to the various model parameters (reaction rate, indoor VOCs emission rates, air exchange rate, etc), the influence of which has not been systematically studied before. In the meanwhile, a ranking of parameter importance according to the sensitivity coefficients has been settled and detailed. In this chapter, we carry out SA (i) address three main purposes of sensitivity analysis. They are (i) to quantify the effects of all reactions and model parameters on indoor [OH] with no previous subjective selections ; (ii) to identify the most important reactions and parameters on indoor [OH] and (iii) to set a guideline for improvement of the indoor air quality.

This chapter is organized as follows : section 2 presents the INCA-Indoor model, section 3 details the sensitivity method, the automatic differentiation TAPENADE tool and the application of TAPENADE to INCA-Indoor model. The results of sensitivity are reported and discussed in section 4. The conclusions are provided in section 5.

5.2 INCA-Indoor Model

INCA-Indoor model has been developed to simulate the concentrations of the indoor chemical species, and to understand the physical and chemical processes leading to indoor air pollution and identify the main contributions to pollutant concentrations. The full chemical mechanism of INCA-Indoor model is based on the SAPRC-07 mechanism [41] in which is taken into account the oxidation processes of almost 640 VOCs through 1400 reactions.

For the purpose of this chapter, the chemistry mechanism was restricted depending on the case studied here. This was done mainly to understand the impact of a limited number of reactions and species, and analyze more easily the results. Due to a limitation of TAPENADE to derive long formulations of some production and losses terms produced by lots of chemistry reactions, the full chemistry scheme cannot be used to compute sensitivities but the less reduced ones gives similar results as the full model. The photolysis in the model is modeled following Nazaroff and Cass, (1986) [45]. The indoor photolysis rates depend on the spherically integrated flux of photons in the ultraviolet (UV) (300-400 nm) and visible (400-760 nm) ranges issued from artificial lighting and sunlight entering through the windows and the skylights. The transmission values of visible and UV light of outdoor light as it passes indoors was adopted from Drakou et al. (1997) [172], 80% of the visible light and 30% of UV light, respectively. While we showed in chapter 4 that those Drakou et al.'s conditions of light are not fully representative of indoor conditions that was measured during the MERMAID project, they were chosen in order to be able to compare the sensitivity analysis results to previous results obtained in literature and especially Mendez et al. (2015) [41].

For the purpose of this chapter, the chemistry mechanism was restricted depending on the case studied here. This was done mainly to understand the impact of a limited number of reactions and species, and analyze more easily the results. Due to a limitation of TAPENADE to derive long formulations of some production and losses terms produced by lots of chemistry reactions, the full chemistry scheme cannot be used to compute sensitivities but the less reduced

ones gives similar results as the full model. The photolysis in the model is modeled following Nazaroff and Cass, (1986) [45]. The indoor photolysis rates depend on the spherically integrated flux of photons in the ultraviolet (UV) (300-400 nm) and visible (400-760 nm) ranges issued from artificial lighting and sunlight entering through the windows and the skylights. The transmission values of visible and UV light of outdoor light as it passes indoors was adopted from Drakou et al. (1997) [172], 80% of the visible light and 30% of UV light, respectively. While we showed in chapter 4 that those Drakou et al.'s conditions of light are not fully representative of indoor conditions that was measured during the MERMAID project, they were chosen in order to be able to compare the sensitivity analysis results to previous results obtained in literature and especially Mendez et al. (2015) [41].

The indoor concentrations of NO, NO_2 and O_3 have been taken from Carslaw (2007) [46] and initialized at 12, 17 and 17ppb, respectively. The initial concentration of HONO is set to 7 ppb. All other model species were initialized at zero.

The outdoor concentration profiles of NO, NO_2 and O_3 are coming from Mendez et al., (2015) [41]. Outdoor concentrations of VOCs are set to values reported by Sarwar et al. (2002) [79]. The air exchange rate (AER) between indoors and outdoors can vary quite widely in a typical residential building. The model run uses 0.7 h^{-1} (0.7 times in one hour that indoor air is completely changed by outdoor air) for this parameter in our simulation cases.

In the absence of available experimental data, many of the deposition velocities were taken from Sarwar et al. (2002) [79]. Indoor emission rates of VOCs have been set to values reported by Sarwar et al. (2002) [79]. A constant temperature of 293.0 K was used for simulations. All simulations began at midnight and were run for one. The simulation time step was 300 seconds.

5.3 Sensitivity Analysis Method

The time-variation of the i^{th} species concentration (C_i) calculated by INCA-Indoor model can be described as :

$$\frac{\partial[C_i]}{\partial t} = f(t, C_1, C_2, ..., C_m, P_1, P_2, ..., P_l) \tag{5.1}$$

where P_j (j = 1,. . . ,l) are the parameters of the model. The sensitivity of C_i with respect to the j^{th} parameter (P_j) is defined as :

$$S_{i,j} = \frac{\partial[C_i]}{\partial[P_j]} \tag{5.2}$$

For example if we obtain the following values

$$S_{i,1} = \frac{\partial[C_i]}{\partial[P_1]} = 0.5, S_{i,2} = \frac{\partial[C_i]}{\partial[P_2]} = 2, S_{i,3} = \frac{\partial[C_i]}{\partial[P_3]} = -10 \tag{5.3}$$

The positive sign of $S_{i,j}$ (j = 1,2,3) means that the concentration C_i increases due to the increase of P_j. The negative sensitivity $S_{i,3}$ indicates a decrease of C_i with increasing of P_j. When these three parameters (P_1, P_2, P_3) have the same units, we can use them to rank the model input parameters according to the absolute magnitudes of $S_{i,j}$. If it is the case, one can conclude that in the example P_3 is the most important input parameter of model. When units are different, the sensitivities $S_{i,j}$ cannot be compared in a fair manner. Consequently, they cannot be used to rank the model inputs and it is needed to use normalized sensitivities.

5.3.1 Normalized sensitivities

A technique to be able to compare the sensitivities is to use the dimensionless sensitivity coefficient (or normalized local sensitivity) which can be defined as :

$$S^*_{i,j} = \frac{\partial[C_i]}{\partial P_j}\frac{P_j}{C_i} = \frac{\partial[C_i]}{C_i}(\frac{\partial P_j}{P_j})^{-1} \tag{5.4}$$

The magnitude of $S^*_{i,j}$ gives the relative change of concentration C_i per unit change of the parameter P_j. For example, $S^*_{i,j} = 1$ can be explained by supposing an increase of $\Delta P_j = 10\%$ of the parameter P_j, which will lead to the same results in a positive variation ($\Delta C_i = \Delta P_j \times S^*_{i,j} = 10\%$) of the concentration C_i. Larger $S^*_{i,j}$ reflects higher influence of parameters/reactions for the concentration C_i. Because of different units of INCA-Indoor model parameters, the normalized local sensitivities have been chosen as sensitivity indices in our work.

In addition, we demonstrated that normalized local sensitivities of species C_i with respect to reaction rate (v) are equaled to those with respect to reaction rate constants (k). Following a simple reaction example, the demonstration follows :

Let us consider the general reaction :

$$\mathrm{aA} + \mathrm{bB} \xrightarrow{\mathrm{k}} \mathrm{cC} + ... \qquad \mathrm{v} = \mathrm{k}\,[\mathrm{A}]^{\mathrm{a}}\,[\mathrm{B}]^{\mathrm{b}} \tag{5.5}$$

where A, B are reactants ; [A], [B] are concentrations of A and B, respectively, a,b,c,... are the stoichiometric coefficients of the reaction, k and v are the reaction rate constant and the reaction rate, respectively.

$$S_{[C],v} = \frac{\partial [C]}{\partial v} = \frac{\partial [C]}{\partial k}\frac{\partial k}{\partial v} = \frac{\partial [C]}{\partial k}(\frac{\partial v}{\partial k})^{-1} = \frac{\partial [C]}{\partial k}([A]^a[B]^b)^{-1} = S_{[C],k}([A]^a[B]^b)^{-1} \tag{5.6}$$

$$S^*_{[C],v} = \frac{\partial [C]}{\partial v}\frac{v}{[C]} = [S_{[C],v}]\frac{v}{[C]} = [S_{[C],k}([A]^a[B]^b)^{-1}]\frac{v}{[C]} = S_{[C],k}\frac{k}{[C]} = S^*_{[C],k} \tag{5.7}$$

Therefore, it is reasonable to assess the importance of reactions for [OH] by comparing normalized local sensitivities of [OH] with respect to reaction rate constants ($S^*_{[OH],k}$), which is easier on a computational point of view.

5.3.2 Differentiation automatic tool TAPENADE

The sensibility analysis method used here is implemented by means of the automatic differentiation (AD) tool TAPENADE from Hascoët and Pascual (2013) [182] to compute sensitivities for all species with respect to all the parameters of the model.

TAPENADE is an AD tool based on source transformation. Application of TAPENADE to a code written in FORTRAN or C language requires the user to choose the independent and dependent variables with respect to differentiation and the differentiation mode (“tangent” mode or “adjoint” mode), and to provide the source program. So TAPENADE can build a new source program that computes both the original simulation and its derivatives. In “tangent” mode, TAPENADE builds a program that computes directional derivatives. In “adjoint” mode, TAPENADE builds a program that computes the gradient of the output with respect to all input parameters. Tapenade is used here in the tangent mode to generate a code that computes sensitivities for all species with respect to all the parameters of the model. The first applications lead to very few modifications of INCA-Indoor to respect modeling rules of TAPENADE. More information could be found on the webpage of the model (https ://www-sop.inria.fr/tropics/tapenade.html). TAPENADE was already applied for many applications in other fields of research [186, 187, 188, 189].

5.3.3 Application TAPENADE to INCA-Indoor model

In order to test the use of TAPENADE to calculate sensitivity coefficients, three test cases were considered. TAPENADE was then applied directly to our original code and generated the “tangent linear code” which allowed the calculation of the partial derivatives (absolute sensitivity). Using the equation (5), the normalized local sensitivities of individual species concentrations with respect to diverse model parameters at each time step have been calculated.

All tests discussed in this section were done with the same conditions : room volume V=250 m^3, surface-volume ratio S/V = 3.0 m^{-1}, temperature T = 293.0 K.

Case study 1 : The indoor initial concentrations of NO, NO_2, O_3 were respectively 12, 17 and 17 ppb as in (Carslaw et al. 2007) [46]. The concentrations of others species were set to zero. Only d-limonene was emitted and 2 species (O_3, d-limonene) are exchanged through the ventilation. Indoor emission rate of d-limonene and the outdoor concentration profiles of the 2 species were taken from Sarwar et al. (2002) [79]. These 2 species were exchanged between the indoor and outdoor environments by ventilation with an air exchange rate of 0.7 h^{-1} between 14 :00 and 15 :00. Only the deposition velocity of O_3 is considered and it was set to 0.036 cm s^{-1} which is issued also from Sarwar et al. (2002) [79]. The photolysis rates were calculated with the TUV model (Madronich et al.,2010) according to the attenuation factor measured by Drakou et al. (1998) [172]. 181 reactions may occur involving 85 species.

Case study 2 : 49 VOCs are emitted indoor and 56 species that were exchanged between the indoor and outdoor environments by ventilation. The depositions of 22 species were considered. In addition, there were 131 species and 351 reactions in the chemical mechanism. The others conditions were the same as in the case 1. The sensitivities averaged of [OH] and [HO_2] between 14 :00 and 15 :00 h are analyzed and discussed too in the next section.

Case study 3 : To avoid the effects of choosing different ventilation time on sensitivity results, ventilation in case 3 has been active within 24h while other conditions were set to the same as for the case 2.

5.4 Results

5.4.1 INCA-Indoor simulations of OH concentrations

Diurnal profiles of indoor [OH] for 3 cases are presented in figure 5.1. Profile of indoor [OH] for case 1 shows that there are two peaks for indoor [OH], which are 3.4×10^6 molecule.cm^{-3}

at 07h :40 and 2.1×10^6 molecule.cm^{-3} at 15h :00, respectively. Indoor [OH] increases significantly before 07h :40 because of the increase of photolysis of HONO and N_2 and then decreases until the ventilation is activated at 14h :00. The decrease of [OH] during this period could be explained by two reasons. Firstly, the reactions of OH with d-limonene and other VOCs resulted in its concentration reduce. Secondly, the decrease of the concentrations of HONO and NO_2 (see figure 5.3) caused the reduce of the direct or indirect production of [OH] through the photolysis of HONO and NO_2. The photolysis of NO_2 generate NO, which react with HO_2 radical to produce OH radical. When the ventilation is active, indoor [OH] reincreases as a consequence of the increases of O_3 concentrations, which increase the OH production by the reaction of d-limonene with O_3. Sensitivities analysis helped to understand this profile and is presented in following sections.

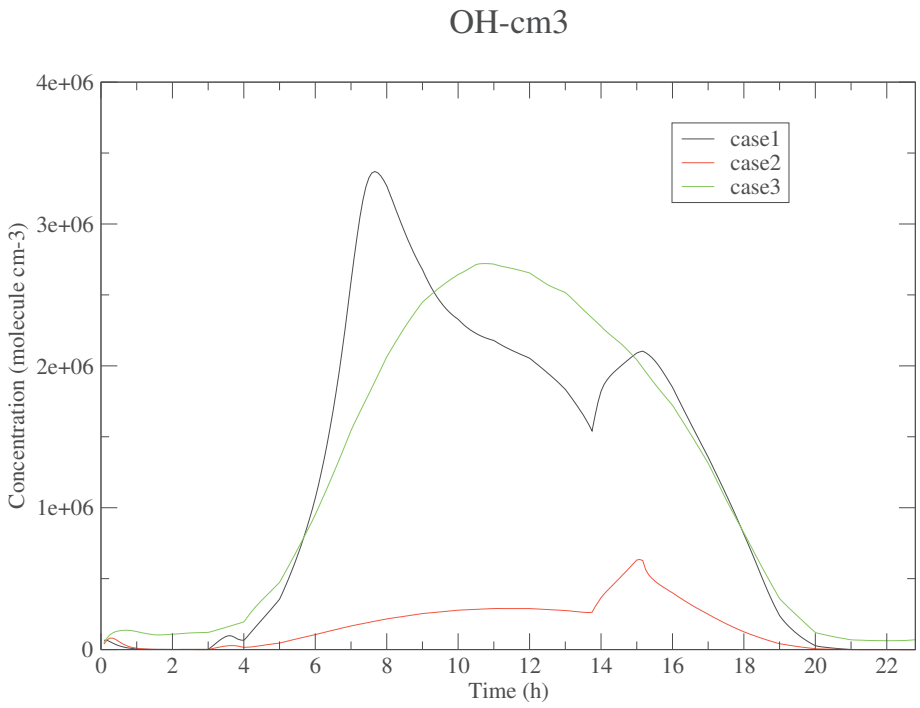

Figure 5.1 – Indoor [OH] (in molecule.cm^{-3}) simulated with the INCA-Indoor model

In case 2, [OH] experiences significant reduction compared with that in case 1 due to higher level of VOCs concentrations consuming more OH radicals. Profile of [OH] in figure 5.1 shows

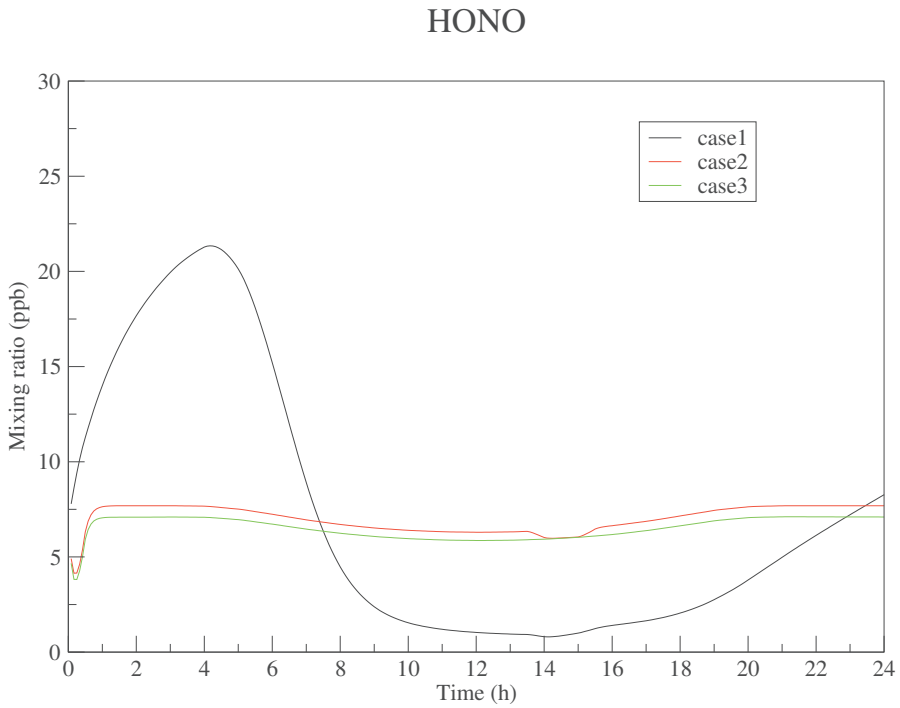

Figure 5.2 – Indoor HONO (in ppb) simulated with the INCA-Indoor model

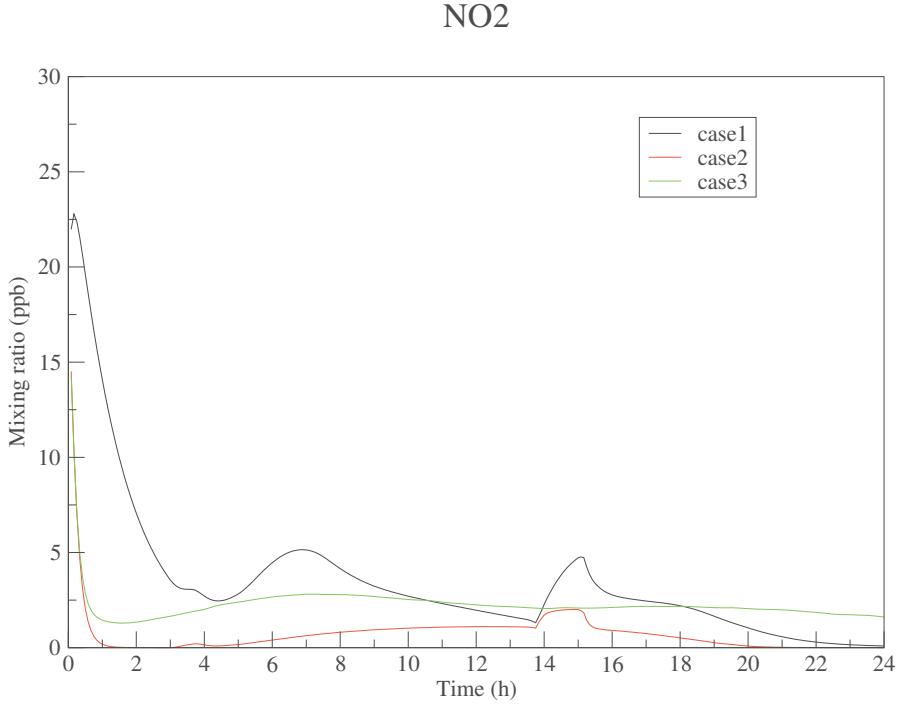

Figure 5.3 – Indoor NO_2 (in ppb) simulated with the INCA-Indoor model

that [OH] increases significantly when the ventilation was active (between 14h :00 and 15h :00) and [OH] reaches a maximum at 15h :05 with the concentration of 6.35×10^5 molecule.cm^{-3}.

In case 3, OH reached its maximum of 2.7×10^6 molecule.cm^{-3} at around 10h :30. The predicted OH maximum concentration is higher than that of Carslaw et al. (2007) [46] who report a maximum of 4.0×10^5 molecule.cm^{-3}. However, low transmission values of visible and UV light to indoors were used in the work of Carslaw et al. (2007) (0.1% in the visible and 0.03% in the UV), resulting in less UV available for HONO photolysis to produce OH. That is why the peak concentration in the work of Carslaw is far less than that in the present work.

Gomez Alvarez et al. (2013) [48] present direct measurements of significant amounts of OH radicals of up to 1.8×10^6 molecule.cm^{-3} during an experimental campaign carried out in a school classroom in Marseille. The concentration in this study is in the same range as the experimental measurements. The maximum concentration of [OH] in case 3 is larger than that in the case 2 but smaller compared to the case 1. Compared with case 2, higher OH peak concentrations can be attributed to two reasons. Firstly, because the ventilation remains active for all the day of simulation in case 3, the concentrations of many VOCs like d-limonene and ethanol are significantly reduced, leading to the decrease of the OH consumption. Secondly, due to the increases of NO and O_3 concentrations transported from outdoor, the OH production increases via reactions of HO_2 with NO and alkenes/monoterpenes with O_3. However, in this last case there are more VOCs consuming OH radicals than in the case 1, which leads to smaller [OH] compared to the case 1.

Comparisons the profiles of three cases, we notice that [OH] is strongly affected by the ventilation and the reactions of VOCs with OH and with O_3. The sensitivity analysis in the later sections help to understand this point.

5.4.2 Validation of sensitivity methodology and application strategy

Taylor test

It was first important to check the validity of the differentiated code, INCA-INDOOR-D created by TAPENADE. In other words, it is necessary to control that the tangent linear model (INCA-INDOOR-D) is well computing the derivative of the direct model (INCA-INDOOR) for each perturbed parameter. To do so, we use the ratio ($r\omega$) to compare derivatives obtained by AD and a finite difference method. This test, called "Taylor test", can be considered as satisfying when the ratio ($r\omega$) tends linearly towards 1 as ω tends to 0. The ratio (r_ω) for "Taylor test" is calculated as :

$$r_\omega = \frac{|C_i(P_j+\omega) - C_i(P_j)|}{\omega} \frac{1}{C_i d(P_j)} \tag{5.8}$$

r_ω tends linearly towards 1 as ω tends to 0. In formula 5.7, C_id is derivative of concentration C_i obtained by Tapenade with respect to parameter P_j in the direction of perturbation P_jd. ω is the step, supposed small.

Taylor tests were realized for a perturbation of selected parameters used in the model for 3 cases and the ratio (r_ω) at each time step was calculated. Table 5.1 shows an example of Taylor test results of mean r_ω with respect to indoor HONO concentration for different ω. Theoretically, small ω are necessary to minimize the truncation error resulting from the finite difference approximation. For example, r_ω tends towards 1 until ω equals 10^{-7} in case 1, which is the optimal value for a finite difference computation. For very small ω, the subtraction of too close floating-point numbers (when $\omega < 10^{-7}$) leads to a large cancellation errors that dominate the truncation errors coming from the finite difference computations. One observes the expected behavior for the ratio r_ω in table 5.1 : the tangent linear code is correct.

Computation and sorting of sensitivities

With INCA-Indoor-D model, sensitivity analysis are performed in three cases presented above. The sensitivities ($S^*_{i,j}$) are sorted according to their absolute values. Indoor [OH] can be considered as sensitive with $S^*_{i,j} > 1$, relatively sensitive with $0.1 < S^*_{i,j} < 1$, insensitive with $S^*_{i,j} < 0.1$, in regard to the changes for the different parameters. Only the parameters with sensibilities larger than 0.1 are shown in following tables.

Table 5.1 – Taylor test results for [OH] with respect to HONO concentrations

ω	Case1(ω)	Case2(ω)	Case3(ω)
10^{-1}	2.793412911	1.038705941	0.992372516
10^{-2}	1.017316830	1.003653484	0.999215919
10^{-3}	1.001291798	1.000363317	0.999921382
10^{-4}	1.000127679	1.000036311	0.999992136
10^{-5}	1.000012753	1.000003621	0.999999214
10^{-6}	1.000001276	1.000000266	0.999999923
10^{-7}	1.000000137	0.999999063	1.000000006
10^{-8}	1.000000218	0.999990122	1.000000163
10^{-9}	1.000001042	0.999900365	1.000002497
10^{-10}	1.000009919	0.999005631	1.000006908

5.4.3 Sensitivity results for case 1

The table 5.2 shows sensitivities of indoor [OH] at two peak concentrations (at 07h :40 and 15h :00) with respect to different parameters : indoor HONO concentration, gas phase reaction rate constants, indoor d-limonene emission rate, air exchange rate, outdoor O_3 concentrations and O_3 deposition velocity.

Table 5.2 – Normalized sensitivities (above 0.1) of [OH] at two peak concentrations with respect to different parameters (processes or reactions) in case 1. Femi is the emission rate. vdepot is the deposition velocity. Cout is the outdoor concentration. Conc is the indoor concentration. RCHO represents lumped C3+ Aldehydes. NO_2ADS indicates the absorbed NO_2 by the materials.

Rank	Parameter	$S^*_{i,j}$ ([OH] the first peak concentration (07h :40))	Parameter	$S^*_{i,j}$ ([OH] the second peak concentration (15h :00
1	Conc(HONO)	39.925	Conc(HONO)	30.938
2	NO_2+hv	8.015	HONO+hv	0.868
3	HONO+hv	1.736	OH+HONO	-0.465
4	femi(d-limonene)	-1.458	femi(d-limonene)	-0.453
5	NO_2->NO_2ADS	-0.816	OH+NO_2	-0.252
6	d-limonene+OH	-0.656	vdepot(O_3)	-0.240
7	Conc(NO_2)	0.357	RCHO+hv	0.172
8	Conc(NO)	0.297	Cout(O_3)	0.156
9	RCHO+OH	-0.209		
10	HO_2+NO	0.177		
11	d-limonene+O_3	0.116		
...	...	...	...	...

Sensitivity of indoor [OH] reaching the first peak concentration

According to the rank of parameters at 07h :40 when [OH] reaching the first peak concentration before the ventilation active (see table 5.2), [OH] is the most sensitive to indoor HONO concentrations. In addition, [OH] is sensitive to reactions directly producing (or consuming) OH or indirectly contributing to OH production (or consuming). The photolysis of HONO,

$$\mathrm{HONO} + \mathrm{hv} \longrightarrow \mathrm{OH} + \mathrm{NO} \tag{5.9}$$

is the most important source of indoor [OH] at this moment. Higher photolysis rate of HONO increases directly indoor OH production. Higher indoor HONO concentration is also to favor indoor [OH] by increasing the HONO photolysis rate. This is consistent with past studies (Alicke, (2003) [190], Alvarez et al., (2013) [48] ; Mendez et al., (2017) [42]). The photolysis of NO_2 also exhibits a significant importance for indoor [OH]. Higher NO_2 photolysis rate

$$\mathrm{NO_2} + \mathrm{hv} \longrightarrow \mathrm{NO} + \mathrm{O_3P} \tag{5.10}$$

produce more NO, which then reacts with HO_2 (R5.10) to produce OH. An increase of NO_2 concentration increase [OH] due to increasing NO_2 photolysis rate, which indirectly increase the [OH] production. Other important reaction sources of indoor [OH] include

$$\mathrm{HO_2} + \mathrm{NO} \longrightarrow \mathrm{OH} + \mathrm{NO_2} \tag{5.11}$$

and oxidation of d-Limonene by O_3

$$\mathrm{d-limonene} + \mathrm{O_3} \longrightarrow 0.729\mathrm{OH} + 0.089\mathrm{HCHO} + \ldots \tag{5.12}$$

An increase of the reaction speeds of HO_2 with NO (R5.10) and d-limonene with O_3 (R5.11) can directly increase [OH].

The main sink reactions for OH are oxidation of d-limonene by OH (R5.12) and aldehydes (RCHO) by OH (R5.13).

$$\mathrm{d-limonene + OH \longrightarrow 0.827xHO_2 + 0.288xHCHO + 0.539xRCHO...} \tag{5.13}$$

$$\mathrm{RCHO + OH \longrightarrow 1.93 * RCO3 + 0.07 * xHO2 + ...} \tag{5.14}$$

In this chapter xHO_2, xOH, xRCHO, etc, are chemical species added in SAPRC07 in order to parametrize the formation respectively of HO_2, OH and RCHO, etc, from alkoxy radicals formed in peroxy radical reactions with NO and NO_3 and RO_2. The use of these so-called "steady state operators" avoid to simulate all reactions and species that could be involved in the oxidation of some VOC but only their impact on HO_2, OH, RCHO. RCHO represents lumped C3+ Aldehydes. In addition, the reaction of NO_2 on the material surface (R5.14) indirectly reduces indoor [OH]. That can be explained by the fact that surface reaction of NO_2 decreases NO_2 concentration, whose photolysis can indirectly increase OH concentrations.

$$\mathrm{NO_2 + surface \longrightarrow NO_2ADS} \tag{5.15}$$

Here NO_2ADS represents the NO_2 absorbed by the surface.

The effects of indoor d-limonene emission rate on [OH] is complex. This is due to the fact that [OH] results of the balance of production and consumption issued from d-limonene. The net effect depends on the reaction rates of d-limonene with OH and with O_3. The d-limonene can be considered primarily as a sink of indoor [OH] because the d-limonene with O_3 (R5.11) reaction rate is smaller than that of d-limonene with OH (R5.12). At the same time, as shown

by the high negative sensitivity of OH to the d-limonene emission rate, the larger indoor d-limonene emission rate, the larger indoor d-limonene concentration resulting in larger indoor [OH] removal rates than production rates, thus having a net negative effect on [OH].

Sensitivity of indoor [OH] reaching the second peak concentration

Figure 5.1 shows that indoor [OH] reaches the second peak concentration at 15h :00 after ventilation active. Compared with the rank of parameters at 07h :40, the most important factor and reaction source for OH are the same, which are the HONO concentration and the photolysis of HONO. However, the most important sink reactions for OH become from reactions of d-limonene (or RCHO) with OH at the first [OH] peak concentration to the reactions of HONO (and NO_2) with OH. That is due to indoor d-limonene concentrations decrease (see figure 5.4).

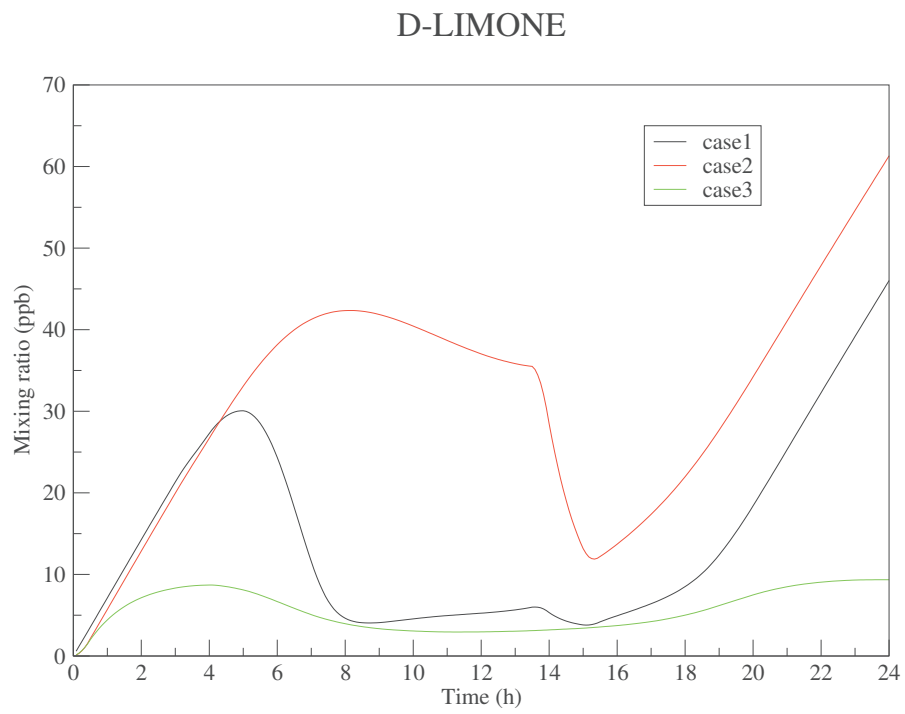

Figure 5.4 – Indoor d-limonene (in ppb) simulated with the INCA-Indoor model

In addition, photolysis of RCHO (Lumped C3+ Aldehydes))

$$\mathrm{RCHO} + \mathrm{hv} \longrightarrow 2\mathrm{CO} + 2\mathrm{HO_2} + \ldots \tag{5.16}$$

shows positive effect on indoor [OH]. Indoor [OH] is increased with increasing photolysis rate of R5.15 where HO_2 radicals are generated and then OH is reproduced by reaction R5.10.

Outdoor O_3 concentration exhibits a positive effect on [OH]. Since indoor O_3 arises mainly from outdoor-to-indoor transport, an increase in outdoor O_3 concentration increases indoor O_3 concentration, leading to higher OH production rates via reactions alkene/monoterpenes with O_3. A higher O_3 deposition rate generates a reduction of the O_3 concentration, leading to reduce the OH production rate via reactions alkene/monoterpenes with O_3, thus resulting in a negative effect on [OH].

5.4.4 Sensitivity results for the case 2

To further study the effects of different parameters/reactions on [OH] and to evaluate the relative importance of the [OH] production and consumption pathways, we conduct sensitivity analysis for [OH] at two different moments, at which [OH] reaching the peak concentration and the larger growing velocity.

Table 5.4.4 shows the sensitivities of indoor [OH] at these two moments to the different following parameters : indoor HONO concentration, gas phase reaction rate constants, indoor VOCs emission rates, air exchange rate, outdoor species concentrations and indoor deposition velocities), and the rank of parameter importance according to the sensitivity coefficient ($S^*_{i,j}$). While only the parameters with sensibilities larger than 0.1 are shown in table 5.4.4. The sensitivity results obtained are discussed below in the following sections.

Table 5.3 – Normalized sensitivities (above 0.1) of [OH] in different time with respect to different parameters (processes or reactions) in case 2. Femi is the emission rate. vdepot is the deposition velocity. Cout is the outdoor concentration. Conc is the indoor concentration

Rank	Parameter	$S^*_{i,j}$ (The largest growing velocity)	Parameter	$S^*_{i,j}$ (peak concentration)
1	AER	2.433	AER	4.159
2	HONO+hv	1.255	HONO+hv	0.914
3	vdepot(HONO)	-1.072	vdepot(HONO)	-0.790
4	NO_2+hv	0.447	NO_2+hv	0.523
5	femi(d-limonene)	-0.436	vdepot(NO_2)	-0.408
6	vdepot(NO_2)	-0.343	femi(d-limonene)	-0.375
7	femi(ethanol)	-0.194	Cout(NO_2)	0.221
8	ethanol+OH	-0.188	femi(ethanol)	-0.198
9	d-limonene+OH	-0.186	ethanol+OH	-0.196
10	femi(isoprene)	-0.128	d-limonene+OH	-0.142
11	HO_2+NO	0.113	HO_2+NO	0.127
12			femi(isoprene)	-0.120
...	...	...	...	...

Sensitivity of indoor [OH] reaching the peak concentration

The most important impact on indoor [OH] is performed by air exchange rate (AER), which has a positive effect on [OH] as shown in table . The air exchange rate influences indoor concentrations of inorganic (i.e. O_3, NO, NO_2) and organic compounds and determines the amount of time available for the chemical reactions to occur. Due to many VOCs mainly originating indoors, higher air exchange rate decreases indoor VOCs concentrations (i.e. d-limonene, Ethanol), resulting in slowing down the OH consumption rates via VOCs oxidation by OH, thus leading to a positive effect on OH.

The most important source reactions of [OH] are the photolysis of HONO (R5.8) and reaction of HO_2 with NO (R5.10), which have positive effects on [OH]. The photolysis of NO_2 exhibits a positive effect on [OH]. While the main sink reactions of [OH] are ethanol with OH and d-limonene with OH (R5.12). The reasons why these reactions have positive or negative effects on [OH] have been discussed in section 5.4.3. However, the role of the photolysis of NO_2

becomes less important compared with that in case 1 maybe due to the smaller concentration of NO_2 in case 2 than in case 1 (see figure 5.3). Deposition velocities of HONO and NO_2 exhibit negative effects on indoor [OH]. The reason why the photolysis of NO_2 and HONO have a positive effect on [OH] have already been discussed previously. Then, higher deposition velocities of HONO and NO_2 will decrease their indoor concentrations, which effects will be to decrease the photolysis rates of NO_2 and HONO, resulting in a negative effect on [OH]. A rise in the outdoor NO_2 concentration is clearly beneficial in accelerating the NO_2 photolysis rate for NO, due to the continually enhanced indoor NO_2 concentration. Followed by reaction of NO with HO_2 (R5.10), more OH is produced and result in positive effect on [OH].

In addition, indoor emission rates of d-limonene (D-LIMONE), ethanol (ETOH) and isoprene (ISOPRENE) have a negative impact on [OH]. Indoor [OH] is more sensitive to indoor d-limonene emission rate than those of ethanol and isoprene. That is because reaction rates of the oxidation by O_3 or OH of the d-limonene are faster than those of ethanol and isoprene. Higher emission rates of d-limonene, ethanol and isoprene increase their indoor concentrations and consume directly OH radicals, resulting in a negative impact on [OH].

Sensitivity of indoor [OH] increasing with the largest velocity

Indoor [OH] increases the most rapidly at 13h :45. Compared with the rank of parameters/reactions at 15h :05, the most influential parameters/reactions are almost the same, but their impacts are different in amplitudes. In addition, outdoor NO_2 concentration does not show importance at this moment, due to the fact that the ventilation was not active. The sensitivities of AER is lower than that at 15h :05 (up to 41.5% decrease) because of lower AER at this moment. The sensitivities of the photolysis of HONO and HONO deposition velocity are higher than those at 15h :05, indicating that OH formation is more affected by the photolysis of HONO, which dominate the increase of [OH]. Lower sensitivities to the photolysis of NO_2 and the rate of HO_2 with NO (R5.10) indicate the importance of NO_2 indirectly contributing to

OH production. The magnitude of other parameters/reactions on [OH] are similar with those at 13h :45.

5.4.5 Sensitivity results for the case 3

Sensitivity of indoor [OH] reaching the peak concentration

Indoor [OH] reaches the maximum at 10h :45. The most influential 6 parameters/reactions for [OH] are the same as those at case 2 when [OH] reaching the maximum, with lower sensibilities than those in case 2. Outdoor NO concentration becomes more important than in case 2 and exhibits a positive effect on [OH], with its effect comparable with outdoor NO_2 concentration. Because of longer time of ventilation in case 3 than in case 2, indoor NO concentration is higher in case 3 than that in case 2 due to the transport of NO from outdoor to indoor (see figure 5.5). The increase of outdoor NO concentration increases [OH] with increasing indoor NO concentration. That can be explained by the fact that a rise of NO concentration favors OH production rate via reaction R2. In addition, indoor [OH] is sensitive to the reaction rate of O_3 with NO in case 3, but is insensitive to it in case 1 and 2. Because the ventilation remains active in case 3 for all the day of simulation but one hour in case 1 and 2, indoor O_3 concentration is higher in case 3 than those in case 1 and 2 due to indoor O_3 arising mainly from outdoor-to-indoor transport. Higher indoor O_3 concentration results in higher reaction rate of O_3 with NO, which directly reduces NO concentration, resulting in less NO available to generate OH by R2. Consequently, reaction of O_3 with NO has a negative effect on [OH].

Sensitivity of indoor [OH] increasing with the largest velocity

The indoor [OH] increases the most rapidly at 06h :55. The sensitivity results reported in table show that the indoor [OH] is still the most sensitive to the AER, which has higher sensitivity than that at 10h :45. Since reactions of d-limonene (reaction R5.12) and ethanol with OH act as

Table 5.4 – Normalized sensitivities (above 0.1) of [OH] in different time with respect to different parameters (processes or reactions) in case 3. Femi is the emission rate. vdepot is the deposition velocity. Cout is the outdoor concentration. Conc is the indoor concentration

Rank	Parameter	$S^*_{i,j}$ (The largest growing velocity)	Parameter	$S^*_{i,j}$ (peak concentration)
1	AER	1.281	AER	0.985
2	HONO+hv	0.583	HONO+hv	0.659
3	NO_2+hv	0.491	vdepot(HONO)	-0.582
4	vdepot(HONO)	-0.456	NO_2+hv	0.513
5	Cout(NO)	0.405	vdepot(NO_2)	-0.382
6	femi(d-Limonene)	-0.344	femi(d-Limonene)	-0.263
7	vdepot(NO_2)	-0.339	Cout(NO)	0.215
8	Cout(NO_2)	0.223	Cout(NO_2)	0.210
9	d-Limonene+OH	-0.185	ethanol+OH	-0.196
10	ethanol+OH	-0.140	femi(ethanol)	-0.173
11	femi(ethanol)	-0.121	HO_2+NO	0.131
12	HO_2+NO	0.114	O_3+NO	-0.106
...	...	...	...	...

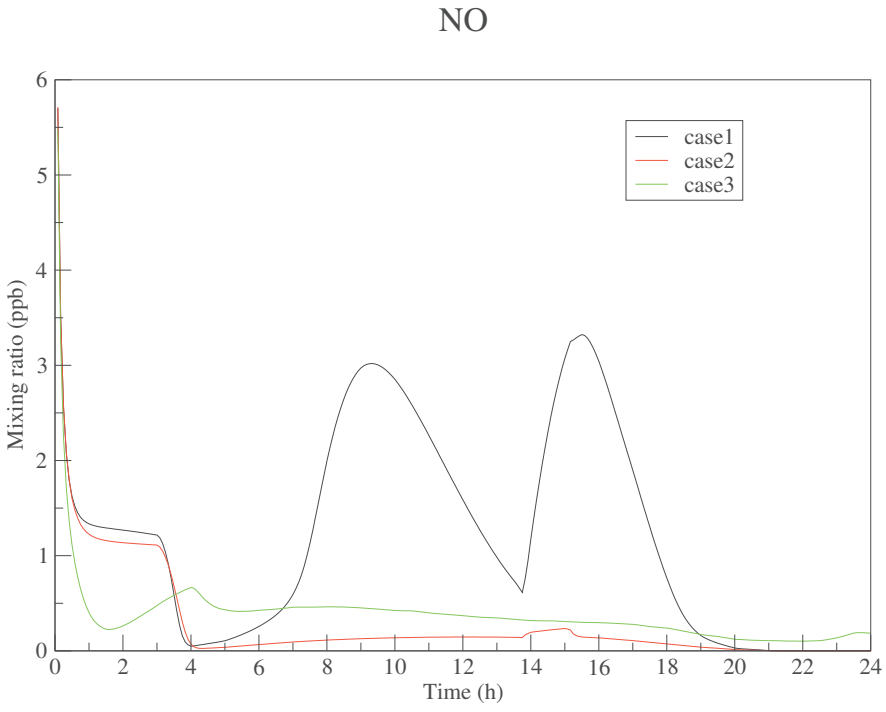

Figure 5.5 – Indoor NO concentration (in ppb) simulated with the INCA-Indoor model

main sinks of [OH] (see in table), an increase of AER can reduce the OH consumption because of significantly decrease of the concentrations of d-limonene and ethanol by ventilation. The most important source reactions of OH are the photolysis of HONO (R5.8) and reaction of HO_2 with NO (R5.10). While the indoor [OH] is mainly governed by the photolysis of HONO (R5.8). The photolysis of NO_2 contributes to the [OH] production. The outdoor concentrations of NO and NO_2 exhibit positive effects on the indoor [OH]. The main negative-influential parameters on the [OH] include the deposition velocities of HONO and NO_2 and the indoor emission rates of d-limonene and ethanol. The reasons why these parameters/reactions show positive or negative effect on the indoor [OH] have already been discussed previously.

5.5 Conclusions

Sensitivity analysis is a powerful tool and can provide insights into the dominant controls of the system and support decision-making. With the comparison of normalized local sensitivities with respect to different parameters/reactions, it facilitates to identify the most important reactions and parameters on the indoor pollutants of interest. An automatic differentiation tool called TAPENADE has been adapted here to calculate the local first order sensitivities defined as partial derivatives of the indoor species concentrations with respect to the model parameters because of its computational efficiency.

The sensitivity results in the three cases show that the effects of the parameters/reactions on the indoor [OH] are different at different moments and in different simulation conditions. The rank of the parameters/reactions at the moments at which the indoor [OH] reached the peak concentration and the maximum growing velocity helps us to point out the most influential parameters/reactions and to evaluate the relative importance of the individual processes for the [OH]. Under the simulation conditions used for this study, the most sensitive parameter is the air exchange rate (in cases 2 and 3) when there is more VOCs existing at the beginning of the

simulations. However, the effect of air exchange rate becomes more important under condition of one hour of duration (in case 2) than one day (in case 3). The main source of [OH] are the photolysis of HONO and the reaction of HO_2 with NO, whether more VOC species are added in the model like for the case 2 or the change of AER in the case 3. However, when there is HONO and its photolysis is possible, the effect of photolysis of HONO on the [OH] is more important than the one of the reaction of HO_2 with NO. This indicates that the photolysis of HONO is the dominant reaction for the increase of the indoor [OH]. While the photolysis of NO_2 shows an important positive impact on the [OH], which is rarely mentioned in the literature. In the presence of more VOCs in the model, the effect of the indoor d-limonene emissions on the [OH] becomes less important in the cases 2 and 3 than in the case 1. The indoor d-limonene emissions are more important than those of other VOCs for the [OH] and even than the reaction of the d-limonene with OH or with O_3.

The sensitivities of the parameters/reactions change significantly through time, thus the rank of parameters/reactions changes also over time. It is essential to choose the important moment of the sensitivity (like the peak concentration and the largest increasing velocity of species of interest), which should illustrate the important influence of parameters and help to make decision to decrease indoor air pollution.

Our work shows that a large-scale sensitivity of a complex model is feasible using the automatic differentiation TAPENADE tool. One emphasis is that local sensitivity is performed around a point of interest of the model parameters. But one must keep in mind that the sensitivity coefficients are only valid near the given parameter values. In addition, it is noted that sensitivity results have been performed for different set of conditions, which sets can change the rank of parameters.

CHAPTER 6

CONCLUSIONS AND PERSPECTIVES

6.1 Conclusions

People spend more than 90 percent of their time indoors : at home, at work, in transportation, and in many other public and private places, where concentrations of some contaminants may be higher indoors than outdoors [7]. Indoor air pollution affects people's well-being and productivity. Furthermore, risks for diverse diseases are increased by indoor air pollution, which may cause diverse symptoms and illnesses, like the symptom now most often referred as SBS (sick building syndrome) [15].

Since indoor air pollution has impacts on human health and people are highly exposed to this air pollution along a day, it is necessary to provide as fast as possible knowledge on the physical and chemical processes that are involved, methodologies that could help to understand the sources and sinks of this air pollution, and develop tools to help to make decisions focusing on its reduction.

Processes taking place indoors and influencing indoor pollutant concentrations have been studied either by measuring or modeling. Direct measuring indoor pollutant concentrations could provide reliable local information of indoor air quality, however, they are limited in numbers and not sufficient to describe properly the processes. On the contrary, modeling indoor air quality has been demonstrated as a powerful tool to investigate indoor air quality issues and

detail contributions and give approximate estimates of the concentrations taking into account the uncertainties of their inputs and parametrizations of the processes. Numerous IAQ models have been developed. INCA-Indoor model is one of the most recent model developed by Mendez et al. (2015) [41]. Its main advantage is to include all the processes existing in confined environments such as ventilation, emissions, deposition, gas phase and heterogeneous chemical processes and aerosol formation. This model can be used to simulate the concentrations of indoor chemical species. Furthermore, this model could provide the information of the contributions of each processes to the pollutant concentrations. It is used in this phd report to analyze indoor air quality.

INCA-Indoor model has been evaluated with other model results [41] and the SURFin data [42]. With data collected during SURFin campaign [36], Mendez et al. (2016) has compared the concentrations of OH and HO_2 between experimental and simulated profiles with INCA-Indoor model and the comparison results shows a relatively good agreement in terms of concentrations for OH and variations for both radicals (OH and HO_2) [42] while precise comparisons were difficult as information on building configuration and materials were missing. In addition, INCA-Indoor model has also been used to evaluate different HONO formation mechanisms due to the important role of the photolysis of HONO being the oxidation driver through OH formation [41, 42]. Comparisons between different HONO formation mechanisms have been carried out with INCA-Indoor model and a new HONO formation mechanism was proposed, which provides a good parameterization for fitting the experimental data.

In this study, INCA-Indoor model is applied to simulate the concentrations of volatile organic compounds (VOC), NO, NO_2 and O_3 measured in a new classroom of a low energy school buildings in France. Those measurements were performed during the MERMAID (Mesures Expérimentales Représentatives et Modélisation Air Intérieur Détaillée) campaign [37, 38] in April-May 2014. The objective is firstly to assess the ability of INCA-Indoor model to simulate the pollutant concentrations in a realistic indoor environment and indoor air dynamics with

high injection experiment. Based on the simulation results, INCA-Indoor model is then used to identify the role of the various processes in determining these concentrations and to quantify the contributions of different processes to the concentrations of NOx, O_3 and 12 VOCs classified as hazardous air pollutants. INCA-Indoor model is validated experimentally using as input data measurement performed during the MERMAID (Mesures Expérimentales Représentatives et Modélisation Air Intérieur Détaillée) compaign [37, 38] in April-May 2014. The comparison with the measurements shows that INCA-Indoor model is able to reproduce correctly the profiles for most of the species measured indoors.

Contribution analysis based on the model indicates that indoor emission is a major source for most of VOCs (i.e. methanol, formaldehyde and acetaldehyde) and the oxidation of VOCs can be an important source for some compounds like acetone. It is showed that the the ventilation can increase indoor concentrations of NOx, O_3. In general, an increase of concentrations of NO and O_3 can enhance the oxidation of VOCs and lead to a production of secondary pollutants (i.e. formaldehyde).

The ventilation is also often a major pathway to reduce most of VOC concentrations, since indoor concentrations are usually higher than outdoor ones. One can note that this is of course really depend on the outdoor pollution. In addition, the deposition is also important for reducing the concentrations of formaldehyde and acetaldehyde. For acetone and acrolein, the sorption accounts for 35.08% and 49.60% respectively of the total consumption rates. Indoor chemistry appears important loss pathway for acrolein, isoprene and d-limonene through their reactions with OH radical or O_3.

The effects of emission, ventilation, deposition and chemistry on indoor concentrations in other buildings will of course vary depending on (1) the emission rates of the furniture, wall surfaces and human activities, (2) the air exchange rates and outdoor air pollution, (3) deposition rates, (4) conditions of light respectively. To reduce indoor concentrations of VOC classified as

hazardous air pollutants in any places, it is obviously necessary to investigate the role of each processes.

Since during MERMAID campaign, the ventilation was varying, and the effect of spatial heterogeneity of materials and light indoors on indoor air pollutants was also investigated, the measurements also allow us to evaluate the sensitivity of the INCA-Indoor simulations to several parameters measured inside their realistic range of values. Not surprisingly, VOC concentrations simulated by INCA-Indoor are very sensitive to their emission rates : when these ones are increasing, indoor VOC concentrations are increasing. The indoor concentrations of NO, NO_2 and O_3 increase with increasing AER : more of those pollutant are imported from outdoor. With increasing AER from 1.08, 2.16 to $4.32h^{-1}$, the maximum concentrations of formaldehyde and acetaldehyde increase due to the reactions of VOC (i.e. d-limonene) with O_3, but the mean and minimum concentrations decrease due to the dilution by the ventilation.

The concentrations for methanol, toluene, which are mainly emitted indoors, decrease with increasing AER. There are minor changes for acrolein and acetone, benzene, isoprene, d-limonene, chlorobenzene and p-dichlorobenzene with increasing AER in our study cases.

The variation of sorption rates (ka and kd) of benzene has a minor influence on benzene concentrations, and there is almost no impact for other VOC and NOx concentrations.

With the measured transmittance spectra of different type of windows, a series of simulations with INCA-Indoor model have carried out to investigate the effect of the transmitted light. Simulation results show that the transmitted light depends on the type of windows and has direct impact on photolysis phenomena occurring indoors and pollutant concentrations. Under indoor conditions of this study, with increasing the transmittance for UV and visible light, concentrations of the HOx radicals and O_3 increase but some VOC (i.e d-limonene, o-xylene, isoprene) decrease due to the reactions of VOC with OH.

The obtained results are very specific to the studied room and one can easily understand that contributions could be very different in other buildings and locations. Nevertheless, it was

interesting to note that understanding indoor air pollution needs details on the contributions of each processes.

Hence how to find out the important parameters is a crucial question before taking action to reduce indoor air pollution : should we open the windows ? Reduce the light ? Or one specific activity inside the room ? Reduce the emission rates is for sure the best way to improve indoor air quality, but for a given room, are we able to guide an inhabitant to reduce the indoor air pollution ? The model can be used with the method of changing parameter value one by one and analyze the results. This is quite time consuming. Therefore we develop a method (or model) that is more convenient to assess the influence of all parameters on pollutant concentration levels, especially for the model with quite a lot of parameters, appear to be necessary.

During the phd work, a tangent linear model of INCA-Indoor model was built using an automatic differentiation tool called TAPENADE to assess the relative importance of different parameters affecting pollutant concentrations. Tangent linear model of INCA-Indoor model has been used to calculate the local fist order sensitivities defined as partial derivatives of indoor species concentrations with respect to the model parameters because of its computational efficiency. Parameter importances are quantified and classified according to their sensitivity values in a very fast way.

The first application of the methodology was performed on [OH], that was intensively studied before. The sensitivity results confirm that [OH] is firstly and mainly sensitive to the air exchange rate and to the photolysis of HONO which produces OH and helped to detail the processes and their contributions. The results were consistent with results in other studies [8] and prove that a large-scale sensitivity of a complex model is feasible using the automatic differentiation TAPENADE tool. One emphasis is that local sensitivity is performed around a point of interest of the model parameters and an exact estimate. But one must keep in mind that the sensitivity coefficients are only valid near the given parameter values. In addition, it is noted that

sensitivity results have been performed for different set of conditions, which sets can change the rank of parameters.

All the results in this study provide useful informations about roles of different processes controlling indoor air quality and the effects of different parameters on indoor pollutant concentrations. INCA-Indoor model can be used as a powerful tool to investigate indoor air issues. In addition, the tangent linear model of INCA-Indoor model developed in the phd work can be used to define the strategies of reducing indoor air pollution

6.2 Perspectives

Further work is needed to address some of the issues that have been encountered during our studies. Firstly, although the comparison between experimental profiles and modeled profiles shows a good agreement, there are still some differences, which may be attributed to the variations of the emission rates, infiltration rate in the room, exchanges with other rooms, heterogeneity in the room (light, concentrations, materials, etc), and also the misunderstand processes that will be needed more measurement and modeling task (like aerosols formation and interaction with gaz phase).

Indeed, emissions can fluctuate over time depending on parameters such as temperature, humidity but also ambient concentrations and materials [164]. INCA-Indoor model considers the emission rates as constants. Hence, quantifying more precisely the emission rates and providing more information of the evolution of emission rates could be helpful to improve the model simulation results, which could provide more reliable information about indoor air quality. Octopus Lab (http ://www.octopuslabs.science/fr), a new company using INCA-Indoor to assess indoor air, developed an interface of the model with PANDORE data (http ://lasie.univ-larochelle.fr). This PANDORE database provides imformations about emission rates of all types of pollutants

(particle, organic and inorganic gases, microorganisms) from indoor sources of the building but also constant emissions.

Secondly, INCA-Indoor model is used to simulate the pollutant concentrations in a classroom with data collected during MERMAID campaign. These measured data were obtained in the classroom where all furnishings were moved out and during the period of scholar holidays for feasibility reasons. Hence, the effect of the emission, sorption or deposition taking place on the surface of these furnishings and human activity like cleaning, opening the windows has not be considered. It is therefore strongly advised, in the future, to simulate the pollutant concentrations in a more realistic environment including the variety of furnishing and the presence of occupants that could greatly interact with indoor air.

CFD simulations inside the room and at the scale of the building would allow a user to take into account the heterogeneity and exchanges with other rooms. Challenging research activities are beyond such kind of work as the dispersion inside a room, or exchanges with other, have strong interactions with the chemistry and coupling will increase time computation.

Thirdly, the effect of air exchange rate of ventilation on indoor air quality has been discussed in this study. It is obvious that some pollutant concentrations can be reduced during the ventilation period. However, when the ventilation is switched off, some pollutant concentrations can reach the same or even higher levels than those before the ventilation is switched on. Further study is necessary to study the effect of ventilation time and to find out moderate ventilation rate and time for improving IAQ. Infiltration is also an issue to investigate. One recommendation for future measurement campaigns would be to measure the infiltration rate as precise as possible and investigate its modeling.

Aerosol particles are regarded as significant pollutant sources in the indoor environment [191] and the concentration of aerosol particle in a room greatly influences the IAQ. It was not possible to discuss this topic in this study, but an aerosol module was also developped in the framework of the MERMAID project. This module needs to be further developped in order to

better simulate the formation of secondary organic aerosol (SOA). Thus studies of the aerosol processes and parameters controlling the indoor air concentrations should be included in the further study.

In addition, the indoor formation mechanism of some species is still not very clear like HONO, which is confirmed to be an important indoor source of OH radical. Although Mendez et al. (2017) [43] has proposed a new formation mechanism of HONO, that mechanism is not yet fully supported by laboratory experiments. More experimantal data are needed to improve the understanding of HONO formation mechanism.

Since IAQ is not the only challenging topic concerning the building, it would be also interesting to couple INCA-Indoor with an energy model and a Heat Air Moisture (HAM) model in order to better address the concept of sustainable buildings. Several new materials are built in order to reduce humidity problem in indoor environment. At the same time ventilation systems are built to reduce humidity too and air pollution, but the air pollutant controlled is usually only CO_2. Optimization of the ventilation rate as a function of energy consumption, humidity and concentrations of several air pollutants would be helpful to optimize the comfort of the inhabitant and respect energy and indoor quality regulations or recommendations. More generally, a building is part of an urban area. Since this urban area, with its associated outdoor air pollution, may impact indoor air pollution, it is necessary design both buildings and quarters in order to reduce the impact on exposure [192, 193].

A first version of a sensitivity model has been built with TAPENADE software and it is proved to be very useful tool to identify the important parameters affecting pollutant concentrations. Further investigations are needed to develop an operational tool that could guide the decision to reduce indoor air pollution since the methodology is for the moment limited to a reduced chemical scheme, and demonstration are needed to be performed to show the capacities of the tool to control several pollutants at the same time.

CHAPTER 7

RÉSUMÉ EN FRANÇAIS

Depuis le siècle dernier, il y a une large compréhension de la menace posée par la pollution atmosphérique à la santé du public [1, 2, 3]. L'histoire et l'évolution de la recherche sur la qualité de l'air intérieur est étroitement liée à la pollution de l'air extérieur [4]. La qualité de l'air intérieur (QAI) se réfère généralement à la qualité de l'air à l'intérieur et autour des bâtiments et des structures et se rapporte surtout à la santé et le confort des occupants du bâtiment [5].

Les polluants extérieurs peuvent pénétrer dans le bâtiment par l'infiltration ou le ventilation. Les polluants d'origine intérieure peuvent provenir de nombreuses sources. Dans les années 1980, l'étude de la méthode de l'exposition totale à la méthodologie (équipe) de l'EPA des États-Unis a fourni un modèle d'évaluation exhaustive des contributions des expositions intérieures et extérieures à l'exposition personnelle totale [6]. Les résultats montrent que les sources de pollution à l'intérieur ont contribué plus à l'exposition personnelle totale aux composés organiques volatils toxiques que les sources de pollution extérieur.

Les personnes passent plus de 90% de leur temps à l'intérieur de bâtiments où les concentrations de certains polluants de l'air peuvent être plus élevées qu'à l'extérieur. Les environnements intérieurs peuvent contenir une variété de polluants atmosphériques. Certains polluants sont émis à partir de matériaux utilisés dans le bâtiment comme l'amiante, le formaldéhyde et le plomb [8, 9, 10]. Certains polluants comme le pollen, les particules, les composés organiques volatils sont générés à partir de moisissures et de pollen [11], fumée de tabac [12], produits

ménagers [13]. La pollution intérieure est souvent exacerbée par des systèmes de ventilation mécanique mal conçus, mal construits et/ou insuffisamment exploités [14]. Les caractéristiques de la QAI pour un environnement intérieur varient en fonction du temps et de l'espace, et peuvent être très différentes dans d'autres bâtiments résidentiels et commerciaux.

La qualité de l'air intérieur affecte la santé, le bien-être et la productivité des personnes. En outre, les risques pour diverses maladies sont augmentés par la pollution de l'air intérieur, qui peut causer divers symptômes et maladies, comme le syndrome maintenant le plus souvent référé comme SBS (syndrome de bâtiment malade) [15]. Des preuves considérables ont été révélées au sujet des conséquences pour la santé du radon intérieur, de la fumée ambiante de tabac, du formaldéhyde, du latex et de nombreux allergènes naturels et synthétiques [16, 17, 18]. L'amiante, un des polluants intérieurs bien connus, peut effrayer le tissu pulmonaire et causer le cancer [19]. Empoisonnement au plomb affecte principalement le système nerveux central, en particulier le développement du cerveau [20]. Selon l'Organisation mondiale de la santé (OMS), 4,3 millions personnes par an meurent prématurément de la maladie attribuable à la pollution de l'air domestique causée par l'utilisation inefficace des combustibles solides (données 2012) pour la cuisson [21].

De nombreuses études présentent les coûts de l'impact de la pollution de l'air intérieur et les avantages des interventions pour la réduire [22, 23, 24]. Par exemple, en France, la pollution à l'intérieur associée aux polluants tels que le benzène, le radon, les particules (PM2.5), la fumée de tabac ambiante (ETS) a été estimée à un coût approximatif de 20 milliards euros en 2004 [**?**]. La recherche de Mendel [26] suggère que l'amélioration des environnements de construction peut entraîner des avantages de plus de 15 millions des 89 millions pour la santé des travailleurs à l'intérieur des États-Unis, avec des avantages économiques estimés de 5 à 75 milliards dollars année.

Par conséquent, l'amélioration de la qualité de l'air intérieur devient un sujet de plus en plus important. Certains guides, règlements et bases de données spécialisées ont établi des normes

primaires pour fixer des limites liées à la protection de la santé publique pour le polluant atmosphérique primaire. Haute priorité fournir des informations pour les applications de qualité de l'air intérieur comprennent la norme ASHRAE 62 [27], les normes nationales de qualité de l'air ambiant, etc. OQAI [28] a proposé une classification des polluants en fonction de leurs impacts sur la santé.

Pour répondre aux problèmes liés aux changements climatiques les secteurs résidentiels et tertiaires doivent également opérer des transformations de manière à produire des bâtiments de moins en moins consommateurs d'énergie. De nouvelles formes urbaines apparaissent, utilisant de nouveaux matériaux et fonctionnalités de ventilation. L'évaluation et le contrôle de la qualité de l'air devient primordiale dès la réflexion de conception du bâtiment pour optimiser le bâtiment et le rendre le plus sain possible.

Avec une reconnaissance croissante des problèmes liés à la pollution de l'air intérieur, de nombreuses méthodes et techniques ont été développées et sont disponibles pour étudier les processus déterminants cette pollution et appuyer les décisions. Deux approches sont la mesure et la modélisation.

Les mesures de la qualité de l'air intérieur se basent souvent sur des instruments de surveillance, qui sont mis en place dans les laboratoires ou dans un environnement de construction réel (mesures in situ). Les mesures in situ à long terme permettent de déterminer les concentrations de crête à court terme, les concentrations moyennes calculées sur n'importe quelle période, et de corréler les variations de concentration en fonction du temps avec la génération de source, infiltration-ventilation, et d'autres caractéristiques. Toutefois, ils sont très coûteux et nécessitent un étalonnage fréquent et un entretien régulier. Ainsi, les mesures à court terme sont plus souvent effectuées et offrent des données limitées pour évaluer pleinement la qualité de l'air intérieur avec ses variations diurnes, saisonnières ou d'autres concentrations à long terme.

Plusieurs campagnes de mesure ont été développées dans le passé. On peut citer par exemple :

En Finlande en 1999, une campagne de mesure de l'air intérieur à Helsinki, Finlande 1999 a été réalisée pour étudier l'effet de la pollution atmosphérique extérieure sur l'air intérieur [29]. Les distributions de taille des particules d'hiver à l'intérieur et à l'extérieur ont été mesurées simultanément avec deux systèmes de granulométrie différentielle de mobilité similaire (DMP) à deux endroits : sur le toit d'un bâtiment (30 m au-dessus du niveau du sol) devant un système de ventilation correspondant à la concentration extérieure, et une salle de bureau (premier étage). On a observé des concentrations de particules intérieures variant de 500 à 10^4 cm^{-3} avec une forte dépendance aux concentrations extérieures. Ceci indique que dans ce scénario, les particules d'intérieur sont principalement d'origine extérieure.

En 1996, l'acide nitreux, le dioxyde d'azote (NO_2) et les concentrations d'ozone (O_3) dans les maisons occupées du sud de la Californie ont été mesuré à l'aide d'échantillonneurs passifs [30]. Les résultats de mesure montrent que la concentration moyenne de HONO à l'intérieur était de 4.6 ppb, comparativement à 0.9 ppb pour les HONO extérieurs. Moyenne concentrations intérieure et extérieure de NO_2 étaient de 28 et de 20,1 ppb, respectivement. Les concentrations de O_3 intérieur étaient faibles (moyenne de 14.9 ppb) par rapport aux niveaux extérieurs (moyenne de 56.5 ppb). Les mesures ont démontré la présence de concentrations et d'associations importantes de HONO intérieur résidentielles parmi les trois polluants intérieurs.

En France en 2002, des mesures de pollution extérieure et intérieure ont été réalisées dans huit écoles de la Rochelle (France) et dans ses banlieues [31]. L'ozone, les oxydes d'azote (NO and NO_2) et les particules aéroportées (numération des particules dans les 15 intervalles de taille variant de 0.3 à 15 mum) ont été surveillées en permanence à l'intérieur et à l'extérieur pendant deux périodes. L'humidité intérieure, la température, la concentration de CO_2 (un indicateur d'occupation), les ouvertures des fenêtres et la perméabilité des bâtiments ont également été mesurées. Les résultats montrent que l'ozone et les oxydes d'azote se comportent différemment, mais aucune corrélation avec la perméabilité des bâtiments n'a été observée pour les oxydes d'azote. Au contraire, l'ozone semble fortement influencé par l'étanchéité à l'air du

bâtiment : plus l'enveloppe du bâtiment est hermétique, plus le ratio [32]. L'occupation, par la resuspension de particules déjà déposées et la génération possible de particules, influence fortement le niveau de concentration intérieur des particules aéroportées.

Entre 1999 et 2001, les concentrations de carbonyle à l'intérieur et à l'extérieur ont été mesurées dans 234 foyers d'air personnel (RIOPA) dans trois zones urbaines des États-Unis [33]. Dans cette étude, les forces de la source intérieure pour différentes concentrations de carbonyle sont présentés. Par exemple, le formaldéhyde et l'acétaldéhyde présentaient les forces de source intérieure les plus fortes avec les valeurs médianes estimées de 3.9 et de 2.6 mg h^{-1}, respectivement. Hexaldehyde a également eu de grandes forces de source intérieure avec une médiane de 0.56 mg h^{-1}. L'acroléine et le crotonaldéhyde avaient les forces de source intérieure les plus faibles, sans sources d'intérieur décelées dans la majorité des maisons RIOPA qui ont été sélectionnées pour n'avoir que des résidents fumeur.

En France, entre 2004 et 2005, les concentrations d'aldéhydes ont été mesurées dans 162 foyers dans la région de Strasbourg (à l'est de la France) dans le cadre d'une étude cas/témoins appariant des personnes asthmatiques et non asthmatiques [34]. Les résultats montrent que le formaldéhyde, l'acétaldéhyde et le hexanal ont été les principaux aldéhydes rencontrés avec des concentrations moyennes de 32.2$\pm$14.6, 14.3$\pm$9.7 et 8.6$\pm$8.1 μg m^{-3}, respectivement. Cependant, il était difficile de déterminer les principaux paramètres influençant les concentrations de formaldéhyde dans l'environnement domestique. Des concentrations plus élevées de hexanal étaient reliées à de nouveaux revêtements tels que la peinture, les papiers peints et le plancher stratifié. La concentration de hexanal a diminué avec les âges de revêtement et de meubles, de sorte que ce composé peut être considéré comme un traceur de ces émissions.

En France, entre 2009 et 2010, un système national de surveillance de la qualité de l'air intérieur dans les locaux publics, en particulier avec des populations vulnérables telles que les enfants, a été réalisé [35]. La première phase d'une étude pilote s'est déroulée du 2009 septembre au 2010 juin et a impliqué 160 écoles et centres de garderie répartis dans 13 régions.

Les autres régions françaises prennent part à une deuxième vague, commencée en septembre 2010. Cette campagne s'est concentrée sur plusieurs paramètres : deux polluants chimiques (le benzène et le formaldéhyde) et l'air congestion. Les résultats montrent, en ce qui concerne les valeurs de gestion avancées par le Comité français pour la santé publique (PCIH), que la qualité de l'air est globalement acceptable dans la plupart des écoles et centres de garde qui ont participé à cette étude. Néanmoins, quelques cas nécessitent des diagnostics supplémentaires ou des mesures correctives. De plus, 16% des salles de classe ont été jugées insuffisamment ventilées (25% dans les écoles primaires). Les maires et les directeurs d'école ont été notifiés, et ont été fournis moyens d'identifier les principales sources de pollution ainsi que de mettre en œuvre des mesures d'assainissement.

En France en 2013, SURFin (les surfaces internes à habitat, une source probable acide nitreux) [36]. La campagne de SURFin a été menée dans une salle de classe inoccupée à Marseille (France) afin de quantifier les radicaux hydroxyle (OH) et hydroperoxyle (HO_2), les HONO, les fréquences de photolyse, les O_3 et les NOx, l'humidité relative, la température et huit différents COV (1-pentène, isobutène, d-limonene, isoprène, acétaldéhyde, acroléine, toluène et xylènes). Pour la première fois dans un environnement intérieur, des expériences sur le terrain pourraient être réalisées pour mesurer les taux de production de HONO et OH. Les résultats montrent que les concentrations de OH peuvent atteindre des niveaux équivalents à ceux de l'atmosphère extérieure dans les zones ensoleillées de la pièce. La photolyse de HONO, produite par la réactivité hétérogène du NO_2, est la principale source de OH.

En France entre 2012 et 2015, MERMAID (mesures expérimentales représentants et modélisation air intérieur détaillée) [37]. L'ADEME PRIMEQUAL projet associé visant à étudier la qualité de l'air intérieur dans le bâtiment à faible énergie. Une campagne intensive permet de mesurer les paramètres physiques de la pièce étudiée, la température et l'humidité relative, le taux de change d'air (AER), les niveaux de NOx (NO and NO_2), O_3, et 50 différents COV. Les

interactions superficielles avec les COV ont également été mesurées in situ afin d'estimer les coefficients d'émission et les facteurs de sorption des matériaux.

En principe, les mesures directes de l'air intérieur du bâtiment donnent les informations les plus réalistes concernant la qualité de l'air intérieur (QAI). En raison des distributions non uniformes des écoulements et des polluants, des mesures doivent être effectuées à de nombreux endroits. La prise de mesures directes des concentrations de polluants à de nombreux endroits ne peut pas être disponible parfois ou est très coûteuse et prend beaucoup de temps lorsqu'elle est disponible. En outre, les concentrations de polluants sont le résultat de divers processus, y compris la ventilation, les émissions, les effets de puits et les réactions chimiques. Ainsi, les mesures des polluants à elles seules ne permettent pas la distinction entre les contributions des processus mentionnés ci-dessus, en particulier le rôle de la chimie ou des autres sources. C'est pourquoi les modèles de QAI peuvent être utiles.

Les coûts élevés et la complexité de la mesure de la qualité de l'air intérieur ont rendu le développement des modèles performants nécessaire. Les modèles existant fournissent un moyen d'analyser les liens entre les sources, les puits et les concentrations de polluants (aux points de mesure ou en dehors des points mesurés) et ainsi constituent une grande potentialité pour l'aide à la décision. En outre, les modèles de QAI peuvent être utilisés pour étudier de nombreux problèmes de QAI sans les dépenses des grandes expériences sur le terrain. Les modèles de QAI ont de nombreux avantages, par exemple :

— Ils peuvent aider à comprendre les sources et les puits de polluants intérieurs et à prévoir les concentrations de polluants intérieurs ;
— Ils fournissent un cadre pour interpréter les résultats expérimentaux et pour concevoir des expériences en fournissant des informations sur les concentrations de polluants ;
— Un modèle est utile pour produire des résultats relatifs aux concentrations de polluants intérieurs avec divers paramètres comme les géométriques, les matériaux, la ventilation, la lumière, l'utilisation de systèmes améliorant la qualité de l'intérieur, etc. ;

— Ils fournissent des informations sur les facteurs importants et peuvent aider à déterminer ce qui doit être mesuré en priorité.

Les utilisations les plus courantes des modèles de QAI sont :

— estimer les concentrations de polluants ;

— estimer l'impact des sources individuelles ou des puits et des options de contrôle de la QAI sur l'exposition personnelle ;

Différents modèles ont été élaborés pour étudier les problèmes de l'air intérieur. Plusieurs de ces modèles sont continuellement mis à jour pour améliorer leur utilité.

Le modèle mathématique de la qualité de l'air intérieur (MIAQ) [45] est développé pour prédire les concentrations des principaux composés chimiquement réactifs dans l'air intérieur. Le modèle tient compte des effets de la ventilation, de la filtration, de l'enlèvement hétérogène, des émissions directes et des réactions photolytiques et chimiques thermiques. Toutefois, ce modèle ne s'adapte pas aux processus tels que l'adsorption et la désorption. En outre, le mécanisme chimique utilisé par ce modèle est simple compte tenu d'un peu plus de 50 réactions chimiques simultanées.

Un progiciel de simulation de la qualité de l'air intérieur (QAI) de Microsoft Windows, appelé trousse d'outils de simulation pour la qualité de l'air intérieur et l'exposition par inhalation (STKi), est conçu principalement pour les utilisateurs expérimentés afin de simuler un large éventail de scénarios de pollution de l'air intérieur [112]. Ce modèle peut estimer le taux de ventilation adéquat lorsque certains critères de qualité de l'air sont donnés. Le STKi se compose d'un programme de simulation à usage général et d'une série de programmes autonomes. Les programmes STKi supposent qu'un bâtiment est divisé en zones aériennes et que, dans chaque zone, l'air est bien mélangé. Le système de chauffage, de ventilation et de climatisation est considéré comme une zone d'air spéciale avec des caractéristiques spécifiques (par exemple, les filtres à l'air sont autorisés dans les voies de retour, le maquillage et les flux d'air d'appro-

visionnement). Toutefois, le STKi ne considère que les réactions chimiques en phase gazeuse, les interactions des polluants avec certaines surfaces ne sont pas prises en compte.

Le modèle de chimie intérieure et d'exposition (ICEM) [79], par exemple, permet de simuler les processus de transport entre les environnements extérieurs et intérieurs, les émissions intérieures, les réactions chimiques intérieures et les dépôts. Cependant, ce modèle ne considère que la chimie homogène et les dépôts hétérogènes irréversibles, d'autres réactions hétérogènes et des processus de surface comme l'adsorption et la désorption ne sont pas pris en compte dans ce modèle.

Un modèle probabiliste (INDAIR) a été mis au point pour prédire les concentrations de polluants atmosphériques dans les microenvironnements domestiques au Royaume-Uni [113]. Dans le modèle INDAIR, il y a trois microenvironnements pour l'environnement résidentiel : cuisine, salon et chambre à coucher. Le modèle INDAIR considère la ventilation, l'émission, la déposition et la sorption effectuées à l'intérieur. Selon les distributions des paramètres d'entrée et pour un grand nombre d'itérations (1000, pour stabiliser les résultats), le modèle INDAIR génère aléatoirement des valeurs de ces distributions pour une utilisation dans l'équation différentielle. Il n'y a pas de mécanisme chimique explicite inclus dans ce modèle.

Le modèle chimique détaillé de l'air intérieur (INDCM) [46, 47] a été mis au point pour étudier la chimie de l'air intérieur à partir d'un mécanisme chimique très détaillé (le principal mécanisme chimique) [114]. Mais ce modèle de boîte chimique ne considère pas les caractérisations détaillées des bâtiments comme les taux d'émission pour les matériaux spécifiques et le processus de sorption.

Un autre est le paquet de modélisation appelé INDAIR-Chem [115], qui utilise un modèle d'exposition à l'air intérieur existant [113] et un modèle détaillé de chimie de l'air intérieur [46]. Il fournit une approche pour évaluer l'exposition à l'intérieur des polluants pertinents à l'intérieur. INDAIR-Chem lie les émissions des principaux polluants intérieur (NOx, ozone, COV primaires et particules ultra fines) aux concentrations des principaux polluants intérieurs

secondaires ayant des effets nocifs présumés sur la santé. En raison de l'application du modèle INDCM en tant que modèle parent, ce modèle ne résout pas les problèmes mentionnés pour le modèle INDCM, comme les caractérisations détaillées des bâtiments comme les taux d'émission pour les matériaux spécifiques utilisés et les processus de sorption.

La dernière détaillée ici est le modèle de la moyenne temporelle qui a été développé pour explorer les magnitudes et les forces de la source de O_3, OH, et NO_3 dans les espaces résidentiels, ainsi que les magnitudes et les déterminants des taux de conversion des COV par ces oxydants [116, 73]. Les entrées du modèle étaient représentées comme des distributions au sein d'une analyse de Monte Carlo, permettant de quantifier l'influence statistique des entrées sur les résultats. Ce modèle est certes une représentation simplifiée de la cinétique réelle et n'est pas explicite. Seulement 20 réactions sont considérées dans le modèle et la sorption des COV sur les surfaces intérieures n'est pas incluse.

Un outil de simulation appelé Musica [117], qui permet de la prédiction dynamique du transport des polluants gazeux dans les sous-marins de la classe triomphant, a été développé. Quatre phénomènes élémentaires ont été identifiés : les flux d'air entre les pièces, les émissions internes, la chimie homogène et la chimie hétérogène. On a pris soin de ce modèle pour simuler avec précision la chimie intérieure homogène et hétérogène.

Mendez et al. (2015) [41] a récemment développé le modèle INCA-Indoor qui a l'avantage d'inclurer tous les processus existants dans des environnements confinés tels que : ventilation, émission, dépôt, processus chimiques de phase gazeuse. INCA-Indoor modèle peut être utilisé pour simuler les concentrations d'espèces chimiques à l'intérieur. De plus, ce modèle pourrait fournir l'information sur les contributions de chaque processus aux concentrations de polluants. Il est utilisé dans ce rapport de doctorat pour analyser leurs contributions relatives.

De nombreux exemples indiquent que les modèles de QAI agissent comme des outils puissants pour étudier l'environnement intérieur. Avec les modèles de QAI, beaucoup de problèmes de QAI peuvent être soigneusement étudiés et analysés avec peu de coût. Une série de modèles

ont été élaborés et adoptés pour étudier les problèmes de QAI. Cependant, peu de ces modèles ont pu être validés avec des résultats expérimentaux, et considèrent tous les processus physiques et chimiques prenant place en air intérieur.

Dans le cadre du projet ADEME PRIMEQUAL MERMAID (Mesures Expérimentales Représentatives et Modélisation Air Intérieur Détaillée), des mesures ont été effectuées dans un bâtiment à basse consommation d'énergie pour documenter la qualité de l'air dans des bâtiments encore rarement mesurée. Le modèle de qualité de l'air intérieur INCA-Indoor a été également développé. Le modèle INCA-Indoor vise à simuler les concentrations de polluants considérant les processus spécifiques de l'air intérieur tels que l'émission, l'infiltration, la ventilation, les interactions de surface (sorption, dépôt), la chimie gazeuse, la chimie hétérogène, formation d'aérosols, etc. Il s'agit d'un modèle numérique à résolution temporelle élaboré afin de comprendre les processus physiques et chimiques qui conduisent à la pollution de l'air intérieur et d'identifier les principales contributions aux concentrations de polluants. La configuration actuelle du modèle suppose que dans une pièce, l'air est complètement mélangé. Via quelques comparaisons mesures-simulations issues d'autres campagnes de mesure, principalement la campagne SURFin, il a pu être montré que le modèle INCA-Indoor permettait de prédire l'évolution des concentrations des espèces en phase gazeuse et des particules au cours du temps de manière satisfaisante et d'évaluer les contributions des différents procédés aux polluants concentrations de polluants.

Comme la pollution de l'air intérieur a des répercussions sur la santé humaine et que les gens sont très exposés à cette pollution atmosphérique le long d'une journée, il est nécessaire de fournir aussi rapidement des connaissances sur les processus physiques et chimiques qui sont impliqués, des méthodologies qui pourraient aider à comprendre les sources et les puits de la pollution de l'air intérieur, et de développer des outils pour aider à prendre des décisions pour le réduire. Cette thèse a été réalisée dans le cadre du projet PRIMEQUAL Mermaid (2012-2016) [37, 38, 39]. Ce projet offre plusieurs types de résultats.

— De nombreuses mesures ont été émises à partir de deux campagnes dans les salles de classe et les environnements extérieurs pendant les vacances universitaires d'avril à mai 2014 et de février à mars 2015 dans un bâtiment à faible énergie et des mesures supplémentaires dans les laboratoires pour détailler peu de processus ;

— Le modèle de la qualité de l'air intérieur INCA-Indoor a été développé en parallèle des campagnes de mesure. Mendez et coll. (2015) [41] a proposé un modèle tenant compte des divers processus physiques et chimiques intérieurs, y compris les émissions, la ventilation, la photochimie gazeuse, le dépôt, la sorption et la chimie hétérogène. Le modèle est de calculer les contributions de chaque processus aux concentrations de polluants ;

— Premières comparaisons du modèle INCA-Indoor avec des mesures émises de la campagne de SURFin et d'autres modèles montrent que le modèle offre des performances assez bonnes pour simuler la qualité de l'air intérieur, et de fournir une nouvelle perspicacité des processus impliqués qualité de l'air intérieur. Mendez et al. (2015) ont évalué l'impact des processus d'oxydation sur la qualité de l'air intérieur avec le modèle INCA-Indoor [41]. Mendez et al. (2017a) ont comparé les concentrations simulées de radicaux HOx (OH + HO_2) avec des mesures in situ et nous fournissent des informations sur les sources et les puits des oxydants radicaux intérieurs [42]. Mendez et al. (2017b) fournit un nouveau mécanisme de formation de HONO à l'intérieur basé sur des mesures in situ et des [43] de modélisation ;

— Les analyses de sensibilité préliminaire ont montré que la sensibilité comme Monte Carlo peut aider à identifier les paramètres d'entrée les plus sensibles qui peuvent influencer les simulations et sur lesquels il est nécessaire d'améliorer les estimations (thèse de Master de Fangfang Guo). Toutefois, l'une des limitations de la méthode de Monte-Carlo est qu'il est difficile d'évaluer la sensibilité de l'impact des variations de

paramètres sur les sorties du modèle au cour du temps. En outre, il est long d'évaluer l'importance relative des paramètres pour un modèle avec beaucoup de paramètres.

Tous ces premiers résultats ont ouvert de nouvelles questions à répondre : le modèle INCA-Indoor est-il capable de reproduire les mesures de MERMAID (nouvellement collectées et analysées) et d'aider à comprendre la qualité de l'air intérieur dans le bâtiment à faible énergie qui a été étudié ? Quels sont les principaux processus en jeu ? Pourrions-nous élaborer une méthodologie de sensibilité pour aider à comprendre la pollution de l'air intérieur et prend les stratégies de réduction des pollutions ?

Fort de ces premiers résultats, l'objectif de cette thèse a été d'analyser et de simuler à l'aide du modèle INCA-Indoor la qualité de l'air intérieur mesurée dans le projet MERMAID, et de développer une nouvelle méthodologie pour étudier les contributions des différents processus impliqués aux concentrations de polluants. Cette nouvelle méthodologie se base sur un nouveau programme de sensibilité INCA-Indoor-D, construit à partir du modèle INCA-Indoor. Ce modèle permet d'identifier rapidement les paramètres les plus sensibles qui peuvent influencer la qualité de l'air intérieur. Il s'agit à terme de développer d'un outil capable d'optimiser les stratégies de réduction de la QAI.

La thèse est organisée en cinq chapitres. Dans le chapitre 1, le contexte socioéconomique international de l'étude ainsi que les principales méthodes d'étude de la qualité de l'air intérieur sont présentés comme la base du travail de la thèse. Le chapitre 2 donne un aperçu des modèles de qualité de l'air intérieur existants et détaille les équations physiques et chimiques du modèle INCA-Indoor qui a servi pour la suite du travail effectué durant la thèse.

Dans le chapitre 3, le modèle INCA-Indoor a été validé expérimentalement en utilisant les données mesurées collectées lors de la campagne MERMAID (2014-2015). Les mesures de terrain pour la première campagne de MERMAID ont été effectuées du 23 avril 2014 au 2 mai 2014. Les paramètres mesurés comprennent les paramètres physiques de la pièce étudiée (volume, surface), la température et l'humidité relative, le taux de change d'air (AER), les

niveaux de NOx, O_3 et les COV. Les 5 fenêtres de la salle de classe sont exposées au sud (210°) afin de favoriser le chauffage solaire. Deux entrées d'air d'une unité de traitement de l'air à double écoulement avec récupération de la chaleur sont présentes dans la salle de classe sur le côté des fenêtres, et une extraction est installée sur le côté du corridor. Les mesures ont été effectuées dans 5 endroits différents dans et hors de la classe.

Pour comparer les résultats de simulation avec les mesures effectuées pendant la MERMAID, INCA-Indoor a été mis en place à la suite de la configuration de la salle de classe (volume = 138,5 m^3, 10 surface). La température et l'humidité relative ont été limitées à leurs valeurs mesurées dans le modèle. Les horaires de fonctionnement de la ventilation suivent le programme de mesures au cours de la première campagne. Les taux d'infiltration ont été mesurés seulement un jour pendant la campagne en suivant la diminution de la concentration de CO_2 et il varie entre 30 et 60 m $^3h^{-1}$. Les taux d'infiltration utilisés comme entrées dans le modèle étaient de 45 m ^{3} h $^{-1}$ (AER : 0.43 h^{-1}) correspondant au taux d'infiltration maximum avec la ventilation éteinte et 300 m ^{3} h^{-1} (AER : 2.2 h^{-1}) avec la ventilation allumée. Afin d'identifier les différences potentielles entre la concentration extérieure et la concentration à l'entrée de ventilation en raison des pertes dans le système ou à la contamination contraire, des mesures ont été effectuées aux deux endroits pendant la campagne. De plus, les concentrations entrant dans la pièce considérées comme concentration d'absorption pour le modèle sont soit les concentrations extérieures mesurées, soit celles mesurées à l'entrée de ventilation. Les deux types de données sont testés ici et discutés dans les sections suivantes. Les taux d'émission et de sorption des COV des 10 surfaces principales mesurées au cours des campagnes [147] sont utilisés dans le modèle. Toutes les simulations commencent à partir du 29 avril 2014 à minuit et se terminent le 30 avril 2014 à minuit avec un pas de temps de 60 secondes.

Deux types de simulations (en tenant compte des données extérieures et de l'entrée de ventilation) ont été effectuées pour les 15 espèces d'intérêt dans le chapitre 3. La simulation avec des données à l'entrée de ventilation représente bien les profils de concentration à l'intérieur,

mais sousestime des concnetrations intérieur en raison de la sous-estimation du taux d'émission lorsque la ventilation est allumée. Toutefois, lorsque la ventilation est désactivée, les simulations mesurées à l'entrée de ventilation ne tiennent pas bien compte de l'effet de l'infiltration. Les simulations avec des données extérieures représentent l'évolution des profils de concentration, mais sous-estiment des concentrations intérieurs en raison de la sous-estimation des taux d'émission. Cependant, les simulations avec des données extérieures mesurées ne pouvaient pas toujours suivre les profils de concentration à l'intérieur en raison de la limitation de détection des instruments utilisés à l'extérieur provoquant l'augmentation de l'incertitude dans le modèle en utilisant des données extérieures.

L'analyse des contributions basée sur la simulation avec des données extérieures mesurées confirme que les émissions intérieures sont les principales sources de la plupart des COV (c.-à-d. le méthanol, le formaldéhyde et l'acétaldéhyde) et que l'oxydation des COV peut être une source importante pour plusieurs composés comme l'acétone.

Des simulations avec des données extérieures mesurées comme entrée de modèle indiquent que les concentrations d'O_3 intérieur et de NOx ont montré une dépendance critique aux valeurs extérieures. Les concentrations d'O_3 intérieur et de NOx augmentent lorsque la ventilation est enclenchée. Bien qu'il y ait un o-xylène émis par des matériaux intérieurs, les comparaisons des données mesurées et simulées ont montré que le o-xylène intérieur était principalement délivré de l'extérieur par la ventilation lorsque la ventilation est allumée. Le retard entre les pics dans les concentrations extérieures et intérieures nous a permis de conclure que le modèle sous-estime probablement les processus d'infiltration, qui n'ont pas été mesurés tous les jours pendant la campagne de MERMAID, mais varient d'un jour à l'autre comme fonction de la météorologie locale. Une de nos premières recommandations serait de mesurer continuellement ce taux d'infiltration dans la future campagne de qualité de l'air intérieur. La sous-estimation de la concentration de o-xylène modélisée est probablement due à la sous-estimation des taux d'émission.

La plupart des autres concentrations de COV sont presque constantes pendant la nuit lorsque la ventilation est éteinte, puis diminuent dès que la ventilation est allumée, mais augmentent lorsque la ventilation est de nouveau éteinte. Ces COV comprennent le formaldéhyde, l'acétaldéhyde, le méthanol, le toluène, l'acroléine, l'acétone et l'isoprène. On montre que le modèle INCA-Indoor simule ces concentrations nocturnes alors que nos simulations sous-estiment probablement les processus d'infiltration à l'aide de données mesurées à l'entrée de ventilation. Le modèle simule très bien la diminution de ces concentrations de COV en raison de la ventilation, mais tend à sous-estimer l'augmentation des concentrations de COV à la fin de la journée et lorsque la ventilation est éteinte à nouveau. Cette augmentation est due aux coefficients d'émission de surface. Les sous-estimations du modèle tendent à montrer que les coefficients d'émission de surface sont également sous-estimés.

L'évolution de la concentration de d-limonene est plus complexe à expliquer. La concentration de d-limonene tend à diminuer avant la mise en marche de la ventilation en raison de la consommation par les réactions de d-limonene avec O_3, le radical nitrate (NO_3) et le radical hydroxyle (OH). Lorsque la ventilation est activée, la concentration de d-limonene dépend de la balance des taux de production et de consommation de d-limonene. Selon les fluctuations non régulières de la concentration de d-limonene, elle suggère que les réactions chimiques peuvent jouer un rôle plus important pour la concentration de d-limonene par rapport aux autres concentrations de COV.

Pour le benzène, le chlorobenzène et le p-dichlorobenzène, il n'y a pas de source d'intérieur observée pendant la campagne Mermaid et les mesures montrent des concentrations faibles près de la limite de leurs incertitudes. Des simulations avec des données mesurées à l'entrée de ventilation montrent que les concentrations de benzène et de chlorobenzène ne sont pas significativement touchées par la ventilation. Cependant, les concentrations de benzène, de chlorobenzène et de p-dichlorobenzène modélisées avec des données extérieures mesurées ont été fortement affectées par la concentration extérieure. Toutefois, le profil extérieur du benzène, du chloro-

benzène et du p-dichlorobenzène ne sont pas réalistes en raison de la limitation de détection des instruments utilisés à l'extérieur, ce qui entraîne l'augmentation de l'incertitude dans le modèle à l'aide de données extérieures.

La ventilation est une voie importante pour réduire la plupart des concentrations de COV. De plus, la déposition est également importante pour réduire les concentrations de formaldéhyde et d'acétaldéhyde. Pour l'acétone et l'acroléine, la sorption représente respectivement 35.08% et 49.60% des taux de consommation totaux. La chimie intérieure apparaît comme une voie de perte importante pour l'acroléine, l'isoprène et le d-limonene par leurs réactions avec OH radical ou O_3.

Bien que les concentrations des espèces ne montrent pas de dépassement des normes de qualité de l'air intérieur dans le bâtiment BBC étudié, elles ont néanmoins permis de vérifier que le modèle était capable de simuler les concentrations de composés organiques volatils, de NO, NO_2 et de O_3 et de permettre une étude de qualité de l'air intérieur. Une analyse de contribution indique que les émissions intérieures de polluants par les surfaces, et les échanges via le système de ventilation avec l'air extérieur sont les deux processus majeurs affectant les concentrations de polluants intérieurs. Le rôle de la chimie est aussi important pour la plupart des COV comme l'acroléïne, l'isoprène et le d-limonène, de par leurs réactions avec les radicaux OH ; la production de ces radicaux OH étant elle-même fortement influencée par la lumière.

Dans le chapitre 4, les influences des taux d'émissions et de la lumière affectant les processus d'oxydation à l'intérieur ont été détaillées. En effet, les variations spatiales et temporelles observées sur les mesures des facteurs d'émissions de polluants à la surface des matériaux ainsi que de l'intensité de la lumière durant la campagne MERMAID ont permis de construire différents scénarios en fonction de ces données d'entrée du modèle. L'analyse des résultats des simulations montre d'une part que les émissions de COV ont, dans les conditions de l'étude, un impact majeur sur les concentrations des espèces à l'intérieur. Les écarts entre les concentrations modélisées et expérimentales pourraient être réduits en détaillant au mieux les variations

spatiales de ces taux d'émissions. D'autre part, les simulations pour lesquelles nous avons fait varier la transmission de la lumière par les fenêtres (qui détermine le flux de photons pénétrant effectivement dans la pièce), montrent qu'en augmentant la transmission des UV et de la lumière visible, les concentrations moyennes diurnes des radicaux HOx (OH et HO_2) et O_3 augmentent par photolyse de HONO par exemple, et par ailleurs, les concentrations de certains COV (comme le d-limonène, le o-xylène, et l'isoprène) diminuent en raison des réactions du COV avec OH. En tant que produits de réactions de COV avec OH, les concentrations de formaldéhyde et d'acétaldéhyde augmentent.

La mise en place de stratégies efficaces pour réduire la pollution de l'air intérieur doit ainsi tenir compte de nombreux paramètres simultanés : concentrations extérieures, flux de rayonnement UV et visible, taux de renouvellement de l'air, taux d'émission, etc. Le renouvellement de l'air ne peut pas toujours permettre de réduire la pollution de l'air intérieur, car l'air extérieur peut aussi apporter des NOx ou d'autres COV. Si l'augmentation de l'intensité lumineuse peut contribuer à diminuer certains COV, en contrepartie elle renforce globalement le pouvoir oxydant de l'atmosphère intérieure. La réduction des émissions dues aux matériaux de construction et à l'activité humaine est certainement la meilleure façon de réduire la pollution de l'air intérieur. Cette option a néanmoins besoin de temps pour être mise en œuvre à grande échelle par les habitants et doit aussi être prise en compte par les industries. Ainsi, afin d'aider les décideur ou/et les habitants à prendre des décisions pour diminuer le plus rapidement la pollution de l'air à l'intérieur des logements, une méthodologie de sensibilité associée au modèle INCA-Indoor a été développée et est présentée dans le chapitre 5. Son objectif est de pouvoir identifier les paramètres les plus influents sur les concentrations des polluants intérieurs et permettre de quantifier les réductions optimales des paramètres nécessaires pour améliorer la qualité de l'air intérieur. La méthodologie s'appuie sur un outil de différenciation automatique appelé TAPENADE, qui a été appliqué pour calculer les sensibilités locales au premier ordre défini comme des dérivées partielles des concentrations d'espèces par rapport aux paramètres du modèle en raison de l'ef-

ficacité de calcul de cet outil. Un exemple d'application a été choisi pour étudier la production du radical OH et la chimie réactive à l'intérieur d'une pièce.

En atmosphère extérieure, une grande partie de la chimie réactive importante est dominée par le radical hydroxyle (OH). En environnement intérieur, les mesures effectuées et les résultats de simulations du modéle indiquent que des quantités de radicaux OH intérieurs sont du même ordre de grandeur que celles en milieu extérieurs. Ceci suggère l'importance de la chimie oxydante par les radicaux OH en atmosphère intérieure qui peut impliquer la formation d'espèces secondaires plus dangereuses que les polluants primaires.

La concentration de radicaux OH intérieure peut être affectée par de nombreux processus. Il s'est avéré nécessaire de déterminer quels étaient les plus importants puis de quantifier leur effet sur les concentrations de radicaux OH et donc sur la qualité de l'air intérieur.

Une analyse de sensibilité des concentrations de OH par rapport aux divers paramètres (concentrations initiales de NO, NO_2, O_3 et HONO, flux d'émission de COV, taux de renouvellement de l'air, concentrations extérieures, vitesses de dépôt et de réaction) a par conséquent été effectuée. Une classification de l'importance de ces paramètres (appelée « rang ») en fonction de la sensibilité a ainsi été effectuée. L'analyse de sensibilité confirme que les concentrations de radicaux OH à l'intérieur sont très sensibles au taux de renouvellement d'air et à la photolyse de HONO, photolyse qui a un impact direct positif sur les concentrations de OH.

En conclusion, ce travail de thèse offre une nouvelle analyse de la pollution de l'air ainsi que de nouvelles perspectives d'études possibles dans un bâtiment basse consommation. Il a permis de confirmer que le modèle INCA-Indoor développé dans le cadre du projet MERMAID permettait de simuler convenablement la pollution de l'air intérieur. A partir de ce modèle, un modèle de sensibilité a été construit afin d'élaborer un nouvel outil d'aide à la décision capable de calculer à la fois les concentrations et leurs sensibilités aux divers paramètres qui ont permis de calculer ces concentrations. Ces sensibilités peuvent ensuite être utilisées pour élaborer, voire optimiser, des stratégies de réduction de la pollution de l'air intérieur et d'identifier les

paramètres les plus importants, sur lesquels il faut se focaliser pour améliorer la modélisation de la pollution de l'air intérieur et la qualité de cet air dans les locaux.

D'autres travaux sont nécessaires pour aborder certaines des questions qui ont été rencontrées au cours de nos études. Tout d'abord, bien que la comparaison entre les profils expérimentaux et les profils modélisés montre un bon accord, il existe encore quelques différences, qui peuvent être attribuées aux variations des taux d'émission, le taux d'infiltration dans la salle, les échanges avec d'autres chambres, l'hétérogénéité dans la salle (lumière, concentrations, matériaux, etc), et aussi les processus mal compris qui seront nécessaires plus de mesure et de la tâche de modélisation (comme la formation des aérosols et l'interaction avec la phase gaz).

En effet, les émissions peuvent fluctuer au cours du temps en fonction des paramètres tels que la température, l'humidité, mais aussi les concentrations ambiantes et les matériaux [164]. INCA-Indoor modèle considère les taux d'émission comme des constantes. Par conséquent, quantifier plus précisément les taux d'émission et fournir plus d'informations sur l'évolution des taux d'émission pourrait être utile pour améliorer les résultats de simulation de modèle, qui pourraient fournir des informations plus fiables sur la qualité de l'air intérieur. Octopus Lab (http ://www.octopuslabs.science/fr), une nouvelle société utilisant INCA-Indoor pour évaluer l'air intérieur, a développé une interface du modèle avec des données Pandore (http ://lAsie.univ-Larochelle.fr). Cette base de données Pandore fournit des imformations sur les taux d'émission de tous les types de polluants (particules, gaz organiques et inorganiques, micro-organismes) des sources intérieures du bâtiment, mais aussi des émissions constantes.

Deuxièmement, INCA-Indoor modèle est utilisé pour simuler les concentrations de polluants dans une salle de classe avec des données collectées lors de la campagne MERMAID. Ces données mesurées ont été obtenues dans la salle de classe où tous les meubles ont été déplacés et pendant la période des vacances universitaires pour des raisons de faisabilité. Par conséquent, l'effet de l'émission, de la sorption ou de la déposition ayant lieu à la surface de ces meubles et de l'activité humaine comme le nettoyage, l'ouverture des fenêtres n'a pas été

pris en considération. Il est donc fortement conseillé, à l'avenir, de simuler les concentrations de polluants dans un environnement plus réaliste, y compris la variété de l'ameublement et la présence d'occupants qui pourraient interagir grandement avec l'air intérieur.

Les simulations CFD à l'intérieur de la pièce et à l'échelle du bâtiment permettraient à un utilisateur de prendre en compte l'hétérogénéité et les échanges avec d'autres pièces. Les activités de recherche difficiles sont au-delà de ce genre de travail que la dispersion à l'intérieur d'une salle, ou des échanges avec d'autres, ont des interactions fortes avec la chimie et le couplage augmentera le calcul du temps.

Troisièmement, l'effet du taux d'échange d'air de la ventilation sur la qualité de l'air intérieur a été discuté dans cette étude. Il est évident que certaines concentrations de polluants peuvent être réduites pendant la période de ventilation. Toutefois, lorsque la ventilation est désactivée, certaines concentrations de polluants peuvent atteindre des niveaux identiques ou même supérieurs à ceux avant que la ventilation ne soit enclenchée. Une étude plus poussée est nécessaire pour étudier l'effet du temps de ventilation et pour trouver le taux de ventilation modéré et le temps pour améliorer la QAI. L'infiltration est aussi une question à étudier. Une des recommandations pour les futures campagnes de mesure consisterait à mesurer le taux d'infiltration le plus précisément possible et à étudier sa modélisation.

Les particules d'aérosol sont considérées comme des sources importantes de polluants dans l'environnement intérieur [191] et la concentration de particules d'aérosol dans une pièce influe grandement sur la QAI. Il n'a pas été possible de discuter de ce sujet dans cette étude, mais un modèle aérosol a également été développé dans le cadre du projet MERMAID. Ce modèle doit être développé afin de mieux simuler la formation d'aérosols organiques secondaires (SOA). Ainsi, les études des procédés et des paramètres des aérosols contrôlant les concentrations de l'air intérieur devraient être incluses dans l'étude ultérieure.

En outre, le mécanisme de formation à l'intérieur de certaines espèces n'est pas encore très clair comme HONO, qui est confirmée comme une source intérieure importante de OH radical.

Bien que Mendez et al. (2017) [43] a proposé un nouveau mécanisme de formation de HONO, ce mécanisme n'est pas encore entièrement soutenu par des expériences en laboratoire. Plus de données expérimentale sont nécessaires pour améliorer la compréhension du mécanisme de formation de HONO.

Puisque la QAI n'est pas le seul sujet difficile concernant le bâtiment, il serait également intéressant de coupler INCA-Indoor avec un modèle d'énergie et un modèle d'humidité de l'air chaud afin de mieux aborder le concept de bâtiments durables. Plusieurs nouveaux matériaux sont construits afin de réduire le problème d'humidité dans l'environnement intérieur. En même temps les systèmes de ventilation sont construits pour réduire l'humidité trop et la pollution de l'air, mais le polluant atmosphérique contrôlé est habituellement seulement CO_2. L'optimisation du taux de ventilation en fonction de la consommation d'énergie, de l'humidité et des concentrations de plusieurs polluants atmosphériques serait utile pour optimiser le confort de l'habitant et respecter les réglementations ou recommandations en matière d'énergie et de qualité intérieure. Plus généralement, un bâtiment fait partie d'une zone urbaine. Puisque cette zone urbaine, avec sa pollution atmosphérique extérieure associée, peut avoir un impact sur la pollution de l'air intérieur, il est nécessaire de concevoir les bâtiments et les quartiers afin de réduire l'impact sur l'exposition [192, 193].

Une première version d'un modèle de sensibilité a été construite avec le logiciel tapenade et il est prouvé qu'il s'agit d'un outil très utile pour identifier les paramètres importants affectant les concentrations de polluants. D'autres investigations sont nécessaires pour développer un outil opérationnel qui pourrait orienter la décision de réduire la pollution de l'air intérieur puisque la méthodologie est pour le moment limitée à un régime chimique réduit, et la démonstration sont nécessaires pour être exécuté pour montrer le capacités de l'outil pour contrôler plusieurs polluants en même temps.

CHAPTER 8

BIBLIOGRAPHY

Bibliographie

[1] Sait C. Sofuoglu, Guler Aslan, Fikret Inal, and Aysun Sofuoglu. An assessment of indoor air concentrations and health risks of volatile organic compounds in three primary schools. *International Journal of Hygiene and Environmental Health*, 214(1) :36–46, January 2011.

[2] G. Zhang, J. Spickett, K. Rumchev, A. H. Lee, and S. Stick. Indoor environmental quality in a 'low allergen' school and three standard primary schools in Western Australia. *Indoor Air*, 16(1) :74–80, February 2006.

[3] Greta Smedje, Dan Norbåck, and Christer Edling. Subjective Indoor Air Quality in Schools in Relation to Exposure. *Indoor Air*, 7(2) :143–150, June 1997.

[4] J. Sundell. On the history of indoor air quality and health. *Indoor Air*, 14 Suppl 7 :51–58, 2004.

[5] OAR US EPA. Introduction to Indoor Air Quality, August 2014.

[6] Office of Research & Development. TOTAL EXPOSURE ASSESSMENT METHODOLOGY (TEAM) STUDY : SUMMARY AND ANALYSIS. VOLUME 1.

[7] European Commission - PRESS RELEASES - Press release - Indoor air pollution : new EU research reveals higher risks than previously thought.

[8] Health Canada and Health Canada. Pollutants from furniture and building materials, January 2012.

[9] Lina Šeduikyte and Raimondas Bliudzius. Pollutants emission from building materials and their influence on indoor air quality and people performance in offices. *Journal of Civil Engineering and Management*, 11(2) :137–144, January 2005.

[10] OAR US EPA. Controlling Pollutants and Sources : Indoor Air Quality Design Tools for Schools, October 2014.

[11] OAR US EPA. Biological Pollutants' Impact on Indoor Air Quality, August 2014.

[12] Daniel Mueller, Stefanie Uibel, Markus Braun, Doris Klingelhoefer, Masaya Takemura, and David A Groneberg. Tobacco smoke particles and indoor air quality (ToPIQ) - the protocol of a new study. *Journal of Occupational Medicine and Toxicology (London, England)*, 6 :35, December 2011.

[13] OAR US EPA. Pesticides' Impact on Indoor Air Quality, August 2014.

[14] The Inside Story : A Guide to Indoor Air Quality, February 2016.

[15] Peder Skov, Ole Valbjørn, and DISG. The "sick" building syndrome in the office environment : The danish town hall study. *Environment International*, 13(4) :339 – 349, 1987.

[16] Anthony V. Nero. Estimated risk of lung cancer from exposure to radon decay products in u.s. homes : A brief review. *Atmospheric Environment (1967)*, 22(10) :2205 – 2211, 1988.

[17] Paul Cameron, John S. Kostin, Jeffrey M. Zaks, John H. Wolfe, Gregory Tighe, Barry Oselett, Richard Stocker, and Jeffrey Winton. The health of smokers' and nonsmokers' children. *Journal of Allergy*, 43(6) :336 – 341, 1969.

[18] Theodore J. Witek, E.Neil Schachter, Tarik Tosun, Brian P. Leaderer, and Gerald J. Beck. Controlled human studies on the pulmonary effects of indoor air pollution : Experiences with sulful dioxide and formaldehyde. *Environment International*, 12(1) :129 – 135, 1986.

[19] Dana Hashim and Paolo Boffetta. Occupational and environmental exposures and cancers in developing countries. *Annals of Global Health*, 80(5) :393 – 411, 2014. A Global Perspective on Cancer Burden.

[20] Talia Sanders, Yiming Liu, Virginia Buchner, and Paul B. Tchounwou. Neurotoxic Effects and Biomarkers of Lead Exposure : A Review. *Reviews on environmental health*, 24(1) :15–45, 2009.

[21] WorldHealthOrganization | Household air pollution and health, 2016.

[22] Guy Hutton, Eva Rehfuess, and Fabrizio Tediosi. Evaluation of the costs and benefits of interventions to reduce indoor air pollution. *Energy for Sustainable Development*, 11(4) :34 – 43, 2007.

[23] Agustin Arcenas, Jan Bojö, Bjorn Larsen, and Fernanda Ruiz Ñunez. The Economic Costs of Indoor Air Pollution : New Results for Indonesia, the Philippines, and Timor-Leste. *Journal of Natural Resources Policy Research*, 2(1) :75–93, January 2010.

[24] Sumi Mehta and Cyrus Shahpar. The health benefits of interventions to reduce indoor air pollution from solid fuel use : a cost-effectiveness analysis. *Energy for sustainable development*, 8(3) :53–59, 2004.

[25] Guillaume Boulanger, Thomas Bayeux, Corinne Mandin, Séverine Kirchner, Benoit Vergriette, Valérie Pernelet-Joly, and Pierre Kopp. Socio-economic costs of indoor air pollution : A tentative estimation for some pollutants of health interest in France. *Environment International*, 104 :14–24, April 2017.

[26] Mark J. Mendell, William J. Fisk, Kathleen Kreiss, Hal Levin, Darryl Alexander, William S. Cain, John R. Girman, Cynthia J. Hines, Paul A. Jensen, Donald K. Milton, Larry P. Rexroat, and Kenneth M. Wallingford. Improving the Health of Workers in Indoor Environments : Priority Research Needs for a National Occupational Research Agenda. *American Journal of Public Health*, 92(9) :1430–1440, September 2002.

[27] American Society of Heating and Air-Conditioning Engineers (ASHAE). The standards for ventilation and indoor air quality, 2016.

[28] OQAI,www.oqai.fr/obsairint.aspx ?idarchitecture=182.

[29] Ismo K. Koponen, Ari Asmi, Petri Keronen, Katri Puhto, and Markku Kulmala. Indoor air measurement campaign in helsinki, finland 1999 – the effect of outdoor air pollution on indoor air. *Atmospheric Environment*, 35(8) :1465 – 1477, 2001.

[30] Kiyoung Lee, Jianping Xue, Alison S Geyh, HalÃ»k Ozkaynak, Brian P Leaderer, Charles J Weschler, and John D Spengler. Nitrous acid, nitrogen dioxide, and ozone concentrations in residential environments. *Environmental Health Perspectives*, 110(2) :145–150, February 2002.

[31] P. Blondeau, V. Iordache, O. Poupard, D. Genin, and F. Allard. Relationship between outdoor and indoor air quality in eight French schools. *Indoor Air*, 15(1) :2–12, jan 2005.

[32] C. J. Weschler. Ozone in indoor environments : concentration and chemistry. *Indoor Air*, 10(4) :269–288, December 2000.

[33] W. Liu, J. Zhang, L. Zhang, B.J. Turpin, C.P. Weisel, M.T. Morandi, T.H. Stock, S. Colome, and L.R. Korn. Estimating contributions of indoor and outdoor sources to indoor carbonyl concentrations in three urban areas of the united states. *Atmospheric Environment*, 40(12) :2202 – 2214, 2006.

[34] C. Marchand, S. Le Calvaand Ph. Mirabel, N. Glasser, A. Casset, N. Schneider, and F. de Blay. Concentrations and determinants of gaseous aldehydes in 162 homes in strasbourg (france). *Atmospheric Environment*, 42(3) :505 – 516, 2008.

[35] Nicolas Michelot, Corinne Mandin, Olivier Ramalho, Jacques Ribaron, Caroline Marchand, Laure Malherbe, Martine Ramel, Marie-Blanche Personnaz, Varonique Delmas, Soizic Urban, and Marie Carrega. Monitoring indoor air quality in french schools and day-care centres results from the first phase of the pilot survey, 2011. http ://dx.doi.org/10.4267/pollution-atmospherique.456.

[36] Sasho GLIGOROVSKI. Les surfaces internes à l'habitat, une source probable d'acide nitreux (SURFIN). 2013.

[37] Coralie Schoemaecker, Marion Blocquet, M. Ward, Benjamin Hanoune, Denis Petitprez, Patrick Lebegue, Sébastien Dusanter, Nadine Locoge, Malak Rizk, Marie Verriele, M. Guglielmino, Stéphane Le Calve, Céline Liaud, R. Nasreddine, C. Trocquet, Nathalie Leclerc, X. Pingenot, Christelle Schneider, Nadège Blond, Didier Hauglustaine, Jean Luc Ponche, Maxence Mendez, Patrice Blondeau, and Marc-Olivier Abadie. Projet MERMAID : Caractérisation détaillée de l'air intérieur des bâtiments performants en énergie par couplage entre Mesures Expérimentales Représentatives et Modélisation Air Intérieur Détaillée. 2015.

[38] M. Verriele, C. Schoemaecker, B. Hanoune, N. Leclerc, S. Germain, V. Gaudion, and N. Locoge. The MERMAID study : indoor and outdoor average pollutant concentrations in 10 low-energy school buildings in France. *Indoor Air*, 26(5) :702–713, October 2016.

[39] Blocquet Marion, Guo Fangfang, Mendez Maxence, Coudert Sébastien, Batut Sébastien, Hecquet Christophe, Blond Nadège, Fittschen Christa, and Schoemaecker Coralie. Im-

pact of the spectral and spatial properties of the light on indoor chemistry : experimental and modeling study. *Indoor Air*, 2017.

[40] M. RIZK, F. GUO, M. WARD, M. VERRIELE, S. DUSANTER, N. BLOND, N. LOCOGE, and C.SCHOEMAECKER. Impact of material emissions and sorption of volatile organic compounds on indoor air quality in a low energy building : field measurements and modelling. *Indoor Air*, 2017.

[41] Maxence Mendez, Nadège Blond, Patrice Blondeau, Coralie Schoemaecker, and Didier A. Hauglustaine. Assessment of the impact of oxidation processes on indoor air pollution using the new time-resolved inca-indoor model. *Atmospheric Environment*, 122 :521 – 530, 2015.

[42] M. Mendez, D. Amedro, N. Blond, D. A. Hauglustaine, P. Blondeau, C. Afif, C. Fittschen, and C. Schoemaecker. Identification of the major HO_x radical pathways in an indoor air environment. *Indoor Air*, July 2016.

[43] M. Mendez, N. Blond, D. Amedro, D. A. Hauglustaine, P. Blondeau, C. Afif, C. Fittschen, and C. Schoemaecker. Assessment of indoor HONO formation mechanisms based on in situ measurements and modeling. *Indoor Air*, 27(2) :443–451, March 2017.

[44] AIRIN,http ://www.airin.fr/.

[45] William W. Nazaroff and Glen R. Cass. Mathematical modeling of chemically reactive pollutants in indoor air. *Environmental Science & Technology*, 20(9) :924–934, September 1986.

[46] Nicola Carslaw. A new detailed chemical model for indoor air pollution. *Atmospheric Environment*, 41(6) :1164 – 1179, 2007.

[47] Nicola Carslaw, Tiago Mota, Michael E. Jenkin, Mark H. Barley, and Gordon McFiggans. A Significant Role for Nitrate and Peroxide Groups on Indoor Secondary Organic Aerosol. *Environmental Science & Technology*, 46(17) :9290–9298, September 2012.

[48] Elena Gómez Alvarez, Damien Amedro, Charbel Afif, Sasho Gligorovski, Coralie Schoemaecker, Christa Fittschen, Jean-Francois Doussin, and Henri Wortham. Unexpectedly high indoor hydroxyl radical concentrations associated with nitrous acid. *Proceedings of the National Academy of Sciences*, 110(33) :13294–13299, August 2013.

[49] Caroline Marchand. *Incidences des teneurs en aldehydes mesurées dans l'air intérieur et extérieur sur des patients sujets à l'asthme*. Strasbourg 1, January 2005.

[50] C. Marchand, B. Bulliot, S. Le CalvÃ©, and Ph. Mirabel. Aldehyde measurements in indoor environments in strasbourg (france). *Atmospheric Environment*, 40(7) :1336 – 1345, 2006.

[51] Dan Norbäck, Jamal Hisham Hashim, Zailina Hashim, and Faridah Ali. Volatile organic compounds (voc), formaldehyde and nitrogen dioxide (no2) in schools in johor bahru, malaysia : Associations with rhinitis, ocular, throat and dermal symptoms, headache and fatigue. *Science of The Total Environment*, 592 :153 – 160, 2017.

[52] H. Gustafsson. *Building materials identified as major sources for indoor air pollutants : a critical review of case studies*. Document (Statens råd för byggnadsforskning (Sweden))). Swedish Council for Building Research, 1992.

[53] Fabian Melchior Gerster, David Vernez, Pascal Pierre Wild, and Nancy Brenna Hopf. Hazardous substances in frequently used professional cleaning products. *International Journal of Occupational and Environmental Health*, 20(1) :46–60, January 2014.

[54] Todd A. Wetzel. Volatile Organic Compounds (VOCs) In Indoor Air : Emission From Consumer Products and the Use of Plants for Air Sampling. 2014.

[55] X Yang, Q Chen, J.S Zhang, R Magee, J Zeng, and C.Y Shaw. Numerical simulation of voc emissions from dry materials. *Building and Environment*, 36(10) :1099 – 1107, 2001.

[56] Zhe Liu, Wei Ye, and John C. Little. Predicting emissions of volatile and semivolatile organic compounds from building materials : A review. *Building and Environment*, 64(Supplement C) :7 – 25, 2013.

[57] Chuck Yu and Derrick Crump. A review of the emission of VOCs from polymeric materials used in buildings. *Building and Environment*, 33(6) :357–374, November 1998.

[58] Fariborz Haghighat and Giovanna Donnini. Emissions of Indoor Pollutants from Building Materials—State of the Art Review. *Architectural Science Review*, 36(1) :13–22, March 1993.

[59] Duy Xuan Ho, Ki-Hyun Kim, Jong Ryeul Sohn, Youn Hee Oh, and Ji-Won Ahn. Emission Rates of Volatile Organic Compounds Released from Newly Produced Household Furniture Products Using a Large-Scale Chamber Testing Method. *The Scientific World Journal*, 11 :1597–1622, September 2011.

[60] Athanasios Katsoyiannis, Paolo Leva, and Dimitrios Kotzias. Voc and carbonyl emissions from carpets : A comparative study using four types of environmental chambers. *Journal of Hazardous Materials*, 152(2) :669 – 676, 2008.

[61] Christophe Yrieix, Alina Dulaurent, Caroline Laffargue, FranÃ§ois Maupetit, Tiphaine Pacary, and Erik Uhde. Characterization of voc and formaldehyde emissions from a wood based panel : Results from an inter-laboratory comparison. *Chemosphere*, 79(4) :414 – 419, 2010.

[62] Thomas J. Kelly, Deborah L. Smith, and Jan Satola. Emission Rates of Formaldehyde

from Materials and Consumer Products Found in California Homes. *Environmental Science & Technology*, 33(1) :81–88, January 1999.

[63] Felix Klein, Naomi J. Farren, Carlo Bozzetti, Kaspar R. Daellenbach, Dogushan Kilic, Nivedita K. Kumar, Simone M. Pieber, Jay G. Slowik, Rosemary N. Tuthill, Jacqueline F. Hamilton, Urs Baltensperger, André S. H. Prévôt, and Imad El Haddad. Indoor terpene emissions from cooking with herbs and pepper and their secondary organic aerosol production potential. *Scientific Reports*, 6 :36623, 11 2016.

[64] Mehdi Amouei Torkmahalleh, Soudabeh Gorjinezhad, Hediye Sumru Unluevcek, and Philip K. Hopke. Review of factors impacting emission/concentration of cooking generated particulate matter. *Science of The Total Environment*, 586(Supplement C) :1046 – 1056, 2017.

[65] Gary WK Wong, Bert Brunekreef, Philippa Ellwood, H Ross Anderson, M Innes Asher, Julian Crane, and Christopher KW Lai. Cooking fuels and prevalence of asthma : a global analysis of phase three of the international study of asthma and allergies in childhood (isaac). *The Lancet Respiratory Medicine*, 1(5) :386–394, 2017/09/16.

[66] Carol Potera. Indoor air quality : Scented products emit a bouquet of vocs. *Environmental Health Perspectives*, 119(1) :A16–A16, 01 2011.

[67] M. H. Sherman and D. J. Wilson. Relating actual and effective ventilation in determining indoor air quality. *Building and Environment*, 21(3) :135–144, January 1986.

[68] O. A. Seppänen, W. J. Fisk, and M. J. Mendell. Association of Ventilation Rates and CO2 Concentrations with Health andOther Responses in Commercial and Institutional Buildings. *Indoor Air*, 9(4) :226–252, December 1999.

[69] M. S. Zuraimi, K. W. Tham, F. T. Chew, and P. L. Ooi. The effect of ventilation strategies

of child care centers on indoor air quality and respiratory health of children in Singapore. *Indoor Air*, 17(4) :317–327, August 2007.

[70] William J. Fisk. Health and productivity gains from better indoor environments and their relationship with building energy efficiency. *Annual Review of Energy and the Environment*, 25(1) :537–566, 2000.

[71] D.J. Clements-Croome, H.B. Awbi, Zs Bakó-Biró, N. Kochhar, and M. Williams. Ventilation rates in schools. *Building and Environment*, 43(3) :362–367, March 2008.

[72] William W. Nazaroff and Charles J. Weschler. Cleaning products and air fresheners : exposure to primary and secondary air pollutants. *Atmospheric Environment*, 38(18) :2841 – 2865, 2004.

[73] Michael S. Waring and J. Raymond Wells. Volatile organic compound conversion by ozone, hydroxyl radicals, and nitrate radicals in residential indoor air : Magnitudes and impacts of oxidant sources. *Atmospheric Environment*, 106 :382 – 391, 2015.

[74] Sasho Gligorovski and Charles J. Weschler. The Oxidative Capacity of Indoor Atmospheres. *Environmental Science & Technology*, 47(24) :13905–13906, December 2013.

[75] C. J. Weschler. Chemistry in indoor environments : 20 years of research. *Indoor Air*, 21(3) :205–218, June 2011.

[76] B. J. Finlayson-Pitts and J. N. Pitts. Tropospheric air pollution : ozone, airborne toxics, polycyclic aromatic hydrocarbons, and particles. *Science (New York, N.Y.)*, 276(5315) :1045–1052, May 1997.

[77] Charles J. Weschler and Helen C. Shields. Potential reactions among indoor pollutants. *Atmospheric Environment*, 31(21) :3487 – 3495, 1997.

[78] Charles J. Weschler and Helen C. Shields. Production of the Hydroxyl Radical in Indoor Air. *Environmental Science & Technology*, 30(11) :3250–3258, October 1996.

[79] Golam Sarwar, Richard Corsi, Yosuke Kimura, David Allen, and Charles J. Weschler. Hydroxyl radicals in indoor environments. *Atmospheric Environment*, 36(24) :3973 – 3988, 2002.

[80] T Wainman, J Zhang, C J Weschler, and P J Lioy. Ozone and limonene in indoor air : a source of submicron particle exposure. *Environmental Health Perspectives*, 108(12) :1139–1145, December 2000.

[81] Charles J. Weschler and Helen C. Shields. Indoor ozone/terpene reactions as a source of indoor particles. *Atmospheric Environment*, 33(15) :2301 – 2312, 1999.

[82] W. W. Nazaroff and A. H. Goldstein. Indoor chemistry : research opportunities and challenges. *Indoor Air*, 25(4) :357–361, August 2015.

[83] A. W. Rollins and S. Pusede. Gas/particle partitioning of total alkyl nitrates observed with TD-LIF in Bakersfield - Rollins - 2013 - Journal of Geophysical Research : Atmospheres - Wiley Online Library.

[84] Effect of Ozone on Nicotine Desorption from Model Surfaces : Evidence for Heterogeneous Chemistry.

[85] C. W. Spicer, D. V. Kenny, G. F. Ward, and I. H. Billick. Transformations, lifetimes, and sources of NO2, HONO, and HNO3 in indoor environments. *Air & Waste : Journal of the Air & Waste Management Association*, 43(11) :1479–1485, November 1993.

[86] T. Wainman, C. J. Weschler, P. J. Lioy, and J. Zhang. Effects of surface type and relative humidity on the production and concentration of nitrous acid in a model indoor environment. *Environmental Science & Technology*, 35(11) :2201–2206, June 2001.

[87] B. J. Finlayson-Pitts, L. M. Wingen, A. L. Sumner, D. Syomin, and K. A. Ramazan. The heterogeneous hydrolysis of NO2 in laboratory systems and in outdoor and indoor atmospheres : An integrated mechanism. *Physical Chemistry Chemical Physics*, 5(2) :223–242, January 2003.

[88] C.W. Spicer, R.W. Coutant, G.F. Ward, D.W. Joseph, A.J. Gaynor, and I.H. Billick. Rates and mechanisms of no2 removal from indoor air by residential materials. *Environment International*, 15(1) :643 – 654, 1989. Indoor Air Quality.

[89] B. J. Finlayson-Pitts and J. N. Jr Pitts. Atmospheric chemistry. Fundamentals and experimental techniques. January 1986.

[90] Jason E. Ham and J. Raymond Wells. Surface chemistry of a pine-oil cleaner and other terpene mixtures with ozone on vinyl flooring tiles. *Chemosphere*, 83(3) :327 – 333, 2011.

[91] Bruce A. Tichenor. Adsorption and Desorption of Pollutants to and from Indoor Surfaces. In *Air Pollution*, The Handbook of Environmental Chemistry, pages 73–87. Springer, Berlin, Heidelberg, 2004. DOI : 10.1007/b94831.

[92] Aruna Suravajala, Larry E. Erickson, and Alok Bhandari. Sorption of Tertiary Butyl Mercaptan to Indoor Materials in Contact with Air or Water. *Journal of Environmental Engineering*, 134(3) :161–168, March 2008.

[93] D. Won, R. L. Corsi, and M. Rynes. Sorptive interactions between VOCs and indoor materials. *Indoor Air*, 11(4) :246–256, December 2001.

[94] Rikke Bramming Jørgensen and Olav Bjørseth. Sorption behaviour of volatile organic compounds on material surfaces — the influence of combinations of compounds and materials compared to sorption of single compounds on single materials. *Environment International*, 25(1) :17 – 27, 1999.

[95] Doyun Won, Daniel M. Sander, C.Y. Shaw, and Richard L. Corsi. Validation of the surface sink model for sorptive interactions between {VOCs} and indoor materials. *Atmospheric Environment*, 35(26) :4479 – 4488, 2001.

[96] Y. An, J. S. Zhang, and C. Y. Shaw. Measurements of {VOC} Adsorption/Desorption Characteristics of Typical Interior Building Materials. *HVAC&R Research*, 5(4) :297–316, October 1999.

[97] R. Meininghaus, L. Gunnarsen, and H. N. Knudsen. Diffusion and Sorption of Volatile Organic Compounds in Building Materials Impact on Indoor Air Quality. *Environmental Science & Technology*, 34(15) :3101–3108, August 2000.

[98] Doyun Won, Richard L. Corsi, and Mike Rynes. New Indoor Carpet as an Adsorptive Reservoir for Volatile Organic Compounds. *Environmental Science & Technology*, 34(19) :4193–4198, October 2000.

[99] B. A. Tichenor, L. A. Sparks, J. B. White, and M. D. Jackson. Evaluating sources of indoor air pollution. *Journal of the Air & Waste Management Association*, 40(4) :487–492, April 1990.

[100] Roman Meininghaus, Tunga Salthammer, and Helmut Knöppel. Interaction of volatile organic compounds with indoor materials—a small-scale screening method. *Atmospheric Environment*, 33(15) :2395 – 2401, 1999.

[101] Jacques J. Piadé, Sandrine D'André, and Edward B. Sanders. Sorption Phenomena of Nicotine and Ethenylpyridine Vapors on Different Materials in a Test Chamber. *Environmental Science & Technology*, 33(12) :2046–2052, June 1999.

[102] De-Ling Liu and William W. Nazaroff. Modeling pollutant penetration across building envelopes. *Atmospheric Environment*, 35(26) :4451 – 4462, 2001.

[103] Tracy L. Thatcher, Melissa M. Lunden, Kenneth L. Revzan, Richard G. Sextro, and Nancy J. Brown. A Concentration Rebound Method for Measuring Particle Penetration and Deposition in the Indoor Environment. *Aerosol Science and Technology*, 37(11) :847–864, November 2003.

[104] Edvard Karlsson. Indoor deposition reducing the effect of toxic gas clouds in ordinary buildings. *Journal of Hazardous Materials*, 38(2) :313 – 327, 1994.

[105] William W. Nazaroff and Glen R. Cass. Mass-transport aspects of pollutant removal at indoor surfaces. *Environment International*, 15(1) :567 – 584, 1989. Indoor Air Quality.

[106] J.A Cano-Ruiz, D Kong, R.B Balas, and W.W Nazaroff. Removal of reactive gases at indoor surfaces : Combining mass transport and surface kinetics. *Atmospheric Environment. Part A. General Topics*, 27(13) :2039 – 2050, 1993.

[107] Terje Grøntoft and Michele R Raychaudhuri. Compilation of tables of surface deposition velocities for o_3, $\{NO_2\}$ and $\{SO_2\}$ to a range of indoor surfaces. *Atmospheric Environment*, 38(4) :533 – 544, 2004.

[108] Ph. D. John D. Spengler, M.D. Jonathan M. Samet, M.S., and Sc.D. John F. McCarthy, C.I.H. INDOOR AIR QUALITY MODELING. In *Indoor Air Quality Handbook*. McGraw Hill Professional, Access Engineering, 2001.

[109] Michael D. Koontz. *Development of a model for assessing indoor exposure to air pollutants*. California Environmental Protection Agency, Air Resources Board, Research Division, Sacramento, CA (2020 L Street, Sacramento, 95814), 1998.

[110] William W. Nazaroff and Glen R. Cass. Mathematical modeling of indoor aerosol dynamics. *Environmental Science & Technology*, 23(2) :157–166, February 1989.

[111] Henrik Brohus and Peter V. Nielsen. Personal Exposure in Displacement Ventilated Rooms. *Indoor Air*, 6(3) :157–167, September 1996.

[112] Zhishi Guo. Development of a windows-based indoor air quality simulation software package. *Environmental Modelling & Software*, 15(4) :403 – 410, 2000.

[113] C. Dimitroulopoulou, M.R. Ashmore, M.T.R. Hill, M.A. Byrne, and R. Kinnersley. Indair : A probabilistic model of indoor air pollution in {UK} homes. *Atmospheric Environment*, 40(33) :6362 – 6379, 2006.

[114] S. M. Saunders, M. E. Jenkin, R. G. Derwent, and M. J. Pilling. Protocol for the development of the Master Chemical Mechanism, MCM v3 (Part A) : tropospheric degradation of non-aromatic volatile organic compounds. *Atmospheric Chemistry and Physics*, 3(1) :161–180, 2003.

[115] Andrew C. Terry, Nicola Carslaw, Mike Ashmore, Sani Dimitroulopoulou, and David C. Carslaw. Occupant exposure to indoor air pollutants in modern european offices : An integrated modelling approach. *Atmospheric Environment*, 82 :9 – 16, 2014.

[116] M. S. Waring. Secondary organic aerosol in residences : predicting its fraction of fine particle mass and determinants of formation strength. *Indoor Air*, 24(4) :376–389, August 2014.

[117] Sylvain Courtey. *Contribution à la modélisation de la phénoménologie des équilibres régissant les atmosphères confinées*. Thèse de doctorat, Université de La Rochelle, France, 2007.

[118] Golam Sarwar, Richard Corsi, David Allen, and Charles Weschler. The significance of secondary organic aerosol formation and growth in buildings : experimental and computational evidence. *Atmospheric Environment*, 37(9–10) :1365 – 1381, 2003. James P. Lodge, Jr. Memorial Issue. Measurement Issues in Atmospheric Chemistry.

[119] R. Kurtenbach, K.H. Becker, J.A.G. Gomes, J. Kleffmann, J.C. Lörzer, M. Spittler, P. Wiesen, R. Ackermann, A. Geyer, and U. Platt. Investigations of emissions and heterogeneous formation of hono in a road traffic tunnel. *Atmospheric Environment*, 35(20) :3385 – 3394, 2001.

[120] Kevin A. Ramazan, Dennis Syomin, and Barbara J. Finlayson-Pitts. The photochemical production of HONO during the heterogeneous hydrolysis of NO2. *Physical Chemistry Chemical Physics*, 6(14) :3836–3843, July 2004.

[121] R. G. Sargent. Verification and validation of simulation models. *Journal of Simulation*, 7(1) :12–24, February 2013.

[122] R. E. Crosbie R. E. Gagne G. S. Innis C. S. Lalwani J. Loch R. J. Sylvester R. D. Wright N. Kheir Schlesinger, S. and D. Bartos. Terminology for model credibility. *SIMULATION*, 32(3) :103–104, March 1979.

[123] American Society for Testing, Materials, ASTM International, ASTM Committee D-22 on Air Quality, and ASTM Subcommittee D-22.05 Subcommittee on Indoor Air. *Standard Guide for Statistical Evaluation of Indoor Air Quality Models*. ASTM International standards. ASTM International, 1997.

[124] Y. Zhao, H. Yoshino, and H. Okuyama. Evaluation of the COMIS Model by Comparing Simulation and Measurement of Airflow and Pollutant Concentration. *Indoor Air*, 8(2) :123–130, June 1998.

[125] Philippe Thunis, Emilia Georgieva, and Anna Pederzoli. A tool to evaluate air quality model performances in regulatory applications. *Environmental modelling & software*, 38 :220–230, 2012.

[126] C. Carnevale, G. Finzi, A. Pederzoli, E. Pisoni, P. Thunis, E. Turrini, and M. Volta. Applying the delta tool to support the Air Quality Directive : evaluation of the TCAM che-

mical transport model. *Air Quality, Atmosphere & Health*, 7(3) :335–346, September 2014.

[127] VERRIELE-M. HANOUN B. PETITPREZ D. LECLERC N. DUSANTER SCHOEMAECKER, C. Characterization of the IAQ in Low Energy Public Buildings in France through a dual experiment and modeling approach | UnivOAK. *Proceedings of the 13th International Conference on Indoor Air Quality and Climate. Hong-Kong*.

[128] D. A. Hauglustaine, F. Hourdin, L. Jourdain, M.-A. Filiberti, S. Walters, J.-F. Lamarque, and E. A. Holland. Interactive chemistry in the Laboratoire de Météorologie Dynamique general circulation model : Description and background tropospheric chemistry evaluation : INTERACTIVE CHEMISTRY IN LMDZ. *Journal of Geophysical Research : Atmospheres*, 109(D4) :n/a–n/a, February 2004.

[129] G. A. Folberth, D. A. Hauglustaine, J. Lathière, and F. Brocheton. Interactive chemistry in the Laboratoire de Météorologie Dynamique general circulation model : model description and impact analysis of biogenic hydrocarbons on tropospheric chemistry. *Atmospheric Chemistry and Physics*, 6(8) :2319, June 2006.

[130] William P.L. Carter. Development of the saprc-07 chemical mechanism. *Atmospheric Environment*, 44(40) :5324 – 5335, 2010. Atmospheric Chemical Mechanisms : Selected Papers from the 2008 Conference.

[131] P. Blondeau, A. L. Tiffonnet, F. Allard, and F. Haghighat. Physically Based Modelling of the Material and Gaseous Contaminant Interactions in Buildings : Models, Experimental Data and Future Developments. *Advances in Building Energy Research*, 2(1) :57–93, January 2008.

[132] Bruce A. Tichenor, Zhishi Guo, James E. Dunn, Leslie E. Sparks, and Mark A. Mason.

The Interaction of Vapour Phase Organic Compounds with Indoor Sinks. *Indoor Air*, 1(1) :23–35, March 1991.

[133] James W. Axley. Adsorption Modelling for Building Contaminant Dispersal Analysis. *Indoor Air*, 1(2) :147–171, July 1991.

[134] James W. Axley. New mass transport elements and components for the NIST IAQ model. *NIST GCR*, pages 95–676, 1995.

[135] Fariborz Haghighat and Hongyu Huang. Integrated iaq model for prediction of voc emissions from building material. *Building and Environment*, 38(8) :1007 – 1017, 2003.

[136] J. Zeng S. Madronich, S.J. Flocke. Tuv : tropospheric ultraviolet and visible radiation model.

[137] J. M. Daisey, W. J. Angell, and M. G. Apte. Indoor air quality, ventilation and health symptoms in schools : an analysis of existing information. *Indoor Air*, 13(1) :53–64, March 2003.

[138] Patrick N. Breysse, Gregory B. Diette, Elizabeth C. Matsui, Arlene M. Butz, Nadia N. Hansel, and Meredith C. McCormack. Indoor Air Pollution and Asthma in Children. *Proceedings of the American Thoracic Society*, 7(2) :102–106, May 2010.

[139] P.N. Pegas, T. Nunes, C.A. Alves, J.R. Silva, S.L.A. Vieira, A. Caseiro, and C.A. Pio. Indoor and outdoor characterisation of organic and inorganic compounds in city centre and suburban elementary schools of aveiro, portugal. *Atmospheric Environment*, 55 :80 – 89, 2012.

[140] S. C. Lee and M. Chang. Indoor and outdoor air quality investigation at schools in Hong Kong. *Chemosphere*, 41(1-2) :109–113, July 2000.

[141] Hakan Pekey and Demet Arslanbaş. The Relationship Between Indoor, Outdoor and Personal VOC Concentrations in Homes, Offices and Schools in the Metropolitan Region of Kocaeli, Turkey. *Water, Air, and Soil Pollution*, 191(1-4) :113–129, June 2008.

[142] M. Stranger, S. S. Potgieter-Vermaak, and R. Van Grieken. Characterization of indoor air quality in primary schools in Antwerp, Belgium. *Indoor Air*, 18(6) :454–463, December 2008.

[143] P.K Srivastava, G.G Pandit, S Sharma, and A.M Mohan Rao. Volatile organic compounds in indoor environments in mumbai, india. *Science of The Total Environment*, 255(1) :161 – 168, 2000.

[144] Celeste Y. S. Siqueira, Adriana Gioda, Fabiana P. Carneiro, Maria da Conceição K. V. Ramos, Aquino Neto, and Francisco R. Distribution of indoor air pollutants in downtown Rio de Janeiro, Brazil. *Journal of the Brazilian Chemical Society*, 22(11) :2127–2138, November 2011.

[145] Charles J. Weschler and Helen C. Shields. Experiments probing the influence of air exchange rates on secondary organic aerosols derived from indoor chemistry. *Atmospheric Environment*, 37(39) :5621 – 5631, 2003. Indoor Air Chemistry and Physics : Papers from Indoor Air 2002.

[146] S. K. Brown, M. R. Sim, M. J. Abramson, and C. N. Gray. Concentrations of Volatile Organic Compounds in Indoor Air – A Review. *Indoor Air*, 4(2) :123–134, June 1994.

[147] Malak Rizk. *Développement, validation et mise en œuvre sur le terrain d'une méthode de caractérisation in-situ des processus de sorption des composés organiques volatils par les matériaux de construction*. Lille 1, September 2015.

[148] OAR US EPA. Initial List of Hazardous Air Pollutants with Modifications, December 2015.

[149] Michael S. Waring and Jeffrey A. Siegel. Indoor Secondary Organic Aerosol Formation Initiated from Reactions between Ozone and Surface-Sorbed d-Limonene. *Environmental Science & Technology*, 47(12) :6341–6348, June 2013.

[150] Ann-Therése Karlberg, Kerstin Magnusson, and Ulrika Nilsson. Air oxidation of d-limonene (the citrus solvent) creates potent allergens. *Contact Dermatitis*, 26(5) :332–340, May 1992.

[151] A.W. Nørgaard, J.D. Kudal, V. Kofoed-Sørensen, I.K. Koponen, and P. Wolkoff. Ozone-initiated VOC and particle emissions from a cleaning agent and an air freshener : Risk assessment of acute airway effects. *Environment International*, 68 :209–218, July 2014.

[152] M. Rizk, M. Verriele, S. Dusanter, C. Schoemaecker, S. Le calve, and N. Locoge. Fast sorption measurements of volatile organic compounds on building materials : Part 1 – methodology developed for field applications. *Building and Environment*, 99 :200 – 209, 2016.

[153] David C. Carslaw. Evidence of an increasing no2/nox emissions ratio from road traffic emissions. *Atmospheric Environment*, 39(26) :4793 – 4802, 2005.

[154] Srinandini Parthasarathy, Randy L. Maddalena, Marion L. Russell, and Michael G. Apte. Effect of temperature and humidity on formaldehyde emissions in temporary housing units. *Journal of the Air & Waste Management Association (1995)*, 61(6) :689–695, June 2011.

[155] Alex B. Guenther, Patrick R. Zimmerman, Peter C. Harley, Russell K. Monson, and Ray Fall. Isoprene and monoterpene emission rate variability : Model evaluations and sensitivity analyses. *Journal of Geophysical Research : Atmospheres*, 98(D7) :12609–12617, July 1993.

[156] Donald M. Murray and David E. Burmaster. Residential Air Exchange Rates in the United States : Empirical and Estimated Parametric Distributions by Season and Climatic Region. *Risk Analysis*, 15(4) :459–465, August 1995.

[157] J. E. Yocom, W. L. Clink, and W. A. Cote. Indoor-outdoor air quality relationships. *Journal of the Air Pollution Control Association*, 21(5) :251–259, May 1971.

[158] Charles J. Weschler. Changes in indoor pollutants since the 1950s. *Atmospheric Environment*, 43(1) :153 – 169, 2009. Atmospheric Environment - Fifty Years of Endeavour.

[159] Peder Wolkoff. Volatile Organic Compounds Sources, Measurements, Emissions, and the Impact on Indoor Air Quality. *Indoor Air*, 5(S3) :5–73, December 1995.

[160] Sait C. Sofuoglu, Guler Aslan, Fikret Inal, and Aysun Sofuoglu. An assessment of indoor air concentrations and health risks of volatile organic compounds in three primary schools. *International Journal of Hygiene and Environmental Health*, 214(1) :36 – 46, 2011.

[161] Shaobin Wang, H.M. Ang, and Moses O. Tade. Volatile organic compounds in indoor environment and photocatalytic oxidation : State of the art. *Environment International*, 33(5) :694 – 705, 2007.

[162] OAR US EPA. Nitrogen Dioxide's Impact on Indoor Air Quality, August 2014.

[163] Kiyoung Lee, William J. Parkhurst, Jianping Xue, Halûk Özkaynak, Donna Neuberg, and John D. Spengler. Outdoor/Indoor/Personal Ozone Exposures of Children in Nashville, Tennessee. *Journal of the Air & Waste Management Association*, 54(3) :352–359, March 2004.

[164] Olaf Wilke, Oliver Jann, and Doris Brödner. VOC- and SVOC-emissions from adhesives, floor coverings and complete floor structures. *Indoor Air*, 14 Suppl 8 :98–107, 2004.

[165] M. D. Pandian, W. R. Ott, and J. V. Behar. Residential air exchange rates for use in indoor air and exposure modeling studies. *Journal of Exposure Analysis and Environmental Epidemiology*, 3(4) :407–416, December 1993.

[166] Hugo Destaillats, Randy L. Maddalena, Brett C. Singer, Alfred T. Hodgson, and Thomas E. McKone. Indoor pollutants emitted by office equipment : A review of reported data and information needs. *Atmospheric Environment*, 42(7) :1371 – 1388, 2008.

[167] Charles J. Weschler and Helen C. Shields. Measurements of the Hydroxyl Radical in a Manipulated but Realistic Indoor Environment. *Environmental Science & Technology*, 31(12) :3719–3722, December 1997.

[168] Zs. Bakó-Biró, D.J. Clements-Croome, N. Kochhar, H.B. Awbi, and M.J. Williams. Ventilation rates in schools and pupils' performance. *Building and Environment*, 48 :215 – 223, 2012.

[169] R. Wålinder, D. Norbäck, G. Wieslander, G. Smedje, C. Erwall, and P. Venge. Nasal patency and biomarkers in nasal lavage – the significance of air exchange rate and type of ventilation in schools. *International Archives of Occupational and Environmental Health*, 71(7) :479–486, October 1998.

[170] H. Guo, L. Morawska, C. He, and D. Gilbert. Impact of ventilation scenario on air exchange rates and on indoor particle number concentrations in an air-conditioned classroom. *Atmospheric Environment*, 42(4) :757 – 768, 2008.

[171] Université de Lille Sciences et Technologies, Mines Douai, Ecole des Mines de Douai, and Université des Sciences et Technologies de Lille (Lille I). Malak RIZK | Profil professionnel | LinkedIn.

[172] G. Drakou, C. Zerefos, I. Ziomas, and M. Voyatzaki. Measurements and numerical

simulations of indoor O3 and NOx in two different cases. *Atmospheric Environment*, 32(4) :595–610, 1998.

[173] Golam Sarwar, Richard Corsi, Yosuke Kimura, David Allen, and Charles J. Weschler. Hydroxyl radicals in indoor environments. *Atmospheric Environment*, 36(24) :3973–3988, 2002.

[174] Charles J. Weschler. Chemical reactions among indoor pollutants : what we've learned in the new millennium. *Indoor air*, 14(s7) :184–194, 2004.

[175] Nicola Carslaw. A mechanistic study of limonene oxidation products and pathways following cleaning activities. *Atmospheric Environment*, 80 :507 – 513, 2013.

[176] P. M. Frank and M. Eslami. Introduction to System Sensitivity Theory. *IEEE Transactions on Systems, Man, and Cybernetics*, 10(6) :337–338, June 1980.

[177] Francesca Pianosi, Keith Beven, Jim Freer, Jim W. Hall, Jonathan Rougier, David B. Stephenson, and Thorsten Wagener. Sensitivity analysis of environmental models : A systematic review with practical workflow. *Environmental Modelling &Software*, 79 :214 – 232, 2016.

[178] Dongming Hwang, Daewon W. Byun, and M. Talat Odman. An automatic differentiation technique for sensitivity analysis of numerical advection schemes in air quality models. *Atmospheric Environment*, 31(6) :879–888, 1997.

[179] Louis B. Rall, G. Goos, J. Hartmanis, W. Brauer, P. Brinch Hansen, D. Gries, C. Moler, G. Seegmüller, J. Stoer, and N. Wirth, editors. *Automatic Differentiation : Techniques and Applications*, volume 120 of *Lecture Notes in Computer Science*. Springer Berlin Heidelberg, Berlin, Heidelberg, 1981. DOI : 10.1007/3-540-10861-0.

[180] Michael Bartholomew-Biggs, Steven Brown, Bruce Christianson, and Laurence Dixon. Automatic differentiation of algorithms. *Journal of Computational and Applied Mathematics*, 124(1) :171 – 190, 2000. Numerical Analysis 2000. Vol. IV : Optimization and Nonlinear Equations.

[181] M Berz and International Workshop on Computational Differentiation, editors. *Computational differentiation : techniques, applications, and tools*. Society for Industrial and Applied Mathematics, Philadelphia, 1996. OCLC : 36430038.

[182] Laurent Hascoet and Valérie Pascual. The Tapenade Automatic Differentiation Tool : Principles, Model, and Specification. *ACM Trans. Math. Softw.*, 39(3) :20 :1–20 :43, May 2013.

[183] A. Dervieux, Y. Mesri, F. Alauzet, A. Loseille, L. Hascoët, and B. Koobus. Continuous mesh adaptation models for CFD. *CFD Journal*, 16(4) :346–355, 2008.

[184] A. Dervieux, Y. Mesri, F. Courty, L. Hascoët, B. Koobus, and M. Vàzquez. Calculs de sensibilité par différentiation pour l'aérodynamique. In *proceedings of CANUM06, ESAIM journal*, 2006. to appear.

[185] C. Lauvernet, L. Hascoët, F.-X. Le Dimet, and F. Barret. Using Automatic Differentiation to study the sensitivity of a crop model. In *Recent Advances in Algorithmic Differentiation*, Lecture Notes in Computational Science and Engineering, pages 59–70. Springer, 2012. Selected papers from AD2012 Fort Collins, july 2012.

[186] Gauthier Hentz, Isabelle Charpentier, and Pierre Renaud. Higher-order continuation for the determination of robot workspace boundaries. *Comptes Rendus Mécanique*, 344(2) :95 – 101, 2016.

[187] B. Ferron and L. Hascoët. Capacités actuelles de la différentiation automatique : l'ad-

joint d'opa par tapenade. In *Colloque National sur l'Assimilation de Données, Toulouse, France*, 2006.

[188] Moulay Hicham Tber, Laurent Hascoet, Arthur Vidard, and Benjamin Dauvergne. Building the Tangent and Adjoint codes of the Ocean General Circulation Model OPA with the Automatic Differentiation tool TAPENADE. *arXiv :0711.4444 [cs]*, November 2007. arXiv : 0711.4444.

[189] C. Lauvernet, Laurent Hascoet, F.X. Le Dimet, and Frédéric Baret. Using Automatic Differentiation to study the sensitivity of a crop model. *Lecture Notes in Computational Science and Engineering*, 87 :p. 59 – p. 69, 2012.

[190] B. Alicke. OH formation by HONO photolysis during the BERLIOZ experiment. *Journal of Geophysical Research*, 108(D4), 2003.

[191] Bin Zhao, Ying Zhang, Xianting Li, Xudong Yang, and Dongtao Huang. Comparison of indoor aerosol particle concentration and deposition in different ventilated rooms by numerical method. *Building and Environment*, 39(1) :1 – 8, 2004.

[192] Jun Gao, Changsheng Cao, Zhiwen Luo, and Xu Zhang. Inhalation exposure to particulate matter in rooms with underfloor air distribution. *Indoor and Built Environment*, 23(2) :236–245, April 2014.

[193] Jian Hang, Zhiwen Luo, Xuemei Wang, Lejian He, Baomin Wang, and Wei Zhu. The influence of street layouts and viaduct settings on daily carbon monoxide exposure and intake fraction in idealized urban canyons. *Environmental Pollution (Barking, Essex : 1987)*, 220(Pt A) :72–86, January 2017.

Annexe 1 : Indoor air quality standards

nom	n° cas	ID Model	Valeurs-guides	unité valeur guide	année de la valeur guide	type de valeur guide	sources valeurs guides
acroléine	#N/A	ACROLEIN	6,9 (1 heure) ; 0,8 (> 1 an)	µg/m3	2013	VGAI	ANSES
Méthyl-t-butyl ether	#N/A	MTBE	367 (15 min) ; 183,5 (moyenne pondérée sur 8 h)	mg/m3	2012	VLEP	INRS
formaldéhyde	50-00-0	FORMALD	50 (2h) ; 10 (> 1 an)	µg/m3	2016	VGAI	ANSES
tétrachlorure de carbone	56-23-5	CCL4	pas de valeur guide française		2005		INERIS
propanediol / propylène gl	57-55-6	PR-GLYCL	100	µg/m3	2006	CLI	Afsset
éthanol	64-17-5	ETOH	1950 (moyenne pondérée sur 8h), 9500 (15 min)	mg/m3	2011	VLEP	INERIS
hexanal	66-25-1	1C6RCHO	640	µg/m3	2006	CLI	Afsset
2-propanol	67-63-0	I-C3-OH	980 (15 min)	mg/m3	1982	VLE	INRS
acétone	67-64-1	ACETONE	1210 (moyenne pondérée sur 8h) ; 2420 (15 min)	mg/m3	2008	VLEP	INRS
chloroforme	67-66-3	CHCL3	250 (15 min) ; 10 (8h)	mg/m3	2015	VLEP	INERIS
1-butanol	71-36-3	N-C4-OH	150 (15 min)	mg/m3	2011	VLEP	INRS

benzène	71-43-2	BENZENE	20 (1 à 14 jours) ; 10 (>1an)	µg/m3	2015	VGAI	ANSES
chlorométhane	74-87-3	CH3-CL	210 (15 min) ; 105 (moyenne pondérée sur 8 heures)	mg/m3	1997	VLE / VME	INRS
acétaldéhyde	75-07-0	ACETALD	3000 (1h), 160 (expo > 1 an)	µg/m3	2014	VGAI	ANSES
dichlorométhane	75-09-2	CL2-ME	356 (15 min) ; 178 (moyenne pondérée sur 8 h)	mg/m3	2014	VLEP	INRS
2-méthyl-1-propanol	78-83-1	I-C4-OH	150 (moyenne pondérée sur 8h)	mg/m3	2011	VLEP	INRS
trichloroethylène	79-01-6	CL3-ETHE	800 (14 jours à 1 an), 2 (expo vie entière)	µg/m3	2009	VGAI	ANSES
alpha-pinene	80-56-8	A-PINENE					

méthyl méthacrylate	80-62-6	ME-MACRT	205 (moyenne pondérée sur 8h), 410 (15 min)	mg/m3	2013	VLEP	INRS
phtalate de ditybutyle	84-74-2	DBU-PTHT	5 (valeur moyenne sur 8h)	mg/m3	2010	VME	INRS
naphtalene	91-20-3	NAPHTAL	10 (> 1 an)	µg/m3	2009	VGAI	Afsset
o-xylène	95-47-6	O-XYLENE	221 (valeur pondérée sur 8h), 442 (15 min)	mg/m3	2009	VLEP	INRS
1,2,4-triméthylbenzène	95-63-6	124-TMB	100 (moyenne pondérée sur 8h), 250 (15min)	mg/m3	2014	VME / VLE	INERIS
Gamma-butyrolactone	96-48-0	GBUTYACT	pas de valeur guide		2003		INRS
éthylbenzène	100-41-4	C2-BENZ	88,4 (moyenne pondérée sur 8h), 442 (15 min)	mg/m3	2010	VLEP	INRS
styrène	100-42-5	STYRENE	215 (valeur pondérée sur 8h)	mg/m3	2012	VLEP	INRS
benzyl alcool	100-51-6	BZ-CH2OH	pas de valeur guide		2010		
benzaldéhyde	100-52-7	BENZALD	pas de valeur guide		2005		
2-éthylhexyl acrylate	103-11-7	2ETHXACR	pas de valeur guide		2011		
2-éthylhexanol	104-76-7	2-ETC6OH	pas de valeur guide		2011		
p-xylène	106-42-3	P-XYLENE	221 (valeur pondérée sur 8h), 442 (15 min)	mg/m3	2009	VLEP	INRS
1,4-dichlorobenzène	106-46-7	CL2-BEN	4,5 (moyenne pondérée sur 8h), 306	mg/m3	2014	VME / VLE	INERIS
M-xylène	108-38-3	M-XYLENE	221 (valeur pondérée sur 8h), 442 (15 min)	mg/m3	2009	VLEP	INRS
toluène	108-88-3	TOLUENE	76,8(8h), 384(15 min)	mg/m3	2012	VLEP	INRS

phénol	108-95-2	PHENOL	7,8 (moyenne pondérée sur 8 h), 15,6 (15 min)	mg/m3	2011	VLEP	INRS
hexane	110-54-3	N-C6	72 (moyenne pondérée sur 8h)	mg/m3	2008	VLEP	INRS
valéraldéhyde	110-62-3	1C5RCHO	175 000 (8h)	µg/m3	2008	VME	ministère du travail
dipropylèneglycol	110-98-5	DPR-GLCL	pas de valeur guide		2004		INERIS
heptanal	111-71-7	1C7RCHO	pas de valeur guide				
2-butoxyéthanol	111-76-2	BUO-ETOH	49 (moyenne pondérée sur 8h), 246 (15 min)	mg/m3	2013	VLEP	INRS
N-nonane	111-84-2	N-C9	1050 (moyenne pondérée sur 8h)	mg/m3	1987	VME	INRS
2-(2-butoxyethoxy)ethanol	112-34-5	DGBE	67,5 (moyenne pondérée sur 8h), 101,2 (15 min)	mg/m3	2007	VME / VLE	INRS
propionaldéhyde	123-38-6	PROPALD	pas de valeur guide		2008		
butyraldéhyde	123-72-8	1C4RCHO	pas de valeur guide		2008		
acétate de n-butyle	123-86-4	BU-ACET	710 (moyenne pondérée sur 8h),940 (15min)	mg/m3	2011	VLEP	INRS
octanal	124-13-0	IC8RCHO	640	µg/m3	2006	CLI	Afsset
décane	124-18-5	N-C10	pas de valeur guide		2013		
tétrachloroéthylène	127-18-4	CL4-ETHE	1380 (1 à 14 jours) , 250 (expo > 1 an)	µg/m3	2010	VGAI	ANSES
N-butyléther	142-96-1	BU-O-BU	pas de valeur guide		2010		
Acide 2-ethylhexanoïque	149-57-5	2ETHXACD	pas de valeur guide		2011		
méthyl isobutyrate	547-63-7	ME-IBUAT					
N-buthyl propionate	590-01-2	BU-PRAT					

isovaléraldéhyde	590-86-3	3MC4RCHO	pas de valeur guide		2008		
tétradécane	629-59-4	N-C14	pas de valeur guide				
Monoxyde de carbone	630-08-0	CO	100 (15 min) ; 60 (30 min) ; 30 (1 heure) ; 10 (8 heures)	mg/m3	2007	VGAI	ANSES
undécane	1120-21-4	N-C11	pas de valeur guide		2013		INERIS
butylcyclohexane	1678-93-9	C46CYCC6	pas de valeur guide				
crotonaldéhyde	4170-30-3	CROTALD	pas de valeur guide		2013		
1-butoxy-2-propanol	5131-66-8	BUOC3OH	pas de valeur guide		2010		
limonène	5989-27-5	D-LIMONE	pas de valeur guide (française)		2010		
2,2,4-trimethyl-1,3-pentanediol diisobutyrate	6846-50-0	TXIB	pas de valeur guide		2011		
chlore	7782-50-5	CL2	1,5 (15 min)	mg/m3	2014	VLE	INERIS
dioxyde d'azote	10102-44-0	NO2	200 (1 heure) ; 20 (> 1 an)	µg/m3	2013	VGAI	ANSES
éthylène glycol	107-21-1	ET-GLYCL	20 (8h) ; 40 (15 min)	mg/m3	2006	VLEP	INRS

Fangfang GUO

Développement d'un modèle pour le contrôle de la qualité de l'air intérieur

Résumé en Français

Ce travail a consisté à analyser et de simuler à l'aide du modèle INCA-Indoor la qualité de l'air intérieur mesurée dans le projet MERMAID, et de développer une nouvelle méthodologie pour étudier les contributions des différents processus aux concentrations de polluants. Cette nouvelle méthodologie se base sur un nouveau programme de sensibilité INCA-Indoor-D, construit à partir du modèle INCA-Indoor. Ce modèle permet d'identifier rapidement les paramètres les plus sensibles qui peuvent influencer la qualité de l'air intérieur.

Le modèle INCA-Indoor a été validé expérimentalement en utilisant les données mesurées lors de la campagne MERMAID (2014-2015). L'application du programme de sensibilité INCA-Indoor-D est pour analyser des sensibilité des concentrations de OH par rapport aux divers paramètres. Une classification de l'importance de ces paramètres (appelée « rang ») en fonction de la sensibilité a ainsi été effectuée. Ce travail de thèse offre une nouvelle analyse de la pollution de l'air ainsi que de nouvelles perspectives d'études possibles dans un bâtiment basse consommation. Il a permis de confirmer que le modèle INCA-Indoor permettait de simuler convenablement la pollution de l'air intérieur. Le modèle de sensibilité a été construit afin d'élaborer un nouvel outil d'aide à la décision capable de calculer à la fois les concentrations et leurs sensibilités aux divers paramètres. Ces sensibilités peuvent ensuite être utilisées pour élaborer, voire optimiser des stratégies de réduction de la pollution de l'air intérieur et d'identifier les paramètres les plus importants.

Mots clés : Qualité de l'air intérieur, modèle INCA-Indoor, sensibilité

Résumé en anglais

This study consisted in the development of a new methodology to study the contributions of different processes taken place indoors and the effect of input data on the indoor air pollution, and especially to develop a fast methodology to identify the most sensitive parameters that could influence indoor air quality. One objective is the development of a tool to support IAQ reduction strategies. The methodology is based on a sensitivity program INCA-Indoor-D for the INCA-Indoor model. This sensitivity program INCA-Indoor-D was built to identify the most important parameters affecting pollutant concentrations.

Since measurement data were newly analyzed and available from MERMAID, it is intended to continue to evaluate the INCA-Indoor model, which was used to analyze the indoor air quality of a low energy building. The first application of the sensitivity program INCA-Indoor-D is performed to develop a comprehensive sensitivity analysis of indoor [OH] with respect to diverse parameters. Sensitivity has been settled with a classification of the parameters. The results in this study provide useful information about roles of different processes controlling indoor air quality and the effects of different parameters on indoor pollutant concentrations. INCA-Indoor model can be used as a powerful tool to investigate indoor air issues. In addition, the tangent linear model of INCA-Indoor model developed can be used to find out the important parameters impacting pollutant concentrations.

Keywords: Indoor air quality, INCA-Indoor model, sensitivity